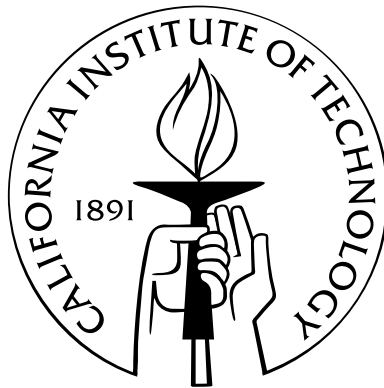


# An Integrated Design approach to Power Systems: from Power Flows to Electricity Markets

Thesis by  
Subhonmesh Bose

In Partial Fulfillment of the Requirements  
for the Degree of  
Doctor of Philosophy



California Institute of Technology  
Pasadena, California

2014  
(Submitted May 28, 2014.)

© 2014

Subhonmesh Bose

All Rights Reserved

To my parents...

# Acknowledgements

The time at Caltech has truly been an enriching experience, both professionally and personally. For the wonderful five years, I would like to extend my heartfelt gratitude to my four advisers: Steven Low, Adam Wierman, Babak Hassibi and K. Mani Chandy. Yes, I had four advisers! Truly, I am indebted for providing such a collaborative research environment with so much latitude. It is, indeed, unique. This is a good opportunity to thank the rest of my thesis committee that includes John Ledyard and Ross Baldick.

The professors, no doubt, have shaped my thoughts. Some of the RSRG (Rigorous Systems Research Group) gang have made this rigorous training a pleasant and interesting experience. First, I would like to thank Elizabeth Bodine-Baron, Dennice Gayme and Sachin Adlakha for providing guidance in my early graduate career. Thank you Desmond Cai and Anish Agrawal for the long discussions at the Atheneum every Friday. Matthew Thill's array of witty remarks have always made the weekly group meetings jovial. Among my long list of remarkable personal friends, I sincerely thank my roommate Kaushik Dasgupta for bearing me for four years.

Finally, I extend my gratitude to my parents. Without their unconditional love and support, this endeavor would never have come to fruition.

# Abstract

Power system is at the brink of change. Engineering needs, economic forces and environmental factors are the main drivers of this change. The vision is to build a smart electrical grid and a smarter market mechanism around it to fulfill mandates on clean energy. Looking at engineering and economic issues in isolation is no longer an option today; it needs an integrated design approach. In this thesis, I shall revisit some of the classical questions on the engineering operation of power systems that deals with the nonconvexity of power flow equations. Then I shall explore some issues of the interaction of these power flow equations on the electricity markets to address the fundamental issue of market power in a deregulated market environment. Finally, motivated by the emergence of new storage technologies, I present an interesting result on the investment decision problem of placing storage over a power network. The goal of this study is to demonstrate that modern optimization and game theory can provide unique insights into this complex system. Some of the ideas carry over to applications beyond power systems.

# Contents

- Acknowledgements** **iv**
  
- Abstract** **v**
  
- 1 Introduction and outline** **1**
  - 1.1 Drivers of change in power system . . . . . 1
    - 1.1.1 The role of engineering . . . . . 2
    - 1.1.2 Rise of economics . . . . . 2
    - 1.1.3 Environment poses a threat . . . . . 3
  - 1.2 The approach to modeling . . . . . 4
  - 1.3 Organization of the thesis . . . . . 7
    - 1.3.1 Chapter 2: Kirchoff’s laws, conic relaxations and their relationships . . . . . 7
    - 1.3.2 Chapter 3: Quadratically constrained quadratic programs on acyclic networks and tight conic relaxations . . . . . 7
    - 1.3.3 Chapter 4: Unifying structural market power analysis in electricity markets . . . . . 8
    - 1.3.4 Chapter 5: Role of market maker in Cournot competition in electricity markets . . . . . 8
    - 1.3.5 Chapter 6: Placing energy storage in a grid for load-shifting . . . . . 9
  - 1.4 Basic notations . . . . . 9
  
- 2 Kirchoff’s laws, conic relaxations and their relationships** **10**
  - 2.1 Background . . . . . 11

2.1.1	Contributions of this chapter . . . . .	12
2.2	Bus injection model and conic relaxations . . . . .	13
2.2.1	OPF formulation . . . . .	14
2.2.2	SDP relaxation: $\mathcal{P}_1$ and $\mathcal{R}_1$ . . . . .	15
2.2.3	Chordal relaxation: $\mathcal{P}_{ch}$ and $\mathcal{R}_{ch}$ . . . . .	18
2.2.4	SOCP relaxation: $\mathcal{P}_2$ and $\mathcal{R}_2$ . . . . .	21
2.2.5	Equivalent and exact relaxations . . . . .	22
2.2.6	Proof of Theorem 1 . . . . .	24
2.3	Branch flow model and SOCP relaxation . . . . .	29
2.3.1	OPF formulation . . . . .	29
2.3.2	SOCP relaxation: $\tilde{\mathcal{P}}_2$ , $\tilde{\mathcal{R}}_2^{nc}$ and $\tilde{\mathcal{R}}_2$ . . . . .	31
2.4	Equivalence of bus injection model and branch flow model . . . . .	34
2.5	Numerics . . . . .	40
2.5.1	A 3-bus example . . . . .	40
2.5.2	IEEE benchmark systems . . . . .	42
<b>3</b>	<b>Quadratically constrained quadratic programs on acyclic networks and tight conic relaxations</b> . . . . .	<b>45</b>
3.1	Background on QCQP . . . . .	45
3.2	Formulation and result for a QCQP in complex variables . . . . .	47
3.3	Proof approaches . . . . .	48
3.3.1	Proof using the dual problem . . . . .	49
3.3.2	Proof using the relaxed problem . . . . .	55
3.4	QCQP in real variables . . . . .	58
3.5	Optimal Power Flow: An application . . . . .	60
3.5.1	Relation to prior work . . . . .	60
3.5.2	Problem Formulation . . . . .	61
3.5.3	Conic relaxation over radial networks . . . . .	64

<b>4</b>	<b>Unifying structural market power analysis in electricity markets</b>	<b>69</b>
4.1	Background on market power analysis . . . . .	70
4.1.1	Prior work . . . . .	71
4.1.2	Our contributions . . . . .	72
4.2	Market power measures . . . . .	73
4.2.1	Residual supply based measures . . . . .	73
4.2.2	Network flow based measures . . . . .	74
4.2.3	Minimal generation based measures . . . . .	75
4.3	Functional measure of market power . . . . .	76
4.3.1	Definition . . . . .	77
4.3.2	Relaxations and approximations . . . . .	79
4.3.2.1	The DC approximation approach . . . . .	79
4.3.2.2	Non-linear optimization technique . . . . .	80
4.3.2.3	The SDP relaxation approach . . . . .	81
4.3.3	Properties of $\text{TCNF}_s$ . . . . .	81
4.4	Case Studies . . . . .	85
4.4.1	IEEE 6-bus Test System . . . . .	86
4.4.2	IEEE 39-bus Test System . . . . .	88
4.4.3	Summary of findings . . . . .	89
4.5	Comparison of Computational Approaches . . . . .	91
4.6	Firm behavior . . . . .	93
4.7	Concluding remarks . . . . .	94
<b>5</b>	<b>Role of market maker in Cournot competition in electricity markets</b>	<b>95</b>
5.1	Background on competition models for electricity markets . . . . .	96
5.1.1	Contributions of this chapter . . . . .	97
5.2	Problem Formulation . . . . .	98
5.2.1	Notation . . . . .	98
5.2.2	Network model . . . . .	99

5.2.3	Generator profit . . . . .	101
5.2.4	Market maker objectives . . . . .	101
5.2.5	Competitive model . . . . .	102
5.3	Existence of equilibrium . . . . .	103
5.4	Regulatory objectives and market outcomes . . . . .	107
5.5	Proofs of main results . . . . .	109
5.6	Concluding remarks and future directions . . . . .	115
<b>6</b>	<b>Placing energy storage in a grid for load-shifting</b>	<b>116</b>
6.1	Background . . . . .	117
6.1.1	Motivation . . . . .	117
6.1.2	Prior work in this area . . . . .	117
6.1.3	Our Contribution . . . . .	118
6.2	Problem formulation . . . . .	119
6.2.1	Network models . . . . .	123
6.3	Simulations using conic relaxation . . . . .	124
6.3.1	Case Studies . . . . .	125
6.3.2	Approximation versus relaxation . . . . .	131
6.4	Storage placement with DC power flow . . . . .	133
6.4.1	Main Result . . . . .	133
6.5	Conclusions and future work . . . . .	144
<b>A</b>	<b>Partial results on storage placement for specific network topologies</b>	<b>145</b>
A.1	Single generator single load network . . . . .	146
A.2	Star network . . . . .	149
A.3	Proofs of results for specific network topologies . . . . .	151
A.3.1	Proofs for single generator single load network . . . . .	151
A.3.2	Proofs for star network . . . . .	157
	<b>Bibliography</b>	<b>162</b>

# List of Figures

1.1	Informal timeline of different driving forces of research in power system. . . .	1
1.2	Visual representation of the structure of electricity spot markets. The arrows represent interactions through bids and control signals. . . . .	6
2.1	Simple graphs to illustrate $G$ -partial matrices. . . . .	16
2.2	Index sets $I_{G_1}$ and $I_{G_2}$ illustrated as entries in a matrix. Entry $(j, k)$ is marked with a tick if $(j, k)$ is in the corresponding index set; otherwise it is marked with a cross. . . . .	16
2.3	Feasible sets of conic formulations and their relaxations, and the relations among these sets. . . . .	39
2.4	A 3-bus network from [1]. . . . .	40
2.5	(a) Projections of feasible regions on $p_1 - p_2$ space for the 3-bus system in Figure 2.4. (b) Zoomed-in Pareto fronts of these sets. . . . .	42
2.6	Projections of feasible regions on $p_1 - p_2$ space for the 3-bus system in Figure 2.4.	44
2.7	Projections of feasible regions on $q_1 - q_2$ space for 3-bus system in Figure 2.4.	44
3.1	(a) and (b) are examples of sets of complex numbers that are linearly separable from the origin. (c) is an example of set that is not. . . . .	47
3.2	$C_{ij}$ and non-zero $[C_p]_{ij}, p = 1, \dots, m$ on the complex plane for OPF for a fixed line $(i, j)$ in tree $\mathcal{T}$ . . . . .	67
4.1	A small network to illustrate market power indices. All quantities are measured in per units (p.u.). $z$ denotes impedance and $b$ denotes line capacity. . . . .	74

4.2	TCNF <sub>s</sub> <sup>DC</sup> (·) of generators in the 3-bus network shown in Figure 4.1. Quantities are measured in per units (p.u.). . . . .	83
4.3	TCNF calculation based on different approaches for various generators in the IEEE 6-bus system. . . . .	87
4.4	TCNF <sup>AC</sup> (ρ) for generators 2 and 3 plotted for load power factors from 0.95 to 0.99 lagging in the IEEE 6-bus system. . . . .	87
4.5	The lower envelope of TCNF, i.e., min <sub>s</sub> TCNF <sub>s</sub> for selected generators in the IEEE 39-bus system. . . . .	90
5.1	Example of a 2-node network. This example illustrates how the model in this chapter can be used to study a caricature of the market in California. Here, northern and southern California are represented as two aggregate nodes connected by a transmission line - Path 15 - that is often congested [2]. . . . .	103
5.2	Plots of various quantities at equilibrium with varying line capacities $f_{12}$ in the 2-node network in Figure 5.1. Parameters chosen for this example are: $a_1 = a_2 = 1$ , $b_1 = 1$ , $b_2 = 0.65$ , $c_1 = c_2 = 1$ . . . . .	108
6.1	Real power balance at node $k \in \mathcal{N}$ . . . . .	122
6.2	The IEEE 14-Bus benchmark system topology. Buses 1, 2, 3, 6, and 8 have generation. . . . .	125
6.3	(a) Peak-normalized real power demand profiles for each of the 14 buses based on an average day in July 2010. The data are reported in half-hour intervals over a 24 hour period. (b) A peak-normalized wind generation profile reported at half-hour intervals over a 24 hour period. . . . .	126

6.4	(a) Total system demand and generation as a function of total storage capacity. (b) Storage placement as a function of total storage capacity. (c) A comparison of total system demand, total generation, individual generator production versus storage level when total storage capacity $h = 1.5$ . The actual transmission over the line between generators 1 and 2 ( $p_{12}$ ) as a function of time is also superimposed. As expected the transmission increases as the generation at bus 1 increases. (d) Storage placement as line limits $f_{12}$ are decreased from the transmission levels shown in (c). For all panels the data is reported in half-hour intervals over a 24 hour period. . . . .	127
6.5	(a), (b) Changes in optimal storage placement in a system with a wind generator. Differences arising from changes in total storage capacity $h$ when the wind is, respectively, placed at bus 1 and 2, which, respectively, represent 43% and 18% of the total system generation capacity. Panels (c) and (d) depict changes in storage siting as the wind generation is moved to each of the generation sites, with the total system storage capacity is, respectively, fixed to $h = 1 pu$ and $h = 2 pu$ Panels (e) and (f) show the effect of changing line limits $f_{12}$ and $f_{15}$ when the wind is placed a bus 1 and fixed $h = 1.5$ . . . . .	130
6.6	Ratios of other eigenvalues to the first eigenvalue. . . . .	132
6.7	A sample network. . . . .	134
6.8	Examples of power networks (a) Single generator single load system (b) A radial network. . . . .	141
6.9	A network with a generator that has multiple connections. . . . .	144
A.1	Single generator single load network. Available storage budget is $h \geq b_1 + b_2$ . .	146
A.2	Plots to illustrate Propositions 20 and 21. (a) Typical hourly load profile and optimal generation portfolio for line flow capacity $f_{12} = 0.85$ , generation capacity $\bar{g}_1 = 1$ and storage budget $h = 1$ (b) $p_*(\bar{g}_1 = 1, f_{12} = 0.85, h)$ . (c) $p_*(\bar{g}_1 = 1, f_{12}, h = 1)$ . . . . .	149
A.3	$P^{DC}(h)$ and $\Pi^{\{1\}}(h)$ for the simple 3-node star network in Figure 6.9. . . . .	150

# List of Tables

2.1	Admittances for the 3-bus network. . . . .	40
2.2	Performance comparison of relaxation techniques for IEEE benchmark systems.	43
4.1	Statistics of $\eta$ for IEEE benchmark systems. . . . .	93
6.1	Comparison of costs from gradient descent for $W^*(t)$ to obtained $V(t)$ . . . . .	132

# Chapter 1

## Introduction and outline

Power system in the United States of America has a rich history starting from the engineering pioneers of the likes of Thomas Alva Edison and Nikola Tesla and business executives like George Westinghouse and Samuel Insull. Over the years, roughly three different factors have played major roles in shaping this system: engineering, economics and the environment. As we argue below, these factors have spurred considerable research interests in different eras, as shown in the timeline in Figure 1.1. Since these factors heavily interact among themselves, modern power system design requires an “integrated systems” viewpoint; looking at individual concerns in isolation is not enough to capture the complexity of the system. In what follows, we first argue the role of each of these factors and delineate our work in that context in Section 1.1. Next, we broadly define the modeling approach towards power system taken in this thesis in Section 1.2. The outline of the ensuing chapters is presented in Section 1.3. Finally, Section 1.4 defines a few recurring notations.

### 1.1 Drivers of change in power system

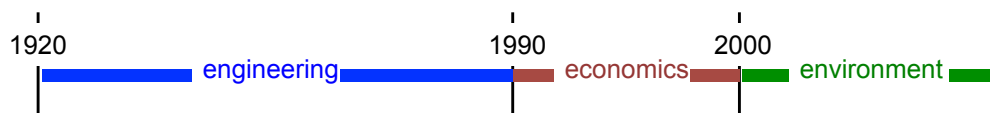


Figure 1.1: Informal timeline of different driving forces of research in power system.

### **1.1.1 The role of engineering**

It is, perhaps, not surprising that engineering problems dominated research in power system till around 1990's. Starting from an alternating current (AC) based generator/ motor model by Tesla, power system evolved into an interconnected network with generators, transmission lines and substations with a plethora of devices designed to convert mechanical energy of turbines to electrical energy and deliver it to geographically distributed customers. For such a massive engineering system, the main focus of research was to optimize generation technologies and costs of production, maximize efficiencies and fault tolerances and control the dynamical system in an optimal yet robust manner. One of the classical problems formulated during this period was the Optimal Power Flow (OPF) problem in 1962 by Carpentier [3]. It attempts to minimize the generation cost subject to all engineering constraints of the system. There has been considerable interest in solving this problem optimally to find "good" operating points in the network. Among others, the nonconvexity of power flow equations defined by Kirchoff's laws have prevented a principled approach to this optimization problem. Recently, however, convex optimization theory has made major breakthroughs in designing polynomial time algorithms for large classes of such problems, specially in conic programming. In this thesis, we revisit this classical problem using the tools and techniques of modern optimization in Chapters 2 and 3.

### **1.1.2 Rise of economics**

As the power system industry moved towards an interconnected grid, the supply side got concentrated under the umbrellas of large regulated utility companies. This business model, with its roots in the ideas of Insull, took advantage of huge economies of scale in the grid. But come 90's, it was realized that such a monopoly would never have incentive to invest in better and more efficient generation technologies. A natural solution to this problem was deregulation; various big utilities were asked to disinvest in generation while they still maintained the transmission and distribution operations of the grid. For example, the three major utility companies in California (Southern California Edison, Pacific Gas & Electric

and San Diego Gas & Electric) divested 40% of their total generation assets [4]. In this era, various prominent economists investigated problems pertaining to the right market design as well as the ensuing dynamics of the electricity market. Deregulation had already proven successful in other industries like railroad, airways and communication technologies, e.g., see [5]. The results, however, in power system was met with an early challenge. The Californian market showed very high price volatility and large utility companies like Pacific Gas and Electric Corporation filed for bankruptcy around 2000. The flaw in the market design became apparent and various market monitoring strategies were laid down to prevent market collapse. In such an environment, there are two natural questions to ask: (a) how do we detect firms with potential market power? (b) given that generators operate strategically, what should be the right market design to mitigate market power? Informally, traditional approaches to answer such questions have emanated from microeconomic theory. The nature of electricity as a commodity, however, makes it difficult to generalize these approaches to electricity markets. Consequently, the literature has remained fractured. In Chapters 4 and 5, we study these aspects in detail to characterize the effect of the network and market clearing mechanisms in electricity markets. This analysis makes use of game-theoretic techniques and optimization and their interaction with Kirchoff's laws.

### **1.1.3 Environment poses a threat**

Electricity generation in the United States primarily depended on fossil fuels, mainly on natural gas and coal. Discovery of large deposits of shale in mainland US has been driving the industry towards a steady uptake of natural gas in place of coal in the recent years. Though generation technologies based on fossil fuels are reliable and economical, a major concern has led us to look elsewhere for our energy needs: fossil fuels leave high carbon footprint. Large quantities of greenhouse gases like carbon dioxide released in the atmosphere due to the production process leads to adverse climate changes, most notably contributes to the increase of earth's average temperature. For example, it has been estimated that global sea surface temperature has increased by  $0.8^\circ$  Celsius in the last century with the last three decades

accounting for more than two-thirds of it [6]. With rapid industrial growth from highly populated areas like India and China, this number is only expected to rise. It is not hard to argue that a shift towards cleaner technologies is a rational choice. Under the leadership of President B. Obama, a new plan called “New Energy for America” [7] was introduced during the presidential campaign in 2008. The goal was to meet 10% of American electricity demand through renewables by 2012; then, increase it to 25% by 2025. The current production is estimated to be at 14.2% during the first half of 2013<sup>1</sup>. It is clear that renewable energy integration is being taken seriously at the policy level. This shift in policy at the federal level has spurred a new era of research in power system to create a so-called smart grid. One major direction is to cope with the intermittency of renewable sources like wind and solar. Meeting an inelastic demand with stochastic supply is not an easy task both for engineering as well as economics, specially when the hallmark of this system is maintaining very high reliability. Electric energy storage, if available, can absorb some of the stochasticity. Though research in storage had begun much earlier, the recent boost in clean energy investment has fueled recent research efforts. The use of electric storage goes beyond mitigating stochasticity. An example of such a use is load-shifting or peak shaving, i.e., to flatten out generation profile to reduce total generation cost. In Chapter 6, we study the problem of optimal placement and sizing of such storage resources with respect to load-shifting in the power grid using tools from convex optimization theory.

## 1.2 The approach to modeling

With the motivation defined above, here we describe the general approach to modeling the power system in this thesis. The following is based on power system dynamics and markets; we refer the reader to [8, 9] for details. This section is meant to serve as a preamble and justification to the problem formulations in the subsequent chapters.

In real-time operation, power system is a coupled dynamical system. The minor imbalances between supply and demand in power manifests as changes in frequencies of generators.

---

<sup>1</sup>For more detailed statistics, please visit <http://www.eia.gov>

The control loop that maintains this delicate balance is sometimes referred to as automatic generation control. This control system has transients that typically settle down within one to two minutes. Thus at five to ten minute time-scale, power system operation can be assumed to be quasi-static. In this mode of operation, the frequency in the entire system is assumed to be at the nominal level (60Hz in USA); this is called the synchronous mode. Also, most power networks (at least in USA) are built as three phase systems. The three phases usually correspond to three different sets of coils in a rotating synchronous machine where the change of flux due to a rotating magnetic field produces voltages in these three sets of coils. When these phases are balanced, the currents and voltages in these three coils are sinusoidal which differ only in phases by  $2\pi/3$  with each other. In this balanced mode of operation, we can simplify the representation of the circuit to a single phase equivalent. Recall that we already assumed the frequencies to be constant throughout the network. With sinusoidal voltage and current generation, the circuit can then be represented in the Fourier frequency domain. In this representation, the voltages at each bus (for the single phase equivalent circuit) is a phasor, which is essentially a complex number representing the sinusoidal signal in the time domain. The transmission lines can then be represented as complex impedances using electromagnetic theory and linear circuit theory. Then we get Kirchoff's laws in the complex domain as a linear relation between the current injections into the circuit and the voltages. In summary, this balanced synchronous mode of operation of power system is succinctly representable using Kirchoff's laws over a single phase equivalent circuit with complex impedances. It should be emphasized that this quasi-static model faithfully represents the large scale power system operation at 5-15 minute interval snapshots. Roughly, the quasi-static model captures the overall operation when transients in the circuit have faded out.

The quasi-static state of a power system defines the set points for the underlying control systems to reach. These set points are calculated through a sequence of market clearing operations. Generators and load-serving entities (LSEs) serve as the supply and demand side of this electricity market with the ISO as the market maker as shown in Figure 1.2. There are different time scales at which the demand and supply for each hour of each day is

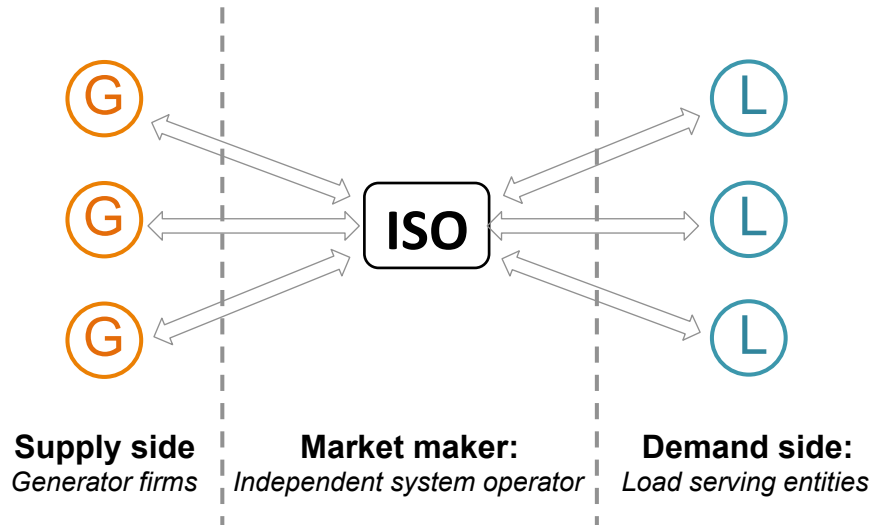


Figure 1.2: Visual representation of the structure of electricity spot markets. The arrows represent interactions through bids and control signals.

cleared. Roughly, the current mode of operations in this wholesale electricity market can be summarized into two steps: (a) Long term or forward contracts that happen through bilateral trades between LSEs and generator firms, (b) Short term or spot market that balances the demand and supply through a market clearing mechanism by the ISO over submitted bids. Spot markets in various regions of USA have different designs. A common design (used in California ISO and Pennsylvania-Jersey-Maryland ISO) consists of a day-ahead market which clears (as the name suggests) a day before the time of realization. Then a real-time market clears the residual imbalance 5-15 minutes before the actual time of consumption. The prices of electricity at each bus is computed from the market clearing mechanism by the ISO, which is usually by solving OPF with the submitted bids. The Lagrange multipliers for real power balance at each bus is used as the price for electricity at that bus. This scheme is popularly known as locational marginal pricing that is based on the seminal work of Schweppe et al. in [10] on spot pricing. The market operations usually use a linearized power flow model to clear the market. The actual dispatch, however, models the circuits with its nonlinearities to obtain a feasible operating point for the quasi-static regime. Then the control system of the network takes over to reach that operating point maintaining a balance between the realized demand and supply. This defines the control hierarchy of the

modern deregulated power system.

## 1.3 Organization of the thesis

### 1.3.1 Chapter 2: Kirchoff's laws, conic relaxations and their relationships

In Chapter 2, we formulate a general optimization over a power network using two different models to write Kirchoff's laws, namely, the *bus injection model* and the *branch flow model*. As would be evident, such an optimization problem is nonconvex due to the nature of Kirchoff's laws. Recently, conic relaxations for nonconvex problems have been proposed in the literature. In Chapter 2, we establish the relationships among these convex relaxations in terms of their feasible sets. In addition, we also provide simulation results for these relaxations on various systems. The results in this chapter have been reported in [11].

### 1.3.2 Chapter 3: Quadratically constrained quadratic programs on acyclic networks and tight conic relaxations

Our next analysis restricts attention to radial networks that are often found in distribution networks. In Chapter 3, we investigate conditions under which the conic relaxations discussed in Chapter 2 are tight, i.e., the optimization over the power network can be solved from the optimal solution of its conic relaxation. To that end, we concentrate on solving optimal power flow type problems that can be cast as quadratically constrained quadratic programs (QCQPs). Power being quadratic in voltage, indeed many OPF type problems can be cast as QCQPs in complex variables. To study these kind of problems, we first identify a class of nonconvex QCQPs that can be efficiently solved through its conic relaxation. This extends known classes of nonconvex QCQPs that admit polynomial time solutions. Then we apply this result to the OPF type problems to obtain sufficient conditions under which their relaxations are tight. The results in this chapter have been reported in [12].

### **1.3.3 Chapter 4: Unifying structural market power analysis in electricity markets**

Next, we turn our attention towards electricity markets. Post deregulation, the OPF problem is solved using submitted bids from the generator firms. As expected, this bidding process is subject to gaming. In Chapter 4, we study the problem of identifying generator firms with potential market power. In a transmission-constrained power network, this structural analysis is supposed to identify must-run generators to successfully meet load requirements. The intuition is simple: if a generator is pivotal in meeting demand, then it can exploit this fact to extract more profits and hence abuse market power. In our studies, we unify different market power measures in the literature and illustrate the complex interaction of economics with the network model through simulations on IEEE benchmark systems. This reiterates the fact that economics or engineering alone cannot faithfully analyze the operations of the modern power system. The results of this chapter have been reported in [13].

### **1.3.4 Chapter 5: Role of market maker in Cournot competition in electricity markets**

One key difference between a general commodity market and electricity market is the presence of a market maker or the independent system operator (ISO). In most networks in USA, the ISO is a regulatory body that facilitates the exchange of power between supply and demand sides. The market clearing mechanism in the spot market, however, is a matter of policy and intuitively should be designed to maximize the benefits of the entire network. In Chapter 5, we study the role of this market mechanism on the equilibrium outcome of the market. With a linearized network model, the game is modeled as a Cournot competition. We consider three different market clearing mechanisms and study the existence of generalized Nash equilibrium of this one-shot Cournot game under such mechanisms. The results of this chapter have been reported in [14].

### 1.3.5 Chapter 6: Placing energy storage in a grid for load-shifting

The problems dealt till Chapter 4 only consider static problems (either optimization or games). We introduce correlation across time through electricity storage in Chapter 5. In particular, we investigate the investment decision problem of placing and sizing bulk storage resources in a power network to flatten out generation profile over time and hence minimize convex cost of conventional generation in the grid under a fixed available storage budget. In the first half of this chapter, we provide simulation results using a conic relaxation framework. Then in the next half, we simplify the model with linearized power flow and analytically characterize some properties of the optimal placement. The results of this chapter have been reported in [15, 16].

## 1.4 Basic notations

Let  $\mathbb{R}$  and  $\mathbb{C}$  denote the sets of real and complex numbers respectively. For a complex number  $z$ , let  $\text{Re } z$  and  $\text{Im } z$  denote the real and imaginary parts of  $z$ . For two vectors  $x, y \in \mathbb{R}^n$ ,  $x \leq y$  denotes inequality componentwise; if  $x, y \in \mathbb{C}^n$ ,  $x \leq y$  means  $\text{Re } x \leq \text{Re } y$  and  $\text{Im } x \leq \text{Im } y$ . For a matrix  $A$ , let  $A_{ij}$  denote the entry in the  $i$ -th row and the  $j$ -th column of  $A$ . For any matrix or vector  $A$ , let  $A^H$  be its hermitian transpose and  $A^\top$  denote its transpose. Let  $\mathbf{i} := \sqrt{-1}$  and for any set  $B$ , let  $|B|$  denote its cardinality.

## Chapter 2

# Kirchoff's laws, conic relaxations and their relationships

In a power network, Kirchoff's laws define a linear relation between the current injections and the voltages at different nodes. Power, being a product of voltage and current, turns out to be quadratic in terms of the voltages. Any optimization problem in terms of power flows in the network introduces quadratic constraints to include Kirchoff's laws. Such a well-studied optimization problem is the optimal power flow (OPF) problem that attempts to minimize total generation cost subject to network constraints. It is well-known that the quadratic constraints arising due to Kirchoff's laws define a nonconvex feasible set and hence solving such a problem is generally NP-hard. Several convex relaxations of the OPF problem have been recently explored. These relaxations arise out of two different ways to write Kirchoff's laws, one using the bus injection model and the other using the branch flow model. In this chapter, we establish relations among these relaxations in terms of feasible sets of these relaxations. Our results imply that, for radial networks, all these relaxations are equivalent and one should always solve a second-order cone relaxation. For mesh networks, we show that a semidefinite relaxation is tighter than the second-order cone based relaxation but requires a heavier computational effort. We further explore another relaxation based on the chordal extension of the network graph and show that this approach strikes a good balance in the tradeoff between speed and accuracy. The main theme of this chapter is to exploit the sparsity pattern of the network graph to study conic relaxations. Simulations are used

to illustrate these results.

## 2.1 Background

The OPF problem is quite central to any optimization framework on a power network; it underlies many applications such as unit commitment, economic dispatch, state estimation, volt/VAR control, and demand response. There has been a great deal of research since Carpentier's first formulation in 1962 [3] and an early solution by Dommel and Tinney [17]; recent surveys can be found in, e.g., [18–29]. OPF is generally nonconvex and NP-hard. A large number of optimization algorithms and relaxations have been proposed, the most popular of which is linearization (called DC OPF) [30–33]; See also [34] for a more accurate linear approximation. An important observation was made in [35] that OPF can be formulated as a quadratically constrained quadratic program and therefore can be approximated by a semidefinite program (SDP). Instead of solving OPF directly, the authors in [36] propose to solve its convex Lagrangian dual problem. Sufficient conditions have been studied by many authors under which an optimal solution for the non-convex problem can be derived from an optimal solution of its SDP relaxation; e.g., [15, 37, 38] for radial networks and in [36, 39, 40] for resistive networks. These papers all use the standard bus injection model where the Kirchhoff's laws are expressed in terms of the complex nodal voltages in rectangular coordinates.

Branch flow models on the other hand formulate OPF in terms of branch power and current flows in addition to nodal voltages, e.g., [41–48]. They have been mainly used for modeling radial distribution networks. A branch flow model has been proposed in [49] to study OPF for both radial and mesh networks and a relaxation based on second-order cone program (SOCP) is developed. Sufficient conditions are obtained in [46, 50, 51] under which the SOCP relaxation is exact for radial networks.

### 2.1.1 Contributions of this chapter

Since the OPF problem in the bus injection model is a quadratically constrained quadratic program it is equivalent to a rank-constrained SDP [35,36]. This formulation naturally leads to an SDP relaxation that removes the rank constraint and solves for a full positive semidefinite matrix. If the rank condition is satisfied at an optimal point, the relaxation is said to be *exact* and an optimal solution of OPF can be recovered through the spectral decomposition of the positive semidefinite matrix. Even though SDP is polynomial time solvable it is nonetheless impractical to compute for large power networks. Practical networks, however, are sparse. In this chapter, we develop two equivalent formulations of OPF using *partial matrices* that involve much fewer variables than the full SDP.

The key idea is to characterize classes of partial matrices that are easy to compute and, when the relaxations are exact, are completable to full positive semidefinite matrices of rank 1 from which a solution of OPF can be recovered through spectral decomposition. One of these equivalent problems leads to an SDP relaxation based on chordal extension of the network graph [52,53] and the other leads to an SOCP relaxation [54,55]. In this chapter, we prove equivalence relations among these problems and their relaxations. Our results imply that, for radial networks, all three relaxations are equivalent and we should always solve the SOCP relaxation. For mesh networks there is a tradeoff between computational effort and accuracy (in terms of exactness of relaxation) in deciding between solving SOCP relaxation or the other two relaxations. Between the chordal relaxation and the full SDP, if all the maximal cliques of a chordal extension of the network graph have been pre-computed offline then solving the chordal relaxation is always better because it has the same accuracy as the full SDP but typically involves far fewer variables and is faster to compute. This is explained in Section 2.2. Chordal relaxation has been suggested in [48,56] for solving OPF, and SOCP relaxation in the bus injection model has also been studied in [12,38,40,57]. Here we provide a framework that unifies and contrasts these approaches.

In Section 2.3 we present the branch flow model of [49] for OPF and the corresponding SOCP relaxation developed in [46,49]. In Section 2.4 we prove the equivalence of the branch

flow model and the bus injection model by exhibiting a bijection between these two models and their relaxations. Indeed the relations among the various problems in this chapter, both in the bus injection model and the branch flow model, are established through relations among their feasible sets.

It is important that we utilize both the bus injection and the branch flow models. Even though they are equivalent, some relaxations are much easier to formulate and some sufficient conditions for exact relaxation are much easier to prove in one model than the other. For instance the semidefinite relaxation of power flows has a much cleaner formulation in the bus injection model. The branch flow model especially for radial networks has a convenient recursive structure that not only allows a more efficient computation of power flows e.g. [58–60], but also plays a crucial role in proving the sufficient conditions for exact relaxation in [61, 62]. Since the variables in the branch flow model correspond directly to physical quantities such as branch power flows and injections it is sometimes more convenient in applications.

In Section 2.5, we illustrate the relations among the various relaxations and OPF through simulations. First, we visualize the feasible sets of a 3-bus example in [1]. Then we compare the running times and accuracies of these relaxations on IEEE benchmark systems provided in Matpower; see [63] for details.

## 2.2 Bus injection model and conic relaxations

In this section we formulate OPF in the bus injection model and describe three equivalent problems. These problems lead naturally to semidefinite relaxation, chordal relaxation, and second-order cone relaxation of OPF. We prove equivalence relations among these problems and their exact relaxations.

### 2.2.1 OPF formulation

Consider a power network modeled by a connected undirected graph  $G(N, E)$  where each node in  $N := \{1, 2, \dots, n\}$  represents a bus and each edge in  $E$  represents a line. For each edge  $(i, j) \in E$  let  $y_{ij}$  be its admittance [8]. A bus  $j \in N$  can have a generator, a load, both or neither. Typically the loads are specified and the generations are variables to be determined. Let  $s_j$  be the net complex power injection (generation minus load) at bus  $j \in N$ . Also, let  $V_j$  be the complex voltage at bus  $j \in N$  and  $|V_j|$  denote its magnitude. Bus 1 is the slack bus with a fixed magnitude  $|V_1|$  (normalized to 1). The *bus injection model* is defined by the following power flow equations that describe Kirchhoff's law<sup>1</sup>:

$$s_j = \sum_{k:(j,k) \in E} V_j(V_j^H - V_k^H)y_{jk}^H \quad \text{for } j \in N. \quad (2.1)$$

The power injections at all buses satisfy

$$\underline{s}_j \leq s_j \leq \bar{s}_j \quad \text{for } j \in N, \quad (2.2)$$

where  $\underline{s}_j$  and  $\bar{s}_j$  are known limits on the net injection at bus  $k$ . It is often assumed that the slack bus (node 1) has a generator and there is no limit of  $s_1$ ; in this case  $-\underline{s}_1 = \bar{s}_1 = \infty$ . We can eliminate the variables  $s_k$  from the OPF formulation by combining (2.1)–(2.2) into

$$\underline{s}_j \leq \sum_{k:(j,k) \in E} V_j(V_j^H - V_k^H)y_{jk}^H \leq \bar{s}_j \quad \text{for } j \in N. \quad (2.3)$$

Then OPF in the bus injection model can be formulated in terms of just the  $n \times 1$  voltage vector  $V$ . All voltage magnitudes are constrained:

$$\underline{V}_j \leq |V_j| \leq \bar{V}_j \quad \text{for } j \in N, \quad (2.4)$$

---

<sup>1</sup>The current flowing from bus  $j$  to bus  $k$  is  $(V_j - V_k)y_{jk}$ .

where  $\underline{V}_j$  and  $\overline{V}_j$  are known lower and upper voltage limits. Typically  $|V_1| = 1 = \underline{V}_1 = \overline{V}_1$ . These constraints define the feasible set of the optimal power flow problem in the bus injection model:

$$\mathbb{V} := \{V \in \mathbb{C}^n \mid V \text{ satisfies (2.3) -- (2.4)}\}. \quad (2.5)$$

Let the cost function be  $c(V)$ . Typical costs include the total cost of generating real power at all buses or line loss over the network. All these costs can be expressed as functions of  $V$ . Thus, we obtain the following optimization problem.

**Optimal power flow problem OPF:**

$$\begin{aligned} & \underset{V}{\text{minimize}} && c(V) \\ & \text{subject to} && V \in \mathbb{V}. \end{aligned}$$

Since (2.3) is quadratic,  $\mathbb{V}$  is generally a nonconvex set. Thus OPF is nonconvex and NP-hard to solve.

**Remark 1.** *The OPF formulation usually includes additional constraints such as thermal or stability limits on power or current flows on the lines, or security constraints; see surveys in [18–22, 24–28]. Our results generalize to OPF with some of these constraints, e.g., line limits [12, 49]. Our model can also include a shunt element at each bus. We omit these refinements for ease of presentation.*

### 2.2.2 SDP relaxation: $\mathcal{P}_1$ and $\mathcal{R}_1$

Note that (2.3) is linear in the variables  $W_{jj} := |V_j|^2$  for  $j \in N$  and  $W_{jk} := V_j V_k^H$  for  $(j, k) \in E$ . This motivates the definition of a  $G$ -partial matrix. Define the index set  $I_G$ :

$$I_G := \left\{ (j, j) \mid j \in N \right\} \cup \left\{ (j, k) \mid (j, k) \in E \right\}.$$

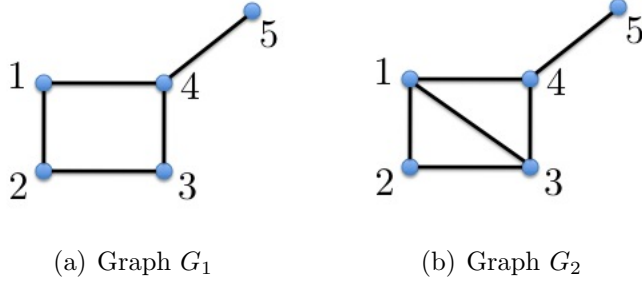


Figure 2.1: Simple graphs to illustrate  $G$ -partial matrices.

✓	✓	×	✓	×
✓	✓	✓	×	×
×	✓	✓	✓	×
✓	×	✓	✓	✓
×	×	×	✓	✓

✓	✓	✓	✓	×
✓	✓	✓	×	×
✓	✓	✓	✓	×
✓	×	✓	✓	✓
×	×	×	✓	✓

(a)  $G_1$ -partial matrix
(b)  $G_2$ -partial matrix

Figure 2.2: Index sets  $I_{G_1}$  and  $I_{G_2}$  illustrated as entries in a matrix. Entry  $(j, k)$  is marked with a tick if  $(j, k)$  is in the corresponding index set; otherwise it is marked with a cross.

A  $G$ -partial matrix  $W_G$  is a collection of complex numbers indexed by the set  $I_G$ , i.e.,  $[W_G]_{jk}$  is defined iff  $j = k \in N$  or  $(j, k) \in E$ . This is illustrated in Figure 2.1. For graph  $G_1$ , we have  $n = 5$  nodes and  $I_{G_1} = \{(1, 1), (2, 2), (3, 3), (4, 4), (5, 5), (1, 2), (2, 1), (2, 3), (3, 2), (3, 4), (4, 3), (1, 4), (4, 1), (4, 5), (5, 4)\}$  as shown in Figure 2.2(a) as a partially filled matrix. For graph  $G_2$  in Figure 2.1(b),  $I_{G_2}$  is represented in Figure 2.2(b). If  $G$  is a *complete graph*, i.e., every pair of nodes share an edge, then  $W_G$  is an  $n \times n$  matrix.

The relations in (2.3)–(2.4) can be rewritten in terms of  $W_G$  as:

$$\underline{s}_j \leq \sum_{k:(j,k) \in E} ([W_G]_{jj} - [W_G]_{jk}) y_{jk}^H \leq \bar{s}_j \quad \text{for } j \in N, \quad (2.7a)$$

$$\underline{V}_j^2 \leq [W_G]_{jj} \leq \bar{V}_j^2 \quad \text{for } j \in N. \quad (2.7b)$$

We assume the cost function  $c(V)$  in OPF depends on  $V$  only through the  $G$ -partial matrix  $W_G$ . For instance, if the objective is to minimize the total real power loss in the

network then

$$c(V) = \sum_{j \in N} \operatorname{Re} s_j = \sum_{j \in N} \sum_{k: (j,k) \in E} \operatorname{Re} ([W_G]_{jj} - [W_G]_{jk}) y_{jk}^H.$$

If the objective is to minimize a weighted sum of real power generation at various nodes then

$$\begin{aligned} c(V) &= \sum_{j \in N} c_j (\operatorname{Re} s_j - p_j^d) \\ &= \sum_{j \in N} c_j \left( \sum_{k: (j,k) \in E} \operatorname{Re} ([W_G]_{jj} - [W_G]_{jk}) y_{jk}^H - p_j^D \right), \end{aligned}$$

where  $p_j^d$  is the given real power demand at bus  $j \in N$ . Henceforth we refer to the cost function as  $c(W_G)$ .

Consider an  $n \times 1$  voltage vector  $V$ . Then  $W = VV^H$  is an  $n \times n$  psd matrix of rank 1. Define the  $G$ -partial matrix  $W(G)$  as the collection of  $I_G$  entries of  $W$ . To describe the constraints  $V \in \mathbb{V}$ , we use the equivalent constraints in terms of  $W(G)$  in (2.7a)-(2.7b). Formally, OPF is equivalent to the following problem with  $n \times n$  Hermitian matrix  $W$ :

**Problem  $\mathcal{P}_1$ :**

$$\begin{aligned} &\underset{W}{\text{minimize}} && c(W(G)) \\ &\text{subject to} && W(G) \text{ satisfies (2.7a) - (2.7b),} \\ &&& W \succeq 0, \text{ rank } W = 1. \end{aligned}$$

Given an  $V \in \mathbb{V}$ ,  $W = VV^H$  is feasible for  $\mathcal{P}_1$ ; conversely given a feasible  $W$  it has a unique spectral decomposition [64]  $W = VV^H$  such that  $V \in \mathbb{V}$ . Hence there is a one-one correspondence between the feasible sets of OPF and  $\mathcal{P}_1$ , i.e., OPF is equivalent to  $\mathcal{P}_1$ . Problem  $\mathcal{P}_1$  is a rank-constrained SDP and NP-hard to solve. The nonconvex rank constraint is relaxed to obtain the following SDP.

**Problem  $\mathcal{R}_1$ :**

$$\begin{aligned} & \underset{W}{\text{minimize}} && c(W(G)) \\ & \text{subject to} && W(G) \text{ satisfies (2.7a) – (2.7b), } W \succeq 0. \end{aligned}$$

$\mathcal{R}_1$  is an SDP [55, 65] and can be solved in polynomial time using interior-point algorithms [66, 67]. Let  $W^*$  be an optimal solution of  $\mathcal{R}_1$ . If  $W^*$  is rank-1 then  $W^*$  also solves  $\mathcal{P}_1$  optimally. We say the relaxation  $\mathcal{R}_1$  is *exact with respect to  $\mathcal{P}_1$*  if there exists an optimal solution of  $\mathcal{R}_1$  that satisfies the rank constraint in  $\mathcal{P}_1$  and hence optimal for  $\mathcal{P}_1$ .

**Remark 2.** *In this chapter we define a relaxation to be exact as long as one of its optimal solutions satisfies the constraints of the original problem, even though a relaxation may have multiple optimal solutions with possibly different ranks. The exactness of  $\mathcal{R}_1$  in general does not guarantee that we can compute efficiently a rank-1 optimal  $W_*$  if non-rank-1 optimal solutions also exist. Many sufficient conditions for exact relaxation in the recent literature, however, do guarantee that every optimal solution of the relaxation is optimal for the original problem, e.g., [37, 40, 68, 69] or they lead to a polynomial time algorithm to construct an optimal solution of  $\mathcal{P}_1$  from any optimal solution of the relaxation, e.g., [12, 70].*

**2.2.3 Chordal relaxation:  $\mathcal{P}_{ch}$  and  $\mathcal{R}_{ch}$** 

To define the next relaxation we need to extend the definitions of Hermitian, psd, and rank-1 for matrices to partial matrices:

1. The complex conjugate transpose of a  $G$ -partial matrix  $W_G$  is the  $G$ -partial matrix  $(W_G)^H$  that satisfies

$$[(W_G)^H]_{jk} = [W_G]_{kj}^H \text{ for all } (j, k) \in I_G.$$

We say  $W_G$  is *Hermitian* if  $W_G = (W_G)^H$ .

2. A matrix  $M$  is psd if and only if all its principal submatrices (including  $M$  itself)

are psd. We extend the definition of psd to  $G$ -partial matrices using this property. Informally a  $G$ -partial matrix is said to be psd if, when viewed as a partially filled  $n \times n$  matrix, all its *fully-specified* principal submatrices are psd. This notion can be formalized as follows. A clique is a complete subgraph of a given graph. A clique on  $k$  nodes is referred to as a  $k$ -clique. For the graph  $G_1$  in Figure 2.1(a), the cliques are the edges. For the graph  $G_2$  in Figure 2.1(b), the cliques consist of the edges and the triangles  $\{1, 2, 3\}$  and  $\{1, 3, 4\}$ . A  $k$ -clique  $C$  in graph  $G$  on nodes  $\{n_1, n_2, \dots, n_k\}$  fully specifies the  $k \times k$  submatrix  $W_G(C)$ <sup>2</sup>:

$$W_G(C) = \begin{pmatrix} [W_G]_{n_1 n_1} & [W_G]_{n_1 n_2} & \cdots & [W_G]_{n_1 n_k} \\ [W_G]_{n_2 n_1} & [W_G]_{n_2 n_2} & \cdots & [W_G]_{n_2 n_k} \\ \vdots & \vdots & \ddots & \vdots \\ [W_G]_{n_k n_1} & [W_G]_{n_k n_2} & \cdots & [W_G]_{n_k n_k} \end{pmatrix}.$$

We say a  $G$ -partial matrix  $W_G$  is *positive semidefinite (psd)*, written as  $W_G \succeq 0$ , if and only if  $W_G(C) \succeq 0$  for all cliques  $C$  in graph  $G$ .

3. A matrix  $M$  has rank one if  $M$  has exactly one linearly independent row (or column). We say a  $G$ -partial matrix  $W_G$  has rank one, written as  $\text{rank } W_G = 1$ , if and only if  $\text{rank } W_G(C) = 1$  for all cliques  $C$  in  $G$ .

If  $G$  is a complete graph then  $W_G$  specifies an  $n \times n$  matrix and the definitions of psd and rank-1 for the  $G$ -partial matrix  $W_G$  coincide with the regular definitions.

A cycle on  $k$  nodes in graph  $G$  is a  $k$ -tuple  $(n_1, n_2, \dots, n_k)$  such that  $(n_1, n_2), (n_2, n_3), \dots, (n_k, n_1)$  are edges in  $G$ . A cycle  $(n_1, n_2, \dots, n_k)$  in  $G$  is minimal if no strict subset of  $\{n_1, n_2, \dots, n_k\}$  defines a cycle in  $G$ . In graph  $G_1$  in Figure 2.1(a) the 4-tuple  $(1, 2, 3, 4)$  defines a minimal cycle. In graph  $G_2$  in Figure 2.1(b) however the same 4-tuple is a cycle but not minimal. The minimal cycles in  $G_2$  are  $(1, 2, 3)$  and  $(1, 3, 4)$ . A graph is said to be *chordal* if all its minimal cycles have at most 3 nodes. In Figure 2.1,  $G_2$  is a chordal graph

---

<sup>2</sup>For any graph  $F$ , a partial matrix  $W_F$ , and a subgraph  $H$  of  $F$ , the partial matrix  $W_F(H)$  is a submatrix of  $W_F$  corresponding to the  $I_H$  entries of  $W_F$ . If subgraph  $H$  is a  $k$  clique, then  $W_F(H)$  is a  $k \times k$  matrix.

while  $G_1$  is not. A *chordal extension* of a graph  $G$  on  $n$  nodes is a chordal graph  $G_{ch}$  on the same  $n$  nodes that contains  $G$  as a subgraph. Note that all graphs have a chordal extension; the complete graph on the same set of vertices is a trivial chordal extension of a graph. In Figure 2.1,  $G_2$  is a chordal extension of  $G_1$ .

Let  $G_{ch}$  be any chordal extension of  $G$ . Define the following optimization problem over a Hermitian  $G_{ch}$ -partial matrix  $W_{ch} := W_{G_{ch}}$ , where the constraints (2.7a)-(2.7b) are imposed only on the index set  $I_G \subseteq I_{G_{ch}}$ , i.e., in terms of the  $G$ -partial submatrix  $W_{ch}(G)$  of the  $G_{ch}$ -partial matrix  $W_{ch}$ .

**Problem  $\mathcal{P}_{ch}$ :**

$$\begin{aligned} & \underset{W_{ch}}{\text{minimize}} && c(W_{ch}(G)) \\ & \text{subject to} && W_{ch}(G) \text{ satisfies (2.7a) -- (2.7b),} \\ & && W_{ch} \succeq 0, \text{ rank } W_{ch} = 1. \end{aligned}$$

Let  $\mathcal{R}_{ch}$  be the rank-relaxation of  $\mathcal{P}_{ch}$ .

**Problem  $\mathcal{R}_{ch}$ :**

$$\begin{aligned} & \underset{W_{ch}}{\text{minimize}} && c(W_{ch}(G)) \\ & \text{subject to} && W_{ch}(G) \text{ satisfies (2.7a) -- (2.7b), } W_{ch} \succeq 0. \end{aligned}$$

Let  $W_{ch}^*$  be an optimal solution of  $\mathcal{R}_{ch}$ . If  $W_{ch}^*$  is rank-1 then  $W_{ch}^*$  also solves  $\mathcal{P}_{ch}$  optimally. Again, we say  $\mathcal{R}_{ch}$  is *exact with respect to*  $\mathcal{P}_{ch}$  if there exists an optimal solution  $W_{ch}^*$  of  $\mathcal{R}_{ch}$  that has rank 1 and hence optimal for  $\mathcal{P}_{ch}$ ; see Remark 2 for more details.

To illustrate, consider graph  $G_1$  in Figure 2.1(a) and its chordal extension  $G_2$  in Figure 2.1(b). The cliques in  $G_2$  are  $\{1, 2\}$ ,  $\{2, 3\}$ ,  $\{3, 4\}$ ,  $\{4, 1\}$ ,  $\{1, 3\}$ ,  $\{1, 2, 3\}$ ,  $\{1, 3, 4\}$  and  $\{4, 5\}$ . Thus the constraint  $W_{ch} \succeq 0$  in  $\mathcal{R}_{ch}$  imposes positive semidefiniteness on  $W_{ch}(C)$  for each clique  $C$  in the above list. Indeed imposing  $W_{ch}(C) \succeq 0$  for maximal cliques  $C$  of  $G$  is sufficient, where a *maximal clique* of a graph is a clique that is not a subgraph of another clique in the same graph. This is because  $W_{ch}(C) \succeq 0$  for a maximal clique  $C$

implies  $W_{ch}(C') \succeq 0$  for any clique  $C'$  that is a subgraph of  $C$ . The maximal cliques in graph  $G_2$  are  $\{1, 2, 3\}$ ,  $\{1, 3, 4\}$  and  $\{4, 5\}$  and thus  $W_{ch} \succeq 0$  is equivalent to  $W_{ch}(C) \succeq 0$  for all maximal cliques  $C$  listed above. Even though listing all maximal cliques of a general graph is NP-complete it can be done efficiently for a chordal graph. This is because a graph is chordal if and only if it has a perfect elimination ordering [71] and computing this ordering takes linear time in the number of nodes and edges [72]. Given a perfect elimination ordering all maximal cliques  $C$  can be enumerated and  $W_{ch}(C)$  constructed efficiently [52]. Moreover the computation depends only on network topology, not on operational data, and therefore can be done offline. For more details on chordal extension see [52]. A special case of chordal relaxation is studied in [70] where the underlying chordal extension extends every basis cycle of the network graph into a clique.

#### 2.2.4 SOCP relaxation: $\mathcal{P}_2$ and $\mathcal{R}_2$

We say a  $G$ -partial matrix  $W_G$  satisfies the *cycle condition* if, over *every* cycle  $(n_1, \dots, n_k)$  in  $G$ , we have

$$\angle[W_G]_{n_1 n_2} + \angle[W_G]_{n_2 n_3} + \dots + \angle[W_G]_{n_k n_1} = 0 \pmod{2\pi}. \quad (2.8)$$

**Remark 3.** Consider any spanning tree of  $G$ . A “basis cycle” in  $G$  is a cycle that has all but one of its edges common with the spanning tree. If (2.8) holds over all basis cycles in  $G$  with respect to a spanning tree then (2.8) holds over all cycles of  $G$  [73].

For any edge  $e = (i, j)$  in  $G$ ,  $W_G(e)$  is the  $2 \times 2$  principal submatrix of  $W_G$  defined by the 2-clique  $e$ . Define the following optimization problem over Hermitian  $G$ -partial matrices  $W_G$ .

**Problem  $\mathcal{P}_2$ :**

$$\begin{aligned} & \underset{W_G}{\text{minimize}} && c(W_G) \\ & \text{subject to} && W_G \text{ satisfies (2.7a) – (2.7b) and (2.8),} \\ & && W_G(e) \succeq 0, \text{ rank } W_G(e) = 1 \text{ for all } e \in E. \end{aligned}$$

Both the cycle condition (2.8) and the rank-1 condition are nonconvex constraints. Relaxing them, we get the following second-order cone program.

**Problem  $\mathcal{R}_2$ :**

$$\begin{aligned} & \underset{W_G}{\text{minimize}} && c(W_G) \\ & \text{subject to} && W_G \text{ satisfies (2.7a) – (2.7b),} \\ & && W_G(e) \succeq 0 \text{ for all } e \in E. \end{aligned}$$

For  $e = (i, j)$  and Hermitian  $W_G$  we have

$$W_G(e) \succeq 0 \quad \Leftrightarrow \quad [W_G]_{ii}[W_G]_{jj} \geq |[W_G]_{ij}|^2. \quad (2.9)$$

The right-hand side of (2.9) is a second-order cone constraint [55] and hence  $\mathcal{R}_2$  can be solved as an SOCP. If an optimal solution  $W_G^*$  of  $\mathcal{R}_2$  is rank-1 and also satisfies the cycle condition then  $W_G^*$  solves  $\mathcal{P}_2$  optimally and we say that relaxation  $\mathcal{R}_2$  is *exact with respect to  $\mathcal{P}_2$* .

### 2.2.5 Equivalent and exact relaxations

So far, we have defined the problems  $\mathcal{P}_1$ ,  $\mathcal{P}_{ch}$  and  $\mathcal{P}_2$  and obtained their convex relaxations  $\mathcal{R}_1$ ,  $\mathcal{R}_{ch}$  and  $\mathcal{R}_2$  respectively. We now characterize the relations among these problems.

Let  $p^*$  be the optimal cost of OPF. Let  $p_1^*$ ,  $p_{ch}^*$ ,  $p_2^*$  be the optimal cost of  $\mathcal{P}_1$ ,  $\mathcal{P}_{ch}$ ,  $\mathcal{P}_2$  respectively and let  $r_1^*$ ,  $r_{ch}^*$ ,  $r_2^*$  be the optimal cost of their relaxations  $\mathcal{R}_1$ ,  $\mathcal{R}_{ch}$ ,  $\mathcal{R}_2$  respectively.

**Theorem 1.** *Let  $G_{ch}$  denote any chordal extension of  $G$ . Then*

(a)  $p_1^* = p_{ch}^* = p_2^* = p^*$ .

(b)  $r_1^* = r_{ch}^* \geq r_2^*$ . *If  $G$  is acyclic, then  $r_1^* = r_{ch}^* = r_2^*$ .*

(c)  $\mathcal{R}_1$  is exact iff  $\mathcal{R}_{ch}$  is exact.  $\mathcal{R}_1$  and  $\mathcal{R}_{ch}$  are exact if  $\mathcal{R}_2$  is exact. *If  $G$  is acyclic, then  $\mathcal{R}_2$  is exact iff  $\mathcal{R}_1$  is exact.*

We make three remarks. First, part (a) says that the optimal cost of  $\mathcal{P}_1$ ,  $\mathcal{P}_{ch}$  and  $\mathcal{P}_2$  are the same as that of OPF. Our proof claims a stronger result: the underlying  $G$ -partial matrices in these problems are the same. Informally the feasible sets of these problems, and hence the problems themselves, are equivalent and one can construct a solution of OPF from a solution of any of these problems.

Second, since  $\mathcal{P}_1$ ,  $\mathcal{P}_{ch}$  and  $\mathcal{P}_2$  are nonconvex we will solve their relaxations  $\mathcal{R}_1$ ,  $\mathcal{R}_{ch}$  or  $\mathcal{R}_2$  instead. Even though exactness is defined to be a relation between each pair (e.g.,  $\mathcal{R}_2$  is exact means  $r_2^* = p_2^*$ ), part (a) says that if any pair is exact then the relaxed problem is exact *with respect to OPF* as well. For instance if  $\mathcal{R}_2$  is exact with respect to  $\mathcal{P}_2$  then any optimal  $G$ -partial matrix  $W_G^*$  of  $\mathcal{R}_2$  satisfies (2.8) and has  $\text{rank } W_G^*(e) = 1$  for all  $e \in E$ . Our proof will construct a psd rank-1  $n \times n$  matrix  $W^*$  from  $W_G^*$  that is optimal for  $\mathcal{P}_1$ . The spectral decomposition of  $W^*$  then yields an optimal voltage vector  $V^*$  in  $\mathbb{V}$  for OPF. Henceforth we will simply say that a relaxation  $\mathcal{R}_1/\mathcal{R}_{ch}/\mathcal{R}_2$  is “exact” instead of “exact with respect to  $\mathcal{P}_1/\mathcal{P}_{ch}/\mathcal{P}_2$ .”

Third, part (c) says that solving  $\mathcal{R}_1$  is the same as solving  $\mathcal{R}_{ch}$  and, in the case where  $G$  is acyclic (a *tree*, since  $G$  is assumed to be connected), is the same as solving  $\mathcal{R}_2$ .  $\mathcal{R}_1$  and  $\mathcal{R}_{ch}$  are SDPs while  $\mathcal{R}_2$  is an SOCP. Though they can all be solved in polynomial time [55, 65], SOCP in general requires a much smaller computational effort than SDP. Part (b) suggests that, when  $G$  is a tree, we should always solve  $\mathcal{R}_2$ . When  $G$  has cycles then there is a tradeoff between computational effort and exactness in deciding between solving  $\mathcal{R}_2$  or  $\mathcal{R}_{ch}/\mathcal{R}_1$ . As our simulation results in Section 2.5 confirm, if all maximal cliques of a chordal extension are available then solving  $\mathcal{R}_{ch}$  is *always better* than solving  $\mathcal{R}_1$  as they have the same accuracy

(in terms of exactness) but  $\mathcal{R}_{ch}$  is usually much faster to solve for large sparse networks  $G$ . Indeed  $G$  is a subgraph of any chordal extension  $G_{ch}$  of  $G$  which is, in turn, a subgraph of the complete graph on  $n$  nodes (denoted as  $C_n$ ), and hence  $I_G \subseteq I_{G_{ch}} \subseteq I_{C_n}$ . Therefore, *typically*, the number of variables is the smallest in  $\mathcal{R}_2$  ( $|I_G|$ ), the largest in  $\mathcal{R}_1$  ( $|I_{C_n}|$ ), with  $\mathcal{R}_{ch}$  in between. However the actual number of variables in  $\mathcal{R}_{ch}$  is generally greater than  $|I_{G_{ch}}|$ , depending on the choice of the chordal extension  $G_{ch}$ . Choosing a good  $G_{ch}$  is nontrivial; see [52] for more details. This choice however does not affect the optimal value  $r_{ch}^*$ .

**Corollary 2.** 1. *If  $G$  is acyclic then  $p_* = p_1^* = p_{ch}^* = p_2^* \geq r_1^* = r_{ch}^* = r_2^*$ .*

2. *If  $G$  has cycles then  $p_* = p_1^* = p_{ch}^* = p_2^* \geq r_1^* = r_{ch}^* \geq r_2^*$ .*

Theorem 1 and Corollary 2 do not provide conditions that guarantee any of the relaxations  $\mathcal{R}_1, \mathcal{R}_{ch}, \mathcal{R}_2$  are exact. See [15, 36–39, 68–70] for such sufficient conditions in the bus injection model. Corollary 2 implies that if  $\mathcal{R}_2$  is exact, so are  $\mathcal{R}_{ch}$  and  $\mathcal{R}_1$ . Moreover Lemma 4 below relates the feasible sets of  $\mathcal{R}_1, \mathcal{R}_{ch}, \mathcal{R}_2$ , not just their optimal values. It implies that  $\mathcal{R}_1, \mathcal{R}_{ch}, \mathcal{R}_2$  are equivalent problems if  $G$  has no cycles.

## 2.2.6 Proof of Theorem 1

We now prove that the feasible sets of OPF and  $\mathcal{P}_1, \mathcal{P}_{ch}, \mathcal{P}_2$  are equivalent when restricted to the underlying  $G$ -partial matrices. Similarly, the feasible sets of their relaxations are equivalent when  $G$  is a tree. When any of the relaxations are exact we can construct an  $n$ -dimensional complex voltage vector  $V \in \mathbb{V}$  that optimally solves OPF.

To define the set of  $G$ -partial matrices associated with  $\mathcal{P}_1, \mathcal{P}_{ch}, \mathcal{P}_2$  suppose  $F$  is a graph on  $n$  nodes such that  $G$  is a subgraph of  $F$ , i.e.,  $I_G \subseteq I_F$ . An  $F$ -partial matrix  $W_F$  is called an  $F$ -completion of the  $G$ -partial matrix  $W_G$  if

$$[W_F]_{ij} = [W_G]_{ij} \text{ for all } (i, j) \in I_G \subseteq I_F,$$

i.e.,  $W_F$  agrees with  $W_G$  on the index set  $I_G$ . If  $F$  is  $C_n$ , the complete graph on  $n$  nodes, then  $W_F$  is an  $n \times n$  matrix.  $W_F$  is a Hermitian  $F$ -completion if  $W_F = W_F^H$ .  $W_F$  is a psd

$F$ -completion if *in addition*  $W_F \succeq 0$ .  $W_F$  is a rank-1  $F$ -completion if  $\text{rank } W_F = 1$ . It can be checked that if  $W_G \not\preceq 0$  then  $W_G$  does not have a psd  $F$ -completion. If  $\text{rank } W_G \neq 1$  then it does not have a rank-1  $F$ -completion. Define

$$\begin{aligned} \mathbb{W}_1 &:= \{W_G \mid W_G \text{ satisfies (2.7a) -- (2.7b)}, \\ &\quad \exists \text{ psd rank-1 } C_n\text{-completion of } W_G\}. \end{aligned}$$

Recall that for  $W$ , an  $n \times n$  matrix,  $W(G)$  is the  $G$ -partial matrix corresponding to the  $I_G$  entries of  $W$ . Given an  $n \times n$  psd rank-1 matrix  $W$  that is feasible for  $\mathcal{P}_1$ ,  $W(G)$  is in  $\mathbb{W}_1$ . Conversely given a  $W_G \in \mathbb{W}_1$ , its psd rank-1  $C_n$ -completion is a feasible solution for  $\mathcal{P}_1$ . Hence  $\mathbb{W}_1$  is the set of  $I_G$  entries of all  $n \times n$  matrices feasible for  $\mathcal{P}_1$  and is nonconvex. Define

$$\begin{aligned} \mathbb{W}_1^+ &:= \{W_G \mid W_G \text{ satisfies (2.7a) -- (2.7b)}, \\ &\quad \exists \text{ psd } C_n\text{-completion of } W_G\}. \end{aligned}$$

$\mathbb{W}_1^+$  is the set of  $I_G$  entries of all  $n \times n$  matrices feasible for  $\mathcal{R}_1$ . It is convex and contains  $\mathbb{W}_1$ .

Similarly define the corresponding sets for  $\mathcal{P}_{ch}$  and  $\mathcal{R}_{ch}$ :

$$\begin{aligned} \mathbb{W}_{ch} &:= \{W_G \mid W_G \text{ satisfies (2.7a) -- (2.7b)}, \\ &\quad \exists \text{ psd rank-1 } G_{ch}\text{-completion of } W_G\}, \\ \mathbb{W}_{ch}^+ &:= \{W_G \mid W_G \text{ satisfies (2.7a) -- (2.7b)}, \\ &\quad \exists \text{ psd } G_{ch}\text{-completion of } W_G\}. \end{aligned}$$

$\mathbb{W}_{ch}$  and  $\mathbb{W}_{ch}^+$  are the sets of  $I_G$  entries of  $G_{ch}$ -partial matrices feasible for problems  $\mathcal{P}_{ch}$  and  $\mathcal{R}_{ch}$  respectively. Again  $\mathbb{W}_{ch}^+$  is a convex set containing the nonconvex set  $\mathbb{W}_{ch}$ . For problems

$\mathcal{P}_2$  and  $\mathcal{R}_2$  define:

$$\begin{aligned}\mathbb{W}_2 &:= \{W_G \mid W_G \text{ satisfies (2.7a) -- (2.7b) and (2.8),} \\ &\quad W_G(e) \succeq 0, \text{ rank } W_G(e) = 1 \text{ for all } e \in E\}, \\ \mathbb{W}_2^+ &:= \{W_G \mid W_G \text{ satisfies (2.7a) -- (2.7b),} \\ &\quad W_G(e) \succeq 0 \text{ for all } e \in E\}.\end{aligned}$$

Informally the sets  $\mathbb{W}_1, \mathbb{W}_1^+, \mathbb{W}_{ch}, \mathbb{W}_{ch}^+, \mathbb{W}_2$  and  $\mathbb{W}_2^+$  describe the feasible sets of the various problems restricted to the  $I_G$  entries of their respective partial matrix variables.

To relate the sets to the feasible set of OPF, consider the map  $f$  from  $\mathbb{C}^n$  to the set of  $G$ -partial matrices defined as:

$$\begin{aligned}f(V) &:= W_G \text{ where } [W_G]_{kk} = |V_k|^2, \text{ } k \in N, \text{ and} \\ &\quad [W_G]_{jk} = V_j V_k^H, \text{ } (j, k) \in E.\end{aligned}$$

Also, let  $f(\mathbb{V}) := \{f(V) \mid V \in \mathbb{V}\}$ .

The sketch of the proof is as follows. We prove Theorem 1(a) in Lemma 3 and then Theorem 1(b) in Lemma 4 below. Theorem 1(c) then follows from these two lemmas.

**Lemma 3.**  $f(\mathbb{V}) = \mathbb{W}_1 = \mathbb{W}_{ch} = \mathbb{W}_2$ .

*Proof.* First, we show that  $f(\mathbb{V}) = \mathbb{W}_1$ . Consider  $V \in \mathbb{V}$ . Then  $W = VV^H$  is feasible for  $\mathcal{P}_1$  and hence the  $G$ -partial matrix  $W(G)$  is in  $\mathbb{W}_1$ . Thus,  $f(\mathbb{V}) \subseteq \mathbb{W}_1$ . To prove  $\mathbb{W}_1 \subseteq f(\mathbb{V})$ , consider the rank-1 psd  $C_n$  completion of a  $G$ -partial matrix in  $\mathbb{W}_1$ . Its unique spectral decomposition yields a vector  $V$  that satisfies (2.3)–(2.4) and hence is in  $\mathbb{V}$ . Hence,  $f(\mathbb{V}) = \mathbb{W}_1$ .

Now, fix a chordal extension  $G_{ch}$  of  $G$ . We now prove:

$$\mathbb{W}_1 \subseteq \mathbb{W}_{ch} \subseteq \mathbb{W}_2 \subseteq \mathbb{W}_1.$$

To show  $\mathbb{W}_1 \subseteq \mathbb{W}_{ch}$ , consider  $W_G \in \mathbb{W}_1$ , and let  $W$  be its rank-1 psd  $C_n$ -completion. Then

it is easy to check that  $W(G_{ch})$  is feasible for  $\mathcal{P}_{ch}$  and hence  $W_G$  is in  $\mathbb{W}_{ch}$  as well.

To show  $\mathbb{W}_{ch} \subseteq \mathbb{W}_2$  consider a  $W_G \in \mathbb{W}_{ch}$  and its psd rank-1  $G_{ch}$ -completion  $W_{ch}$ . Since every edge  $e$  of  $G$  is a 2-clique in  $G_{ch}$ ,  $W_G(e) = W_{ch}(e)$  is psd rank-1 by the definition of psd and rank-1 for  $W_{ch}$ . We are thus left to show that  $W_G$  satisfies the cycle condition (2.8).

Consider the following statement  $T_k$  for  $3 \leq k \leq n$ :

$S_k$ : For all cycles  $(n_1, n_2, \dots, n_k)$  of length  $k$  in  $G_{ch}$  we have:

$$\angle[W_{ch}]_{n_1 n_2} + \angle[W_{ch}]_{n_2 n_3} + \dots + \angle[W_{ch}]_{n_k n_1} = 0 \pmod{2\pi}.$$

For  $k = 3$ , a cycle  $(n_1, n_2, n_3)$  defines a 3-clique in  $G_{ch}$  and thus  $W_{ch}(n_1, n_2, n_3)$  is psd rank-1 and  $W_{ch}(n_1, n_2, n_3) = uu^H$  for some  $u := (u_1, u_2, u_3) \in \mathbb{C}^3$ . Then

$$\begin{aligned} & \angle[W_{ch}]_{n_1 n_2} + \angle[W_{ch}]_{n_2 n_3} + \angle[W_{ch}]_{n_3 n_1} \\ &= \angle[(u_1 u_2^H)(u_2 u_3^H)(u_3 u_1^H)] = 0 \pmod{2\pi}. \end{aligned}$$

Let  $T_r$  be true for all  $3 \leq r \leq k$  and consider a cycle  $(n_1, n_2, \dots, n_{k+1})$  of length  $k+1$  in  $G_{ch}$ . Since  $G_{ch}$  is chordal, this cycle must have a chord, i.e., an edge between two nodes, say,  $n_1$  and  $n_{k'}$ , that are not adjacent on the cycle. Then  $(n_1, n_2, \dots, n_{k'})$  and  $(n_1, n_{k'}, n_{k'+1}, \dots, n_k)$  are two cycles in  $G_{ch}$ . By hypothesis,  $T_{k'}$  and  $T_{k-k'+2}$  are true and hence

$$\begin{aligned} & \angle[W_{ch}]_{n_1 n_2} + \angle[W_{ch}]_{n_2 n_3} + \dots + \angle[W_{ch}]_{n_{k'} n_1} \\ &= \angle[W_{ch}]_{n_1 n_{k'}} + \angle[W_{ch}]_{n_{k'} n_{k'+1}} + \dots + \angle[W_{ch}]_{n_k n_1} \\ &= 0 \pmod{2\pi}. \end{aligned}$$

We conclude that  $T_{k+1}$  is true by adding the above equations and using  $\angle[W_{ch}]_{n_1 n_{k'}} = -\angle[W_{ch}]_{n_{k'} n_1} \pmod{2\pi}$  since  $W_{ch}$  is Hermitian. By induction,  $W_{ch}$  satisfies the cycle condition. Also,  $W_G = W_{ch}(G)$  satisfies the cycle condition and hence is in  $\mathbb{W}_2$ . This completes the proof of  $\mathbb{W}_{ch} \subseteq \mathbb{W}_2$ .

To show  $\mathbb{W}_2 \subseteq \mathbb{W}_1$  suppose  $W_G \in \mathbb{W}_2$ . We now construct a psd rank-1  $C_n$ -completion of

$W_G$  to show  $W_G \in \mathbb{W}_1$ . Define  $\theta \in \mathbb{C}^n$  as follows. Let  $\theta_1 := 0$ . For  $j \in N \setminus \{1\}$  let  $(1, n_2), (n_2, n_3), \dots, (n_k, j)$  be any path from node 1 to node  $j$ . Define

$$\theta_j := -(\angle[W_G]_{1n_2} + \angle[W_G]_{n_2n_3} + \dots + \angle[W_G]_{n_kj}) \pmod{2\pi}.$$

Note that the above definition is well-defined: if there is another sequence of edges from node 1 to node  $j$ , the above relation still defines  $\theta_j$  uniquely because  $W_G$  satisfies the cycle condition. Let

$$V := \left[ \sqrt{[W_G]_{11}} e^{i\theta_1}, \dots, \sqrt{[W_G]_{nn}} e^{i\theta_n} \right].$$

Then it can be verified that  $W := VV^H$  is a psd rank-1  $C_n$ -completion of  $W_G$ . Hence  $W_G \in \mathbb{W}_1$ . This completes the proof of the lemma.  $\square$

**Lemma 4.**  $\mathbb{W}_1^+ = \mathbb{W}_{ch}^+ \subseteq \mathbb{W}_2^+$ . If  $G$  is acyclic, then  $\mathbb{W}_1^+ = \mathbb{W}_{ch}^+ = \mathbb{W}_2^+$ .

*Proof.* It suffices to prove

$$\mathbb{W}_{ch}^+ \subseteq \mathbb{W}_1^+ \subseteq \mathbb{W}_{ch}^+ \subseteq \mathbb{W}_2^+. \quad (2.10)$$

To show  $\mathbb{W}_{ch}^+ \subseteq \mathbb{W}_1^+$ , suppose  $W_G \in \mathbb{W}_{ch}^+$ . Let  $W_{ch}$  be a psd  $G_{ch}$ -completion of  $W_G$  for a chordal extension  $G_{ch}$ . Since any psd partial matrix on a chordal graph has a psd  $C_n$ -completion [74, Theorem 7],  $W_{ch}$  has a psd  $C_n$ -completion. Obviously, any psd  $C_n$ -completion of  $W_{ch}$  is also a psd  $C_n$ -completion of  $W_G$ , i.e.,  $W_G \in \mathbb{W}_1^+$ . The relation  $\mathbb{W}_1^+ \subseteq \mathbb{W}_{ch}^+ \subseteq \mathbb{W}_2^+$  follows a similar argument to the proof of Lemma 3.

If  $G$  is acyclic, then  $G$  is itself chordal and hence  $W_G$  has a psd  $C_n$ -completion, i.e.,  $\mathbb{W}_2^+ \subseteq \mathbb{W}_1^+$ . This implies  $\mathbb{W}_1^+ = \mathbb{W}_{ch}^+ = \mathbb{W}_2^+$ .  $\square$

To prove Theorem 1(c) note that parts (a) and (b) imply

$$p^* = p_1^* = p_{ch}^* = p_2^* \geq r_1^* = r_{ch}^* \geq r_2^*.$$

Hence  $\mathcal{R}_1$  is exact ( $p_1^* = r_1^*$ ) iff  $\mathcal{R}_{ch}$  is exact ( $p_{ch}^* = r_{ch}^*$ ). If  $\mathcal{R}_2$  is exact, i.e.,  $p_2^* = r_2^*$ , then both inequalities above become equalities, proving Theorem 1(c). This completes the proof of Theorem 1.

## 2.3 Branch flow model and SOCP relaxation

### 2.3.1 OPF formulation

The branch flow model of [49] adopts a directed connected graph  $\tilde{G} = (N, \tilde{E})$  to represent a power network where each node in  $N := \{1, \dots, n\}$  represents a bus and each edge in  $\tilde{E}$  represents a line. The orientations of the edges are taken to be arbitrary. Denote the directed edge from bus  $i$  to bus  $j$  by  $i \rightarrow j \in \tilde{E}$  and define  $m := |\tilde{E}|$  as the number of directed edges in  $G$ . For each edge  $i \rightarrow j \in \tilde{E}$ , define the following quantities:

- $z_{ij}$ : The complex impedance on the line. Thus  $z_{ij} = 1/y_{ij}$ .
- $I_{ij}$ : The complex current from bus  $i$  to bus  $j$ .
- $S_{ij}$ : The *sending-end* complex power from buses  $i$  to  $j$ .

Recall that for each node  $i \in N$ ,  $V_i$  is the complex voltage at bus  $i$  and  $s_i$  is the net complex power injection (generation minus load) at bus  $i$ .

The *branch flow model* of [49] is defined by the following set of power flow equations:

$$s_j = \sum_{k:j \rightarrow k} S_{jk} - \sum_{i:i \rightarrow j} (S_{ij} - z_{ij}|I_{ij}|^2) \quad \text{for } j \in N, \quad (2.11a)$$

$$S_{ij} = V_i I_{ij}^H \quad \text{and} \quad I_{ij} = y_{ij}(V_i - V_j) \quad \text{for } i \rightarrow j \in \tilde{E}, \quad (2.11b)$$

where (2.11a) imposes power balance at each bus and (2.11b) defines branch power and describes Ohm's law. The power injections at all buses satisfy

$$\underline{s}_j \leq s_j \leq \bar{s}_j \quad \text{for } j \in N, \quad (2.12)$$

where  $\underline{s}_j$  and  $\bar{s}_j$  are known limits on the net generation at bus  $j$ . It is often assumed that the slack bus (node 1) has a generator and there is no limit of  $s_1$ ; in this case  $-\underline{s}_j = \bar{s}_j = \infty$ . As in the bus injection model, we can eliminate the variables  $s_j$  by combining (2.11a) and (2.12) into:

$$\underline{s}_j \leq \sum_{k:j \rightarrow k} S_{jk} - \sum_{i:i \rightarrow j} (S_{ij} - z_{ij}|I_{ij}|^2) \leq \bar{s}_j \quad \text{for } j \in N. \quad (2.13)$$

All voltage magnitudes are constrained as follows:

$$\underline{V}_j \leq |V_j| \leq \bar{V}_j \quad \text{for } j \in N, \quad (2.14)$$

where  $\underline{V}_j$  and  $\bar{V}_j$  are known lower and upper voltage limits, with  $|V_1| = 1 = \underline{V}_1 = \bar{V}_1$ . Denote the variables in the branch flow model by  $\tilde{x} := (S, I, V) \in \mathbb{C}^{n+2m}$ . These constraints define the feasible set of the OPF problem in the branch flow model:

$$\mathbb{X} := \{\tilde{x} \in \mathbb{C}^{n+2m} \mid \tilde{x} \text{ satisfies (2.11b), (2.13), (2.14)}\}. \quad (2.15)$$

To define OPF, consider a cost function  $c(\tilde{x})$ . For example, if the objective is to minimize the real power loss in the network, then we have

$$c(\tilde{x}) = \sum_{j \in N} \text{Re } s_j = \sum_{j \in N} \text{Re} \left[ \sum_{k:j \rightarrow k} S_{jk} - \sum_{i:i \rightarrow j} (S_{ij} - z_{ij}|I_{ij}|^2) \right].$$

Similarly, if the objective is to minimize the weighted sum of real power generation in the network, then

$$\begin{aligned} c(\tilde{x}) &= \sum_{j \in N} c_j (\text{Re } s_j - p_j^d) \\ &= \sum_{j \in N} c_j \left[ \text{Re} \left( \sum_{k:j \rightarrow k} S_{jk} - \sum_{i:i \rightarrow j} (S_{ij} - z_{ij}|I_{ij}|^2) \right) - p_j^d \right], \end{aligned}$$

where  $p_j^d$  is the given real power demand at bus  $j \in N$ .

**Optimal power flow problem *OPF*:**

$$\underset{\tilde{x}}{\text{minimize}} \quad c(\tilde{x}) \quad \text{subject to} \quad \tilde{x} \in \mathbb{X}. \quad (2.16)$$

Since (2.11) is quadratic,  $\mathbb{X}$  is generally a nonconvex set. As before, OPF is a nonconvex problem.

### 2.3.2 SOCP relaxation: $\tilde{\mathcal{P}}_2$ , $\tilde{\mathcal{R}}_2^{nc}$ and $\tilde{\mathcal{R}}_2$

The SOCP relaxation of (2.16) developed in [49] consists of two steps. First, we use (2.11b) to eliminate the phase angles from the complex voltages  $V$  and currents  $I$  to obtain for each  $i \rightarrow j \in \tilde{E}$ ,

$$v_j = v_i - 2 \operatorname{Re}(z_{ij}^H S_{ij}) + |z_{ij}|^2 \ell_{ij}, \quad (2.17)$$

$$\ell_{ij} v_i = |S_{ij}|^2. \quad (2.18)$$

where  $v_i := |V_i|^2$  and  $\ell_{ij} := |I_{ij}|^2$ . This is the model first proposed by Baran-Wu in [41, 42] for distribution systems. Second the quadratic equalities in (2.18) are nonconvex; relax them to inequalities:

$$\ell_{ij} v_i \geq |S_{ij}|^2 \quad \text{for } i \rightarrow j \in \tilde{E}. \quad (2.19)$$

Let  $x := (S, \ell, v) \in \mathbb{R}^{n+3m}$  denote the new variables. Note that we use  $S$  to denote both a complex variable in  $\mathbb{C}^m$  and the real variables  $(\operatorname{Re} S, \operatorname{Im} S)$  in  $\mathbb{R}^{2m}$  depending on context. Define the nonconvex set:

$$\mathbb{X}_2^{nc} := \{x \in \mathbb{R}^{n+3m} \mid x \text{ satisfies (2.13), (2.14), (2.17), (2.18)}\},$$

and the convex superset that is a second-order cone:

$$\mathbb{X}_2^+ := \{x \in \mathbb{R}^{n+3m} \mid x \text{ satisfies (2.13), (2.14), (2.17), (2.19)}\}.$$

As we discuss below solving OPF over  $\mathbb{X}_2^+$  is an SOCP and hence efficiently computable. Whether the solution of the SOCP relaxation yields an optimal for OPF depends on two factors [49]: (a) whether the optimal solution over  $\mathbb{X}_2^+$  actually lies in  $\mathbb{X}_2^{nc}$ , (b) whether the phase angles of  $V$  and  $I$  can be recovered from such a solution, as we now explain.

For an  $n \times 1$  vector  $\theta \in [-\pi, \pi)^n$  define the map  $h_\theta : \mathbb{R}^{n+3m} \rightarrow \mathbb{C}^{n+2m}$  by  $h_\theta(S, \ell, v) = (S, I, V)$  where

$$\begin{aligned} V_i &:= \sqrt{v_i} e^{i\theta_i} \quad \text{for } i \in N, \\ I_{ij} &:= \sqrt{\ell_{ij}} e^{i(\theta_i - \angle S_{ij})} \quad \text{for } i \rightarrow j \in \tilde{E}. \end{aligned}$$

Given an  $x := (S, \ell, v) \in \mathbb{X}_2^+$  our goal is to find  $\theta$  so that  $h_\theta(x) \in \mathbb{X}$  is feasible for OPF. To determine whether such a  $\theta$  exists, define  $\beta(x) \in \mathbb{R}^m$  by

$$\beta_{ij}(x) := \angle(v_i - z_{ij}^H S_{ij}) \quad \text{for } i \rightarrow j \in \tilde{E}. \quad (2.20)$$

Essentially,  $x \in \mathbb{X}_2^+$  implies a phase angle difference across each line  $i \rightarrow j \in \tilde{E}$  given by  $\beta_{ij}(x)$  [49, Theorem 2]. We are interested in the set of  $x$  such that  $\beta_{ij}(x)$  can be expressed as  $\theta_i - \theta_j$  where  $\theta_i$  can be the phase of voltage at node  $i \in N$ . In particular, let  $C$  be the  $n \times m$  incidence matrix of  $\tilde{G}$  defined as

$$C_{ie} = \begin{cases} 1 & \text{if edge } e \in \tilde{E} \text{ leaves node } i \in N, \\ -1 & \text{if edge } e \in \tilde{E} \text{ enters node } i \in N, \\ 0 & \text{otherwise.} \end{cases}$$

The first row of  $C$  corresponds to the slack bus. Define the  $m \times (n - 1)$  *reduced* incidence matrix  $B$  obtained from  $C$  by removing the first row and taking the transpose. Consider the set of  $x$  such that

$$\exists \theta \text{ that solves } B\theta = \beta(x) \pmod{2\pi}. \quad (2.21)$$

A solution  $\theta$ , if exists, is unique in  $[-\pi, \pi)^n$ . Moreover the necessary and sufficient condition for the existence of a solution to (2.21) has a familiar interpretation: the implied voltage angle differences  $\beta(x)$  sum to zero (mod  $2\pi$ ) around any cycle [49, Theorem 2].

Define the set:

$$\mathbb{X}_2 := \{x \in \mathbb{R}^{n+3m} \mid x \text{ satisfies (2.13), (2.14), (2.17), (2.18), (2.21)}\}.$$

Clearly  $\mathbb{X}_2 \subseteq \mathbb{X}_2^{nc} \subseteq \mathbb{X}_2^+$ . These three sets define the following optimization problems.<sup>3</sup>

**Problem  $\tilde{\mathcal{P}}_2$ :**

$$\underset{x}{\text{minimize}} \quad c(x) \quad \text{subject to} \quad x \in \mathbb{X}_2.$$

**Problem  $\tilde{\mathcal{R}}_2^{nc}$ :**

$$\underset{x}{\text{minimize}} \quad c(x) \quad \text{subject to} \quad x \in \mathbb{X}_2^{nc}.$$

**Problem  $\tilde{\mathcal{R}}_2$ :**

$$\underset{x}{\text{minimize}} \quad c(x) \quad \text{subject to} \quad x \in \mathbb{X}_2^+.$$

We say  $\tilde{\mathcal{R}}_2$  is exact with respect to  $\tilde{\mathcal{R}}_2^{nc}$  if there exists an optimal solution  $x^*$  of  $\tilde{\mathcal{R}}_2$  that attains equality in (2.19), i.e.,  $x^*$  lies in  $\mathbb{X}_2^{nc}$ . We say  $\tilde{\mathcal{R}}_2^{nc}$  is exact with respect to  $\tilde{\mathcal{P}}_2$  if there exists an optimal solution  $x^*$  of  $\tilde{\mathcal{R}}_2^{nc}$  that satisfies (2.21), i.e.,  $x^*$  lies in  $\mathbb{X}_2$  and solves  $\tilde{\mathcal{P}}_2$  optimally.

The problems  $\tilde{\mathcal{P}}_2$  and  $\tilde{\mathcal{R}}_2^{nc}$  are nonconvex and hence NP-hard, but problem  $\tilde{\mathcal{R}}_2$  is an SOCP and hence can be solved in polynomial time [55, 75]. Let  $p^*$  be the optimal cost of OPF (2.16) in the branch flow model. Let  $\tilde{p}_2^*$ ,  $\tilde{r}_2^{nc}$ ,  $\tilde{r}_2^*$  be the optimal costs of  $\tilde{\mathcal{P}}_2$ ,  $\tilde{\mathcal{R}}_2^{nc}$ ,  $\tilde{\mathcal{R}}_2$  respectively. The next result follows directly from [49, Theorems 2, 4].

---

<sup>3</sup>Recall that cost  $c(\cdot)$  was defined over  $(S, I, V) \in \mathbb{C}^{n+2m}$ . For the cost functions considered, it can be equivalently written as a function of  $(S, \ell, v) \in \mathbb{R}^{n+3m}$ .

**Theorem 5.** (a) *There is a bijection between  $\mathbb{X}$  and  $\mathbb{X}_2$ .*

(b)  $p^* = \tilde{p}_2^* \geq \tilde{r}_2^{nc} \geq \tilde{r}_2^*$  where the first inequality is an equality if  $\tilde{G}$  is acyclic.

We make two remarks on this relaxation over radial (tree) networks  $\tilde{G}$ . First, for such a graph, Theorem 5 says that if  $\tilde{\mathcal{R}}_2$  is exact with respect to  $\tilde{\mathcal{R}}_2^{nc}$ , then it is exact with respect to OPF (2.16). Indeed, for any optimal solution  $x^*$  of  $\tilde{\mathcal{R}}_2$  that attains equality in (2.19), the relation in (2.21) always has a unique solution  $\theta^*$  in  $[-\pi, \pi]^n$  and hence  $h_{\theta^*}(x^*)$  is optimal for OPF.

Second, Theorem 5 does not provide conditions that guarantee  $\tilde{\mathcal{R}}_2$  or  $\tilde{\mathcal{R}}_2^{nc}$  is exact. See [46, 49–51] for sufficient conditions for exact SOCP relaxation in radial networks. Even though, here, we define a relaxation to be exact as long as one of its optimal solutions satisfies the constraints of the original problem, all the sufficient conditions in these papers guarantee that *every* optimal solution of the relaxation is optimal for the original problem.

## 2.4 Equivalence of bus injection model and branch flow model

In this section we establish equivalence relations between the bus injection model and the branch flow model and their relaxations. Specifically we establish two sets of bijections (a) between the feasible sets of problems  $\mathcal{P}_2$  and  $\tilde{\mathcal{P}}_2$ , i.e.,  $\mathbb{W}_2$  and  $\mathbb{X}_2$ , and (b) between the feasible sets of problems  $\mathcal{R}_2$  and  $\tilde{\mathcal{R}}_2$ , i.e.,  $\mathbb{W}_2^+$  and  $\mathbb{X}_2^+$ .

For a Hermitian  $G$ -partial matrix  $W_G$ , define the  $(n+3m) \times 1$  vector  $x = (S, \ell, v) := g(W_G)$  as follows. For  $i \in N$  and  $i \rightarrow j \in \tilde{E}$ ,

$$v_i := [W_G]_{ii}, \tag{2.25}$$

$$S_{ij} := y_{ij}^H ([W_G]_{ii} - [W_G]_{ij}), \tag{2.26}$$

$$\ell_{ij} := |y_{ij}|^2 ([W_G]_{ii} + [W_G]_{jj} - [W_G]_{ij} - [W_G]_{ji}). \tag{2.27}$$

Define the mapping  $g^{-1}$  from  $\mathbb{R}^{n+3m}$  to the set of Hermitian  $G$ -partial matrices as follows.

Let  $W_G := g^{-1}(x)$  where

$$[W_G]_{ii} := v_i \quad \text{for } i \in N, \quad (2.28)$$

$$[W_G]_{ij} := v_i - z_{ij}^H S_{ij} = [W_G]_{ji}^H \quad \text{for } i \rightarrow j \in \tilde{E}. \quad (2.29)$$

The next result implies that  $g$  and  $g^{-1}$  restricted to  $\mathbb{W}_2^+$  ( $\mathbb{W}_2$ ) and  $\mathbb{X}_2^+$  ( $\mathbb{X}_2$ ) respectively are indeed inverse of each other. This establishes a bijection between the respective sets.

**Theorem 6.** (a) *The mapping  $g : \mathbb{W}_2 \rightarrow \mathbb{X}_2$  is a bijection with  $g^{-1}$  as its inverse.*

(b) *The mapping  $g : \mathbb{W}_2^+ \rightarrow \mathbb{X}_2^+$  is a bijection with  $g^{-1}$  as its inverse.*

Before we present its proof we make three remarks. First, Lemma 3 implies a bijection between  $\mathbb{W}_2$  and the feasible set  $V$  of OPF in the bus injection model. Theorem 5(a) implies a bijection between  $\mathbb{X}_2$  and the feasible set  $\mathbb{X}$  of OPF in the branch flow model. Theorem 6 hence implies a bijection between the feasible sets  $\mathbb{V}$  and  $\mathbb{X}$  of OPF in the bus injection model and the branch flow model respectively. It is in this sense that these two models are equivalent.

Second, it is important that we utilize both models because some relaxations are much easier to formulate and some sufficient conditions for exact relaxation are much easier to prove in one model than the other. For instance the semidefinite relaxation of power flows has a much cleaner formulation in the bus injection model. The branch flow model especially for radial networks has a convenient recursive structure that not only allows a more efficient computation of power flows e.g. [58–60], but also plays a crucial role in proving the sufficient conditions for exact relaxation in [61, 62]. Since the variables in the branch flow model correspond directly to physical quantities such as branch power flows and injections it is sometimes more convenient in applications.

Third, define the set of  $G$ -partial matrices that are in  $\mathbb{W}_2^+$  but do not satisfy the cycle

condition (2.8):

$$\begin{aligned} \mathbb{W}_2^{nc} &:= \{W_G \mid W_G \text{ satisfies (2.7a) – (2.7b)}, \\ &W_G(e) \succeq 0, \text{rank } W_G(e) = 1 \text{ for } e \in E\}. \end{aligned} \quad (2.30)$$

Clearly,  $\mathbb{W}_2 \subseteq \mathbb{W}_2^{nc} \subseteq \mathbb{W}_2^+$ . Then the same argument as in Theorem 6 implies that  $g$  and  $g^{-1}$  define a bijection between  $\mathbb{W}_2^{nc}$  and  $\mathbb{X}_2^{nc}$ .

*Proof of Theorem 6.* We only prove part (a); part (b) follows similarly. Recall the definitions of sets  $\mathbb{W}_2$  and  $\mathbb{X}_2$ :

$$\begin{aligned} \mathbb{W}_2 &:= \{W_G \mid W_G \text{ satisfies (2.7a) – (2.7b) and (2.8)}, \\ &W_G(e) \succeq 0, \text{rank } W_G(e) = 1 \text{ for all } e \in E\}, \\ \mathbb{X}_2 &:= \{x \in \mathbb{R}^{n+3m} \mid x \text{ satisfies (2.13), (2.14), (2.17), (2.18), (2.21)}\}. \end{aligned}$$

We need to show that

- (i)  $g(\mathbb{W}_2) \subseteq \mathbb{X}_2$  so that  $g : \mathbb{W}_2 \rightarrow \mathbb{X}_2$  is well defined.
- (ii)  $g$  is injective, i.e.,  $g(x) \neq g(x')$  if  $x \neq x'$ .
- (iii)  $g$  is surjective and hence its inverse exists; moreover  $g^{-1}$  defined in (2.28)–(2.29) is indeed  $g$ 's inverse.

The proof of (i) is similar to that of (iii) and omitted. That  $g$  is injective follows directly from (2.25)–(2.27). To prove (iii), we need to show that given any  $x := (S, \ell, v) \in \mathbb{X}_2$ ,  $W_G := g^{-1}(x)$  defined by (2.28)–(2.29) is in  $\mathbb{W}_2$  and  $x = g(W_G)$ . We now prove this in four steps.

*Step 1: Proof that  $W_G$  satisfies (2.7a)–(2.7b).* Clearly (2.7b) follows from (2.14). We now show that (2.7a) is equivalent to (2.13). For node  $j \in N$ , separate the edges in the summation in (2.7a) into outgoing edges  $j \rightarrow k \in \tilde{E}$  from node  $j$  and incoming edges  $k \rightarrow j \in \tilde{E}$  to

node  $j$ . For each incoming edge  $k \rightarrow j \in \tilde{E}$  we have from (2.28)–(2.29)

$$\begin{aligned} [W_G]_{jj} - [W_G]_{jk} &= v_j - (v_k - z_{kj}^H S_{kj})^H \\ &= - (v_k - v_j - z_{kj} S_{kj}^H) \\ &= - (z_{kj}^H S_{kj} - |z_{kj}|^2 \ell_{kj}), \end{aligned}$$

where the last equality follows from (2.17). Substituting this and (2.28)–(2.29) into (2.7a) we get, for each  $j \in N$ :

$$\begin{aligned} &\sum_{k:(j,k) \in E} ([W_G]_{jj} - [W_G]_{jk}) y_{jk}^H \\ &= \sum_{k:j \rightarrow k \in \tilde{E}} ([W_G]_{jj} - [W_G]_{jk}) y_{jk}^H \\ &\quad + \sum_{k:k \rightarrow j \in \tilde{E}} ([W_G]_{jj} - [W_G]_{jk}) y_{jk}^H \\ &= \sum_{k:j \rightarrow k \in \tilde{E}} (v_j - (v_j - z_{jk}^H S_{jk})) y_{jk}^H \\ &\quad - \sum_{k:k \rightarrow j \in \tilde{E}} (z_{kj}^H S_{kj} - |z_{kj}|^2 \ell_{kj}) y_{kj}^H \\ &= \sum_{k:j \rightarrow k} S_{jk} - \sum_{k:k \rightarrow j} (S_{kj} - z_{kj} \ell_{kj}). \end{aligned}$$

Hence, (2.7a) is equivalent to (2.13).

*Step 2: Proof that  $W_G$  satisfies (2.8).* Without loss of generality let  $c := (1, 2, \dots, k)$  be a cycle. For each *directed* edge  $i \rightarrow j \in \tilde{E}$ , recall  $\beta_{ij}(x) := \angle(v_i - z_{ij}^H S_{ij})$  defined in (2.20) and define  $\beta_{ji}(x) = -\beta_{ij}(x)$  in the opposite direction. Since  $x = (S, \ell, v)$  satisfies (2.21), [49, Theorem 2] implies that

$$\beta_{12}(x) + \dots + \beta_{k1}(x) = 0 \pmod{2\pi}, \quad (2.31)$$

where each  $(i, j)$  in  $c$  may be in the same or opposite orientation as the orientation of the

directed graph  $\tilde{G}$ . Observe from (2.29) that, for each directed edge  $i \rightarrow j \in \tilde{E}$ ,  $\angle[W_G]_{ij} = \beta_{ij}(x)$  and  $\angle[W_G]_{ji} = \beta_{ji}(x)$ . Hence (2.31) is equivalent to (2.8), i.e.,  $\sum_{(i,j) \in c} \angle[W_G]_{ij} = 0 \pmod{2\pi}$ .

*Step 3: Proof that  $W_G(e) \succeq 0$ , rank  $W_G(e) = 1$  for all  $e \in E$ .* For each edge  $i \rightarrow j \in \tilde{E}$  we have

$$[W_G]_{ii}[W_G]_{jj} - [W_G]_{ij}[W_G]_{ij}^H \quad (2.32)$$

$$\begin{aligned} &= v_i v_j - |v_i - z_{ij}^H S_{ij}|^2 \\ &= v_i v_j - (v_i^2 - v_i(z_{ij} S_{ij}^H + z_{ij}^H S_{ij}) + |z_{ij}|^2 |S_{ij}|^2) \\ &= -v_i (v_i - v_j - (z_{ij} S_{ij}^H + z_{ij}^H S_{ij}) + |z_{ij}|^2 \ell_{ij}), \end{aligned} \quad (2.33)$$

where the last equality follows from (2.18). Substituting (2.17) into (2.33) yields  $[W_G]_{ii}[W_G]_{jj} = |[W_G]_{ij}|^2$ . This together with  $[W_G]_{ii} \geq 0$  (from (2.28)) means  $W_G(i, j) \succeq 0$  and rank  $W_G(i, j) = 1$ .

*Step 4: Proof that  $g(W_G) = x$ .* Steps 1–3 show that  $W_G := g^{-1}(x) \in \mathbb{W}_2$  and hence  $g$  has an inverse. We now prove this inverse is  $g^{-1}$  defined by (2.28)–(2.29). It is easy to see that (2.25)–(2.26) follow directly from (2.28)–(2.29). We hence are left to show that  $W_G$  satisfies (2.27). For each edge  $i \rightarrow j \in \tilde{E}$  we have from (2.28)–(2.29)

$$\begin{aligned} &|y_{ij}|^2 ([W_G]_{ii} + [W_G]_{jj} - [W_G]_{ij} - [W_G]_{ji}) \\ &= |y_{ij}|^2 (v_i + v_j - 2 \operatorname{Re} (v_i - z_{ij}^H S_{ij})) \\ &= |y_{ij}|^2 (v_j - v_i + 2 \operatorname{Re} (z_{ij}^H S_{ij})) \\ &= \ell_{ij}, \end{aligned}$$

where the last equality follows from (2.17). Hence  $W_G$  satisfies (2.27) and  $g(W_G) = x$ .  $\square$

We end this section with a visualization of Theorems 1, 5 and 6 in Figure 2.3. For any chordal extension  $G_{ch}$  of graph  $G$ , the bus-injection model leads to three sets of problems  $\mathcal{P}_1, \mathcal{P}_{ch}$ , and  $\mathcal{P}_2$  and their corresponding relaxations  $\mathcal{R}_1, \mathcal{R}_{ch}$  and  $\mathcal{R}_2$  respectively. The branch

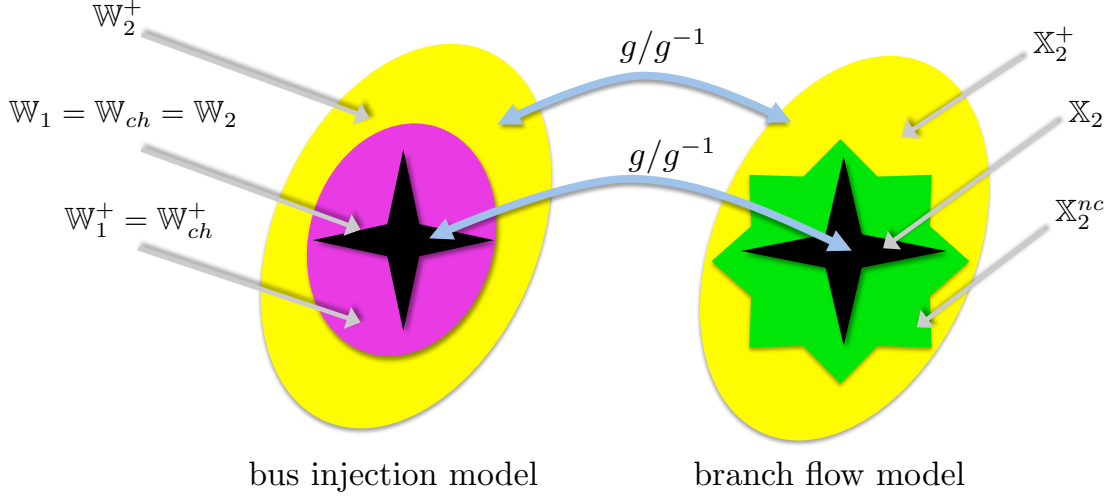


Figure 2.3: Feasible sets of conic formulations and their relaxations, and the relations among these sets.

flow model leads to an equivalent OPF problem  $\tilde{\mathcal{P}}_2$ , a nonconvex relaxation  $\tilde{\mathcal{R}}_2^{nc}$  obtained by eliminating the voltage phase angles, and its convex relaxation  $\tilde{\mathcal{R}}_2$ . The feasible sets of these problems, their relations, and the equivalence of the two models are shown in Figure 2.3. As evident from the figure, the sets  $\mathbb{W}_1 = \mathbb{W}_{ch} = \mathbb{W}_2$  on the left are the nonconvex feasible sets of equivalent OPF problems  $\mathcal{P}_1, \mathcal{P}_{ch}, \mathcal{P}_2$  respectively in the bus injection model, and  $\mathbb{W}_1^+ = \mathbb{W}_{ch}^+ \subseteq \mathbb{W}_2^+$  are the convex feasible sets of their respective relaxations  $\mathcal{R}_1, \mathcal{R}_{ch}, \mathcal{R}_2$ . On the right,  $\mathbb{X}_2$  is the nonconvex feasible set of an equivalent OPF problem  $\tilde{\mathcal{P}}_2$  in the branch flow model.  $\mathbb{X}_2^{nc}$  is the nonconvex feasible set of the relaxation  $\tilde{\mathcal{R}}_2^{nc}$  obtained by eliminating the voltage phase angles and  $\mathbb{X}_2^+$  is the convex feasible set of the relaxation  $\tilde{\mathcal{R}}_2$ . The equivalence of the sets  $\mathbb{W}_2$  (or  $\mathbb{W}_2^+$ ) and  $\mathbb{X}_2$  (or  $\mathbb{X}_2^+$ ) is represented by the linear maps  $g/g^{-1}$ . When  $G$  is a tree,  $\mathbb{W}_1^+ = \mathbb{W}_{ch}^+ = \mathbb{W}_2^+$  in the bus injection model and  $\mathbb{X}_2^{nc} = \mathbb{X}_2^+$  in the branch flow model. Note that neither of  $\mathbb{W}_1^+$  and  $\mathbb{X}_2^{nc}$  (or, more precisely  $g^{-1}(\mathbb{X}_2^{nc})$ ) contains the other.

## 2.5 Numerics

We now illustrate the theory developed so far through simulations. First we visualize in Section 2.5.1 the feasible sets of OPF and their relaxations for a simple 3-bus example from [1]. Next we report in Section 2.5.2 the running times and accuracies (in terms of exactness) of different relaxations on IEEE benchmark systems.

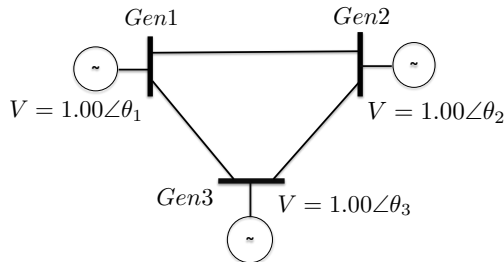


Figure 2.4: A 3-bus network from [1].

Parameter	Value
$y_{11}$	$\mathbf{i}0.3750$
$y_{22}$	$\mathbf{i}0.5$
$y_{33}$	$\mathbf{i}0.5750$
$y_{12}$	$0.0517 - \mathbf{i}1.1087$
$y_{13}$	$0.1673 - \mathbf{i}1.5954$
$y_{23}$	$0.0444 - \mathbf{i}1.3319$

Table 2.1: Admittances for the 3-bus network.

### 2.5.1 A 3-bus example

Consider the 3-bus example in Figure 2.4 taken from [1] (but we do not impose line limits) with line parameters in per units in Table 2.1. Note that this network has shunt elements. For this example,  $\mathcal{P}_1$  is the same problem as  $\mathcal{P}_{ch}$  and  $\mathcal{R}_1$  is the same problem as  $\mathcal{R}_{ch}$ . Hence we will focus on the feasible sets of  $\mathcal{P}_1$  (which is the same as that of  $\mathcal{P}_2$ ) and the feasible sets of  $\mathcal{R}_1, \mathcal{R}_2$ . Each problem has a Hermitian  $3 \times 3$  matrix  $W$  as its variable. Recall that  $s_j = p_j + \mathbf{i}q_j$  is the complex power injection at node  $j \in N$  and thus for each Hermitian

matrix  $W$ , we have the following map:

$$p_j(W) + \mathbf{i}q_j(W) = W_{jj} y_{jj} + \sum_{k:(j,k) \in E} (W_{jj} - W_{jk}) y_{jk}^H.$$

To visualize the various feasible sets, define the following set in 2 dimensions:

$$\begin{aligned} \mathcal{A}_1 &:= \{(p_1(W), p_2(W)) \mid W \in \mathbb{W}_1, \\ &W_{11} = W_{22} = W_{33} = 1, p_3(W) = -0.95\}. \end{aligned} \quad (2.34)$$

This is the projection of the feasible set of  $\mathcal{P}_1$  on the  $p_1 - p_2$  plane. Similarly, define the sets  $\mathcal{A}_1^+$  and  $\mathcal{A}_2^+$  where the Hermitian matrix  $W$  is restricted to be in  $\mathbb{W}_1^+$  and  $\mathbb{W}_2^+$ , respectively. We plot  $\mathcal{A}_1$ ,  $\mathcal{A}_1^+$  and  $\mathcal{A}_2^+$  in Figure 2.5(a). It illustrates the relationship among the sets in Figure 2.3, i.e.,  $\mathbb{W}_1 \subseteq \mathbb{W}_1^+ \subseteq \mathbb{W}_2^+$ . From Figure 2.5(a),  $\mathcal{A}_1$  is non-convex while  $\mathcal{A}_1^+$  and  $\mathcal{A}_2^+$  are convex. Since  $W \rightarrow (p_1(W), p_2(W))$  is a linear map, this confirms that  $\mathbb{W}_1$  is non-convex while  $\mathbb{W}_1^+$  and  $\mathbb{W}_2^+$  are convex. To investigate the exactness of relaxations, consider the Pareto fronts of the various sets (magnified in Figure 2.5(b)). The Pareto front of  $\mathcal{A}_1^+$  coincides with that of  $\mathcal{A}_1$  and thus relaxation  $\mathcal{R}_1$  is exact; relaxation  $\mathcal{R}_2$ , however, is not.<sup>4</sup>

Consider the set  $\mathbb{W}_2^{nc}$  defined in (2.30) that is equivalent to  $\mathbb{X}_2^{nc}$ . For this example,  $\mathbb{W}_2^{nc}$  is the set of  $3 \times 3$  matrices  $W$  that satisfy (2.7a)-(2.7b) and the submatrices  $W(1, 2)$ ,  $W(2, 3)$ ,  $W(1, 3)$  are psd rank-1. The full matrix  $W$ , however, may not be psd or rank-1. Extend the definition of  $\mathcal{A}_1$  in (2.34) to define the set  $\mathcal{A}_2^{nc}$  where the matrix  $W$  is restricted to be in  $\mathbb{W}_2^{nc}$ . In Figure 2.6, we plot  $\mathcal{A}_2^{nc}$  along with  $\mathcal{A}_2^+$  and  $\mathcal{A}$ . This equivalently illustrates the relation of the sets on the right in Figure 2.3.

---

<sup>4</sup>SDP here are exact while some of the simulations in [1] are not exact because we do not impose line limits here.

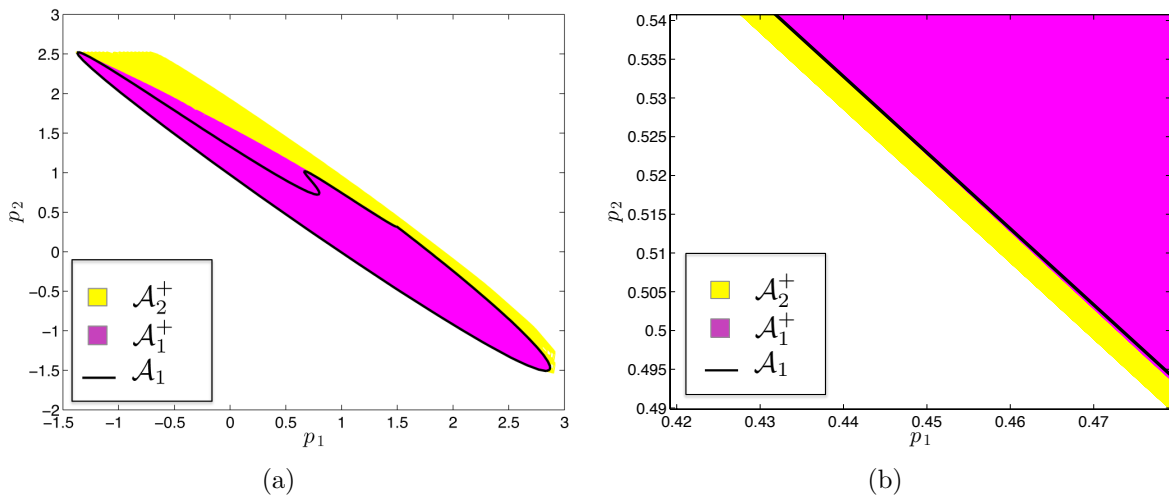


Figure 2.5: (a) Projections of feasible regions on  $p_1 - p_2$  space for the 3-bus system in Figure 2.4.  
(b) Zoomed-in Pareto fronts of these sets.

For the projections on the  $q_1 - q_2$  plane define the set

$$\mathcal{B}_1 := \{(q_1(W), q_2(W)) \mid W \in \mathbb{W}_1, \\ W_{11} = W_{22} = W_{33} = 1, p_3(W) = -0.95\}.$$

As before, extend the definitions to  $\mathcal{B}_1^+$ ,  $\mathcal{B}_2^+$ , and  $\mathcal{B}_2^{nc}$ . We plot  $\mathcal{B}_1$ ,  $\mathcal{B}_1^+$  and  $\mathcal{B}_2^+$  in Figure 2.7(a) and  $\mathcal{B}_1$ ,  $\mathcal{B}_2^{nc}$  and  $\mathcal{B}_2^+$  in Figure 2.7(b). This plot illustrates that the set  $\mathbb{W}_2^{nc}$  is not simply connected (a set is said to be simply connected if any 2 paths from one point to another can be continuously transformed, staying within the set). Note that neither of  $\mathcal{B}_1^+$  and  $\mathcal{B}_2^{nc}$  contains the other.

## 2.5.2 IEEE benchmark systems

For IEEE benchmark systems [63], we solve  $\mathcal{R}_1$ ,  $\mathcal{R}_2$  and  $\mathcal{R}_{ch}$  in MATLAB using CVX [76] with the solver SeDuMi [77] after some minor modifications to the resistances on some lines [36]<sup>5</sup>. The objective values and running times are presented in Table 2.2. The problems

<sup>5</sup>A resistance of  $10^{-5}$  p.u. is added to lines with zero resistance.

Test case	Objective value		Running times			Lambda ratio
	$R_1, R_{ch}$	$R_2$	$R_1$	$R_{ch}$	$R_2$	
9 bus	5297.4	5297.4	0.2	0.2	0.2	$1.15 \times 10^{-9}$
14 bus	8081.7	8075.3	0.2	0.2	0.2	$8.69 \times 10^{-9}$
30 bus	574.5	573.6	0.4	0.3	0.3	$1.67 \times 10^{-9}$
39 bus	41889.1	41881.5	0.7	0.3	0.3	$1.02 \times 10^{-10}$
57 bus	41738.3	41712.0	1.3	0.5	0.3	$3.98 \times 10^{-9}$
118 bus	129668.6	129372.4	6.9	0.7	0.6	$2.16 \times 10^{-10}$
300 bus	720031.0	719006.5	109.4	2.9	1.8	$1.26 \times 10^{-4}$
2383wp bus	1840270	1789500.0	-	1005.6	155.3	median = $3.33 \times 10^{-5}$ , max = 0.0034.

Table 2.2: Performance comparison of relaxation techniques for IEEE benchmark systems.

$\mathcal{R}_1$  and  $\mathcal{R}_{ch}$  have the same optimal objective value, i.e.,  $r_1^* = r_{ch}^*$ , as predicted by Theorem 1. We also report the ratios of the first two eigenvalues of the optimal  $W^*$  in  $\mathcal{R}_1$ <sup>6</sup>; for most cases, it is small indicating that the relaxation is exact. The optimal objective value of  $\mathcal{R}_2$  is lower ( $r_2^* < r_1^*$ ), indicating that the optimum of the SOCP relaxation that is computed is not feasible for  $\mathcal{P}_1$ . As Table 2.2 shows,  $\mathcal{R}_{ch}$  is much faster than  $\mathcal{R}_1$  for large networks. The chordal extensions of the graphs are computed *a priori* for each case [53].  $\mathcal{R}_2$  is faster than both  $\mathcal{R}_1$  and  $\mathcal{R}_{ch}$ , but yields an infeasible solution for most IEEE benchmark systems considered.

---

<sup>6</sup>For the 2383-bus system, we only run  $\mathcal{R}_{ch}$ . For the optimal  $G_{ch}$ -partial matrix  $W_{ch}^*$ , we report the maximum and the median of the non-zero ratios of the first and second eigenvalues of  $W_{ch}^*(C)$  over all cliques  $C$  in  $G_{ch}$ .

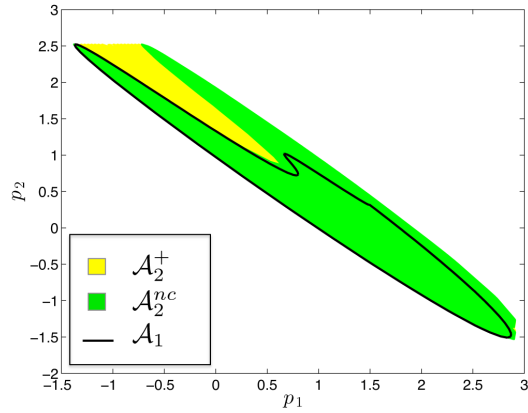


Figure 2.6: Projections of feasible regions on  $p_1 - p_2$  space for the 3-bus system in Figure 2.4.

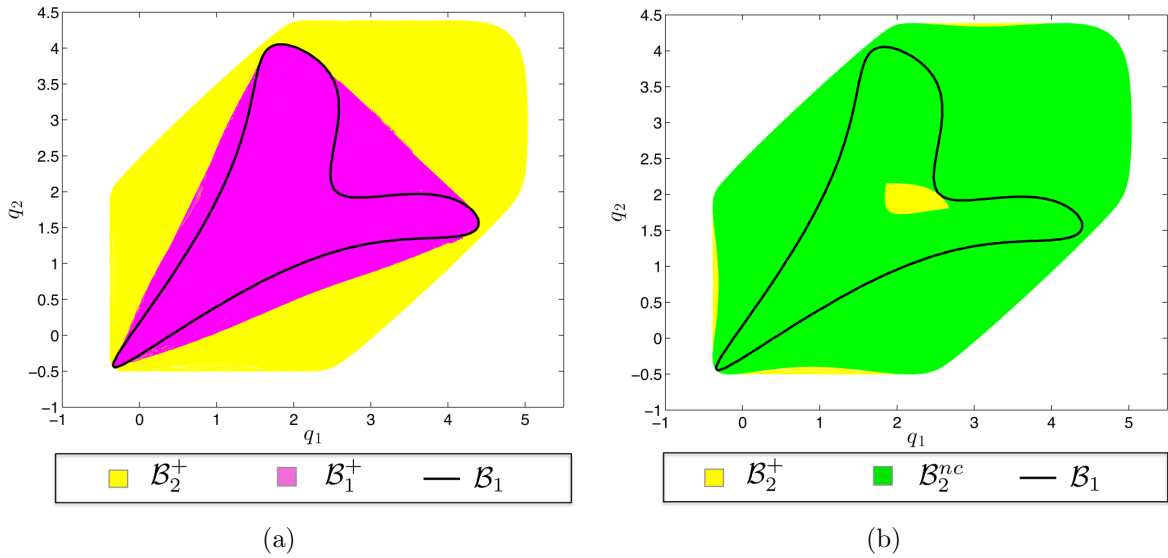


Figure 2.7: Projections of feasible regions on  $q_1 - q_2$  space for 3-bus system in Figure 2.4.

## Chapter 3

# Quadratically constrained quadratic programs on acyclic networks and tight conic relaxations

As we saw in the last chapter, Kirchoff's laws can be written in two ways using the bus injection and branch flow models. The power flow equations arising from such models can then be relaxed to convex sets; hence the feasible sets of the optimal power flow (OPF) problem can be represented as intersection of second-order or semidefinite cones. In this chapter, we explore sufficient conditions under which the nonconvex OPF problem can be solved using its conic relaxations. To that end, we restrict our attention to the bus injection model of Kirchoff's laws. As we have mentioned before, the OPF problem can be formulated as a quadratically constrained quadratic program (QCQP). We first prove a general result on QCQP on acyclic graphs that extends the class of nonconvex QCQPs solvable in polynomial time. Then we explore the application of this result to the OPF problem on acyclic networks.

### 3.1 Background on QCQP

A quadratically constrained quadratic program (QCQP) is an optimization problem in which both the objective function and the constraints are quadratic. Many engineering problems can be represented as QCQPs, e.g., [78–81], sensor network localization [82], principal component analysis [83] and optimal power flow [35, 36, 45]. A wide-range of combinatorial

problems can also be cast as QCQPs, e.g., the max-cut problem [84, 85] and the maximum stable set problem [86, 87]. In general, QCQPs are nonconvex, and therefore lack computationally efficient solution methods. The contribution of this chapter is to identify a class of nonconvex QCQPs for which globally optimal solutions can be guaranteed. The standard approach in the literature to solving a QCQP, optimally or approximately, is to relax this nonconvex problem to a convex conic program [55, 65]. There are polynomial-time interior-point algorithms to solve these relaxed programs cast as second-order cone programs (SOCP) or semidefinite programs (SDP) [66, 67, 88]. For applications of this technique to engineering problems, we refer the reader to [65, 89]. Several authors have investigated the accuracy of these relaxations [84] [90–93]. Others have studied conditions under which a conic relaxation of the QCQP is exact, i.e., an optimal solution of the QCQP can be computed from an optimal solution of its relaxation [94, 95]. We extend such results by proving a sufficient condition under which QCQPs with complex variables whose underlying graph structures are acyclic admit an efficient polynomial time solution through an SOCP or SDP relaxation. Note that QCQPs in complex variables can be recast as QCQPs in real variables; our result, however, is not implied by previous results. The result here generalizes our earlier result in [15] using a Lagrangian dual argument. For completeness, we also present an alternative proof using the optimal solution of the conic relaxation that is equivalent to an earlier independent result in [70].

In Section 3.2, we present a sufficient condition for a nonconvex QCQP over acyclic graphs to be solvable in polynomial time and prove it using two different techniques in Section 3.3. In Section 3.4, we compare our result with known results in the literature. Finally we discuss the application of our result on QCQP to the OPF problem in Section 3.5.

## 3.2 Formulation and result for a QCQP in complex variables

Consider the following QCQP with complex variable  $x \in \mathbb{C}^n$ , where  $\mathbb{C}$  is the set of complex numbers.

**Primal problem  $P$ :**

$$\begin{aligned} & \underset{x \in \mathbb{C}^n}{\text{minimize}} && x^H C_0 x \\ & \text{subject to:} && x^H C_p x \leq b_p, \quad p = 1, 2, \dots, m. \end{aligned}$$

where  $x^H$  denotes the conjugate transpose of  $x$ ,  $b_0, b_1, \dots, b_m$  are scalars and  $\mathcal{C} := \{C_0, C_1, \dots, C_m\}$  is a set of  $n \times n$  complex Hermitian matrices. If the matrices  $C_0, C_1, \dots, C_m$  are positive semidefinite, then problem  $P$  is a convex program and can be solved in polynomial time [55, 96]. Otherwise, problem  $P$  is generally non-convex and NP-hard. The main result of this chapter is to characterize the set  $\mathcal{C}$  such that problem  $P$  can be solved in polynomial time.

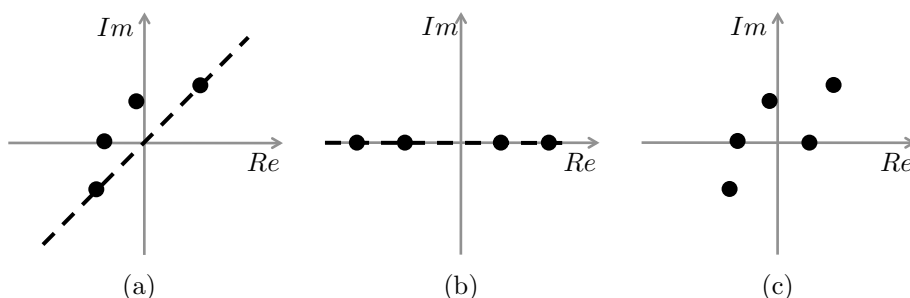


Figure 3.1: (a) and (b) are examples of sets of complex numbers that are linearly separable from the origin. (c) is an example of set that is not.

We first define some notation. For a Hermitian matrix  $Q$ , we define the *graph of matrix*  $Q$  (denoted by  $G(Q)$ ) as the undirected graph on  $n$  nodes, where nodes  $j$  and  $k$  ( $j \neq k, 1 \leq j, k \leq n$ ) share an edge if and only if  $Q_{jk} \neq 0$ . Intuitively, the graph  $G(Q)$  represents the sparsity pattern of the matrix  $Q$ . For the collection of matrices  $\mathcal{C}$ , extend this definition to the *graph of  $\mathcal{C}$*  (denoted by  $G(\mathcal{C})$ ) as the undirected graph on  $n$  nodes, where  $j$  and  $k$

$(j \neq k, 1 \leq j, k \leq n)$  share an edge if and only if  $j$  and  $k$  share an edge in at least one among  $G(C_0), G(C_1), \dots, G(C_m)$ , i.e., the complex numbers  $\{[C_0]_{jk}, [C_1]_{jk}, \dots, [C_m]_{jk}\}$  are not all identically zero.

A set of complex numbers is said to be *linearly separable from the origin* if there exists a line through the origin of the complex plane such that the points represented by this set of complex numbers lie on one side of that line. To illustrate this, consider the sets of complex numbers in Figure 3.1. While the sets in (a) and (b) are linearly separable from the origin, the set in (c) is not. The collection  $\mathcal{C}$  is said to be *off-diagonally linearly separable from the origin* if for each  $j \neq k, 1 \leq j, k \leq n$ , the set of complex numbers  $\{[C_0]_{jk}, [C_1]_{jk}, \dots, [C_m]_{jk}\}$  are linearly separable from the origin. Using this notation, we now present the main result of the chapter.

**Theorem 7.** *For QCQP  $P$ , suppose the feasible set is non-empty and bounded and the collection of matrices  $\mathcal{C}$  satisfies:*

1.  $G(\mathcal{C})$  is acyclic,
2.  $\mathcal{C}$  is off-diagonally linearly separable from the origin.

*Then,  $P$  can be solved in polynomial time.*

For a continuous optimization problem, we say it can be *solved in polynomial time* if given any  $\zeta > 0$ , there is an algorithm that finds a feasible solution to the optimization problem with an objective value within  $\zeta$  of the theoretical optimum in polynomial time [55, 65, 96].

### 3.3 Proof approaches

We now provide two proof techniques in Sections 3.3.1 and 3.3.2. Without loss of generality, assume throughout that the graph  $G(\mathcal{C})$  is connected and acyclic, i.e., it is a *tree*.

### 3.3.1 Proof using the dual problem

Here we prove Theorem 7 by characterizing the optimal solution of the Lagrangian dual problem of  $P$ . This approach requires an additional assumption: problem  $P$  is strictly feasible. It generalizes the result of [15].

For vector  $a$ , let  $a \gg 0$  denote that all its elements are strictly positive. The proof proceeds in two steps:

1. First, we prove the result for the following case. For all  $a \gg 0$ , suppose:

$$a_0[C_0]_{jk} + a_1[C_1]_{jk} + \dots + a_m[C_m]_{jk} \neq 0. \quad (3.1)$$

The relation in (3.1) implies that the convex hull of the set of complex numbers  $[C_0]_{jk}, [C_1]_{jk}, \dots, [C_m]_{jk}$  does not contain the origin of the complex plane in its interior. If this set is linearly separable from the origin, then (3.1) is generally satisfied unless all the points lie on a line through the origin of the complex plane.

2. Next, we relax the condition in equation (3.1).

Step 1: Consider the following semidefinite program  $RP$  where  $W$  is an  $n \times n$  complex positive semidefinite matrix.

**Relaxed Problem  $RP$ :**

$$\begin{aligned} & \underset{W \succeq 0}{\text{minimize}} && \text{tr}(C_0 W) \\ & \text{subject to:} && \text{tr}(C_p W) \leq b_p, \quad p = 1, 2, \dots, m. \end{aligned} \quad (3.2)$$

$RP$  is an SDP and hence can be solved in polynomial time using interior-point methods [66, 67, 88]. Define  $p_*$  and  $r_*$  as the optimum values of the objective functions for problems  $P$  and  $RP$  respectively.

**Lemma 8.**  $p_*, r_*$  are finite and  $p_* \geq r_*$ . If  $W_*$  solves  $RP$  optimally and  $\text{rank } W_* \leq 1$ , then  $p_* = r_*$  and  $x_*$  solves  $P$  optimally, where  $x_*$  uniquely solves  $W_* = x_* x_*^H$ .

*Proof.* Since the feasible set of  $P$  (and hence of  $RP$ ) are bounded,  $p_*$  and  $r_*$  are finite. Given any feasible solution  $x$  of  $P$ ,  $W := xx^H$  is a feasible solution of  $RP$ . Hence  $RP$  is feasible and  $p_* \geq r_*$ . If  $\text{rank } W_* = 0$ , then  $W_* = 0$ , and an optimal solution to  $P$  is  $x_* = 0$ , and therefore  $r_* = p_*$ . If  $\text{rank } W_* = 1$  then  $W_*$  has a unique decomposition  $W_* = x_*x_*^H$ , where  $r_* = \text{tr}(C_0W_*) = x_*^H C_0 x_* = p_*$ .  $\square$

Next, we show that there exists a finite  $W_*$  that solves  $RP$  optimally and has  $\text{rank } W_* \leq 1$ . Let the Lagrange multipliers for the inequalities in (3.2) be  $\lambda_p \geq 0$  for  $p = 1, 2, \dots, m$ . Then the Lagrangian dual of  $P$  (and also of  $RP$ ) is

**Dual problem  $DP$ :**

$$\begin{aligned} & \underset{\lambda \geq 0}{\text{maximize}} && - \sum_{p=1}^m \lambda_p b_p \\ & \text{subject to:} && \underbrace{C_0 + \sum_{p=1}^m \lambda_p C_p}_{:=A(\lambda)} \succeq 0. \end{aligned}$$

It can be checked that the graph of the matrix  $A(\lambda)$  (denoted by  $G(A(\lambda))$ ) is a subgraph of  $G(\mathcal{C})$ . For some values of  $\lambda$  however, edge  $(j, k)$  may exist in  $G(\mathcal{C})$  but not in  $G(A(\lambda))$ ; in this case  $G(A(\lambda))$  is acyclic but may not be connected, and hence it may be a forest of two or more disconnected trees rather than a single connected tree that spans all vertices in the graph. From the relation in (3.1), it follows that for all  $\lambda \gg 0$ , the graph  $G(A(\lambda))$  is connected.

Next we characterize the relationship between the optimal points of  $RP$  and  $DP$ . The feasible sets of  $P$  (and hence of  $RP$ ) are bounded. Thus  $r_*$  is attained by a finite optimum. Let  $d_*$  denote the optimal objective value of problem  $DP$ . Problems  $P$  and hence  $RP$  are strictly feasible. From Slater's condition [55], it then follows that  $r_* = d_*$  and  $d_*$  is attained. Thus,  $RP/DP$  has a finite primal dual optimal point  $(W_*, \lambda_*)$ .

For convenience, define  $A_* := A(\lambda_*)$ .

**Lemma 9.** *If  $G(A_*)$  is connected then  $\text{rank } W_* \leq 1$ .*

*Proof.* We observe that  $\text{rank } A_* \geq n - 1$ . This follows from a result in the literature [97], [98, Theorem 3.4] and [99, Corollary 3.9] that states that for any  $n \times n$  positive semidefinite matrix  $Q$  where the associated graph  $G(Q)$  is a connected acyclic graph (i.e., a tree),  $\text{rank } Q \geq n - 1$ .

Next we show that  $\text{rank } W_* \leq 1$ . The complementary slackness condition for optimality of  $(W_*, \lambda_*)$  implies  $\text{tr}(A_* W_*) = 0$ . Let  $W_* = \sum_i \rho_i w_i w_i^H$  be the spectral decomposition of  $W_*$ . Then,  $\text{tr}(A_* W_*) = \sum_i \rho_i w_i^H A_* w_i = 0$ . Since  $A_* \succeq 0$ , the eigenvectors  $w_i$  of  $W_*$  corresponding to nonzero eigenvalues  $\rho_i$  are all in the null space of  $A_*$ . The rank of  $A_*$  is at least  $n - 1$  and hence its null space has dimension at most 1, from which it follows that  $\text{rank } W_* \leq 1$ .  $\square$

$G(A_*)$  can be connected in one of two ways: (a) For each edge  $(j, k)$  in  $G(\mathcal{C})$ , the origin of the complex plane lies strictly outside the convex hull of the points  $[C_0]_{jk}, [C_1]_{jk}, \dots, [C_m]_{jk}$ , or (b)  $\lambda_* \gg 0$ . In both cases, lemma 9 guarantees that  $\text{rank } W_* \leq 1$ .

If the origin lies on the boundary of the convex hull, then  $G(A_*)$  may not be connected when  $\lambda_* \not\gg 0$  and  $\text{rank } W_* \leq 1$  may not hold. We use a perturbation [100, 101] of  $RP/DP$ , where  $G(A_*)$  is connected in the perturbed problem. In particular, define the perturbed problems for parameter  $\varepsilon > 0$ :

**Perturbed relaxed problem  $RP^\varepsilon$ :**

$$\begin{aligned} & \underset{W \succeq 0}{\text{minimize}} && \text{tr}(C_0 W) - \varepsilon \sum_{p=1}^m [b_p - \text{tr}(C_p W)] \\ & \text{subject to:} && \text{tr}(C_p W) \leq b_p, \quad p = 1, 2, \dots, m. \end{aligned}$$

**Perturbed dual problem  $DP^\varepsilon$ :**

$$\begin{aligned} & \underset{\lambda}{\text{maximize}} && - \sum_{p=1}^m \lambda_p b_p \\ & \text{subject to:} && A(\lambda) \succeq 0, \quad \lambda_p \geq \varepsilon, \quad p = 1, 2, \dots, m. \end{aligned}$$

For any variable  $z$  in the original problem, let  $z^\varepsilon$  denote the corresponding variable in the perturbed problem with perturbation parameter  $\varepsilon$ . The feasible sets of  $RP$  and  $RP^\varepsilon$  are

identical and hence bounded. Thus,  $r_*^\varepsilon$  is finite and attained. Moreover,  $RP^\varepsilon$  is strictly feasible. From Slater's condition, it follows that  $r_*^\varepsilon = d_*^\varepsilon$  and  $RP^\varepsilon/DP^\varepsilon$  has a finite primal dual optimal point  $(W_*^\varepsilon, \lambda_*^\varepsilon)$ . Moreover,  $\lambda_*^\varepsilon \geq \varepsilon \mathbf{1} \gg 0$  and hence  $G(A_*^\varepsilon)$  is connected. Then it implies  $\text{rank } W_*^\varepsilon \leq 1$ .

Now consider a decreasing sequence of  $\varepsilon \downarrow 0$ . For each  $\varepsilon > 0$ , the optimal solution  $W_*^\varepsilon$  of  $RP^\varepsilon$  has rank at most 1 and lies in the (bounded) feasible set of  $RP^\varepsilon$ . Since the space of positive semidefinite matrices with rank at most 1 is a closed set [64], the sequence  $W_*^\varepsilon$  resides in a compact space and hence admits a convergent subsequence. It is easy to check that the limit point  $\hat{W}$  of this convergent subsequence is indeed feasible for  $RP$  and satisfies  $\text{rank } \hat{W} \leq 1$ . Next, we show that  $\hat{W}$  solves  $RP$  optimally, i.e.,  $r_* = \text{tr}(C_0 \hat{W})$ .

For any matrix  $W$  feasible for  $RP$  (and  $RP^\varepsilon$ ), we have

$$\text{tr}(C_0 W) - \varepsilon \sum_{p=1}^m [b_p - \text{tr}(C_p W)] \leq \text{tr}(C_0 W).$$

Minimizing over the feasible sets of  $RP$  (or equivalently  $RP^\varepsilon$ ), we obtain  $r_*^\varepsilon \leq r_*$ . Taking limit over the convergent subsequence, we have  $\text{tr}(C_0 \hat{W}) \leq r_*$ . Moreover,  $r_*$  is the optimum value of  $RP$  and hence  $r_* \leq \text{tr}(C_0 \hat{W})$ . Thus,  $r_* = \text{tr}(C_0 \hat{W})$ .

So far we have shown that  $RP$  has a minimizer  $\hat{W}$  that satisfies  $\text{rank } \hat{W} \leq 1$  and  $p_* = r_*$ . But in general, it is hard to guarantee that solving  $RP$  would yield the minimum rank optimizer if the set of optimizers of  $RP$  is non-unique. Next, we provide an algorithm to use the perturbed problems to solve  $P$  in polynomial time.

First, solve  $RP$  in polynomial time to obtain  $r_*$ . If the associated optimizer  $W_*$  has rank at most 1, then construct  $x_*$  from  $W_*$  as in lemma 8 and we are done. Otherwise, fix a small  $\varepsilon_0$  and solve  $RP^{\varepsilon_0}$  in polynomial time. For any  $\varepsilon$  in  $(0, \varepsilon_0)$ , we have

$$r_*^\varepsilon = \text{tr}(C_0 W_*^\varepsilon) - \varepsilon \sum_{p=1}^m [b_p - \text{tr}(C_p W_*^\varepsilon)] \leq r_* \leq \text{tr}(C_0 W_*^\varepsilon),$$

Also, comparing the objective function values of  $RP^\varepsilon$  and  $RP^{\varepsilon_0}$  at  $W_*^\varepsilon$  and  $W_*^{\varepsilon_0}$ , respectively,

we obtain

$$\sum_{p=1}^m [b_p - \text{tr}(C_p W_*^\varepsilon)] \leq \sum_{p=1}^m [b_p - \text{tr}(C_p W_*^{\varepsilon_0})].$$

Combining the above two equations, we get

$$|r_* - \text{tr}(C_0 W_*^\varepsilon)| \leq \varepsilon \sum_{p=1}^m [b_p - \text{tr}(C_p W_*^{\varepsilon_0})].$$

Given  $\zeta > 0$ , choose  $\varepsilon$  in  $(0, \varepsilon_0)$  such that  $\varepsilon \sum_{p=1}^m [b_p - \text{tr}(C_p W_*^{\varepsilon_0})] \leq \zeta$ . Now solve  $RP^\varepsilon$  in polynomial time to get  $W_*^\varepsilon$  that satisfies  $\text{rank } W_*^\varepsilon \leq 1$  and compute  $x_*^\varepsilon$  from it. Then  $x_*^\varepsilon$  is a feasible point of  $P$  and  $p_* \leq (x_*^\varepsilon)^H C_0(x_*^\varepsilon) \leq p_* + \zeta$  and we have computed  $x_*^\varepsilon$  in polynomial time. This completes Step 1.

Step 2: Here we relax the extra condition required in (3.1). The proof relies on another perturbation of  $RP$  such that the matrices in the perturbed problem satisfies (3.1). We use Step 1 to solve this perturbed problem in polynomial time and use it to solve  $P$  in polynomial time.

Suppose there exists an edge  $(j, k)$ , such that the set of complex numbers  $[C_0]_{jk}, [C_1]_{jk}, \dots, [C_m]_{jk}$  lie on a line through the origin. This set does *not* satisfy (3.1) but is linearly separable from the origin. Given the set  $[C_0]_{jk}, [C_1]_{jk}, \dots, [C_m]_{jk}$ , there exists a complex number  $u^{jk}$  such that for all  $a \gg 0$ , we have

$$a_0 ([C_0]_{jk} - u^{jk}) + a_1 [C_1]_{jk} + \dots + a_m [C_m]_{jk} \neq 0.$$

Construct an  $n \times n$  Hermitian matrix  $U^{jk}$ , where all entries are zeros, except  $[U^{jk}]_{jj} = [U^{jk}]_{kk} = |u^{jk}|$  and  $[U^{jk}]_{jk} = [U^{jk}]_{kj}^H = -u^{jk}$ . Then  $U^{jk} \succeq 0$ . Now, suppose (3.1) is violated at edges  $(j_1, k_1), (j_2, k_2), \dots, (j_s, k_s)$  in  $G(\mathcal{C})$ . Then construct  $U^{j_1 k_1}, U^{j_2 k_2}, \dots, U^{j_s k_s}$  as above and define

$$U := U^{j_1 k_1} + U^{j_2 k_2} + \dots + U^{j_s k_s} \succeq 0.$$

Consider the perturbed problems for  $\delta > 0$ :

**Perturbed primal problem  $P^{(\delta)}$ :**

$$\begin{aligned} & \underset{x \in \mathbb{C}^n}{\text{minimize}} && x^H (C_0 + \delta U) x \\ & \text{subject to:} && x^H C_p x \leq b_p, \quad p = 1, 2, \dots, m. \end{aligned}$$

**Perturbed relaxed problem  $RP^{(\delta)}$ :**

$$\begin{aligned} & \underset{W \succeq 0}{\text{minimize}} && \text{tr}[(C_0 + \delta U)W] \\ & \text{subject to:} && \text{tr}(C_p W) \leq b_p, \quad p = 1, 2, \dots, m, \end{aligned}$$

For any variable  $z$  in  $P/RP$ , let  $z^{(\delta)}$  denote the corresponding variable in  $P^{(\delta)}/RP^{(\delta)}$ . First, we show that  $RP$  has an optimizer  $W_*$  with rank at most 1 and conclude  $p_* = r_*$ . Then we use this to provide a polynomial time computation for  $P$ .

The matrices in the perturbed problems satisfy the relation in (3.1). From Step 1, there exists  $W_*^{(\delta)} \succeq 0$  that solves  $RP^{(\delta)}$  and  $\text{rank } W_*^{(\delta)} \leq 1$ . Following the arguments for Lemma 8, we have

$$p_*^{(\delta)} = r_*^{(\delta)} = \text{tr}[(C_0 + \delta U)W_*^{(\delta)}].$$

The feasible region of  $RP$  (and hence of  $RP^{(\delta)}$ ) is bounded. Taking  $\delta \downarrow 0$  and following the perturbation argument for  $RP^\varepsilon$ , we have a convergent subsequence of  $W_*^{(\delta)}$  with the limit point  $\hat{W}$ . Then  $\hat{W}$  is feasible for  $RP$ . Now, we show that it is optimal for  $RP$ , i.e.,  $r_* = \text{tr}(C_0 \hat{W})$ .

$r_*^{(\delta)}$  is non-decreasing in  $\delta$ . Then  $r_* \leq \text{tr}(C_0 \hat{W}) \leq r_*^{(\delta)}$ . Suppose  $r_* < \text{tr}(C_0 \hat{W})$ , i.e., the inequality is strict. Let  $W'_*$  be any optimizer of  $RP$  and choose a small enough  $\delta > 0$ , such that

$$r_* + \delta \text{tr}(UW'_*) < \text{tr}(C_0 \hat{W}) \leq r_*^{(\delta)}.$$

For this  $\delta$ ,  $(W'_* + W_*^{(\delta)})/2$  is a feasible point of  $RP^{(\delta)}$ . Since  $r_*^{(\delta)}$  is the optimal objective

value of  $RP^{(\delta)}$ , it follows that

$$\begin{aligned} r_*^{(\delta)} &\leq \text{tr} \left[ (C_0 + \delta U) \left( \frac{W_*' + W_*^{(\delta)}}{2} \right) \right] \\ &= \frac{1}{2} r_*^{(\delta)} + \frac{1}{2} [r_* + \delta \text{tr}(UW_*')] \\ &< r_*^{(\delta)}. \end{aligned}$$

This is a contradiction and hence  $r_* = \text{tr}(C_0 \hat{W})$ .

Now, we show how to use this perturbation technique to solve  $P$  in polynomial time. Solve  $RP$  to get  $r_* = p_*$ . If the optimizer  $W_*$  of  $RP$  has rank at most 1, compute  $x_*$  from  $W_*$  as in lemma 8 then we have solved  $P$  in polynomial time. Otherwise, choose a small  $\delta_0 > 0$  and solve  $RP^{(\delta_0)}$  in polynomial time to get the minimizer  $W_*^{(\delta_0)}$  and the minimum  $r_*^{(\delta_0)} = p_*^{(\delta_0)}$ . For any  $\delta$  in  $(0, \delta_0)$ ,

$$p_* = r_* \leq \text{tr}(C_0 W_*^{(\delta)}) \leq p_*^{(\delta)}. \quad (3.3)$$

Also,  $p_*^{(\delta)}$  is convex in  $\delta$  [101] and hence

$$p_*^{(\delta)} \leq p_* + \frac{\delta}{\delta_0} (p_*^{(\delta_0)} - p_*). \quad (3.4)$$

Given  $\zeta > 0$ , choose  $\delta$  sufficiently small so that  $\frac{\delta}{\delta_0} (p_*^{(\delta_0)} - p_*) \leq \zeta$ . For this  $\delta$ , solve  $RP^{(\delta)}$  arbitrarily closely in polynomial time to get  $W_*^{(\delta)}$  that has rank at most 1 and compute  $x_*^{(\delta)}$ . From equations (3.3) and (3.4),  $x_*^{(\delta)}$  satisfies  $p_* \leq (x_*^{(\delta)})^H C_0 (x_*^{(\delta)}) \leq p_* + \zeta$ . In summary, we have computed  $x_*^{(\delta)}$  in polynomial time, that is feasible for  $P$  with an objective value within  $\zeta$  of the theoretical optimum. This completes Step 2.

### 3.3.2 Proof using the relaxed problem

Here we use an optimal solution of the relaxed problem  $RP$  to construct an optimal solution of  $P$ . It is equivalent to an earlier proof in [70] and included here for completeness.

The feasible set of  $RP$  is bounded (since feasible set of  $P$  is bounded) and hence  $RP$  can be solved in polynomial time [66, 67, 88] to obtain a finite optimizer  $W_*$ . Now we construct an optimal solution of  $P$  from  $W_*$ , thus solving  $P$  in polynomial time.

**Lemma 10.** *Suppose  $x \in \mathbb{C}^n$  satisfies  $x^H C x \leq \text{tr}(C W_*)$  for all  $C \in \mathcal{C}$ . Then  $x$  is an optimal solution of  $P$ .*

*Proof.* We have  $x^H C_p x \leq \text{tr}(C_p W_*) \leq b_p$ ,  $p = 1, 2, \dots, m$  and hence  $x$  is feasible. Also,  $x^H C_0 x = \text{tr}(C_0 x x^H) \leq \text{tr}(C_0 W_*)$ . But  $x x^H$  is feasible in  $RP$ . Since  $W_*$  is optimal for  $RP$ , we obtain  $x^H C_0 x = \text{tr}(C_0 W_*)$ . The result then follows from the fact that  $x$  achieves the optimal objective value of its relaxation  $RP$ .  $\square$

In what follows, we construct such an  $n$ -dimensional complex vector  $x$ , in two steps. First we construct an  $n \times n$  Hermitian matrix  $R$  with  $R_{jj} R_{kk} = |R_{jk}|^2$  for each  $(j, k)$  in  $G(\mathcal{C})$  that satisfies  $\text{tr}(C R) \leq \text{tr}(C W_*)$  for all  $C \in \mathcal{C}$ . Next we construct  $x$  from  $R$  that satisfies

$$x^H C x = \text{tr}(C R) \leq \text{tr}(C W_*) \quad \text{for all } C \in \mathcal{C} \quad (3.5)$$

Step 1: Constructing  $R$  from  $W_*$ . For each  $(j, k)$  in  $G(\mathcal{C})$ , the set of complex numbers  $[C_0]_{jk}, [C_1]_{jk}, \dots, [C_m]_{jk}$  is linearly separable from the origin. Thus for each  $(j, k)$  in  $G(\mathcal{C})$ , there exists an angle  $\alpha_{jk} \in [0, 2\pi]$ , such that for all  $p = 0, 1, \dots, m$ ,

$$\alpha_{jk} \leq \angle [C_p]_{jk} \leq \alpha_{jk} + \pi. \quad (3.6)$$

Since the matrices in  $\mathcal{C}$  are Hermitian,  $\alpha_{kj} = \pi - \alpha_{jk} \pmod{2\pi}$ . Define  $R_{jj} := [W_*]_{jj}$ . For each  $(j, k)$  in  $G(\mathcal{C})$ , let

$$R_{kj} = [W_*]_{kj} + w_{kj} \exp[\mathbf{i}(-\pi/2 + \alpha_{kj})],$$

for some  $w_{kj} \geq 0$  to be determined below. Note that we leave  $R_{jk}$  unspecified for  $(j, k)$  not in  $G(\mathcal{C})$ ; we will return to this point later.

We now show that the inequality in (3.5) is satisfied as long as  $w_{kj} \geq 0$  and then choose  $w_{kj}$  to satisfy  $R_{jj}R_{kk} = |R_{jk}|^2$  for each  $(j, k)$  in  $G(\mathcal{C})$ . We have for each  $C \in \mathcal{C}$ ,

$$\begin{aligned}
& \text{tr}[C(R - W_*)] \\
&= \sum_{j=1}^n C_{jj} \underbrace{(R_{jj} - [W_*]_{jj})}_{=0 \text{ by construction}} + \sum_{\substack{j \neq k, \\ 1 \leq j, k \leq n}} C_{jk} (R_{kj} - [W_*]_{kj}) \\
&= \sum_{(j,k) \text{ in } G(\mathcal{C})} \text{Re} \{C_{jk} (R_{kj} - [W_*]_{kj})\} \\
&= \sum_{(j,k) \text{ in } G(\mathcal{C})} |C_{jk}| w_{kj} \cos \underbrace{(\angle C_{jk} - \pi/2 + \alpha_{kj})}_{\in [\pi/2, 3\pi/2] \text{ from (3.6)}} \\
&\leq 0
\end{aligned}$$

as required in (3.5). We now choose  $w_{kj}$  such that  $R_{jj}R_{kk} = |R_{jk}|^2$ , i.e.,

$$[W_*]_{jj}[W_*]_{kk} = \left| [W_*]_{kj} + w_{kj} \exp[\mathbf{i}(-\pi/2 + \alpha_{kj})] \right|^2.$$

This is a quadratic in  $w_{kj}$  and admits a solution  $w_{kj} = \sqrt{b^2 + c} - b$ , where

$$\begin{aligned}
b &:= \text{Re} \{ [W_*]_{kj} \exp[\mathbf{i}(\pi/2 - \alpha_{kj})] \}, \\
c &:= [W_*]_{jj}[W_*]_{kk} - |[W_*]_{kj}|^2.
\end{aligned}$$

Since  $W_* \succeq 0$ , the  $2 \times 2$  principal minor corresponding to the  $i$ -th and  $j$ -th rows and columns is positive semidefinite. Thus,  $[W_*]_{jj}[W_*]_{kk} - |[W_*]_{kj}|^2 = c \geq 0$  that implies  $w_{kj} \geq 0$ .

Step 2: Constructing  $x$  from  $R$ .

1. Define  $|x_j| := \sqrt{R_{jj}}$  for each  $1 \leq j \leq n$ .
2. Define  $\angle x_1 := 0$ . For any node  $2 \leq j \leq n$ , find the unique path from node 1 to node  $j$  in the acyclic graph  $G(\mathcal{C})$ , given by the sequence of edges  $(\ell_0 = 1, \ell_1), (\ell_1, \ell_2), \dots, (\ell_i, \ell_{i+1} = j)$ . Then define  $\angle x_j := -\sum_{k=0}^i \angle R_{\ell_k \ell_{k+1}}$ .

Note that for  $(j, k)$  in  $G(\mathcal{C})$ ,  $\angle R_{kj} = \angle x_k - \angle x_j$ . Then the equality in (3.5) is satisfied since

$$\begin{aligned}
& x^H C x - \text{tr}(CR) \\
&= \sum_{j=1}^n C_{jj} \underbrace{(|x_j|^2 - R_{jj})}_{=0 \text{ by construction}} + \sum_{\substack{j \neq k, \\ 1 \leq j, k \leq n}} C_{jk} (x_j^H x_k - R_{kj}) \\
&= \sum_{(j,k) \text{ in } G(\mathcal{C})} \text{Re} \{ C_{jk} (x_j^H x_k - R_{kj}) \} \\
&= \sum_{(j,k) \text{ in } G(\mathcal{C})} \text{Re} \{ C_{jk} (|x_j| |x_k| \exp[\mathbf{i}(\angle x_k - \angle x_j)] - R_{kj}) \} \\
&= \sum_{(j,k) \text{ in } G(\mathcal{C})} \text{Re} \left\{ C_{jk} \underbrace{(\sqrt{R_{jj} R_{kk}} \exp[\mathbf{i} \angle R_{kj}])}_{=R_{kj} \text{ by construction}} - R_{kj} \right\} \\
&= 0.
\end{aligned}$$

Note that our construction does not require  $R_{jk}$  nor  $[W_*]_{jk}$  for  $(j, k)$  not in  $G(\mathcal{C})$ . We only use the fact that  $[W_*]_{jj}[W_*]_{kk} - |[W_*]_{kj}|^2 \geq 0$  for  $(j, k)$  in  $G(\mathcal{C})$ . We can indeed formulate another relaxation of  $P$  in terms of the variables  $\{W_{jj}, 1 \leq j \leq n\}$  and  $\{W_{jk}, W_{kj} = W_{jk}^H, (j, k) \text{ in } G(\mathcal{C})\}$  with the constraint

$$W_{jj}W_{kk} - |W_{jk}|^2 \geq 0.$$

The above defines a second-order cone [55] and hence this relaxation is an SOCP. The feasible set of this relaxation is bounded and can be solved in polynomial time. The above construction then yields an optimal solution of  $P$  from the optimal solution of this SOCP relaxation.

### 3.4 QCQP in real variables

In the QCQP  $P$ , suppose the matrices in set  $\mathcal{C}$  are real and symmetric, then all off-diagonal elements of the matrices in  $\mathcal{C}$  are always linearly separable from the origin. If in addition,

the graph  $G(\mathcal{C})$  is acyclic, then Theorem 7 implies an optimal solution  $x_* \in \mathbb{C}^n$  of  $P$  can be solved in polynomial time.

Let  $\mathbb{R}$  denote the set of real numbers. Authors of [94, 95] have considered the case where  $P$  is solved over  $x \in \mathbb{R}^n$  and  $RP$  is solved over real symmetric matrices  $W \in \mathbb{R}^{n \times n}$ . The authors of [94] consider QCQPs where  $G(\mathcal{C})$  may contain cycles, but require a particular sign pattern of its off-diagonal entries. Restricted to acyclic graphs, this condition is equivalent to  $[C_0]_{jk}, [C_1]_{jk}, \dots, [C_m]_{jk}$  having the same sign for each edge  $(j, k)$  in  $G(\mathcal{C})$ . It can be checked that the proof technique in Section 3.3.2 is a generalization of the approach in [94, Theorem 3.4] and can be used to prove the result in [94, Theorem 3.4] with minor modifications. Theorem 7, however, generalizes to complex QCQPs and cannot be obtained by transforming a QCQP in the complex domain to an equivalent QCQP in the real domain using the following transformation [55, 65] of the quadratic forms:

$$x^H C x = \begin{pmatrix} \operatorname{Re} x \\ \operatorname{Im} x \end{pmatrix}^T \begin{pmatrix} \operatorname{Re} C & -\operatorname{Im} C \\ \operatorname{Im} C & \operatorname{Re} C \end{pmatrix} \begin{pmatrix} \operatorname{Re} x \\ \operatorname{Im} x \end{pmatrix},$$

where for any vector or matrix  $y$ ,  $y^T$  denotes its transpose. This discussion is summarized in the following.

**Corollary 11.** *Suppose QCQP  $P$  has a non-empty and bounded feasible set. For all  $C \in \mathcal{C}$  let  $C$  be symmetric and in  $\mathbb{R}^{n \times n}$ . If  $G(\mathcal{C})$  is acyclic,*

1. *Then an optimal solution  $x_* \in \mathbb{C}^n$  of  $P$  can be obtained in polynomial time.*
2. *If for each edge  $(j, k)$  in  $G(\mathcal{C})$ , the real numbers  $C_{jk}, C \in \mathcal{C}$  have the same sign, then an optimal solution  $x_* \in \mathbb{R}^n$  of  $P$  can be obtained in polynomial time.*

**Remark 4.** *The authors in [94, 95] consider an additional convex constraint in  $P$  of the form  $x^2 \in \mathcal{F}$ , where  $x^2$  is the  $n \times 1$  vector with  $(x_i)^2$  as its  $i$ -th component and  $\mathcal{F}$  is a bounded convex set. This adds the constraint  $\operatorname{diag}(W) \in \mathcal{F}$  in the relaxation  $RP$ . Our proofs in Section 3.3.1 and 3.3.2 remain unchanged with this additional constraint on the diagonal elements of  $W$ .*

## 3.5 Optimal Power Flow: An application

As previously discussed, OPF can be cast as a QCQP. In Chapter 2, we discussed the formulations of OPF and its conic relaxations through the bus injection and branch flow models. In this section, we only use the bus injection model. In what follows, we examine the application of Theorem 7 to derive sufficient conditions on the tightness of such conic relaxations. For completeness of this chapter, we start by summarizing recent results on OPF relaxations in Section 3.5.1, though most have been discussed in detail in Chapter 2. In Section 3.5.2 we formulate OPF as a QCQP. Our formulation here is a much more detailed exposition of the formulation of the bus injection model presented in the chapter before. Then, we restrict ourselves to OPF over radial networks and use Theorem 7 to provide a sufficient condition under which the OPF problem can be solved efficiently in Section 3.5.3. Notice that radial networks are important for power systems because most distribution systems are indeed radial.

### 3.5.1 Relation to prior work

The SDP based relaxation for OPF is proposed in [35,102] and its use is illustrated on several IEEE test systems in [63] using an interior-point method. The authors in [36] propose to solve the convex Lagrangian dual of the OPF problem and derive a sufficient condition that allows the optimal solution for the OPF to be recovered from that of the dual. Though an SDP relaxation recovers an OPF solution for most IEEE test systems, it does not work on all problem instances; such limitations have been most recently discussed in [1]. The non-convexity of power flow solutions, has however, been studied earlier, e.g., in [37,103–105]. This motivates the study of sufficient conditions under which the SDP-based conic relaxation provides an optimal solution of the OPF problem.

Recently a series of works have studied OPF over radial networks and proved a variety of sufficient conditions that guarantee exact convex relaxations. It has been independently reported in [15,37,38] that the semidefinite relaxation of OPF is exact for radial networks provided certain conditions on the power flow constraints are satisfied. Note that such

sufficient conditions have also been explored for the branch flow models, e.g., authors in [46, 50, 51] prove that this relaxation is exact for radial networks when there are no upper bounds on loads, or when there are no upper bounds on voltage magnitudes. Using the equivalence result from Chapter 2, we notice that such results also carry over to the bus injection models.

### 3.5.2 Problem Formulation

Consider a power system network with  $n$  nodes (buses). The admittance-to-ground at bus  $i$ , for  $1 \leq i \in \mathbb{Z} \leq n$ , is  $y_{ii}$  and the admittance of the line between connected nodes  $i$  and  $j$  (denoted by  $i \sim j$ ) is  $y_{ij} = g_{ij} - \mathbf{i}b_{ij}$ . Typically,  $g_{ij} \geq 0$  and  $b_{ij} \geq 0$ , i.e., the lines are resistive and inductive. Define the corresponding  $n \times n$  admittance matrix  $Y$  as

$$Y_{ij} = \begin{cases} y_{ii} + \sum_{j \sim i} y_{ij}, & \text{if } i = j, \\ -y_{ij}, & \text{if } i \neq j \text{ and } i \sim j, \\ 0 & \text{otherwise.} \end{cases}$$

**Remark 5.**  $Y$  is symmetric but not necessarily Hermitian.

The remaining circuit parameters and their relations are defined as follows.

- $V$  and  $I$  are  $n$ -dimensional complex voltage and current injection vectors, where  $V_k, I_k$  denote the nodal voltage and the injection current at bus  $1 \leq k \leq n$  respectively. The voltage magnitude  $|V_k|$  is bounded as

$$0 < \underline{W}_k \leq |V_k|^2 \leq \overline{W}_k.$$

- $S_k = P_k + \mathbf{i}Q_k$  is the complex power injection at node  $1 \leq k \leq n$ , where  $P_k$  and  $Q_k$ , respectively, denote the real and reactive power injections and

$$S_k = V_k I_k^H. \tag{3.7}$$

- $P_k^D$  and  $Q_k^D$  are the real and reactive power demands at bus  $1 \leq k \leq n$ , which are assumed to be fixed and given.
- $P_k^G$  and  $Q_k^G$  are the real and reactive power generation at bus  $1 \leq k \leq n$ . They are decision variables that satisfy the constraints  $\underline{P}_k \leq P_k^G \leq \overline{P}_k$  and  $\underline{Q}_k \leq Q_k^G \leq \overline{Q}_k$ .

Power balance at each bus  $1 \leq k \leq n$  requires  $P_k^G = P_k^D + P_k$  and  $Q_k^G = Q_k^D + Q_k$ , which leads us to define

$$\begin{aligned}\underline{P}_k &:= \underline{P}_k^G - P_k^D, & \overline{P}_k &:= \overline{P}_k^G - P_k^D \\ \underline{Q}_k &:= \underline{Q}_k^G - Q_k^D, & \overline{Q}_k &:= \overline{Q}_k^G - Q_k^D.\end{aligned}$$

The power injections at each bus  $1 \leq k \leq n$  are then bounded as

$$\underline{P}_k \leq P_k \leq \overline{P}_k, \quad \underline{Q}_k \leq Q_k \leq \overline{Q}_k.$$

The branch power flows and their limits are defined as follows.

- $S_{ij} = P_{ij} + \mathbf{i}Q_{ij}$  is the sending-end complex power flow from node  $i$  to node  $j$ , where  $P_{ij}$  and  $Q_{ij}$  are the real and reactive power flows respectively. The real power flows are constrained as  $|P_{ij}| \leq \overline{F}_{ij}$  where  $\overline{F}_{ij}$  is the line-flow limit between nodes  $i$  and  $j$  and  $\overline{F}_{ij} = \overline{F}_{ji}$ .
- $L_{ij} = P_{ij} + P_{ji}$  is the power loss over the line between nodes  $i$  and  $j$ , satisfying  $L_{ij} \leq \overline{L}_{ij}$  where  $\overline{L}_{ij}$  is the thermal line limit and  $\overline{L}_{ij} = \overline{L}_{ji}$ . Also, observe that since  $L_{ij} \geq 0$ , we have  $|P_{ij}| \leq \overline{F}_{ij}, |P_{ji}| \leq \overline{F}_{ji}$  if and only if  $P_{ij} \leq \overline{F}_{ij}, P_{ji} \leq \overline{F}_{ji}$ .

For  $1 \leq k \leq n$ , let  $J_k = e_k e_k^H$  where  $e_k$  is the  $k$ -th canonical basis vector in  $\mathbb{C}^n$ . Define  $Y_k := e_k e_k^H Y$ . Substituting these expressions into (3.7) yields

$$\begin{aligned}S_k &= e_k^H V I^H e_k = \text{tr}(V V^H (Y^H e_k e_k^H)) = V^H Y_k^H V \\ &= V^H \underbrace{\left( \frac{Y_k^H + Y_k}{2} \right)}_{=: \Phi_k} V + \mathbf{i} V^H \underbrace{\left( \frac{Y_k^H - Y_k}{2\mathbf{i}} \right)}_{=: \Psi_k} V,\end{aligned}$$

where  $\Phi_k$  and  $\Psi_k$  are Hermitian matrices. Thus, the two quantities  $V^H \Phi_k V$  and  $V^H \Psi_k V$  are real numbers and

$$P_k = V^H \Phi_k V, \quad Q_k = V^H \Psi_k V.$$

The real power flow from  $i$  to  $j$  can be expressed as a quadratic form as follows.

$$P_{ij} = \text{Re} \{V_i (V_i - V_j)^H y_{ij}^H\} = V^H M^{ij} V,$$

where  $M^{ij}$  is an  $n \times n$  Hermitian matrix.

The thermal loss of the line connecting buses  $i$  and  $j$  is

$$L_{ij} = L_{ji} = P_{ij} + P_{ji} = V^H T^{ij} V$$

where  $T^{ij} = T^{ji} := M^{ij} + M^{ji} \succeq 0$ . The entries of the matrices  $\Psi_k, \Phi_k, 1 \leq k \leq n, M^{ij}, T^{ij}, i \sim j$  are described in detail in the appendix.

We can now write the OPF problem. Given a Hermitian  $n \times n$  matrix  $C_0$ , we have

**Optimal power flow problem OPF:**

$$\underset{V \in \mathbb{C}^n}{\text{minimize}} \quad V^H C_0 V$$

$$\text{subject to:} \quad \underline{P}_k \leq V^H \Phi_k V \leq \overline{P}_k, \quad 1 \leq k \leq n, \quad (3.8a)$$

$$\underline{Q}_k \leq V^H \Psi_k V \leq \overline{Q}_k, \quad 1 \leq k \leq n, \quad (3.8b)$$

$$\underline{W}_k \leq V^H J_k V \leq \overline{W}_k, \quad 1 \leq k \leq n, \quad (3.8c)$$

$$V^H M^{ij} V \leq \overline{F}_{ij}, \quad i \sim j, \quad (3.8d)$$

$$V^H T^{ij} V \leq \overline{L}_{ij}, \quad i \sim j, \quad (3.8e)$$

where (3.8a)–(3.8e) are, respectively, constraints on the real and reactive powers, the voltage magnitudes, the line flows and thermal losses.

We do not include line-flow constraints that impose an upper bound on the apparent

power  $\sqrt{P_{ij}^2 + Q_{ij}^2}$  on each branch  $i \sim j$  because such constraints are not quadratic in the voltages and hence beyond the scope of our model.

**Remark 6** (Objective Functions). *We can consider different optimality criteria by changing  $C_0$  as follows:*

(i) *Voltages:  $C_0 = \mathcal{I}_{n \times n}$  (identity matrix) where we aim to minimize  $\|V\|^2 = \sum_k |V_k|^2$ .*

(ii) *Power loss:  $C_0 = (Y + Y^H)/2$  where we aim to minimize  $\sum_i g_{ii}|V_i|^2 + \sum_{i < j} g_{ij}|V_i - V_j|^2$ .*

(iii) *Production costs:  $C_0 = \sum_k c_k \Phi_k$  where we aim to minimize  $\sum_k c_k P_k^G$ ,  $c_k \geq 0$ .*

### 3.5.3 Conic relaxation over radial networks

Assume hereafter that OPF is feasible. To conform to the notation of problem  $P$  in Section 3.2, we replace the constraint in (3.8a) by the equivalent constraints

$$\begin{aligned} V^H[\Phi_k]V &\leq \bar{P}_k, & 1 \leq k \leq n, \\ V^H[-\Phi_k]V &\leq -\underline{P}_k, & 1 \leq k \leq n. \end{aligned}$$

Similarly we rewrite (3.8b) and (3.8c). Then the set of matrices  $\{C_1, \dots, C_m\}$  and the set of scalars  $\{b_1, \dots, b_m\}$  in the OPF problem are defined as

$$\begin{aligned} \{C_1, \dots, C_m\} &:= \{\Phi_k, -\Phi_k, \Psi_k, -\Psi_k, J_k, -J_k, 1 \leq k \leq n\} \\ &\quad \cup \{M^{ij}, T^{ij}, i \sim j\}, \\ \{b_1, \dots, b_m\} &:= \{\bar{P}_k, -\underline{P}_k, \bar{Q}_k, -\underline{Q}_k, \bar{W}_k, -\underline{W}_k, 1 \leq k \leq n\} \\ &\quad \cup \{\bar{F}^{ij}, \bar{L}^{ij}, i \sim j\}. \end{aligned}$$

We now limit the discussion to OPF instances where the graph of the power network is acyclic and denote this graph on  $n$  nodes as  $\mathcal{T}$ . Then, one can show that for all objective

functions considered, the set  $\mathcal{C} = \{C_0, C_1, \dots, C_m\}$  for OPF satisfies

$$G(\mathcal{C}) = \mathcal{T}, \quad (3.9)$$

i.e., the sparsity pattern of the matrices in the set  $\mathcal{C}$  follows the acyclic graph  $\mathcal{T}$  of the power network. To explore the linear separability condition for OPF over  $\mathcal{T}$ , consider an edge  $(i, j)$  in  $\mathcal{T}$  with  $y_{ij} = g_{ij} - \mathbf{i}b_{ij}$ . Next, we compute the complex numbers  $[C_p]_{ij}, p = 1, \dots, m$  from the matrices described as follows. For  $1 \leq k \leq n$ , and  $(p, q)$  and  $(i, j)$  in  $\mathcal{T}$ , we have:

$$[\Phi_k]_{ij} = \begin{cases} \frac{1}{2}Y_{ij} = \frac{1}{2}(-g_{ij} + \mathbf{i}b_{ij}) & \text{if } k = i \\ \frac{1}{2}Y_{ij}^{\mathcal{H}} = \frac{1}{2}(-g_{ij} - \mathbf{i}b_{ij}) & \text{if } k = j \\ 0 & \text{otherwise,} \end{cases} \quad (3.10)$$

$$[\Psi_k]_{ij} = \begin{cases} \frac{-1}{2\mathbf{i}}Y_{ij} = \frac{1}{2}(-b_{ij} - \mathbf{i}g_{ij}) & \text{if } k = i \\ \frac{1}{2\mathbf{i}}Y_{ij}^{\mathcal{H}} = \frac{1}{2}(-b_{ij} + \mathbf{i}g_{ij}) & \text{if } k = j \\ 0 & \text{otherwise,} \end{cases} \quad (3.11)$$

$$[M^{pq}]_{ij} = \begin{cases} g_{pq} & \text{if } i = j = p \\ \frac{1}{2}(-g_{pq} + \mathbf{i}b_{pq}) & \text{if } (i, j) = (p, q) \\ \frac{1}{2}(-g_{pq} - \mathbf{i}b_{pq}) & \text{if } (i, j) = (q, p) \\ 0 & \text{otherwise,} \end{cases} \quad (3.12)$$

$$[T^{pq}]_{ij} = \begin{cases} g_{pq} & \text{if } i = j = p \text{ or } i = j = q \\ -g_{pq} & \text{if } (i, j) = (p, q) \text{ or } (i, j) = (q, p) \\ 0 & \text{otherwise.} \end{cases} \quad (3.13)$$

Succinctly, the  $(i, j)$  entries of the matrices that contribute are given as:

$$\begin{aligned} \text{(a) } [\Phi_i] &: -g_{ij}/2 + \mathbf{i}b_{ij}/2, & \text{(e) } [M^{ij}] &: -g_{ij}/2 + \mathbf{i}b_{ij}/2, \\ \text{(b) } [\Phi_j] &: -g_{ij}/2 - \mathbf{i}b_{ij}/2, & \text{(f) } [M^{ji}] &: -g_{ij}/2 - \mathbf{i}b_{ij}/2, \\ \text{(c) } [\Psi_i] &: -b_{ij}/2 - \mathbf{i}g_{ij}/2, & \text{(g) } [T^{ij}] &: -g_{ij}, \\ \text{(d) } [\Psi_j] &: -b_{ij}/2 + \mathbf{i}g_{ij}/2, & \text{(h) } [T^{ji}] &: -g_{ij}. \end{aligned}$$

For the same edge  $(i, j) \in \mathcal{T}$ , the objective functions in Remark 6 will respectively have the following entries

$$\begin{aligned} \text{(i) Voltages: } [C_0]_{ij} &= 0, \\ \text{(ii) Power loss: } [C_0]_{ij} &= -g_{ij}, \\ \text{(iii) Production costs: } [C_0]_{ij} &= -g_{ij}(c_i + c_j)/2 + \mathbf{i}b_{ij}(c_i - c_j)/2. \end{aligned}$$

For the purpose of this discussion, consider power loss minimization as the objective, i.e.,  $[C_0]_{ij} = -g_{ij}$  and assume  $g_{ij} > b_{ij} > 0$ . We plot the non-zero  $(i, j)$ -th entries of the matrices in  $\mathcal{C}$  on the complex plane in Figure 3.2 and label each point with its corresponding matrix. Clearly if we consider all the points in Figure 3.2, they are not linearly separable from the origin. To apply Theorem 7 to OPF, consider an index-set  $\mathcal{M} \subseteq \{1, 2, \dots, m\}$  such that the set of matrices  $C_0$  and  $\{C_p, p \in \mathcal{M}\}$  are off-diagonally linearly separable. This corresponds to removing certain inequalities in OPF, i.e.,  $b_p = +\infty$  for  $p \in \{1, 2, \dots, m\} \setminus \mathcal{M}$ . For example, removing  $-\Phi_j$  from the set  $\{C_1, \dots, C_m\}$  corresponds to setting  $\underline{P}_j = -\infty$ . Then Theorem 7 can be used to prove the following result.

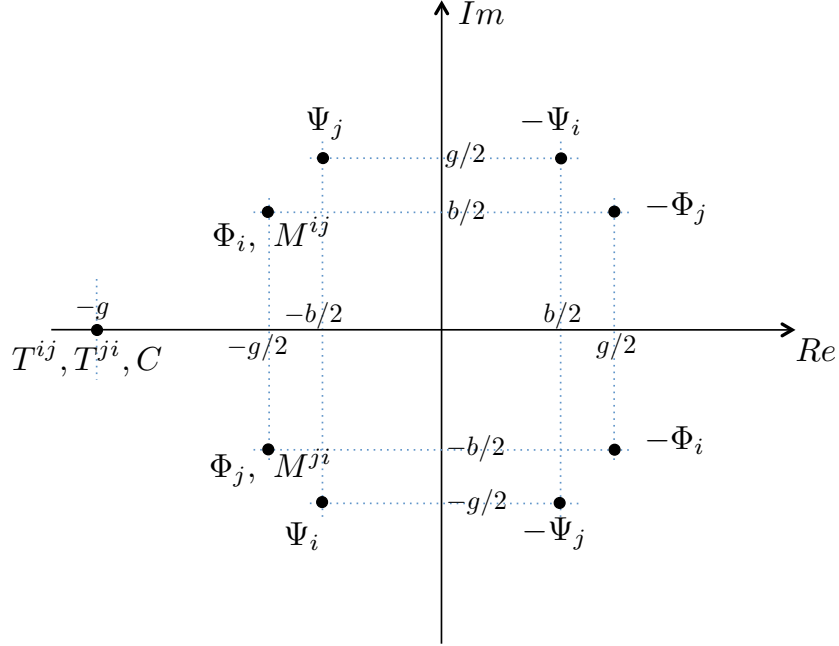


Figure 3.2:  $C_{ij}$  and non-zero  $[C_p]_{ij}, p = 1, \dots, m$  on the complex plane for OPF for a fixed line  $(i, j)$  in tree  $\mathcal{T}$ .

**Corollary 12.** *The OPF problem over an acyclic power network  $\mathcal{T}$  with an off-diagonally linearly separable set of matrices  $\tilde{\mathcal{C}} = \{C_0, C_p, p \in \mathcal{M}\}$  can be solved in polynomial time using its SDP or SOCP relaxation.*

We next explore, through examples, some constraint patterns for OPF over  $\mathcal{T}$  for which the conic relaxations can be used to solve OPF.

*Example 1:* In Figure 3.2, consider the  $(i, j)$ -th elements of the following set of matrices:

$$\{\Phi_i, \Phi_j, \Psi_i, \Psi_j, -\Psi_i, M^{ij}, M^{ji}, T^{ij} = T^{ji}, C_0\}.$$

This set of points is linearly separable from the origin. With these points, associate a constraint pattern defined as follows. For any point in the diagram that is not a part of this set, the inequality associated with that matrix is removed from OPF. For example, the

matrices  $-\Phi_j$ ,  $-\Phi_i$  and  $-\Psi_j$  are removed, which leads to

$$\underline{P}_j = \underline{P}_i = \underline{Q}_j = -\infty.$$

This can be generalized to a constraint pattern over  $\mathcal{T}$  by removing the lower bounds on the real powers at all nodes and the lower bounds on reactive powers at alternate nodes.

*Example 2:* Suppose  $\underline{P}_k = \underline{Q}_k = -\infty$  for all nodes  $k$  in  $\mathcal{T}$ . This corresponds to considering points only on the left-half plane in Figure 3.2 for all edges  $(i, j)$  in  $\mathcal{T}$  and constitutes a set that is linearly separable from the origin. In Figure 3.2, we assume  $g_{ij} > b_{ij} > 0$ . However, regardless of the ordering between  $g_{ij}$  and  $b_{ij}$  for edges  $(i, j)$  in  $\mathcal{T}$ , the set of points considered in this constraint pattern always lies in the left half of the complex plane.

Removing the lower bounds on the real and reactive power can be interpreted as load over-satisfaction, i.e., the real and reactive powers supplied to a node  $1 \leq k \leq n$  can be greater than their respective real and reactive power demands  $P_k^D$  and  $Q_k^D$ . Results showing that OPF on a radial network with load over-satisfaction can be efficiently solved were previously reported in [15, 37, 38].

*Example 3:* Consider voltage minimization, i.e.,  $C_0$  is the  $n \times n$  identity matrix. In Figure 3.2, consider the  $(i, j)$ -th entries of the following set of matrices:

$$\{-\Phi_i, \Phi_j, -\Phi_j, \Psi_i, -\Psi_j, C_0\}.$$

The constraint pattern associated with this set of points is

$$\overline{P}_i = \overline{Q}_j = \overline{L}_{ij} = \overline{L}_{ji} = \overline{F}_{ij} = \overline{F}_{ji} = +\infty, \underline{Q}_i = -\infty.$$

We can construct a constraint pattern for the OPF problem using the above that can be solved efficiently.

# Chapter 4

## Unifying structural market power analysis in electricity markets

In the 1990s, the Federal Energy Regulatory Commission (FERC) began to deregulate electricity markets in various states by replacing cost-of-service regulated rates with market-based prices. The goal was to increase competition among generators and lower prices to end-consumers. However, the consequences of deregulation were unexpected; in 2000 and 2001, market manipulations led to the California electricity crisis which involved multiple large-scale blackouts and skyrocketing prices [4]. It is estimated that about \$5.55 billion was paid in excess of costs between 1998 and 2001 alone [106]. Subsequently, various measures were introduced in the markets to curb such behavior. Nevertheless, market manipulation continues to exist. For instance, JP Morgan was fined \$410 million for market manipulation in electricity markets in California and the Midwest from September 2010 to November 2012 [107]. To avoid such over-payments, monitoring and mitigating market power is essential. It is expected to become even more critical as new smart grid technologies such as intermittent renewable generation, energy storage, and demand-response programs start picking up presenting more opportunities to exploit. In this chapter, we propose a new functional market power measure, termed *transmission constrained network flow* (TCNF), that unifies different classes of structural market power indices in the literature. We study this measure with three different models for the power flow equations: (a) a DC approximation, (b) a semidefinite relaxation, and (c) interior-point algorithms from Matpower. Finally,

we provide extensive simulations on IEEE benchmark systems and highlight the complex interaction of engineering constraints with market power assessment.

## 4.1 Background on market power analysis

The Department of Justice defines market power as the ability of a firm to profitably alter prices away from competitive levels [108, 109]. In other words, market power is a form of market “dominance”, where a player can increase its profitability by behaving independently of competitors and consumers. The major reason for the potential to exploit is that electricity markets are complex and operate on multiple time-scales. Power delivered at a particular instant of time is first procured months (or even years) ahead via long-term bilateral contracts between generators and retailers. Between one week and one day ahead of delivery, generators and retailers begin to trade in centralized electricity markets to clear imbalances. These centralized markets typically operate over multiple stages to allow market participants to exploit the increased information about supply and demand closer to delivery. The procedures for each stage are similar – generators and retailers submit offers and bids respectively and the market operator clears the market by solving a centralized dispatch problem to minimize system costs subject to operating constraints. Payments are calculated based on locational marginal prices (LMP) which are designed to reflect local costs of generation.

Market power in generic markets has been extensively studied using microeconomics, e.g., in [110]. The theory, however, does not apply directly to *electricity markets* due to various reasons, such as: (a) Unlike in most commodity markets, electricity cannot be stored cheaply; therefore generators have significant short-run capacity constraints. (b) Electricity demand is typically inelastic because of limited price-responsiveness of consumers. (c) Trade agreement between a supplier and a consumer is not enough to guarantee feasible power delivery over a transmission grid since power transfer respects physical laws as well as market outcomes. Economics or engineering alone cannot handle such issues adequately. In electricity market, such dominance can be global, e.g., by a supplier with a large enough generation capacity, or local, e.g., by a supplier in a region which has limited ability to import less expensive

electricity due to transmission constraints [111].

### 4.1.1 Prior work

Classically, the literature on market power is fractured. Recently, however, a principled design has begun to emerge, e.g., see [109] for a survey. The analysis of market power can be divided into three distinct categories: (a) structural analysis, (b) competition models, and (c) behavioral analysis.

Structural analysis of market power is based on an *ex ante* approach where the emphasis is on identifying firms that own “must-run” generators and hence have strategic advantage in terms of market share, location in the network, etc. Such market power studies are also useful in the long-run to evaluate mergers, plan transmission capacity expansions, etc. Competition models analyze the electricity market either as a supply function or a Cournot competition with or without transmission constraints and establish competitive benchmarks for firm behavior using extensive simulations, e.g., see [112–115]. Real data is then compared *ex post* to such benchmarks to identify abuses of market power. In contrast, the behavioral analysis is another *ex post* approach that detects actual supply withholding or high price-to-cost markups in the spot market as opposed to comparing it with perfectly competitive behavior. We make two observations. First, such *ex post* analysis indeed correlates with structural indices [116, 117]. Second, *ex post* analysis with real data can be highly challenging to identify intentional abuse of market power [118, 119]. Thus *ex ante* structural analysis helps to prevent rather than cure such abuse. In this chapter, we focus on the same.

Early work on structural market power analysis, emerging from microeconomics, suggested measures that focussed exclusively on market share based on generator capacities, e.g., *Herfindahl-Hirschmann index* (HHI) [120]. The major shortcoming of such an analysis in electricity markets is in defining the *relevant market*. Due to demand variations and lack of storage, electricity across different periods of time are not substitutes. Similarly supplies that are geographically located on different ends of a congested transmission line are not substitutes as well. Thus, market power indices that are agnostic to demand variations and

transmission constraints have limited applicability to electricity markets.

To incorporate the demand side, Bushnell et al. introduced the *pivotal supplier index* (PSI) as a binary indicator examining whether the capacity of a generator is larger than the supply surplus, i.e., the difference between the total supply and the total demand [121]. Later, Sheffrin et al. refined PSI by measuring market power on a continuous scale, and proposed the *residual supply index* (RSI) in [122]. This index is used by the California ISO to assure price competitiveness [123]. The electric reliability council of Texas (ERCOT) uses a similar measure called the *element competitiveness index* (ECI) [124], based on HHI [120].

Issues arising due to transmission constraints have also been addressed in the literature. A traditional approach used the SSNIP (small but significant non-transitory increase in price) test [125] to identify geographically isolated “load pockets”. Many authors have studied Cournot-based or supply-function based markets with congestion, e.g., see [112–115, 126, 127]. Structural indices on a transmission constrained network, however, have remained fractured. We have attempted to bridge that gap in this work.

### 4.1.2 Our contributions

The contributions of this chapter are as follows: (1) we introduce a *functional* market power measure for structural analysis that unifies the theory<sup>1</sup> (2) we incorporate a detailed AC model of the underlying power system to study the complex interactions of this measure with the engineering constraints. Structural indices identify pivotal suppliers, i.e., generators that are crucial to meet demand subject to engineering constraints. These constraints, however, are not limited to transmission capacities of the network only. Our study shows that an AC power flow model significantly affects the conclusions. The new measure, termed “transmission constrained network flow” unifies the three broad classes of long-term structural measures in the literature: “network flow based” [129, 130], “residual supply based” [126, 131], and “minimal generation based” [132, 133]. We introduce each of these classes in detail in Section 4.2. Calculating the new measure in Section 4.3 requires us to solve a nonconvex

---

<sup>1</sup>A preliminary version of this work has appeared in [128].

optimization program resulting from the nature of the AC power flow equations. We deal with this nonconvexity in three ways: (a) use DC approximation [134,135] and solve a linear program (LP) , (b) use interior-point based methods implemented in Matpower [63], (c) use recent advances in semidefinite programming (SDP) based relaxations [65] to AC power flow equations [11, 12, 35, 36]. In Section 4.4, we provide extensive simulations on IEEE benchmark systems [63] and illustrate the importance of modeling engineering constraints in identifying market power. We compare the different computational approaches in Section 4.5 and extend the index to the case where firms can own generators at multiple locations in Section 4.6.

## 4.2 Market power measures

Recently, many indices have been introduced to include the effect of transmission constraints in structural market power indices; we categorize them as: “residual supply based”, “network flow based”, and “minimal generation based”. In what follows, we introduce each of them in detail.

### 4.2.1 Residual supply based measures

Residual supply based measures propose to quantify the maximum total load that the transmission-constrained electricity market can meet if generator of interest,  $s$ , is excluded. Following [126,131], the *transmission-constrained residual supply index* (TCRSI) for generator  $s$  is defined as:

$$\begin{aligned}
 \text{TCRSI}_s = \underset{q,t}{\text{maximize}} \quad & t \\
 \text{subject to} \quad & \mathbf{1}^\top q = \mathbf{1}^\top (\bar{d}t), \\
 & -b \leq H_q q - H_d(\bar{d}t) \leq b, \\
 & q_s = 0, \quad 0 \leq q_i \leq \bar{q}_i, i \neq s.
 \end{aligned} \tag{4.1}$$

where  $q$  is the supply vector,  $t$  is the demand scaling parameter,  $H_q$  is the generation shift factor matrix,  $H_d$  is load shift factor matrix,  $b$  is the transmission line capacity vector,  $\bar{q}_i$  is the capacity of generator  $i$ ,  $\bar{d}_j$  is the demand of load  $j$ ,  $\mathbf{1}$  is a unit vector, and  $\top$  denotes transposition. If  $\text{TCRSI}_s < 1$ , then generator  $s$  can potentially exercise market power. Consider the network in Figure 4.1. For  $G_1$ , TCRSI is  $3.2/7$ , the fraction of demand that can be met with available supply.

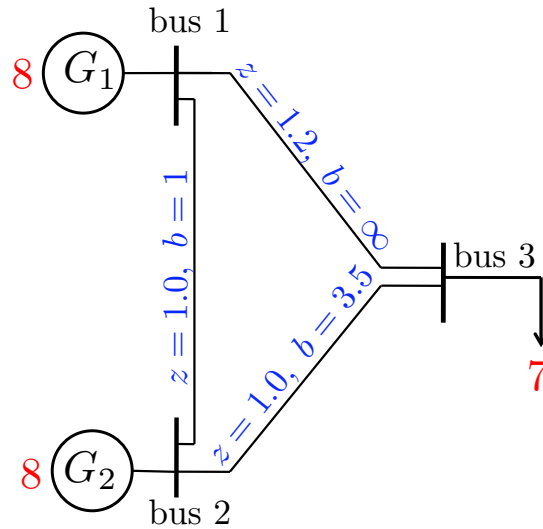


Figure 4.1: A small network to illustrate market power indices. All quantities are measured in per units (p.u.).  $z$  denotes impedance and  $b$  denotes line capacity.

## 4.2.2 Network flow based measures

Network flow based measures are exemplified by [129,130], which model market power in the presence of transmission constraints in terms of the *maximal network flow* (MNF) achievable without the generator of interest. Conceptually, these measures are similar to TCRSI, but they do not use power flow equations to model the underlying power systems. A key result in [129,130] is that market power is supermodular, i.e., there is always an incentive for generators to collude. This conclusion, however, does not hold if the power flow respects impedance and follows Kirchoff's laws. See Section 4.6 for an example in IEEE test systems. Intuitively, one would expect that there is always an incentive to collude since any individual

strategy for generators would likely be a valid strategy for a collusion of generators. Market power index, however, measures the demand shortfall due to the absence of a generator. Consider the network in Figure 4.1. When  $G_1$  withholds generation,  $G_2$  can only supply  $3.2pu$ ; demand shortfall is  $3.8pu$ . Similarly, when  $G_2$  withholds generation, demand shortfall is  $4.33pu$ . When both generators withhold, shortfall is the total demand of  $7pu$ , which is lower than the sum of the two shortfalls computed before. Thus market power is *not* supermodular. Roughly, when power injection from two different generators lead to opposing power flows on a capacity-limited transmission line, then these two generators acting together may not be able to cause more demand shortfall than shortfalls due to each generator withholding alone. This intuition holds for the network in Figure 4.1.

### 4.2.3 Minimal generation based measures

The above two definitions of market power focus on the fraction of unmet demand when generator at bus  $s$  is not in service. An alternate approach is to calculate the minimum generation required from generator  $s$  to meet the total target demand. In particular, minimal generation based measures typically identify “must run generators”, e.g., [132, 133] are exemplified by the *transmission-constrained minimal generator index* (TCMGI):

$$\begin{aligned}
\text{TCMGI}_s &= \underset{q}{\text{minimize}} \quad q_s \\
&\text{subject to} \quad \mathbf{1}^\top q = \mathbf{1}^\top \bar{d}, \\
&\quad -b \leq H_q q - H_d \bar{d} \leq b, \\
&\quad 0 \leq q_i \leq \bar{q}_i.
\end{aligned} \tag{4.2}$$

Note that in (4.1), we have  $q_s = 0$  and the total load is scaled by a variable factor  $t$ . In (4.2), however, the output of generator  $s$  is a variable and the total demand is a constant. If  $\text{TCMGI}_s > 0$ , then generator  $s$  can exercise market power. In general,  $\text{TCMGI}_s$  does *not* equal the unmet demand in the network when generator at bus  $s$  is not operational. For example, consider the network in Figure 4.1. It can be checked that  $\text{TCMGI}_1 = 4.2pu$

while the shortfall is actually  $3.8pu$  when the same generator is not in service.  $TCRSI_s$  and  $TCMGI_s$  are indeed related; we explore this below.

### 4.3 Functional measure of market power

Prior work on long term market power measures in Section 4.2 suggests that while a wide variety of measures exist, the literature lacks a unified theory that incorporates economic and engineering constraints. Here we propose a *functional* market power measure rather than a market power *index* that represents a step toward such a unifying measure.

To motivate the measure, consider the following informal definition:

$$\begin{aligned} \text{TCNF}_s(\rho) = & \mathbf{maximize} \quad \text{total demand met} \\ & \mathbf{subject\ to} \quad \text{supply from generator } s \leq \rho, \\ & \quad \quad \quad \text{other network constraints.} \end{aligned}$$

The functional  $\text{TCNF}_s$  maps every scalar  $\rho \in [0, \bar{q}_i]$  into the maximum demand that can be satisfied when the (real) power output of generator  $s$  is no more than  $\rho$ .  $\text{TCNF}_s(\rho)$  can also be interpreted as a measure of the minimum amount of load that has to be shed (or dispatched, through demand-side management<sup>2</sup>), provided that the supply of generator  $s$  is up to  $\rho$ . At different levels of  $\rho$ , it measures the relative importance of each generator to meet additional demand, abiding by the network constraints.

The definition can also be interpreted as follows. Consider the optimal power flow (OPF) problem where the objective is to only satisfy demand and the production level of generator  $s$  is upper bounded by the parameter  $\rho$ . Then, the optimal objective value of this OPF type problem is a function of that variable  $\rho$  and hence defines a “functional” measure of market power for generator  $s$ .

In the rest of this section, we show how a detailed power flow model can be included to arrive at a unifying market power measure that is applicable to the evolving smart grid.

---

<sup>2</sup>When there is a deficit in electricity supply, the system operator may call upon consumers to adjust their demand so as to match the supply – an approach which is usually referred to as demand response.

Next, we formally define  $\text{TCNF}_s(\rho)$  with the engineering constraints.

### 4.3.1 Definition

We begin with some notation. Let  $\mathbf{i} = \sqrt{-1}$  and for any complex matrix or number  $z$ , let  $z^H$  be the complex conjugate transpose of  $z$ . Consider a network on  $n$  nodes (buses) labeled  $1, 2, \dots, n$ . Let  $p_k^G$  and  $q_k^G$  be the real and reactive power generations at node  $k$ . Also let  $p_k^D$  and  $q_k^D$  be the real and reactive power demands that are met at node  $k$ . We denote  $s_{kj} := p_{kj} + \mathbf{i}q_{kj}$  as the apparent power flowing from bus  $k$  to bus  $j$ , where  $p_{kj}$  and  $q_{kj}$  are the real and reactive power flows, respectively. Thus, power balance equation at each node  $k$  becomes

$$(p_k^G - p_k^D) + \mathbf{i}(q_k^G - q_k^D) = \sum_{j:j \sim k} s_{kj}, \quad (4.3)$$

where  $j \sim k$  denotes that buses  $k$  and  $j$  are connected in the power network. The power generations are assumed to satisfy

$$0 \leq p_k^G \leq \bar{p}_k^G, \quad -\beta_k p_k^G \leq q_k^G \leq \beta_k p_k^G, \quad (4.4)$$

where  $\beta_k > 0$  is a known constant that depends on the technology, i.e., each generator is assumed to vary its reactive power output within a certain power factor of the real power generation. The total load to be supported at bus  $k$  has a target real demand  $\bar{p}_k^D$  and a target power factor  $\alpha_k$ . The target power factor depends on the type of load at bus  $k$ . Thus, the supported demand  $p_k^D + \mathbf{i}q_k^D$  satisfies

$$0 \leq p_k^D \leq \bar{p}_k^D, \quad q_k^D = \tan(\cos^{-1} \alpha_k) p_k^D. \quad (4.5)$$

Power factors typically range from 0.95 to 0.98 lagging. The apparent power flowing from bus  $k$  to bus  $j$  is  $s_{kj}$  and is bounded by the thermal and stability limits of the transmission

lines as

$$|s_{kj}| \leq f_{kj}, \quad (4.6)$$

where  $f_{kj}$  is the known capacity of the line between buses  $k$  and  $j$ . Let the voltage at bus  $k$  be  $V_k$ , and the admittance of the line between buses  $k$  and  $j$  be  $y_{kj}$ . The current flowing from bus  $k$  to bus  $j$  is  $y_{kj}(V_k - V_j)$  and we have

$$s_{kj} = V_k [y_{kj}(V_k - V_j)]^H. \quad (4.7)$$

To maintain power quality and the system stability, the voltage magnitude  $|V_k|$  at bus  $k$  is required to be bounded as follows:

$$\underline{W}_k \leq |V_k|^2 \leq \overline{W}_k, \quad (4.8)$$

where  $\underline{W}_k$  and  $\overline{W}_k$  are known constants.

Using the notations introduced above, we are now ready to formally introduce a measure the market power of a generator at node  $s$  as follows:

$$\begin{aligned} \text{TCNF}_s(\rho) = & \mathbf{maximize} \quad \sum_k p_k^D \\ & \mathbf{subject\ to} \quad p_s^G \leq \rho, \\ & (4.3), (4.4), (4.5), (4.6), (4.7), (4.8), \\ & \mathbf{over} \quad p_k^G, q_k^G, p_k^D, q_k^D, k = 1, \dots, n, \\ & s_{kj}, \quad k \sim j. \end{aligned} \quad (4.9)$$

We refer to this measure as the *transmission-constrained network flow*. The constraints in (4.3)-(4.8) impose the impact of the network topology, the underlying circuits, and the transmission line capacities. These constraints make our analysis different from a traditional economic approach to market power. Note that,  $\text{TCNF}_s(\rho)$  is a *functional* measure, i.e., it

evaluates market power for every given value of parameter  $\rho$ .

In Section 4.3.3, we describe how this measure in (4.9) unifies the three general classes of long-term market power measures discussed in Section 4.2. Next, we describe the solution approaches to the optimization program to calculate  $\text{TCNF}_s$ .

### 4.3.2 Relaxations and approximations

Perhaps the first observation one makes about the definition of  $\text{TCNF}_s$  is that it requires solving optimization problems that are NP-hard. This is because the relation in (4.7) is a quadratic equality and hence the feasible set is, in general, non-convex. This makes it difficult to compute (4.9) to quantify market power. There are three general approaches to compute the measure: (i) linearizing the quadratic constraint around a set-point and use DC approximation (ii) using heuristic iterative nonconvex optimization techniques, (iii) relaxing the non-convex quadratic equality constraint to a convex semidefinite constraint and use conic program solvers.

Nonconvexity of power-flow equations have played a significant role in optimization problems over power networks [23]. Traditionally, the engineering problems and market computations have differed in the approaches taken to deal with this nonconvexity. While market outcomes have relied on the DC approximation [121, 122, 124, 128, 129, 131], engineering problems such as real-time economic dispatch have applied heuristics or iterative techniques to reach an implementable operating point [22, 63]. The conic relaxation approach, however, is a recent development and is finding applications in both the engineering and market considerations, e.g., see [11, 35, 36] for its use in optimal power flow and see [136, 137] for its use in electricity markets. Next, we present all three computational approaches; we compare them in Section 4.5.

#### 4.3.2.1 The DC approximation approach

The most popular approximation for power flow equations is linearization, e.g., see [134, 135]. This approach makes the following assumptions:

- Voltage magnitude  $|V_k|$  at each node  $k$  is assumed to be at its nominal value, where  $V_k = |V_k| \exp(\mathbf{i}\theta_k)$ . Thus  $|V_k| = 1pu$ .
- Transmission lines are assumed to be loss-less, i.e.,  $y_{kj} = \mathbf{i}b_{kj}$  is purely imaginary for all pairs  $k \sim j$ .
- For any pair of buses  $k \sim j$ , the voltage phase angle differences  $\theta_k - \theta_j$  are assumed to be small, i.e.,  $\sin(\theta_k - \theta_j) \approx \theta_k - \theta_j$  and  $\cos(\theta_k - \theta_j) \approx 1$ .

Using this approximation, for any pair  $k \sim j$ , we have

$$s_{kj} = p_{kj} = b_{kj}(\theta_k - \theta_j).$$

It can be checked that there is no reactive power that flows in this model and hence ignoring the reactive power demand constraint in (4.5), this definition of  $\text{TCNF}_s$  coincides with the one studied in [128] and can be solved as an LP. Henceforth, we refer to this computation as the *DC case*, denoted by  $\text{TCNF}_s^{DC}(\rho)$ .

#### 4.3.2.2 Non-linear optimization technique

Many iterative techniques have been used to solve optimization problems in power systems, specifically the optimal power flow problem; see [22, 23] for surveys. Some notable examples are quadratic programming, variations of gradient methods, Newton-based techniques, sequential quadratic programming, and interior-point based methods. The problem is NP-hard, these iterative algorithms are not guaranteed to converge to the global optimal solution, though some of them provably converge to local minima in polynomial time. For many test cases, these approaches have been known to converge to “good” operating points. In this work, we use the primal-dual interior-point solver in Matpower [63]. When this converges, we refer to it as  $\text{TCNF}_s^{NL}$  and call this computation as the *NL case*. Though it is hard to comment on the optimality of the point obtained through this heuristic, the use of Matpower solver provides insights as we explore the simulations on the IEEE benchmark systems.

### 4.3.2.3 The SDP relaxation approach

Recently, a conic relaxation has been proposed to deal with the nonconvexity of power-flow equation in (4.7), e.g., see [11,12,35,36]. In particular, consider the  $n \times n$  positive semidefinite matrix  $W = VV^H$  that has rank one (denoted as  $W \succeq 0, \text{rank } W = 1$ ). For each pair of buses  $k \sim j$ , we express  $s_{kj}$  as a linear matrix relation in  $W$  as follows. Define an  $n \times n$  matrix  $M^{kj}$ , where

$$[M^{kj}]_{kk} = y_{kj}^H, \quad [M^{kj}]_{jk} = -y_{kj}^H,$$

and rest of the entries of  $M^{kj}$  are zero. In terms of  $M^{kj}$ , the equality in (4.7) can be written as

$$s_{kj} = \text{tr}(M^{kj}W).$$

Accordingly, the optimization problem to calculate TCNF becomes a rank-constrained SDP [65] in terms of matrix  $W$ . It still remains nonconvex due to the rank constraint. Next, we relax the rank constraint to obtain  $\text{TCNF}_s^{AC}(\rho)$  and refer to this computation as the *AC case*.

### 4.3.3 Properties of $\text{TCNF}_s$

In Section 4.3.2, we introduced the functional measure  $\text{TCNF}_s(\rho)$  and its computational versions  $\text{TCNF}_s^{DC}(\rho)$ ,  $\text{TCNF}_s^{AC}(\rho)$  and  $\text{TCNF}_s^{NL}(\rho)$  to assess market power. Now, we explore their salient features.

$\text{TCNF}_s^{DC}(\rho)$  generalizes network flow based and residual supply based measures. When  $\rho = 0$ , it indicates the maximal network flow satisfying the DC power flow constraints when generator  $s$  withholds generation.  $\text{TCNF}_s^{AC}(0)$  and  $\text{TCNF}_s^{NL}(0)$  measure the same with AC power flow models.

To relate  $\text{TCNF}_s$  to the minimum generation based measure, consider the *transmission-*

constrained minimal generation  $\text{TCMG}_s(D)$  for generator  $s$  to be defined as follows:

$$\begin{aligned}
\text{TCMG}_s(D) = & \mathbf{minimize} \quad p_s^G, \\
& \mathbf{subject\ to} \quad \sum_k p_k^D = D, \\
& (4.3), (4.4), (4.5), (4.6), (4.7), (4.8), \\
& \mathbf{over} \quad p_k^G, q_k^G, p_k^D, q_k^D, k = 1, \dots, n, \\
& s_{kj}, k \sim j.
\end{aligned}$$

This generalizes the minimum generation based measures in [129, 130] to a functional form and uses AC power flow to model the physical power system. It is easy to extend the definition of  $\text{TCMG}_s(\cdot)$  to the following computable versions:  $\text{TCMG}_s^{DC}(\cdot)$  with the DC-approximation and  $\text{TCMG}_s^{AC}(\cdot)$  with the SDP-based relaxation. First, we explore the relationship of the functions  $\text{TCNF}_s(\cdot)$  and  $\text{TCMG}_s(\cdot)$  for the DC and the AC cases; proof is included in the appendix.

**Theorem 13.** *For each generator  $s$ :*

1.  $\text{TCNF}_s^{DC}(\cdot)$  is a continuous, concave, piecewise linear and non-decreasing function;  $\text{TCMG}_s^{DC}(\cdot)$  is a continuous, convex, piecewise linear and non-decreasing function. Moreover,  $\text{TCNF}_s^{DC}(\cdot)$  and  $\text{TCMG}_s^{DC}(\cdot)$  are inverses of each other, i.e., for any  $0 \leq D \leq \text{TCNF}_s^{DC}(\infty)$ ,

$$\text{TCNF}_s^{DC} [\text{TCMG}_s^{DC}(D)] = D.$$

2.  $\text{TCNF}_s^{AC}(\cdot)$  is a continuous, concave, and non-decreasing function;  $\text{TCMG}_s^{AC}(\cdot)$  is a continuous, convex, and non-decreasing function. Moreover,  $\text{TCNF}_s^{AC}(\cdot)$  and  $\text{TCMG}_s^{AC}(\cdot)$  are inverses of each other, i.e., for any  $0 \leq D \leq \text{TCNF}_s^{AC}(\infty)$ ,

$$\text{TCNF}_s^{AC} [\text{TCMG}_s^{AC}(D)] = D.$$

Before we present the proof, we make a few observations about the result. Note that the

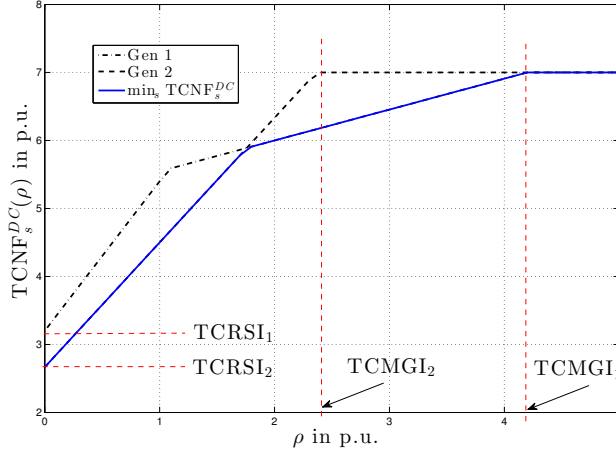


Figure 4.2:  $\text{TCNF}_s^{DC}(\cdot)$  of generators in the 3-bus network shown in Figure 4.1. Quantities are measured in per units (p.u.).

functions  $\text{TCNF}_s^{DC}(\cdot)$  satisfies all properties of  $\text{TCNF}_s^{AC}(\cdot)$ ; in addition, it is also piecewise linear, because the optimization problem to compute  $\text{TCNF}_s^{DC}$  is a linear-parametric LP. This property does not generalize to linear-parametric SDPs; see [65] for a counterexample. The concavity and monotonicity follow from standard arguments on the feasible set of the respective optimization programs.

The inverse relationship between  $\text{TCNF}_s^{DC}(\cdot)$  and  $\text{TCMG}_s^{DC}(\cdot)$  holds for all  $0 \leq D \leq \text{TCNF}_s^{DC}(\infty)$ . Here,  $\text{TCNF}_s^{DC}(\infty)$  is the total demand in the network that can be met when the power generated by generator  $s$  is not constrained (it, however, satisfies the generation capacity constraint  $0 \leq p_s^G \leq \bar{p}_s^G$  in (4.4)). Beyond that, the network cannot satisfy the target demand and hence  $\text{TCMG}_s^{DC}(D)$  only exists for  $0 \leq D \leq \text{TCNF}_s^{DC}(\infty)$ . Similar result holds for the AC case. Unlike the DC and AC approximations, when  $\text{TCNF}_s(\cdot)$  is instantiated with the true AC power flow equations (i.e., not the SDP relaxation), then it may not be concave since the feasible set of the corresponding optimization problem is not convex. The function  $\text{TCNF}_s(\cdot)$  may not be monotonically increasing in the interval  $[0, \text{TCMG}_s(\text{TCNF}_s(\infty))]$  in this case, and thus not invertible. The NL case is similar.

Next, we illustrate the result of Theorem 13 through an example. Consider the network shown in Figure 4.1.  $\text{TCNF}_s^{DC}(\cdot)$  is plotted for generators at buses 1 and 2 in Figure 4.2.

Functions  $\text{TCNF}_1^{DC}(\cdot)$  and  $\text{TCNF}_2^{DC}(\cdot)$  are continuous, convex, piecewise linear and non-decreasing. As noted earlier,  $\text{TCNF}_s^{DC}(0)$  equals the TCRSI for generator  $s$ . Also, TCMGI for generator  $s$  is given by  $\min\{\rho \geq 0 \mid \text{TCNF}_s(\rho) = \text{TCNF}_s(\infty)\}$ . TCRSI and TCMGI for each generator are indicated in the figure.

Lower the value of  $\text{TCNF}_s^{DC}(\cdot)$ , higher the market power of generator  $s$ . Thus we plot  $\min_s \text{TCNF}_s^{DC}$  by considering the lower envelope of  $\text{TCNF}_1^{DC}(\cdot)$  and  $\text{TCNF}_2^{DC}(\cdot)$  to indicate the market power of the dominant generator for each  $\rho \geq 0$ . In this example, the generator with maximum market power changes as  $\rho$  changes. This suggests that market power assessment is complex and cannot be sufficiently captured through a single index.

*Proof of Theorem 13.* We only prove the DC case; proof for the AC case is similar and is omitted for brevity. For the DC-case, the optimization is an LP linearly parameterized by  $\rho$ . Then it is well-known that the optimal objective function (in this case  $\text{TCNF}_s^{DC}(\rho)$ ) is continuous and piecewise linear in the parameter  $\rho$ ; see [65]. Thus,  $\text{TCNF}_s^{DC}(\rho)$  is a continuous and piecewise linear function of  $\rho \geq 0$ . For  $0 \leq \rho_1 < \rho_2$ , the feasible set for the optimization problem to compute  $\text{TCNF}_s^{DC}(\rho_1)$  is a subset of that of  $\text{TCNF}_s^{DC}(\rho_2)$  and thus  $\text{TCNF}_s^{DC}(\rho)$  is non-decreasing in  $\rho \geq 0$ . Let the optimal points for problems  $\text{TCNF}_s^{DC}(\rho_1)$  and  $\text{TCNF}_s^{DC}(\rho_2)$  be  $x_1$  and  $x_2$ , respectively. For any  $0 \leq \gamma \leq 1$ , the point  $\gamma x_1 + (1 - \gamma)x_2$  is a feasible point for the problem  $\text{TCNF}_s^{DC}(\gamma\rho_1 + (1 - \gamma)\rho_2)$ . Then it follows that  $\text{TCNF}_s^{DC}(\rho)$  is concave.

Next, we show that  $\text{TCNF}_s^{DC}(\cdot)$  and  $\text{TCMG}_s^{DC}(\cdot)$  are inverses of each other. For any  $\rho \geq 0$ , consider the optimal point for the optimization problem to compute  $\text{TCNF}_s^{DC}(\rho)$ . This optimum is feasible for the optimization problem  $\text{TCMG}_s^{DC}[\text{TCNF}_s^{DC}(\rho)]$  and we have

$$\text{TCMG}_s^{DC}[\text{TCNF}_s^{DC}(\rho)] \leq \rho. \quad (4.10)$$

Similarly, it can be checked that for any  $0 \leq D \leq \text{TCNF}_s^{DC}(\infty)$ ,

$$\text{TCNF}_s^{DC}[\text{TCMG}_s^{DC}(D)] \geq D. \quad (4.11)$$

For  $\rho \in [0, \text{TCMG}_s^{DC}[\text{TCNF}_s^{DC}(\infty)]]$ , replacing  $D = \text{TCNF}_s^{DC}(\rho)$  in (4.11), we obtain

$$\text{TCNF}_s^{DC}[\text{TCMG}_s^{DC}(\text{TCNF}_s^{DC}(\rho))] \geq \text{TCNF}_s^{DC}(\rho). \quad (4.12)$$

Now, for  $\rho \in [0, \text{TCMG}_s^{DC}[\text{TCNF}_s^{DC}(\infty)]]$ , we have  $\text{TCNF}_s^{DC}(\rho)$  is concave and non-decreasing. Then it is easy to check that  $\text{TCNF}_s^{DC}(\rho)$  is monotonically increasing in this interval and hence from (4.12), it follows that

$$\text{TCMG}_s^{DC}[\text{TCNF}_s^{DC}(\rho)] \geq \rho.$$

Combining the above relation with (4.10), we have

$$\text{TCMG}_s^{DC}[\text{TCNF}_s^{DC}(\rho)] = \rho. \quad (4.13)$$

The rest follows from the fact that for  $0 \leq \rho \leq \text{TCMG}_s^{DC}[\text{TCNF}_s^{DC}(\infty)]$ , the map  $\text{TCNF}_s^{DC}(\rho)$  is monotonically increasing and hence one-one in this interval.  $\square$

## 4.4 Case Studies

In this section, we use our proposed unifying measure to assess market power of generators in various IEEE test systems [63]. In particular, we show how market power can be affected by different factors such as the variation of target demand due to distributed renewable generation, changes in dispatchable load in presence of demand-response programs, and changes in load power-factors. We also compare the results obtained from  $\text{TCNF}_s^{DC}$ ,  $\text{TCNF}_s^{AC}$  and  $\text{TCNF}_s^{NL}$  and point out the important role of nonconvexity of power flow equations in assessing market power. This underlines the significance of engineering constraints on market outcomes in electricity markets.

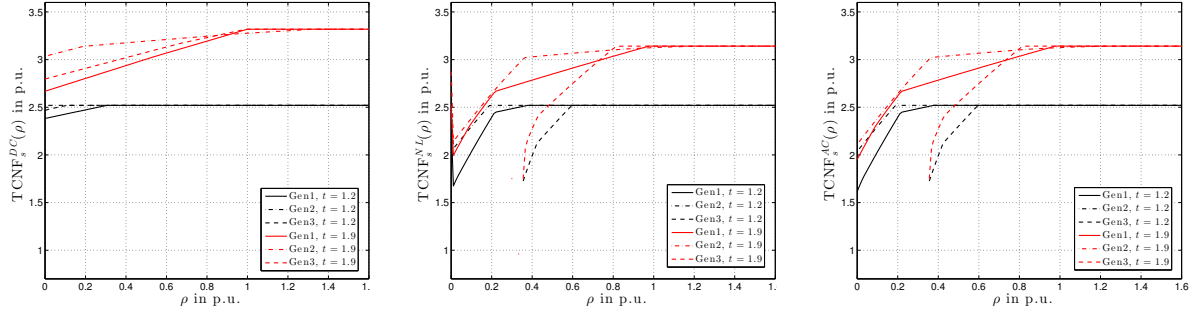
In our simulations, we consider the IEEE 6-bus and 39-bus test systems. In each case, we look at a variety of scalings of the target demands in the test systems to understand the impact of demand fluctuation and distributed renewable generation. Specifically, target

demands are scaled uniformly by a scalar  $t \geq 0$ , i.e., each target demand  $\bar{p}_k^D$  in the database is multiplied by a factor  $t$  to obtain the new target demand for our simulations. We assume that for all generators, the minimum level of generation is zero, i.e.,  $p_k^G \geq 0$ . Most systems have a reactive generation capability defined by  $\underline{q}_k^G \leq q_k^G \leq \bar{q}_k^G$ . We modify this box constraint on  $q_k^G$  to  $-\beta_k p_k^G \leq q_k^G \leq \beta_k p_k^G$  as in (4.4), where  $\beta_k$  is chosen accordingly for each case study. To compute  $\text{TCNF}_s^{DC}(\cdot)$  and  $\text{TCNF}_s^{AC}(\cdot)$ , we use the convex programming package CVX [76] in MATLAB with SDPT3 as the SDP solver [138]. Finally,  $\text{TCNF}_s^{NL}$  is computed using the primal-dual interior-point method in Matpower [63].

#### 4.4.1 IEEE 6-bus Test System

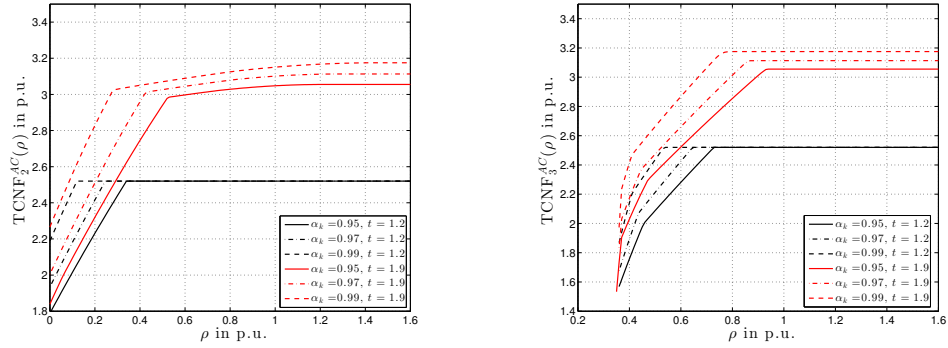
The IEEE 6-bus test system has three generators at nodes 1, 2 and 3. For all generators, we assume that  $\beta_k = 0.6$  and for all loads we assume that the power-factors are  $\alpha_k = 0.98$  lagging. In Figure 4.3, we plot  $\text{TCNF}_s^{DC}(\rho)$ ,  $\text{TCNF}_s^{NL}(\rho)$ , and  $\text{TCNF}_s^{AC}(\rho)$  for demand scalings of  $t = 1.2$  and  $t = 1.9$ . Note that, there is a remarkable difference between the AC and the DC cases, while the results from the NL case are similar to that of the AC model. Therefore, we can conclude that in this case study, the SDP relaxation finds a feasible and close to optimal solution of the non-convex optimization problem in (4.9).

In Theorem 13, the TCNF functions for the DC and AC cases in Figure 4.3 are increasing and concave for all generators. This property does not generalize for the NL case. Note that, for generator 3, the optimization problem for calculating  $\text{TCNF}_s^{AC}$  remains infeasible for  $\rho \leq 0.35pu$ . This indicates that generator 3 is needed to supply at least  $0.35pu$  in order to maintain system stability. It is interesting to note that if the SDP relaxation is infeasible, so is the non-linear optimization problem in (4.9) and hence the interior-point method does not converge to a feasible point for  $\rho \leq 0.35pu$ . We can also see that  $\text{TCNF}_s^{NL}$  and  $\text{TCNF}_s^{AC}$  are quite similar except for generators 1 and 2 at  $\rho = 0$ , where  $\text{TCNF}_s^{NL}$  is greater than  $\text{TCNF}_s^{AC}$ . For such a non-convex optimization problem, determining feasibility is NP-hard and hence it is hard to comment whether the problem in (4.9) is infeasible at  $\rho = 0$ . The SDP relaxation  $\text{TCNF}_s^{AC}$ , however, is feasible. Moreover, it is continuous at  $\rho = 0$  as expected



(a) TCNF with DC power flow      (b) TCNF with Matpower      (c) TCNF with AC power flow

Figure 4.3: TCNF calculation based on different approaches for various generators in the IEEE 6-bus system.



(a)  $\text{TCNF}^{AC}$  of generator 2      (b)  $\text{TCNF}^{AC}$  of generator 3

Figure 4.4:  $\text{TCNF}^{AC}(\rho)$  for generators 2 and 3 plotted for load power factors from 0.95 to 0.99 lagging in the IEEE 6-bus system.

from Theorem 13.

The results in Figure 4.3 can be further interpreted as follows. For the AC case at  $t = 1.9$ , consider the total demand level (y-axis) of  $3pu$ , which is lower than the total target demand level. At this demand level,  $\text{TCNF}_3^{AC}$  has a larger slope than  $\text{TCNF}_1^{AC}$ . Therefore, to satisfy an extra unit of demand at  $3pu$ , generator 3 has to supply less additional power and hence it is more valuable to the system operator. This means that generator 3 has more market power in an *incremental market*.

Another key observation is about the importance of each generator at various demand levels, in presence of *dispatchable load*. In this regard, we see that at the same demand level,

TCNF<sub>s</sub><sup>DC</sup> in Figure 4.3(a) and TCNF<sub>s</sub><sup>AC</sup> in Figure 4.3(c) give conflicting conclusions, while TCNF<sub>s</sub><sup>NL</sup> in Figure 4.3(b) agrees with TCNF<sub>s</sub><sup>AC</sup>, indicating that the relaxation approach of AC power flow model is efficient in quantifying market power in the IEEE 6-bus system. This further confirms that the market outcome depends on the underlying power engineering model.

Finally, to illustrate the importance of reactive power flows, consider TCNF<sub>s</sub><sup>AC</sup>( $\rho$ ) in Figures 4.4(a) for generator 2 and in Figure 4.4(b) for generator 3, respectively. The plots have been generated with  $t = 1.2$  and  $t = 1.9$  and the load power factors have been varied from 0.95 to 0.99 lagging uniformly for all buses in each case. TCNF<sub>2</sub><sup>AC</sup>( $\rho$ ) and TCNF<sub>3</sub><sup>AC</sup>( $\rho$ ) show considerable variations with changes in load power factors and thus reactive power flow has a significant effect on market power and must be taken into consideration for an efficient long-term planning. For example, as load power factor decreases, generators 1 and 3 are needed to supply more power in order to meet the same level of demand, placing these generators in better positions to gain market power. Another interesting observation is that although changing the load power factor can significantly change the slope of the TCNF<sub>s</sub><sup>AC</sup>( $\rho$ ) function at different points, it does not have direct impact on the cut off rate of TCNF<sub>3</sub><sup>AC</sup>( $\rho$ ), i.e., the choice of  $\rho$  for which the optimization problem in (4.9) for  $s = 3$  becomes infeasible. Similar results can be observed for TCNF<sub>s</sub><sup>NL</sup>( $\rho$ ) (not shown here).

#### 4.4.2 IEEE 39-bus Test System

We now assess our proposed approach for market power analysis in a larger IEEE test system with 39 buses. At each bus  $s$ , the value of parameter  $\rho$  in function TCNF<sub>s</sub>( $\rho$ ) can be interpreted as the amount of curtailable load that is available for dispatch at bus  $s$ , in case of losing the generator at bus  $s$ . The higher the amount of dispatchable load at a bus, the better the grid operator can handle the loss of a generator at that bus, preventing such generator from gaining market power. However, the effectiveness of the same amount of dispatchable load in mitigating market power may not be the same at different buses. In other words, dispatchable load can be more (or less) valuable at certain locations. For example, consider

the simulation results in Figure 4.5. Here, we are considering the  $\text{TCNF}_s$  for generators at buses 31, 35 and 38. For the purpose of our analysis, we plot the lower envelope of  $\text{TCNF}_s$  only, namely  $\min_{s \in \{31, 35, 38\}} \text{TCNF}_s(\cdot)$  for demand levels ranging from  $t = 1.0$  to  $t = 1.15$ . For the case where  $t = 1.15$ , increasing the dispatchable load capacity is most beneficial when it is done at bus 38 because the generator at bus 38 has the highest potential to gain market power in this case. As another example, for the case where  $t = 1.05$ , if there is  $1pu$  of dispatchable load capacity already in place in all generator buses, then increasing the dispatchable load capacity is most beneficial at bus 31, but if there is  $3pu$  of dispatchable load capacity already in place in all generator buses, then increasing the dispatchable load capacity at bus 35 is most beneficial.

We can also make the following observations based on the results in Figure 4.5: (a) In the DC approximation case, depending on the value of  $\rho$ , different generators may gain the maximum market power. However, in the AC case, it is only generator 38 that always maintains the maximum market power for all values of  $\rho$ . (b) The DC and the NL cases are more similar to each other than the corresponding AC case. (c) For demand scaling of  $t = 1.15$ , the DC and NL cases indicate that the total demand that can be met is lower than the total target demand. In the AC case, however, the total target demand of about  $71.1pu$  can be satisfied.

### 4.4.3 Summary of findings

First, our proposed market power measure can capture the impact of changes in load power factor. Specifically, it can identify *reliability must-run* generators. Note that, this capability in our measure is the direct result of using the more accurate AC power flow models. Second, our proposed measure is suitable to incorporate the impact of demand-response in market power analysis. One option is to analyze demand response by looking at the results at a certain demand level, as we explained in Section 4.4.1. Another option is to analyze demand response in form of quantifying the value of dispatchable loads at different buses, as we explained in Section 4.4.2. Note that, since we study structural market power, our

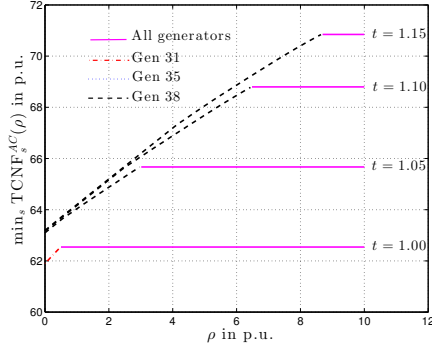
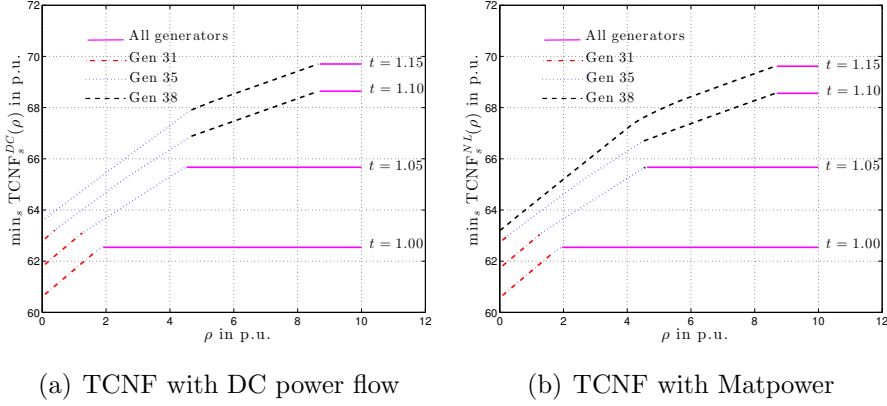


Figure 4.5: The lower envelope of TCNF, i.e.,  $\min_s \text{TCNF}_s$  for selected generators in the IEEE 39-bus system.

analysis does not involve pricing. Accordingly, it does not address price-elasticity in load demand. However, our case study in Section 4.4.2 provided an example on how we can utilize dispatchable loads as an *elastic demand resource* to mitigate market power. Finally, the results in our case studies can also be used to understand the role of renewable generation. For example, similar to the analysis in Section 4.4.2, we can assess renewable generators by examining their impact on parameter  $\rho$ . Note that, at a bus where a traditional generator is *co-located* with a renewable generator, the value of  $\rho$  is calculated as the *total* power injection by both generators combined. Therefore, we can analyze how the variations in the output of renewable generator may aggravate or mitigate market power of a co-located traditional generator.

## 4.5 Comparison of Computational Approaches

Now that we have presented our simulation results, we discuss the relative pros and cons of the three computational approaches to evaluate market power, namely,  $\text{TCNF}_s^{DC}(\cdot)$ ,  $\text{TCNF}_s^{NL}(\cdot)$  and  $\text{TCNF}_s^{AC}(\cdot)$ .

### DC Approximation Case

This approach uses an approximation of the underlying system and formulates the optimization as an LP that is fast and scalable with the size of the network. Since  $\text{TCNF}_s^{DC}(\cdot)$  is continuous and piecewise linear, we can characterize the slopes of the linear segments of  $\text{TCNF}_s^{DC}(\cdot)$  using Lagrangian duality [65]; furthermore, we can use these slopes to provide an efficient way to compute the function. Specifically, for generator  $s$ , let  $\mu$  be the Lagrange multiplier for the constraint  $p_s^G \leq \rho$ . For any function  $f(z)$  in variable  $z$ , define  $(df(z)/dz)^+$  as its right-hand derivative. We can relate the slopes of the linear segments of the functions  $\text{TCNF}_s^{DC}(\rho)$  as follows:

$$\left( \frac{d}{d\rho} \text{TCNF}_s^{DC}(\rho) \right)^+ = \mu_*, \quad (4.14)$$

where  $\mu_*$  is the Lagrange multiplier at the optimum. Recall that  $\text{TCNF}_s(\rho)$  is piecewise linear and is non-differentiable at the end-points of each line segment, but the right-hand derivative in (4.14) is well-defined. Using (4.14), a recursive algorithm can be developed to compute  $\text{TCNF}_s^{DC}(\rho)$  for  $\rho$  in any interval  $[a, b]$ ; see [128] for details.

### Using Matpower

Matpower is a MATLAB toolbox that implements a primal-dual interior-point algorithm to solve the power flow equations [63]. Interior-point methods were popularized by Karmarkar for LPs [139] and Nesterov et al. for SDPs [140]. For LPs and SDPs, it is proved that interior point methods converge to a *global* optimal solution in polynomial time. For nonlinear nonconvex problems, they rather provide a heuristic approach to obtain a *local* optimal

solution. Matpower has been known to perform well for economic dispatch problems over various IEEE test systems. As evidenced by our simulations, the NL case often shows similarity to the DC and the AC cases and provides a yard stick to measure the performance of our proposed DC approximation and the AC relaxation approaches. However, we reiterate that computing TCNF in (4.9) is NP-hard and thus it is hard to comment on the optimality of the solution obtained using Matpower.

### AC Relaxation Approach

The DC approximation completely ignores the reactive power flows; our studies on IEEE benchmark systems, however, indicate that reactive power flows play an important role in characterizing market power potential. To tackle such limitations, we use the SDP relaxation approach with an AC power flow model. When the relaxation is exact, it indeed provides a global optimal solution as opposed to the heuristic NL case. The sufficient conditions for exact relaxation, however, are specific to particular network topologies and constraint patterns [12, 36]. When line-flow constraints are active, the relaxation is often inexact, as in [1] and the optimization yields a non rank-1 optimal  $W_*$ . We encounter similar results in our simulations. To better understand the accuracy of our simulations, we report the statistics of the quantity  $\eta := \lambda_2(W_*)/\lambda_1(W_*)$  for the IEEE benchmark systems in Table 4.1, where  $\lambda_1(W_*)$ ,  $\lambda_2(W_*)$  are the first and second eigenvalues of the positive semidefinite matrix  $W_*$ , respectively. A lower value for this ratio indicates a smaller optimality gap and hence more accurate results. We see that  $\eta$  is typically very small in our simulations. However, the optimality gaps may not be accurate to find optimal operating points in economic dispatch, but as far as structural market power analysis is concerned, the results provide valuable insights to the system planner that is often not obvious using the DC power flow model. We comment that the SDP relaxation approach is known to scale poorly with the size of the network. Recent results in [11, 48], suggest that the sparsity of the power network can be suitably exploited to obtain fast and scalable conic relaxations; these ideas have been extensively explored in Chapter 2.

Test Case	# of Scenarios	Mean $\eta$	Max $\eta$
6-bus	834	0.0015	0.0044
9-bus	900	0.0034	0.0093
39-bus	900	0.0099	0.0171

Table 4.1: Statistics of  $\eta$  for IEEE benchmark systems.

## 4.6 Firm behavior

Our focus so far has been on identifying market power of a single generator. However, our analysis can easily be extended to the case where a single firm owns multiple generators at different locations. Let  $\mathcal{S}$  denote the set of locations (buses) where the firm has a generator. The TCNF index of the firm can be defined using the optimization problem (4.9) with a modified constraint that the *total* supply of the firm’s generators does not exceed  $\rho$ , i.e.,  $\sum_{s \in \mathcal{S}} p_s^G \leq \rho$ . Similarly, the TCMG index of a firm can be defined as the minimum *total* supply needed from the generators of this firm in order to meet a certain demand level  $D$ . This index can be calculated by modifying the objective function to  $\sum_{s \in \mathcal{S}} p_s^G$  in the definition of  $\text{TCMG}_s$ .

Note that, if an “adversarial” firm acts strategically to degrade the performance of the grid, then the behavior of each individual generator (of the firm) might be potentially different if it acted as a separate entity. A game theoretic analysis will be needed to measure the “worst-case” market power of an adversarial firm, which is an area left for future work.

We end this discussion with a note on supermodularity of market power. When market power is supermodular, it suggests that there is an incentive for generators to collude and form large firms. In fact, previous work in [129, 130] has suggested that there is always such an incentive. However, [129, 130] did not use power-flow equations in their study, and so we revisit this question here. Interestingly, it is indeed the case that, most of the time, market power is supermodular. This is not always the case though, e.g., for the IEEE 39-bus system, supermodularity does not hold for  $\text{TCNF}_s^{DC}(0)$  for generators at nodes  $s = 31$  and  $s = 32$  when the line-flow limits are uniformly scaled down to 70% of their given values. Other examples can also be found. While it is often the case that firms have incentive to collude,

this is not universally true.

## 4.7 Concluding remarks

In this chapter, we proposed a functional market power measure for structural analysis, called the *transmission constrained network flow*. This measure unifies three directions within market power research – residual supply based measures, network flow based measures, and minimal generation based measures. Additionally, our analysis uses detailed power flow equations to model the underlying physical power system. In current practice, units that impact voltages or reactive powers alone are separately identified as reliability must-run units; market power is then calculated among the other generators to identify pivotal units with respect to real power supply. In this work, we unify this in a common framework and identify must-run generators from an operational standpoint. Our simulations on the IEEE benchmark systems highlight that this distinction is of fundamental importance, i.e., using the detailed AC model as opposed to the DC model yields fundamentally different conclusions about market power. This highlights the fact that a pure economic analysis is not enough to accurately analyze market power in electricity markets.

# Chapter 5

## Role of market maker in Cournot competition in electricity markets

In the last chapter, we formulated the problem of detecting market power through structural analysis. Perhaps, the first thing a curious reader notices is that we did not model the strategic interaction of the generator firms explicitly. Rather our approach only assessed the potential to exploit for each firm. In this chapter, we turn toward filling that gap, i.e., we model the spot market as a Cournot game between the generator firms and the market maker or the independent system operator (ISO). Our goal is specifically to study the role of the ISO on the equilibrium outcome of the game. To make it precise, notice that the spot market is cleared using a specific market clearing mechanism, like solving the optimal power flow (OPF) problem with the submitted supply bids of the generators. In this chapter, we consider three such different market clearing mechanisms. First, we study the existence of equilibria in such settings. Then we illustrate through a 2-node network that the equilibrium outcome can be very different with the employed mechanism. The main goal of this chapter is to emphasize the role of a market maker in the electricity market.

## 5.1 Background on competition models for electricity markets

Electricity markets are challenging to model and analyze due to the multiple time-scales, non-convex generation costs, network constraints and generation supply constraints. Nevertheless, there is a sizable literature focused on analyzing the key strategic incentives of generators. The models that have been used can be largely classified into two categories – supply function competition and Cournot competition. In both approaches, it is common to assume that demand is exogenous and focus on analyzing the resulting strategic game among generators. Here, we briefly review prior work using supply function and Cournot competition in single-stage settings. We recognize that there is also significant work in multi-stage models, but we do not discuss that here as forward contracting is not the focus of the current chapter.

*Supply function competition:* Introduced by Klemperer et al. in [141], the key feature of supply function competition is that firms (or generators) compete by choosing supply functions specifying how much power it is willing to supply at each price. This model is appealing due to its similarity to how electricity markets operate in practice where generators typically submit step-wise increasing offer functions. Hence, this model has been frequently used both analytically and numerically to obtain insights on generator behavior [142–148]. In certain cases, strong theoretical results were obtained by restricting the functional form of the supply functions to a parameterized class [143, 147–149] (typically affine or logarithmic). More recent work has analyzed supply function competition in settings with network transmission constraints [126, 127, 150]. However, to our knowledge, no work has addressed the role of the market maker under supply function competition.

*Cournot competition:* Cournot competition is a well-known competitive model in economics dating back to 1838 [151]. In contrast with the supply function approach where generators submit an offer function, in Cournot competition, generators submit a single quantity specifying how much they are willing to supply at any price. Hence, this formula-

tion amounts to generators specifying a supply function with zero price elasticity. Although this offer model is significantly different from how electricity markets operate in practice, it was found that the Cournot model often provides good explanations of observed price variations [152, 153]. Further, the Cournot model is appealing due to its tractability, e.g. bounds on the loss in system efficiency due to strategic behavior have been obtained [154–156].

*Networked Cournot competition:* Cournot competition has also been applied to settings with network transmission constraints [157–163]. Such frameworks have also been applied to domains outside electricity within a broader framework referred to as networked Cournot competition [164]. However, the results in [164] are not directly applicable to electricity markets because they ignore network flow constraints. To our knowledge, in both non-networked and networked Cournot competition, no work has studied the role of the market maker which is the main focus of this chapter.

### 5.1.1 Contributions of this chapter

We make two main contributions: (i) we characterize the existence of equilibria under each of the three market maker objectives, and (ii) we show that, when equilibria exists, the equilibrium flow could be completely different under the three objectives. Our results highlight the importance of designing the market in a way that takes into account strategic generator behavior and physical system constraints. The equilibrium concept we adopt in this chapter is known as Generalized Nash Equilibrium (GNE). As will be clear in Section 5.2, the strategy set of the market maker depends on the actions of generators, and so the conventional Nash equilibrium framework does not apply to our setting. Hence, we resort to GNE which is an extension of Nash equilibrium for such settings.

Our first main result is that a GNE always exists under the social welfare and residual social welfare objectives but it might not exist under the consumer surplus objective. For the latter, we provide a simple 2-node example under which GNE does not exist. Our proof shows that one of the key factors that leads to non-existence of GNE is that the consumer surplus is not a concave function of the market maker’s decision variable. Non-existence

of equilibria could have numerous negative implications on market efficiency, e.g. more volatile prices leading to higher risk premium that eventually translates into higher costs for consumers. Also, market power measures might need to be adjusted to use longer-term metrics in order to account for the unreliable observations of market outcomes (e.g. see Chapter 4).

Our second main result shows that, when equilibria exist, the market outcomes could differ significantly under the three regulatory objectives. In particular, we focus on a 2-node example and show that the equilibrium flow could be positive with social welfare maximization, zero with residual social welfare maximization, and negative with consumer surplus maximization. Hence, although all three regulatory objectives attempt to maximize consumer benefit, the exact methodology by which system costs are reflected in the objective impacts how generators behave in the market and determines the resulting equilibrium and system efficiency.

## 5.2 Problem Formulation

Our goal in this chapter is to understand how the decision of the market maker impacts the strategic incentives and the resulting market equilibrium of generators in an electricity market. Hence, we model the market as a game between two entities: generators located at different nodes of the network, and a market maker that balances demand and supply. Since nodal pricing is a key feature in many electricity markets, we seek to capture this feature in our model by having generators and demand face different prices depending on their location in the network.

### 5.2.1 Notation

Let  $\mathbb{R}$  denote the set of real numbers and  $\mathbb{R}_+$  denote the set of non-negative real numbers. For any two vectors  $u, v$  of the same size, we say  $u \geq v$  if the vector  $u - v$  is element-wise non-negative. Also, let  $\mathbf{1}$  denote the vector of all ones of appropriate size. For any vector

$v \in \mathbb{R}^n$ , we denote its transpose by  $v^\top$ . We also let  $v_{-i} = (v_1, \dots, v_{i-1}, v_{i+1}, \dots, v_n)$  denote the vector of all elements other than the  $i$ -th element.

## 5.2.2 Network model

We consider a power network with  $n$  nodes  $1, 2, \dots, n$  and  $\ell$  edges. Each node  $k$  has a generator  $G_k$  that supplies a quantity of power  $q_k \geq 0$  and incurs a cost  $c_k q_k^2$  for some  $c_k > 0$ . We assume that demand at each node  $k$  can be represented by a linear demand function:

$$p_k(d_k) := a_k - b_k d_k,$$

for some  $a_k > 0$  and  $b_k \geq 0$ . Here,  $p_k(d_k)$  is the price that demand at node  $k$  is willing to pay as a function of the quantity of power  $d_k$  it receives. This form of demand function is a common assumption in economics [151] and prior studies of electricity markets models [160–162] and corresponds to an aggregate consumer having a quadratic utility function. We also assume that all demand functions are fixed and known to all market participants, which is reasonable when demand is highly predictable.

We assume that there is a single market maker  $M$  that balances supply and demand by choosing *re-balancing quantities*  $r_k$  at each node such that demand at node  $k$  receives a quantity:

$$d_k := q_k + r_k.$$

At each node  $k$ , the market maker charges the demand and pays the generator at a price  $p_k(q_k + r_k)$ . This model for nodal pricing is motivated by prior studies of electricity markets, e.g. [160–162].

Let the vector  $q := (q_1, q_2, \dots, q_n)$  denote the production quantities of the generators and the vector  $r := (r_1, r_2, \dots, r_n)$  denote the re-balancing quantities chosen by the market maker. We assume that the market maker chooses the vector  $r$  of re-balancing quantities subject to the following constraints:

- (i) Demand at each node is non-negative, i.e.,  $q + r \geq 0$ .

$$W_{soc}(q, r) := \sum_{1 \leq k \leq n} \left( \int_0^{q_k + r_k} p_k(w_k) dw_k - \tilde{c}_k(q_k) \right). \quad (5.1)$$

$$W_{res}(q, r) := W_{soc}(q, r) - \sum_{1 \leq k \leq n} \pi_k^G(q, r) = \sum_{1 \leq k \leq n} \left( \int_0^{q_k + r_k} p_k(w_k) dw_k - q_k p_k(q_k + r_k) \right). \quad (5.2)$$

$$W_{con}(r, q) := \sum_{1 \leq k \leq n} \left( \int_0^{q_k + r_k} p_k(w_k) dw_k - (q_k + r_k) p_k(q_k + r_k) \right). \quad (5.3)$$

- (ii) Power flow on each transmission line respects the line limits, i.e.,  $-f \leq -Hr \leq f$ , where  $H \in \mathbb{R}^{\ell \times n}$  is the shift-factor matrix that relates the flows on all  $\ell$  lines as a function of the power injection vector  $-r$  and  $f \in \mathbb{R}^\ell$  is the vector of all line capacities.
- (iii) Re-balancing quantities sum to zero, i.e.,  $\mathbf{1}^\top r = 0$ .

Note that the set of allowable re-balancing quantities depends on the production quantities  $q$ . We denote the set of allowable re-balancing quantities by:

$$S^M(q) := \left\{ r \in \mathbb{R}^n \mid q + r \geq 0, |Hr| \leq f, \mathbf{1}^\top r = 0 \right\}.$$

Figure 5.1 shows an example of a 2-node network, which we study in detail in Section 5.4.

We remark that the shift-factor matrix depends on the admittances of the transmission lines of the power network and encapsulates Kirchoff's laws [108]. This representation assumes a linearized DC power-flow model [32] for the network. Though widely used in the literature, this representation of the power flow equations has its limitations for power system operation, e.g., see [33]. However, in electricity markets, locational marginal prices are typically calculated using the DC power-flow model [165–167]. Hence, this is a reasonable model for the purpose of studying generator bidding behavior in the market.

### 5.2.3 Generator profit

Within the context described above, the profit of generator  $G_k$  is given by:

$$\pi_k^G(q_k, q_{-k}, r) := q_k p_k(q_k + r_k) - c_k q_k^2. \quad (5.4)$$

We assume that each generator seeks to maximize its profit  $\pi_k^G(q_k, q_{-k}, r)$  over its production quantity  $q_k \in S_k^G$  where  $S_k^G = \mathbb{R}_+$  denotes the set of allowable production quantities of generator  $k$ . That is, we assume that generators have infinite capacities.

This is a common assumption in prior studies of market power [142, 143]. The analysis of the case of finite generation capacities is clearly important, but it is left for future work.

Notice that, without the strategic market-maker and geographically distributed generators, this model reduces to the standard Cournot oligopoly in the microeconomics literature [151].

### 5.2.4 Market maker objectives

Our focus in this chapter is on the role of the market maker. In electricity markets, the market makers are often regulatory authorities, e.g., ISOs; thus our goal is to study the role of market design in this regulatory framework.

The market maker designs we consider assume that the market maker maximizes some objective function  $\pi^M(q, r)$  over the re-balancing quantities  $r \in S^M(q)$ . Note that the market maker is a regulatory authority and is free to choose a suitable payoff function. This is the *market design* question of interest, and in this chapter we analyze different candidates for the payoff function  $\pi^M(q, r)$ .

Specifically, inspired from the microeconomics literature [151], we consider the following candidates for  $\pi^M(q, r)$ :

- (a) *Social welfare*: This is the net benefit to society. It refers to the consumers' utility less generation costs (also referred to as overall network utility). We denote it by  $W_{soc}(q, r)$  in (5.1). If generators are not strategic, this corresponds to the original optimal power

flow formulation in [3].

- (b) *Residual social welfare*: In practice, generator costs are unlikely to be known to the market maker. Hence, an alternative regulatory objective is to maximize the social welfare, less the profits of the generators. This is equivalent to the consumers' utility less the revenue of the generators. We denote it by  $W_{res}(q, r)$  in (5.2).
- (c) *Consumer surplus*: This is the net benefit to consumers. It refers to the consumers' utility less their payments. We denote it by  $W_{con}(q, r)$  in (5.3).

We remark that at each node  $k$ , the amount paid by the consumers is  $(q_k + r_k)p_k(q_k + r_k)$ , and the amount paid to the generator  $G_k$  is  $q_k p_k(q_k + r_k)$ . Hence, the market is not necessarily budget-balanced. The difference between the total payment by demand and the total revenue of the generators has previously been referred to as *merchandising surplus* [168]. A consequence of the market not being always budget-balanced is that the residual social welfare is not necessarily equal to the consumer surplus. Hence, it is important to explore the impact of both objectives on the market.

### 5.2.5 Competitive model

Given the models of the generators and the market maker, we now need to model their interaction. To do this, we consider a game with: (a) players  $(G_1, G_2, \dots, G_n, M)$ ; (b) strategy sets  $(S_1^G, S_2^G, \dots, S_n^G, S^M)$ ; and (c) payoffs  $(\pi_1^G, \pi_2^G, \dots, \pi_n^G, \pi^M)$ , where  $\pi^M$  is chosen to be one of the functions in  $\{W_{soc}, W_{res}, W_{con}\}$ . Throughout, we assume that the game is feasible, i.e., the set  $\{(q \in \mathbb{R}_+^n, r \in \mathbb{R}^n) \mid (q, r) \in (S_k^G, 1 \leq k \leq n, S^M(q))\}$  is non-empty.

Since the strategy set  $S^M(q)$  of the market-maker depends on the actions  $q$  of the generators, we focus on a type of equilibrium known as *Generalized Nash Equilibria* (GNE). Formally, an action profile  $(q^*, r^*)$  constitutes a GNE if, for each  $1 \leq k \leq n$ , we have:

$$\begin{aligned} \pi_k^G(q_k^*, q_{-k}^*, r^*) &\geq \pi_k^G(q_k, q_{-k}^*, r^*) \text{ for all } q_k \in S_k^G, \\ \pi^M(q^*, r^*) &\geq \pi^M(q^*, r) \text{ for all } r \in S^M(q^*). \end{aligned}$$

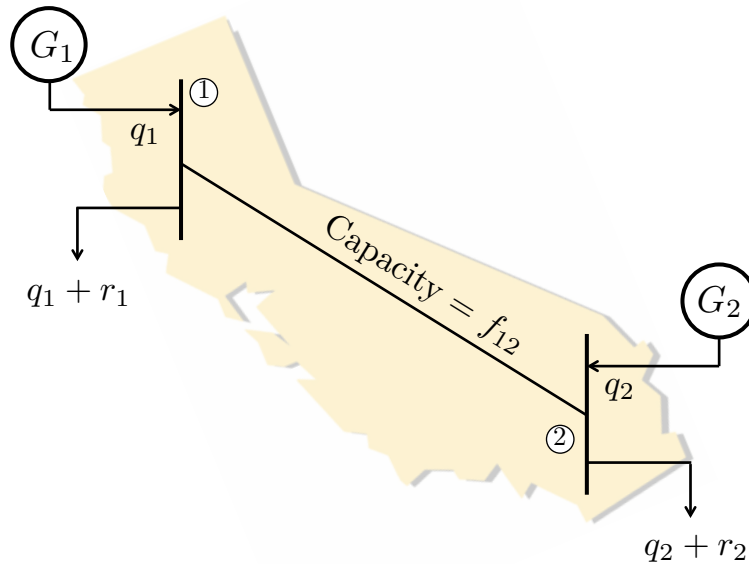


Figure 5.1: Example of a 2-node network. This example illustrates how the model in this chapter can be used to study a caricature of the market in California. Here, northern and southern California are represented as two aggregate nodes connected by a transmission line - Path 15 - that is often congested [2].

This equilibrium concept was first introduced in 1952 by Debreu [169]. It is an extension of Nash equilibrium where the strategy sets of players do not depend on the actions of the other players. We refer the reader to [170] for a detailed survey.

### 5.3 Existence of equilibrium

Within the context of the model described in the previous question, we seek to investigate the following two questions in this chapter:

1. Does a GNE always exist for every each of the market maker objectives we have described, i.e.,  $\pi^M \in \{W_{soc}, W_{res}, W_{con}\}$ ?
2. In the cases where a GNE exists, how do the market outcomes (in terms of flows, profits of generators and social welfare) differ for different market maker objectives?

We focus on the first question in this section and treat the second question in Section 5.4.

The following is our main result on the existence of GNE.

**Theorem 14.** *A GNE exists if  $\pi^M = W_{soc}$  or  $\pi^M = W_{res}$ . However, a GNE may not exist if  $\pi^M = W_{con}$ .*

The theorem shows that the market maker objective has a significant impact on the existence of a GNE in the market. One of the key factors that lead to non-existence of GNE is that the consumer surplus  $W_{con}$  is not a concave function of the re-balancing quantities  $r$ . Hence, when  $\pi^M = W_{res}$ , the optimal re-balancing quantities are at the boundaries of the feasible set  $S^M(q)$ . When the generator production  $q$  changes, the optimal re-balancing quantities  $r^*$  could jump from one boundary point to another, i.e. it is not always continuous in  $q$ , especially when network capacity constraints are binding. Hence, there does not necessarily exist a fixed-point in  $(q, r)$ . In the proof, we explicitly construct an example that exhibits this phenomena using the 2-node network in Figure 5.1.

Given Theorem 14, let us briefly emphasize the importance of choosing a regulatory objective that leads to existence of equilibria. Non-existence of equilibria could have numerous negative implications. It could lead to volatile market prices as the market oscillates between different outcomes which would increase the risk premium and the cost of forward contracting. Market power measures might need to be adjusted to use longer-term metrics in order to account for the unreliable observations of market outcomes (e.g. see [13]). Further, more sophisticated models and equilibria concepts (e.g. repeated game models, dynamic equilibria) might have to be used in theoretical and empirical analysis of market behavior.

To prove the existence results in Theorem 14, we use a result that can be traced back to Debreu [169]. However, the version we apply is a slightly simplified statement given in [170, 171]. Below, we state Debreu's theorem before giving a proof of Theorem 14.

**Theorem.** *(Debreu [169]) Consider a game between  $N$  players defined as follows. For each player  $\nu$ , denote its action by  $x_\nu \in \mathbb{R}^{n_\nu}$  and its payoff function by  $\theta_\nu : \mathbb{R}^n \rightarrow \mathbb{R}$  where  $n = \sum_{\nu=1}^N n_\nu$ . Assume that each player  $\nu$  has a strategy set  $X_\nu(x_{-\nu}) \subseteq \mathbb{R}^{n_\nu}$  that could*

depend on the actions  $x_{-\nu}$  of all other players. Hence, given the actions  $x_{-\nu}$  of all other players, each player  $\nu$  chooses a strategy  $x_\nu$  that solves:

$$\max_{x_\nu \in X_\nu(x_{-\nu})} \theta_\nu(x_\nu, x_{-\nu}).$$

Suppose that:

1. There exists  $N$  nonempty, convex and compact sets  $K_\nu \subset \mathbb{R}^{n_\nu}$  such that for every  $x \in \mathbb{R}^n$  with  $x_\nu \in K_\nu$  for every  $\nu$ ,  $X_\nu(x_{-\nu})$  is nonempty, closed and convex,  $X_\nu(x_{-\nu}) \subseteq K_\nu$ , and  $X_\nu$ , as a point-to-set map, is both upper and lower semicontinuous.
2. For every player  $\nu$ , the function  $\theta_\nu(\cdot, x_{-\nu})$  is quasi-concave on  $X_\nu(x_{-\nu})$ .

Then a GNE exists.

*Proof of Theorem 14.* We divide the proof into three cases, depending on the form of the market maker objective  $\pi^M$ .

*Case 1:*  $\pi^M = W_{soc}$ . Here, we prove that a GNE always exists. Condition 1 in Debreu's Theorem requires strategy sets to be compact. It can be shown that the shift-factor matrix  $H$  has rank  $n - 1$  for any power network and  $\mathbf{1}^\top$  is linearly independent from the rows of  $H$ . It then follows that the feasible region of injection is compact and hence the strategy set  $S^M(q)$  of the market maker is also compact. Now, we turn our attention to the strategy sets of generators  $S_k^G$ . Though  $S_k^G$  of generators are not compact, they can be restricted to some compact subset  $[0, \bar{s}]$  since any equilibrium production  $q_k^*$  can be upper bounded by some  $\bar{s}$ . To see the latter, first observe that, if  $r_k^*$  is an equilibrium re-balancing quantity, then it is bounded from above since:

$$\int_0^{q_k + r_k^*} p_k(w_k) dw_k = a_k(q_k + r_k^*) - \frac{b_k}{2}(q_k + r_k^*)^2,$$

and that for large  $r_k^*$ , the quadratic term (which has a negative coefficient) dominates the linear term. Hence, suppose  $r_k^* \leq \bar{r}$  for all  $k$ . Let  $\bar{s} = a_k/b_k + (n - 1)\bar{r}/b_k$ . Note that, if

$q_k^* > \bar{s}$ , then the equilibrium price at node  $k$  is:

$$p_k^* = a_k - b_k \left( q_k^* - \sum_{k' \neq k} r_{k'}^* \right) < 0.$$

This is a contradiction since generator  $k$  cannot be facing a negative price  $p_k^* < 0$  and yet producing a positive quantity  $q_k^* > \bar{s}$ . For the rest of this proof, we shall assume that  $S_k^G = [0, \bar{s}]$ .

It is straightforward to show that our game satisfies conditions 1 and 2 in Debreu's Theorem. Condition 2 holds trivially since the generator and market maker payoffs are strictly concave over their respective strategy sets. To see that condition 1 holds, choose  $K_\nu$  in Debreu's Theorem in the following manner: (a) for each generator  $k$ , choose  $K_\nu = S_k^G$ ; and (b) for the market maker, choose  $K_\nu = \{r \in \mathbb{R}^n \mid |Hr| \leq f, \mathbf{1}^\top r = 0\}$ . It is clear that  $K_\nu$  are nonempty, convex, and compact.

While the generator strategy sets  $S_k^G$  are constant correspondences, the market maker strategy set  $S^M(q)$  is a polytope that is linearly parametric. Thus, the strategy sets are both upper and lower semicontinuous in terms of players' actions.

*Case 2:*  $\pi^M = W_{res}$ . Here, we prove that a GNE always exists. Observe that any equilibrium re-balancing quantity  $r_k^*$  is bounded from above since:

$$\int_0^{q_k+r_k} p_k(w_k) dw_k - q_k p_k(q_k + r_k) = a_k r_k - \frac{b_k}{2} (r_k^2 - q_k^2).$$

The rest of the proof is similar to that for case 1.

*Case 3:*  $\pi^M = W_{con}$ . Here, we construct an example where GNE does not exist using the 2-node network in Figure 5.1. Our construction is based on the following lemma, proven in Section 5.5.

**Lemma 15.** *Consider the 2-node network in Figure 5.1. Let  $\pi^M = W_{con}$ . Suppose  $a_1 =$*

$a_2 = a$ ,  $1 < b_1/b_2 \leq 3$ ,  $c_1 = c_2 = c$ , and  $f_{12}$  satisfies:

$$\frac{a}{3b_1 + 2c} < f_{12} < \min \left\{ \frac{a}{b_2 + 2c}, \frac{a}{b_1}, f_0 \right\}, \quad (5.5)$$

where:

$$f_0 := \frac{ab_2 [b_1 + b_2 + c(3 - b_1/b_2)]}{b_1 b_2 (b_1 + b_2) + b_1 (b_1 + 5b_2)c + 2(b_1 + b_2)c^2}.$$

Then there does not exist a GNE.

The following parameter values:  $a = 10$ ,  $b_1 = 1.2$ ,  $b_2 = 1$ ,  $c = 1$  and  $f_{12} = 2$ , satisfy the conditions in the lemma and provides an example in which GNE does not exist.  $\square$

## 5.4 Regulatory objectives and market outcomes

Given the existence results in the previous section, we now move to analyzing the impact of regulatory objectives on the market outcomes. To provide clear insight, we focus our analysis on the case of a the 2-node network in Figure 5.1, which represents a caricature of the situation in California. Though simple, this 2-node network is already enough to highlight significant differences in the impact of regulatory objectives.

We begin with a case of unbounded line capacities. This allows us to consider a situation where the market equilibrium always exists for each regulatory objective. Additionally, it highlights that the behaviors of the three regulatory objectives we are studying can differ dramatically even in the simplest of settings. The proof is included in Section 5.5

**Theorem 16.** *Consider the 2-node network in Figure 5.1. Let  $a_1 = a_2 := a$ ,  $1 < b_1/b_2 \leq 3$ ,  $c_1 = c_2 := c$  and  $f_{12} = \infty$ . Then a GNE exists for all  $\pi^M \in \{W_{soc}, W_{res}, W_{con}\}$ . Moreover, the equilibrium re-balancing quantity  $r_1^* = -r_2^*$  under the three regulatory objectives are as follows:*

(a) If  $\pi^M = W_{soc}$ , then  $r_1^* < 0$ ,

(b) if  $\pi^M = W_{res}$ , then  $r_1^* = 0$ ,

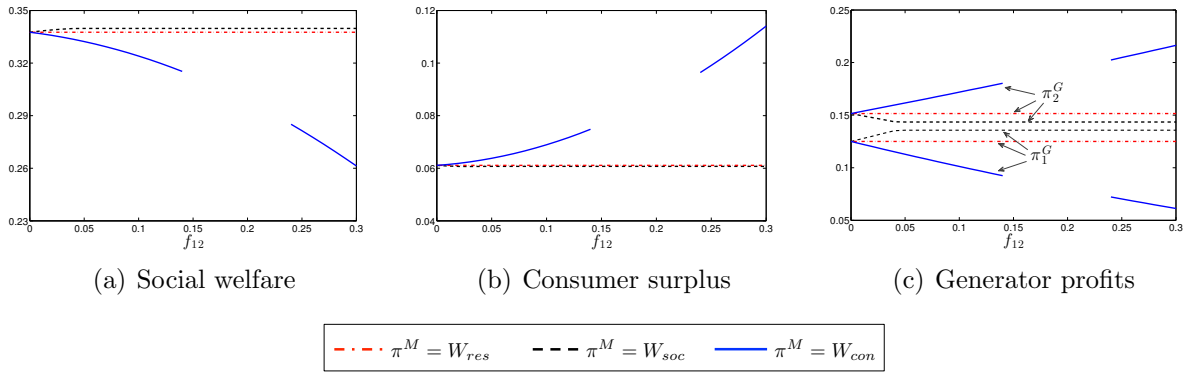


Figure 5.2: Plots of various quantities at equilibrium with varying line capacities  $f_{12}$  in the 2-node network in Figure 5.1. Parameters chosen for this example are:  $a_1 = a_2 = 1$ ,  $b_1 = 1$ ,  $b_2 = 0.65$ ,  $c_1 = c_2 = 1$ .

(c) If  $\pi^M = W_{con}$ , then  $r_1^* > 0$ .

Note that, even though there are no line constraints (i.e.,  $f_{12} = \infty$ ), the 2-node network is not equivalent to an aggregated market since the price at each node is a function of the local demand function at that node.

Our result illustrates how a simple market can exhibit very different equilibria under different regulatory objectives. In particular, though all three market maker objectives are motivated qualitatively by the identical goal of maximizing consumer benefit; one results in flow going north, one in flow going south, and one in no flow between the nodes. So, the exact choice of how costs are reflected in the objective is a significant determinant of how generators behave in the market, which affects the equilibrium power flows and system efficiency dramatically. Hence the market design question is important in the operation of a deregulated market. Although Theorem 16 assumes that the line capacity  $f_{12} = \infty$ , our numerical calculations indicate that the sign of  $r_1^*$  exhibit the same properties even under a binding line constraint.

To further emphasize the significance of the market maker objective on the efficiency of the market, we compare the social welfare (Figure 5.2(a)), consumer surplus (Figure 5.2(b)), and generator profits (Figure 5.2(c)), at the unique equilibrium under each of the three market maker objectives as the line capacity  $f_{12}$  is increased. Here, we choose the parameters in the following manner:  $a_1 = a_2 = 1$ ,  $b_1 = 1$ ,  $b_2 = 0.65$ , and  $c_1 = c_2 = 1$ ; but the qualitative

features in the plots continue to hold for other parameter values that we experimented with. For the case where  $\pi^M = W_{con}$ , the gap in the plot indicates that equilibrium does not exist for those values of  $f_{12}$ . The plots reveal the counter-intuitive phenomena that: increasing the line capacity could decrease social welfare if  $\pi^M = W_{con}$ . There is also a clear tradeoff between market maker objectives: having  $\pi^M = W_{soc}$  leads to higher social welfare but lower consumer surplus versus having  $\pi^M = W_{con}$ .

The three market maker objectives also lead to completely different scaling of generator profits as the line capacity  $f_{12}$  is increased – generator  $G_1$  benefits from line expansion when  $\pi^M = W_{soc}$  but generator  $G_2$  benefits from line expansion when  $\pi^M = W_{con}$ . This implies that, although the market maker objective is only used in the short-term market, it also has implications on long-term incentives to expand transmission.

## 5.5 Proofs of main results

Here we present the proofs of Lemma 15 and Theorem 16. These results are specific to the 2-node network in Figure 5.1. Hence, we simplify the notation by defining  $r := r_1 = -r_2$ . Furthermore, we drop the subscript in  $f_{12} := f$ .<sup>1</sup>

By applying the assumption that  $a_1 = a_2 := a$ , we can write the derivatives of the generator profits with respect to their production quantities as:

$$\frac{\partial \pi_1}{\partial q_1} = (a - b_1 r) - 2(b_1 + c)q_1, \quad (5.6)$$

$$\frac{\partial \pi_2}{\partial q_2} = (a + b_2 r) - 2(b_2 + c)q_2. \quad (5.7)$$

We make repeated references to these expressions throughout the proofs.

---

<sup>1</sup>The notations  $f$  and  $r$  in this proof should not be confused with the vectors in Section 5.2.

## Proof of Lemma 15:

Here  $\pi^M(q_1, q_2, (r, -r)) = W_{con}(q_1, q_2, (r, -r))$ . From equation (5.3), we get:

$$\pi^M((q_1, q_2), (r, -r)) = \underbrace{\frac{b_1}{2}(q_1 + r)^2 + \frac{b_2}{2}(q_2 - r)^2}_{:=\Pi(r)/2}.$$

The market maker maximizes  $\Pi(r)$  subject to  $-q_1 \leq r \leq q_2$  and  $-f \leq r \leq f$ . Our proof technique is to completely characterize all possible equilibria  $(q_1^*, q_2^*, r^*)$  and the conditions on  $f$  that lead to each of the equilibria. Since those conditions on  $f$  do not contain the relation in (5.5), we then infer that GNE does not exist when  $f$  satisfies (5.5).

We divide our analysis into two cases based on whether  $f \geq a/(b_2 + 2c)$  or  $f < a/(b_2 + 2c)$ . The first case can be interpreted as the scenario in which network constraints are not tight.

**Case 1:**  $f \geq a/(b_2 + 2c)$ . Here, we show that a GNE always exists by constructing one. In particular, we construct a GNE such that  $r^* = q_2^*$ . Note that, since  $\Pi$  is convex, its maximizers occur at  $-q_1^*$ ,  $q_2^*$ ,  $-f$ , or  $f$ . By using  $b_1 > b_2$ , we can check that, for any  $q_1^*, q_2^* \geq 0$ , we have:

$$\Pi(q_2^*) \geq \Pi(\max\{-q_1^*, -f\}).$$

Since  $a + b_2 r^* = a + b_2 q_2^* \geq 0$ , we can solve for  $q_2^*$  by setting  $\left. \frac{\partial \pi_2}{\partial q_2} \right|_{q_2^*} = 0$  in (5.7), which gives:

$$q_2^* = r_* = \frac{a}{b_2 + 2c}.$$

Now note that  $q_2^* < f$  which verifies that  $q_2^*$  maximizes  $\Pi(r)$  over  $r \in [-q_1^*, q_2^*] \cap [-f, f]$ .

Next, using (5.6) to solve for  $q_1^*$  gives:

$$q_1^* = \begin{cases} a \frac{2c + b_2 - b_1}{2(b_1 + c)(b_2 + 2c)}, & \text{if } b_1 < b_2 + 2c, \\ 0, & \text{otherwise.} \end{cases}$$

This defines a GNE.

**Case 2:**  $f < a/(b_2 + 2c)$ . First, we argue that any equilibrium must satisfy  $q_2^* \geq f$ .

Suppose there exists an equilibrium with  $q_2^* < f$ . The analysis in case 1 implies that  $r^* = q_2^*$ . However, the first-order condition for generator 2 (c.f. (5.7)) implies that  $q_2^* = r^* = a/(b_2 + 2c) > f$  which is a contradiction. Hence, any equilibrium must satisfy  $q_2^* \geq f$ .

Recall that  $\Pi$  is strictly convex. The condition that  $q_2^* \geq f$  imply that the maximizers of  $\Pi$  can only occur at  $-q_1^*$ ,  $-f$ , or  $f$ . We consider each case separately. Due to lack of space, we only give the proof of the case where  $-f \leq -q_1^*$  and  $r^* = +f$  in this chapter. However, the approach for the other cases is similar.

Suppose  $-f \leq -q_1^*$  and  $r^* = +f$ . From (5.6) and (5.7), we have:

$$q_2^* = \frac{a + b_2 f}{2(b_2 + c)}, \quad q_1^* = \begin{cases} \frac{a - b_1 f}{2(b_1 + c)}, & \text{if } f \leq \frac{a}{b_1}, \\ 0, & \text{otherwise.} \end{cases}$$

For this case, we need the following conditions to be satisfied: (a)  $q_2^* \geq f$ , (b)  $q_1^* \leq f$ , and (c)  $\Pi(+f) \geq \Pi(-q_1^*)$ . We derive conditions on  $f$  for (a), (b) and (c) to hold. It can be checked that  $f < a/(b_2 + 2c)$  implies (a) is always satisfied. To deal with conditions (b) and (c), we consider the two possibilities separately: (i)  $f \leq a/b_1$ , and (ii)  $f > a/b_1$ .

(i) Suppose  $f \leq a/b_1$ . Then (b)  $q_1^* \leq f$  if and only if:

$$f \geq \frac{a}{3b_1 + 2c}.$$

Also, (c)  $\Pi(+f) \geq \Pi(-q_1^*)$  is true if and only if the following quantity is non-negative.

$$\begin{aligned} & \Pi(+f) - \Pi(-q_1^*) \\ &= b_1(q_1^* + f)^2 + b_2(q_2^* - f)^2 - b_2(q_1^* + q_2^*)^2 \\ &= \underbrace{(q_1^* + f)}_{\geq 0} \underbrace{\left[ b_1(q_1^* + f) - b_2(2q_2^* - f + q_1^*) \right]}_{:=\lambda}. \end{aligned}$$

Substituting the expressions for  $q_1^*$  and  $q_2^*$  for this case, it can be verified that  $\lambda \geq 0$  if and

only if:

$$f \geq \frac{ab_2 \left[ b_1 + b_2 + c(3 - b_1/b_2) \right]}{b_1 b_2 (b_1 + b_2) + b_1 (b_1 + 5b_2)c + 2(b_1 + b_2)c^2} := f_0.$$

(ii) Suppose  $f > a/b_1$ . Then (b)  $q_1^* = 0 \leq f$  is trivially satisfied. Also, (b)  $\Pi(+f) \geq \Pi(-q_1^*)$  if and only if  $\lambda \geq 0$ , where:

$$\begin{aligned} \lambda &= b_1(q_1^* + f) - b_2(2q_2^* - f + q_1^*) \\ &= (b_1 + b_2)f - 2b_2 \left[ \frac{a + b_2 f}{2(b_2 + c)} \right] \\ &= \frac{b_1 b_2 + c(b_1 + b_2)}{(b_2 + c)} f - \frac{ab_2}{(b_2 + c)}. \end{aligned}$$

Now, we also have:

$$f \geq \frac{a}{b_1} > \frac{a}{b_1 + c(1 + b_1/b_2)} \implies \lambda \geq 0.$$

By working through the other cases in a similar manner, we discover that there exists a GNE if and only if:

1.  $f \geq a/(b_2 + 2c)$ ; or,
2.  $f < a/(b_2 + 2c)$ ,  $f \leq a/b_1$ ,  $f \geq a/(3b_1 + 2c)$ , and  $f \geq f_0$ ; or,
3.  $f < a/(b_2 + 2c)$  and  $f > a/b_1$ ; or,
4.  $f < a/(b_2 + 2c)$ ,  $f \leq a/b_1$ ,  $f \leq a/(3b_1 + 2c)$ , and  $f \leq f_1$ ,

where  $f_1 := \frac{ac(b_1 - b_2)}{b_1 b_2 (b_1 + b_2) + c(b_1^2 + b_2^2)}$ . Since the relation in (5.5) is not contained in any of the above cases, this completes the proof of Lemma 15. ■

## Proof of Theorem 16:

Case (a):  $\pi^M = W_{soc}$ . Simplifying the expression for  $W_{soc}$  in (5.1) gives:

$$2\pi^M(q_1, q_2, (r, -r)) = \underbrace{-b_1(q_1 + r)^2 - b_2(q_2 - r)^2}_{:=\Pi(r)} + 2a(q_1 + q_2) - 2c_1q_1^2 - 2c_2q_2^2.$$

Maximizing  $\pi^M(q_1, q_2, r)$  is equivalent to maximizing  $\Pi(r)$  over  $r \in [-q_1, +q_2]$ . It can be checked that  $\Pi(r)$  is always maximized at an interior point and hence, at equilibrium, the quantities  $q_1^*, q_2^*, r^*$  satisfy:

$$r^* = \frac{b_2q_2^* - b_1q_1^*}{b_1 + b_2}. \quad (5.8)$$

To compute  $q_1^*$  and  $q_2^*$ , note that there are four possible configurations of equilibria depending on the signs of  $a - b_1r^*$  and  $a + b_2r^*$ . We deal with each case separately.

(i)  $a - b_1r^* < 0, a + b_2r^* < 0$ : From (5.6) and (5.7), it follows that  $q_1^* = q_2^* = r^* = 0$ . But then we have  $a - b_1r^* = a > 0$  and hence a contradiction. Hence, an equilibrium of this form does not exist.

(ii)  $a - b_1r^* < 0, a + b_2r^* \geq 0$ : From (5.6) and (5.7), we have  $q_1^* = 0$ , and  $q_2^* = (a + b_2r^*)/(2b_2 + 2c)$ . Substituting this into (5.8) and simplifying, we get:

$$r^* = \frac{b_2}{b_1 + b_2}q_2^* = \frac{ab_2}{2(b_1 + b_2)(b_2 + c) - b_2^2}.$$

But it can be checked that  $a - b_1r^* \geq 0$  which is a contradiction. Hence, an equilibrium of this form does not exist.

(iii)  $a - b_1r^* \geq 0, a + b_2r^* < 0$ : From (5.6), (5.7) and using arguments similar to the last

case, we have  $q_2^* = 0$  and:

$$r^* = \frac{-ab_1}{2(b_1 + b_2)(b_1 + c) - b_1^2}.$$

Again, it can be checked that  $a + b_2r^* \geq 0$  which is a contradiction. Hence, an equilibrium of this form does not exist.

(iv)  $a - b_1r^* \geq 0$ ,  $a + b_2r^* \geq 0$ : For this case the triplet  $(q_1^*, q_2^*, r^*)$  satisfies the relation in (5.8) and:

$$q_1^* = \frac{a - b_1r^*}{2(b_1 + c)}, \text{ and } q_2^* = \frac{a + b_2r^*}{2(b_2 + c)}.$$

Solving these linear equations, we obtain:

$$r^* = \frac{ac(b_2 - b_1)}{(b_1 + b_2)(b_1b_2 + 2c^2) + c(b_1^2 + b_2^2 + 4b_1b_2)} < 0.$$

With some algebraic manipulations, it can be shown that indeed  $a - b_1r^* \geq 0$  and  $a + b_2r^* \geq 0$ . This defines an equilibrium.

This proves the claim in Theorem 16(a).

*Case (b):*  $\pi^M = W_{res}$ . Simplifying the expression for  $W_{res}$  in (5.2) gives:

$$2\pi^M(q_1, q_2, (r, -r)) = -(b_1 + b_2)r^2 + b_1q_1^2 + b_2q_2^2.$$

Since  $\pi^M$  is strictly concave in  $r$ , it is maximized at  $r^* = 0$ . The resulting equilibria values for  $q_1^*$  and  $q_2^*$  can be computed from the generator profits. This proves the claim in Theorem 16(b).

*Case (c):*  $\pi^M = W_{con}$ . Since  $f > a/(b_2 + 2c)$ , this corresponds to case 1 in the proof of Lemma 15. Hence, equilibrium always exists and we have:

$$r^* = \frac{a}{b_2 + 2c} > 0.$$

This proves the claim in Theorem 16(c), which completes the proof of the theorem. ■

## 5.6 Concluding remarks and future directions

In this chapter, we introduce a networked Cournot model for studying the impact of regulatory objectives on the outcomes in electricity markets. In particular, the model we introduce formulates a game between the electricity market maker (or the ISO) and generators. Within this game, our main results explore the contrasts between three natural market maker objectives – social welfare, residual social welfare, and consumer surplus. The results in this chapter reveal that the design of the market has significant implications on both the existence and form of equilibria. In particular, equilibria might not exist when the market maker maximizes the consumer surplus and the network is capacity constrained. Further, even when equilibria exist, the equilibrium allocation of power flows can be completely different under the three market maker objectives. Hence, the results in this chapter highlight that design of market maker objective is delicate and needs to be further investigated in a principled manner.

# Chapter 6

## Placing energy storage in a grid for load-shifting

An optimization or game over a time horizon reduces to a one stage problem when the states of the system are not coupled across time. The problems considered in Chapters 2 – 5 belong to this category. In this chapter, we introduce electric energy storage that couples the system states across time. Energy storage has many potential applications in power systems. On a fast time scale (on a seconds to minutes scale), it can mitigate intermittency of renewable sources like wind and solar. On a slower time scale (across hours), it can flatten out generation profile rather than supply simply following demand. In this chapter, we concentrate on the second application, that is often referred to as load-shifting. Recall that cost of conventional generation is often quadratic and hence convex. Given such a convex cost, a flatter generation profile reduces total cost over a time horizon. Our focus is on placement and sizing of storage resources across a network to reduce the system-wide generation cost, given an available storage budget. The investment decision problem, by construction, is an infinite horizon problem. With cyclic variation in demand, it is sufficient to optimize the cost over one time period of the cycle. We do two studies in this chapter: (1) simulations using a semidefinite relaxation of AC optimal power flow on IEEE benchmark systems, (2) theoretical characterization of a property of the optimal placement using DC power flow approximations.

## 6.1 Background

### 6.1.1 Motivation

One key difference between electricity and other commodities is the concept of inventory, i.e., ability to store excess supply at one point in time and use that in conjunction with current supply to serve demand. This is precisely the flexibility that electric energy storage would provide to the power grid; in essence balancing any realized demand with instantaneous supply would no longer be necessary. This flexibility is envisioned to have many potential applications to the grid, see [172, 173] for a detailed survey. There has been much interest in building the physical devices; technologies such as pumped hydro, compressed air and Lithium ion electrochemical batteries have shown promise. No doubt, grid scale storage is still very expensive to deploy. However, their costs have shown significant drops over the last decade or so [174, 175]. For a more comprehensive literature review on storage technologies, we refer the reader to [172, 176–183]. This chapter is devoted to integration of storage in the power grid.

As argued before, storage can reduce variability of intermittent sources of energy like wind or solar [184–187]. At slower time scales, it can be used for load shifting [174, 180], i.e., generate when it is cheaper and use storage dynamics to follow the demand. Our focus in this chapter is on the latter. In this setting, there are two natural questions to ask: (a) What is the optimal investment policy for storage? Where to place them, and how to size them? (b) Once installed, what is the optimal control policy for the storage as well as the generation schedule to minimize generation costs? In this chapter, we formulate both problems for slower time-scales in a common framework and present results on the optimal placement, sizing and control of storage units.

### 6.1.2 Prior work in this area

Optimal control policy for installed storage units has received a lot of attention recently. While the authors in [188–190] examine the control of a single storage device without a

network, the authors in [191,192] explicitly model the role of the networks in the operation of distributed storage resources. Storage resources at each node in the network are assumed to be known *a priori* in these settings.

Sizing of storage devices has been studied in the literature too. The works in [193,194] use purely economic arguments, without explicitly considering the network constraints of the physical system. Authors in [189,195] have looked at optimal sizing of storage devices in single-bus power system, while Kanoria et al. [191] compute the effect of sizing of distributed storage resources to optimize generation cost for specific networks.

### 6.1.3 Our Contribution

In this chapter, we study the investment decision problem of placement and sizing of storage in power networks. The formulation, however, builds the investment problem on top of an optimal control problem for storage. We present this formulation in Section 6.2 where the objective is to minimize system-wide general cost subject to an available storage budget. The works in [189,191] consider a similar control problem over an infinite horizon. Since aggregate demands over large geographical locations often show periodicity [196], we effectively reduce this problem to an optimization over one time period. The generators have finite capacities with convex nondecreasing costs [8,190,191]. We model the network, once using a conic relaxation of the AC power flow equations. Next, we use the linearized DC power flow model to simplify the formulation.

The semidefinite relaxation in Section 6.3 attempts to find some properties of the optimal placement of storage in the network. Our results here indicate that optimal storage placement in the absence of line-flow limits is largely dependent on the network structure and fairly robust to the position of renewable generation in the network. The locations (or buses) where a significant amount of storage is allocated does not change much as the total storage budget for the system is increased. However, the line-flow limits have a significant effect on where the storage is placed. When conventional generation is changed to wind generation with zero marginal cost, the distribution of storage roughly remains similar to the case of

conventional generation. In this study, we assumed perfectly efficient storage systems.

The focus of the analysis with the DC power flow approximation in Section 6.4 is the derivation of a structural result on the distribution of storage. Our main contribution in this section is the result in Theorem 17: when minimizing a convex and nondecreasing generation cost with any fixed available storage budget over a slow time-scale of operation, there always exists an optimal storage allocation that assigns zero storage at nodes with only generation that connect via single transmission lines to the rest of the network. This holds for arbitrary demand profiles and other network parameters. The result provides (partial) analytic justification of the observation made empirically in Section 6.3 that optimal storage allocation seldom places storage capacities at generator-only buses.

We finally conclude in Section 6.5 with directions for future work.

## 6.2 Problem formulation

Consider a power network defined by an undirected connected graph on  $n$  nodes (or buses)  $\mathcal{N} = \{1, 2, \dots, n\}$ . For two nodes  $k$  and  $l$  in  $\mathcal{N}$ , let  $k \sim l$  denote that  $k$  is connected to  $l$  in  $G$  by a transmission line with admittance  $y_{kl}$ .

Time is discrete and is indexed by  $t$ . Akin to Chapter 3 Section 3.5 and Chapter 4, we define the following notation.

- $p_k^D(t) + \mathbf{i}q_k^D(t)$  is the apparent power demand at bus  $k \in \mathcal{N}$  and time  $t$ , which are assumed to be known. Demand profiles often show diurnal variations [196], i.e., they exhibit cyclic behavior with each day being the time period of the cycle. Let  $T$  time-steps denote the cycle length of the variation. In particular, for all  $k \in \mathcal{N}$ ,  $t \geq 0$ , assume

$$p_k^D(t + T) + \mathbf{i}q_k^D(t + T) = p_k^D(t) + \mathbf{i}q_k^D(t).$$

- $p_k^G(t) + \mathbf{i}q_k^G(t)$  is the apparent power generation at bus  $k \in \mathcal{N}$  and time  $t$ . These decision variables are constrained by the real and reactive generation capacities at each node

as

$$\underline{p}_k^G \leq p_k^G(t) \leq \overline{p}_k^G, \quad \text{and} \quad \underline{q}_k^G \leq q_k^G(t) \leq \overline{q}_k^G. \quad (6.1)$$

- $c_k(p_k^G)$  denotes the cost of generating power  $p_k^G$  at bus  $k \in \mathcal{N}$ . The cost of generation is assumed to be independent of time  $t$  and depends only on the generation technology at bus  $k$ . Also, suppose that the function  $c_k : \mathbb{R}^+ \rightarrow \mathbb{R}^+$  is non-decreasing and convex. These assumptions apply to commonly used cost functions in the literature [8, 12, 36, 192], e.g., convex and nondecreasing piecewise linear or quadratic ones.
- $V_k(t)$  be the complex voltage at bus  $k \in \mathcal{N}$  and time  $t$ . Voltage magnitudes at nodes are bounded as

$$\underline{V}_k \leq |V_k(t)| \leq \overline{V}_k. \quad (6.2)$$

- For  $k \sim l$  in  $G$ ,  $p_{kl}(t) + \mathbf{i}q_{kl}(t)$  be the apparent power flow from bus  $k$  to bus  $l$  at time  $t$  which satisfies

$$p_{kl}(t) + \mathbf{i}q_{kl}(t) = V_k(t) (V_k(t) - V_l(t))^H y_{kl}^H, \quad (6.3)$$

$p_{kl}(t)$  is constrained by capacity limit  $f_{kl}$ . Thus we have

$$|p_{kl}(t)| \leq f_{kl}. \quad (6.4)$$

Note that in this study, we chose to constrain the real power flow  $p_{kl}$  as opposed to the apparent power flow on the line joining buses  $k$  and  $l$ .

- $\gamma_k(t)$  and  $\delta_k(t)$  are the average charging and discharging powers of the storage unit at bus  $k \in \mathcal{N}$  at time  $t$ , respectively. The energy transacted over a time-step is converted to power units by dividing it by the length of the time-step. This transformation conveniently allows us to formulate the problem in units of power [137]. Let  $0 <$

$\alpha_\gamma, \alpha_\delta \leq 1$  denote the charging and discharging efficiencies, respectively of the storage technology used, i.e., the power flowing in and out of the storage device at node  $k \in \mathcal{N}$  at time  $t$  is  $\alpha_\gamma \gamma_k(t)$  and  $\frac{1}{\alpha_\delta} \delta_k(t)$ , respectively [189,197]. The roundtrip efficiency of this storage technology is  $\alpha = \alpha_\gamma \alpha_\delta \leq 1$ . Note that we assume that the storage units only transact in real power.

- $s_k(t)$  denotes the storage level at node  $k \in \mathcal{N}$  at time  $t$  and  $s_k^0$  is the storage level at node  $k$  at time  $t = 0$ . From the definitions above, we have that

$$s_k(t) = s_k^0 + \sum_{\tau=1}^t \left( \alpha_\gamma \gamma_k(\tau) - \frac{1}{\alpha_\delta} \delta_k(\tau) \right). \quad (6.5)$$

For each  $k \in \mathcal{N}$ , assume  $s_k^0 = 0$ , so that the storage units are empty at installation time.

- $b_k \geq 0$  is the storage capacity at bus  $k$ . Thus,  $s_k(t)$  for all  $t$  satisfies the following:

$$0 \leq s_k(t) \leq b_k. \quad (6.6)$$

- $h$  is the available storage budget and denotes the total amount of storage capacity that can be installed in the network. Our optimization algorithm decides the allocation of storage capacity  $b_k$  at each node  $k \in \mathcal{N}$  and thus, we have

$$\sum_{k \in \mathcal{N}} b_k \leq h. \quad (6.7)$$

- Charging and discharging rates of each storage device are assumed to be upper-bounded by ramp limits. These limits are proportional to the capacity of the corresponding device, i.e., for all  $k \in \mathcal{N}$ ,

$$0 \leq \gamma_k(t) \leq \epsilon_\gamma b_k, \quad (6.8a)$$

$$0 \leq \delta_k(t) \leq \epsilon_\delta b_k, \quad (6.8b)$$

where  $\epsilon_\gamma \in (0, \frac{1}{\alpha_\gamma}]$  and  $\epsilon_\delta \in (0, \alpha_\delta]$  are fixed constants.

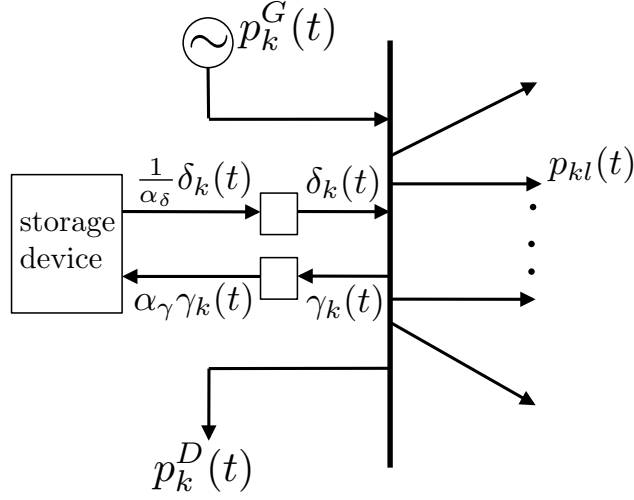


Figure 6.1: Real power balance at node  $k \in \mathcal{N}$ .

Balancing real power that flows in and out of bus  $k \in \mathcal{N}$  at time  $t$ , as shown in Figure 6.1, we have:

$$p_k^G(t) - p_k^D(t) - \gamma_k(t) + \delta_k(t) = \sum_{l \sim k} p_{kl}(t). \quad (6.9)$$

Also, maintaining reactive power balance, we have

$$q_k^G(t) - q_k^D(t) = \sum_{l \sim k} q_{kl}(t). \quad (6.10)$$

Now, optimally placing storage over an infinite horizon is equivalent to solving this problem over a single cycle, provided the state of the storage levels at the end of a cycle is the same as its initial condition [137]. Thus, for each  $k \in \mathcal{N}$ , we have

$$\sum_{t=1}^T \left( \alpha_\gamma \gamma_k(t) - \frac{1}{\alpha_\delta} \delta_k(t) \right) = 0. \quad (6.11)$$

For convenience, denote  $[T] := \{1, 2, \dots, T\}$ . Using the above notation, we define the following optimization problem.

**Storage placement problem  $P$ :**

$$\begin{aligned}
& \text{minimize} && \sum_{k \in \mathcal{N}} \sum_{t=1}^T c_k (p_k^G(t)) \\
& \text{over} && (p_k^G(t), q_k^G(t), \gamma_k(t), \delta_k(t), V(t), p_{kl}(t), b_k), \\
& && k \in \mathcal{N}, k \sim l, t \in [T], \\
& \text{subject to} && (6.1), (6.2), (6.3), (6.4), (6.5), (6.6), (6.7), (6.8), (6.9), (6.11),
\end{aligned}$$

where, (6.1) represents generation constraints, (6.2) represents voltage magnitude constraints, (6.3) links the power flows to the voltages, (6.6), (6.7),(6.8),(6.11) represent the constraints imposed on the charging/discharging policy of the energy storage devices, (6.9) represents the power balance constraints at each bus of the network and (6.7) represents the constraint on the sum of the capacities of all storage devices being no greater than the available storage budget. With the demand profiles and network parameters as input,  $P$  defines the optimal investment decision strategy for sizing storage units at different buses, the economic dispatch of the various generators and the optimal control policy of the installed storage units. For any variable  $z$ , define  $z_*$  as its value at optimum.

### 6.2.1 Network models

As with the market power problem in Chapter 4, we investigate  $P$  with two network models. First in Section 6.3, we solve  $P$  using the conic relaxation of the AC power flow model. Thus, we represent (6.2) – (6.3) in terms of  $W(t) = V(t)[V(t)]^H$ , which is a positive semidefinite matrix of rank 1 for each  $t \in [T]$ . Then the resultant nonconvex program is replaced by a semidefinite program (SDP) by relaxing the rank constraint as discussed in Chapters 2 and 3. We call this problem  $P^{AC}$ . Note that any of the conic relaxations based on chordal SDP or SOCP can also be used for studying the optimal solution of  $P^{AC}$ . However, in Section 6.3, we use the SDP approach to study  $P^{AC}$  for some IEEE benchmark systems.

In Section 6.3, we make a few observations about storage placement in networks. However, the SDP formulation is not amenable to characterize any of these properties analytically.

Hence, we simplify the formulation with the DC approximation [32, 33], first presented in Chapter 4. Thus, the voltage limits in (6.2) are dropped (since voltage magnitudes are assumed to be at nominal value in this approximation) and the relation in (6.3) is modified to

$$p_{kl} = (\theta_k - \theta_l)/x_{kl},$$

where for each node  $k \in \mathcal{N}$ ,  $\theta_k$  represents the voltage angle at bus  $k$  and  $x_{kl}$  is the purely reactive impedance of line  $k \sim l$ . In essence, the admittance  $y_{kl} = (\mathbf{i}x_{kl})^{-1}$  is purely imaginary as losses are neglected under DC approximation. For the storage placement problem (denote by  $P^{DC}$ ) with this simplified linearized version of the constraints, we prove a result characterizing the optimal placement of the storage resources in Section 6.4. We further prove some results on the placement for networks with specific topologies.

### 6.3 Simulations using conic relaxation

Here we present some simulation results of  $P^{AC}$  on the IEEE 14 bus system [63], shown in Figure 6.2. For the purpose of these simulations, we make a few modifications as follows:

- We assume that the cost of generation  $c_k(\cdot)$  for conventional generators is quadratic, i.e.,

$$c_k(p_k^G) := c_k^{(2)}(p_k^G)^2 + c_k^{(1)}p_k^G.$$

We include this as a linear matrix inequality (LMI) as in [36, 192]. The objective function of  $P^{AC}$  is modified to

$$\sum_{k \in \mathcal{N}} \sum_{t=1}^T \xi_k(t),$$

where  $\xi_k(t)$  is an auxiliary variable that adds two extra constraints in the formulation:

$$\begin{aligned} & c_k^{(2)}(p_k^G)^2 + c_k^{(1)}p_k^G \leq \xi_k(t), \\ & \begin{pmatrix} c_k^{(1)}p_k^G(t) - \gamma_k(t) & \sqrt{c_k^{(2)}}p_k^G(t) \\ \sqrt{c_k^{(2)}}p_k^G(t) & -1 \end{pmatrix} \preceq 0. \end{aligned}$$

For wind generators, cost of production is assumed to be zero.

- We assume perfectly efficient storage devices, i.e.,  $\alpha = 1$ . Thus, define the net charging rate for the storage device as

$$r_k(t) := \gamma_k(t) - \delta_k(t).$$

- Also, assume fixed ramping rates for this section, i.e., we use the above equation and replace the relations in (6.8) by the following.

$$\underline{R}_k \leq r_k(t) \leq \overline{R}_k.$$

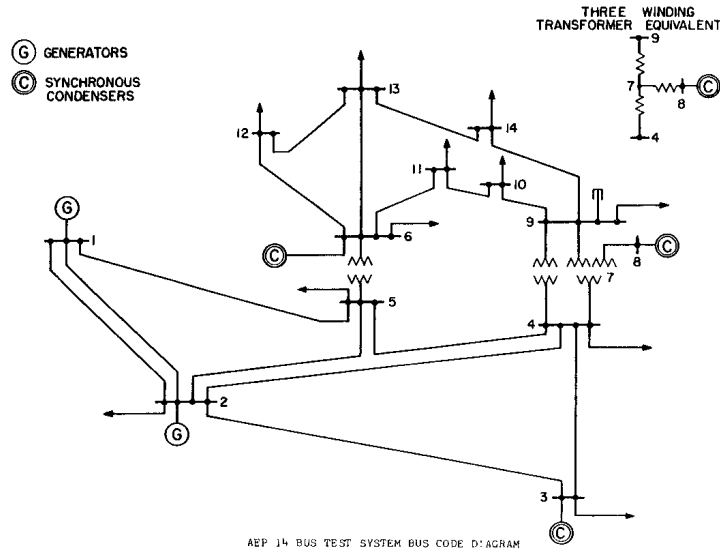


Figure 6.2: The IEEE 14-Bus benchmark system topology. Buses 1, 2, 3, 6, and 8 have generation.

### 6.3.1 Case Studies

Now we are ready to study the simulation results of  $P^{AC}$  on the IEEE 14 bus benchmark system [63] with both conventional generation and a combination of conventional and wind

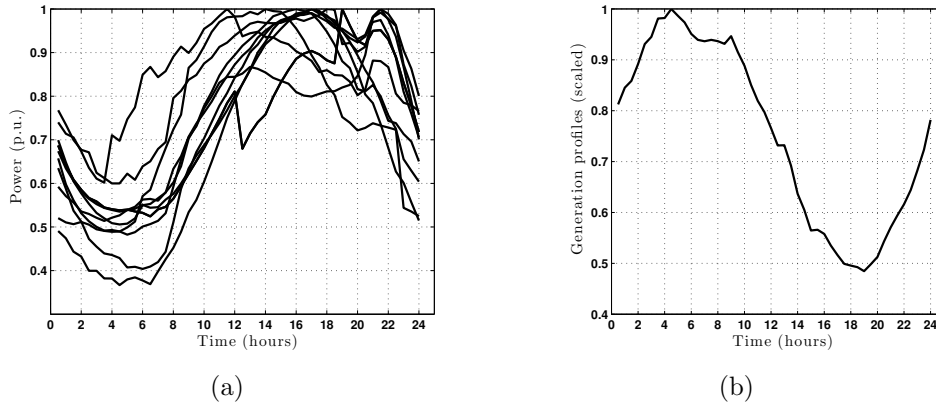


Figure 6.3: (a) Peak-normalized real power demand profiles for each of the 14 buses based on an average day in July 2010. The data are reported in half-hour intervals over a 24 hour period. (b) A peak-normalized wind generation profile reported at half-hour intervals over a 24 hour period.

generation. Similar tests have been performed on the IEEE 30 bus system but for brevity only the results on the 14 bus case is presented here. This system, shown in Figure 6.2, has five generators at buses 1, 2, 3, 6 and 8. We simulate the effects of changes in total storage budget and line-flow limits on the placement of storage capacity. The SDP of  $P^{AC}$  is solved in MATLAB using YALMIP [198] with SeDuMi [77] as the solver.

While we adopt its network topology, admittance matrix and its voltage and generation bounds, we augment the benchmark system with storage at each location. The ramp limits for the storage  $\bar{R}_k$  and  $\underline{R}_k$  are assumed to be  $\pm 0.8 pu$  for all of the numerical studies. The static demand data at each bus is also replaced with a time-varying demand profile. These profiles follow the hourly power consumption data from 14 feeders in Southern California averaged over the month of July in 2010<sup>1</sup>. The data is interpolated to get half-hour time intervals. They are then peak scaled to match the demands in the benchmark circuit. Any linear trends in these profiles are also removed to ensure cyclic behavior over each 24 hour period. The resulting peak-normalized demand profiles at each of the 14 buses is shown in Figure 6.3(a).

<sup>1</sup>This dataset was obtained from personal communication with Southern California Edison.

## Conventional generation only

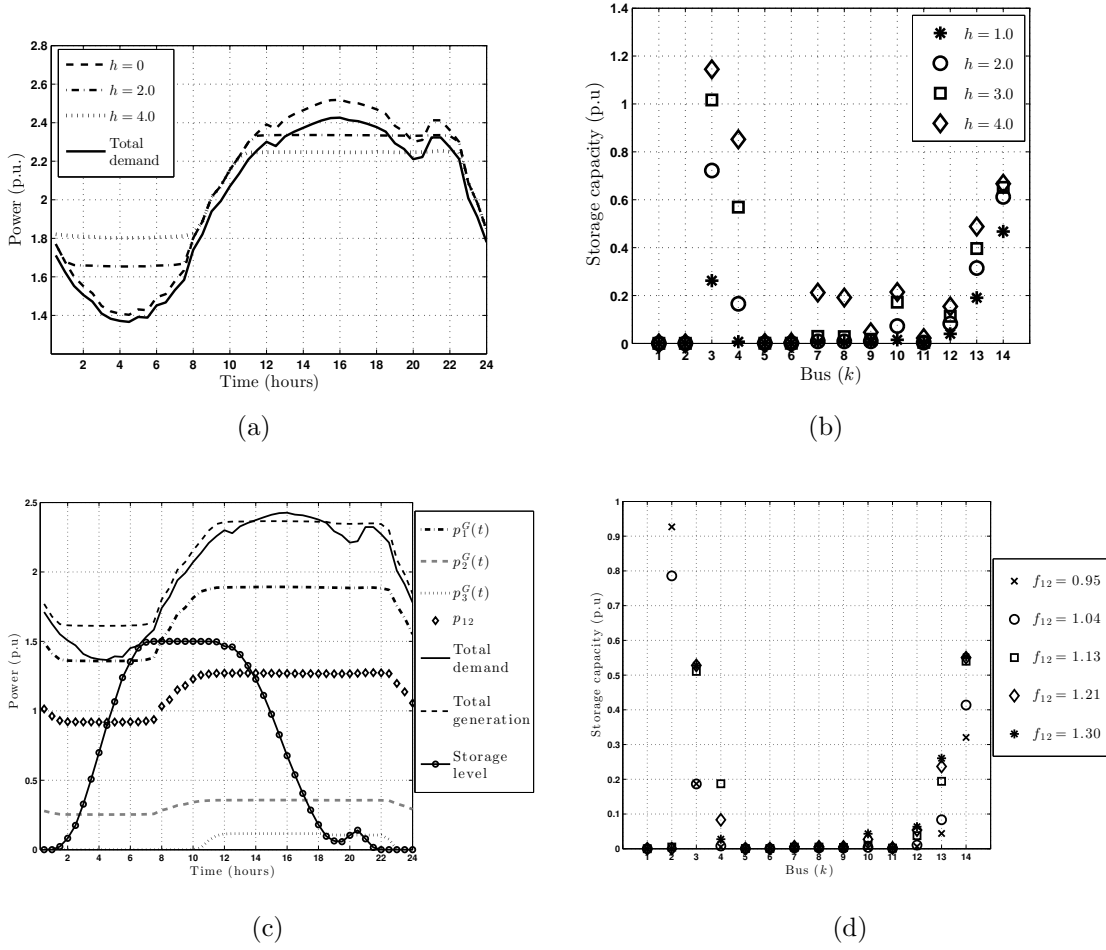


Figure 6.4: (a) Total system demand and generation as a function of total storage capacity. (b) Storage placement as a function of total storage capacity. (c) A comparison of total system demand, total generation, individual generator production versus storage level when total storage capacity  $h = 1.5$ . The actual transmission over the line between generators 1 and 2 ( $p_{12}$ ) as a function of time is also superimposed. As expected the transmission increases as the generation at bus 1 increases. (d) Storage placement as line limits  $f_{12}$  are decreased from the transmission levels shown in (c). For all panels the data is reported in half-hour intervals over a 24 hour period.

The cost structures of the generators are defined in [63]. Generation at bus 1 has the largest capacity (among the five generators) and is the cheapest, followed by the one at bus 2. The cost function in  $P^{AC}$  is quadratic and strictly convex in the variables ( $p_k^G(t), k \in \mathcal{N}, t \in [T]$ ). Figure 6.4(a) shows that as the storage budget increases, the total

generation flattens out, which leads to a lower cost function value. In other words, more storage installed in the system results in greater peak shaving. However, as we continue increasing  $h$  beyond a certain level, the ramp limits bound the ability of the storage to flatten the generation.

In Figure 6.4(b), we explore how storage placement changes as a function of the storage budget  $h$ . Buses 3 and 14 get the highest capacities (i.e., the highest  $b_k$ 's at optimality). Any bus with high demand would be expected to get a larger storage capacity and that explains why bus 3 gets a high share. On the other hand, we conjecture that it is the relative position of bus 14 in the network that leads to a higher capacity. Validation of this conjecture is subject to ongoing work.

To understand the role of line-flow limits, we study the effect of changing  $f_{12}$ , i.e., the line-flow limit on the line linking buses 1 and 2. Levels of power for various signals are plotted in Figure 6.4(c) with a storage budget of 1  $pu$ . With an unimpeded flow on the edge (1, 2), we observed a maximum of  $p_{12} = 1.27 pu$ . The figure also shows how much each generator is producing and the total storage level as a function of time. The flow-limit was systematically brought down on the edge connecting buses 1 and 2 from 1.3 to 0.9 to study its effect on the storage placement. As in Figure 6.4(d), we observe that more capacity is installed at bus 2 when the limits are tighter. This trend is expected since the largest and cheapest generator is at node 1 and the times of peak demand will also be the times when the line flows are likely to be saturated. Therefore, energy is stored at the end of the limited capacity line during the times of low demand so the cheapest cost energy from generator 1 is still accessible when the limits bind the amount of power that can flow from node 1 to 2.

## Wind and conventional generation

For generator buses, we have performed simulations with conventional generators as well as wind generation data. The wind generation profiles were obtained from the National Renewable Energy Laboratory (NREL) Western Wind Integration Dataset from the study in [199] and are based on five different Southern Californian locations. At each location we

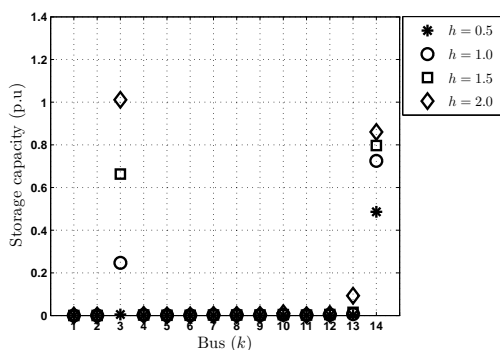
average over five wind farm sites and then average over 31 days from July 2006. The original data is provided in 10 minute increments and we down-sample it to half-hourly intervals and remove any drift in the data. The resulting peak-normalized wind generation profiles are shown in Figure 6.3(b).

The cost of generation for wind is assumed to be zero. Further, we assume that the available wind generation at time  $t$  is captured by varying the real power generation limit with time, i.e., we have  $p_k^G(t) \leq \bar{p}_k^G(t)$  where  $\bar{p}_k^G(t)$  is matched to the wind profile. The reactive power limits satisfy  $-\beta_k \bar{p}_k^G(t) \leq q_k^G(t) \leq \beta_k \bar{p}_k^G(t)$ , where  $\beta_k$  is uniformly assumed to be 0.6.

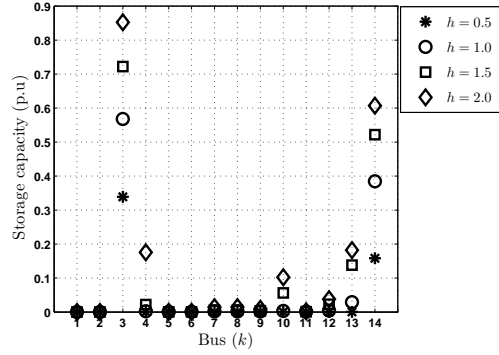
For all of the studies with wind generation, the wind profile is peak-scaled to the capacity of the conventional generator at the corresponding bus. First, we study the effect of changing the storage budget with wind at bus 1. The results are shown in Figure 6.5(a). The storage is not placed directly at the wind generation site but it rather gets distributed to buses 3 and 14, potentially due to the same reasons as in the previously discussed case with solely conventional generation. The results suggest that a bus' load and position in the network is more important than the location of the intermittent source of generation. To gain additional insight into the relationship between storage placement and the location of the wind generator, we moved the wind generation location to bus 2 and simulated the system with the same wind profile (peak-scaled accordingly). In these results, shown in Figure 6.5(b), we observe the same phenomenon.

Since the wind generators in our formulation have zero marginal cost, the algorithm always uses wind power whenever possible. But surprisingly, it does not allocate storage right at that bus to compensate for the intermittency of the source. To further confirm our conjecture, we keep the storage budget fixed at  $h = 1 pu$  and simulate the system using the same wind profile at each of the remaining generator buses (3, 6 and 8). The results with the wind at all five generator buses are shown in Figure 6.5(c). This study is repeated with  $h = 2 pu$  in Figure 6.5(d). In each of these cases, the observed trends remain the same.

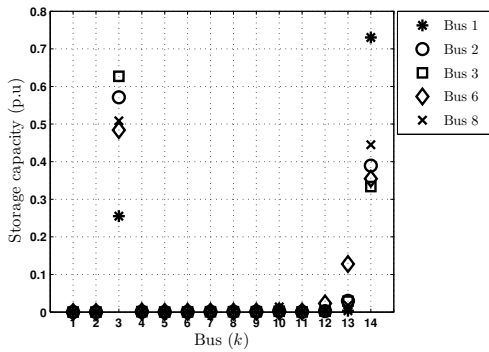
Next, we present results when the line-flow limits are changed. Wind generation is only at bus 1 with a fixed storage budget of  $h = 1.5 pu$ . We change the limits on the line joining buses



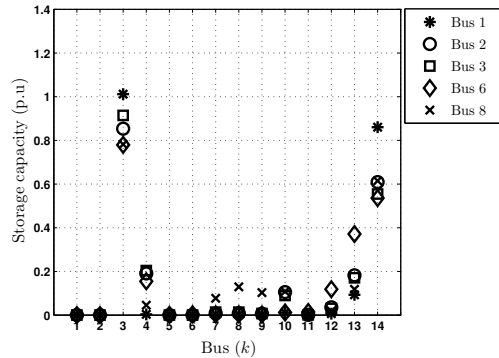
(a)



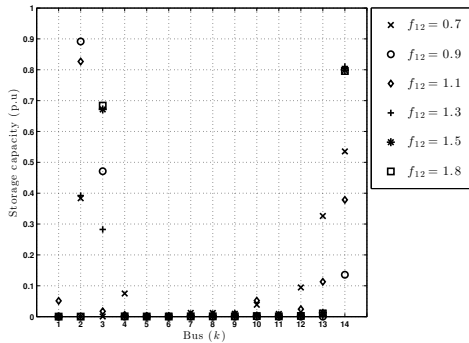
(b)



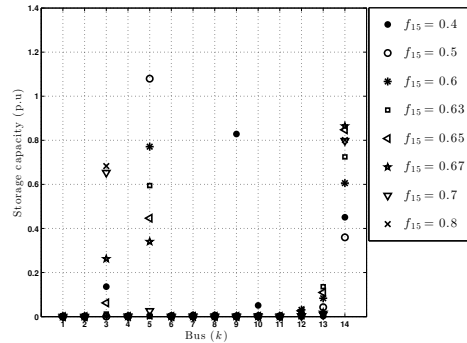
(c)



(d)



(e)



(f)

Figure 6.5: (a), (b) Changes in optimal storage placement in a system with a wind generator. Differences arising from changes in total storage capacity  $h$  when the wind is, respectively, placed at bus 1 and 2, which, respectively, represent 43% and 18% of the total system generation capacity. Panels (c) and (d) depict changes in storage siting as the wind generation is moved to each of the generation sites, with the total system storage capacity is, respectively, fixed to  $h = 1 pu$  and  $h = 2 pu$ . Panels (e) and (f) show the effect of changing line limits  $f_{12}$  and  $f_{15}$  when the wind is placed a bus 1 and fixed  $h = 1.5$ .

1 and 2 in Figure 6.5(e). The results are very similar to the conventional case. Note that the conventional generator at bus 1 is the least cost generator. Even with wind generation at bus 1, it remains the bus with the least cost of generation. Hence, the optimization tries to use the generation there by either placing storage at bus 2 or trying to push the power into the rest of the network through bus 5. We observe the same behaviour when the capacity of the line joining buses 1 and 5 are limited in Figure 6.5(f). However, we draw the attention of the reader to the case for which  $f_{15} = 0.4 pu$ . This result seems to be very different from the other data points. This discrepancy may be due to the fact that the SDP becomes highly inaccurate at this point and the relaxation is thus no longer a good approximation of the original problem, this observation is also noted in [1]. We explore this further in the next section.

### 6.3.2 Approximation versus relaxation

$P^{AC}$  has a nonconvexity similar to that of the optimal power flow (OPF) problem. As discussed in Chapters 2 and 3, the rank relaxation guarantees optimality if and only if  $\text{rank } W^*(t) = 1$  for  $t \in [T]$ . In our simulations, we observe that the rank of the obtained optimal matrices  $W^*(t)$  is often greater than 1. Though OPF on IEEE benchmark systems with its original parameter set defined in the database admits rank one solutions [35,36], existence of nonzero duality gaps have been reported before, e.g., see [1]. Akin to our simulation results for  $\text{TCNF}^{AC}$  in Chapter 4, we plot  $\lambda_2(W^*(t))/\lambda_1(W^*(t))$  and  $\lambda_3(W^*(t))/\lambda_1(W^*(t))$  for one run of  $P^{AC}$  in Figure 6.6, where  $\lambda_1(\cdot) \geq \lambda_2(\cdot) \geq \lambda_3(\cdot)$  are the three largest eigenvalues of the corresponding matrix. Observe that  $\lambda_2(W^*(t))$  is much smaller than  $\lambda_1(W^*(t))$ , but not quite negligible. Note that our argument in Chapter 4 Section 4.5 applies to this problem as well. Clearly the relaxation  $P^{AC}$  does not solve the original nonconvex problem  $P$  optimally. However, the eigenratios in Figure 6.6 are small enough to gain insights from.

Further, we explore a gradient descent method to reach a “nearby” feasible point  $V(t)$  from  $W^*(t)$ . All simulations in this section are done with  $h = 1pu$  ignoring line-flow limits. We summarize the cost of operation in Table 6.1. In most cases, the local search method

Wind location	Cost with $W^*(t)$ (K\$/day)	Cost with $V(t)$ (K\$/day)	% change
None	138	139	0.6
Bus 1	16.0	17.0	6.3
Bus 2	61.6	64.1	4.1
Bus 3	77.5	78.1	0.7
Bus 6	79.0	81.4	3.0
Bus 8	78.1	102.3	30.9

Table 6.1: Comparison of costs from gradient descent for  $W^*(t)$  to obtained  $V(t)$ .

finds a feasible  $V(t)$  near the  $W^*(t)$  with a slight cost increase, though it sometimes fails, e.g., when there is wind generation at bus 8.

We end this section with a remark. Notice that the DC approximation ignores all losses in the network and hence cannot quite capture the placement when line capacities are large since any storage placement scheme is optimal.  $P^{AC}$ , however, still gives a principled approach to gain insights into the storage placement problem. We investigate the properties of  $P^{DC}$  in the next section that characterizes the interaction of storage with the line flow limits.

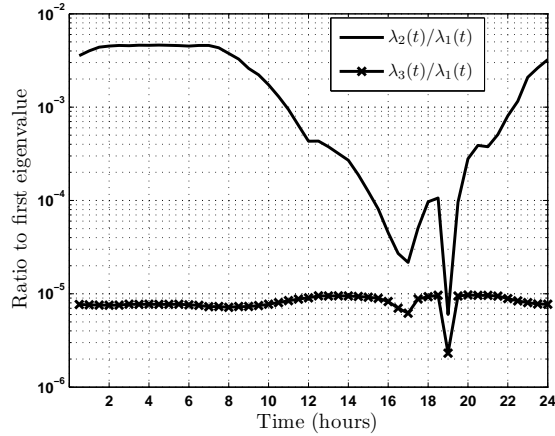


Figure 6.6: Ratios of other eigenvalues to the first eigenvalue.

## 6.4 Storage placement with DC power flow

In this section, we characterize the property of  $P^{DC}$ , that is the storage placement problem  $P$  with the DC approximation to model the power flow equations. As mentioned before, there is no reactive power flow. Also, voltage constraints are redundant. We make a few simplifying assumptions in this section to present our result as follows. Restrict attention to network topologies where each bus either has generation or load but not both. Any intermediate bus (one that has no generation or load) is modeled as a load bus with zero demand at all times. Partition the set of buses  $\mathcal{N}$  into two groups  $\mathcal{N}_G$  and  $\mathcal{N}_D$  where they represent the generation-only and load-only buses respectively and assume  $\mathcal{N}_G$  and  $\mathcal{N}_D$  are non-empty.

Next, we introduce some new notations for convenience. Since there is no reactive power generation, we define  $g_k(t) := p_k^G(t)$  as the real power generation at the  $k$ -th bus. Let  $\underline{p}_k^G = 0$  and define  $\bar{g}_k := \bar{p}_k^G$  for each  $k \in \mathcal{N}_G$ . Similarly, let  $d_k(t) := p_k^D(t)$  denote the real power demand at bus  $k \in \mathcal{N}_D$ .

For any subset  $\mathcal{K}$  of  $\mathcal{N}_G$ , define the *restricted storage placement problem*  $\Pi^{\mathcal{K},DC}$  as  $P^{DC}$  with an additional constraint  $b_i = 0$ ,  $i \in \mathcal{K}$ , i.e., there is no installed storage capacity at generation buses in the set of nodes in  $\mathcal{K}$ . We study the relation between the problems  $P^{DC}$  and  $\Pi^{\mathcal{K},DC}$  in the rest of the chapter.

We say bus  $k \in \mathcal{N}$  has a *single connection* if it has exactly one neighboring node  $l \sim k$ . Similarly, a bus  $k \in \mathcal{N}$  has *multiple connections* if it has more than one neighboring node in  $\mathcal{G}$ . We illustrate the notation using the network in Figure 6.7.  $\mathcal{N}_G = \{1, 2, 7\}$  and  $\mathcal{N}_D = \{3, 4, 5, 6\}$ . Buses 1 and 2 have single connections and all other buses in the network have multiple connections.

### 6.4.1 Main Result

For a subset  $\mathcal{K} \subseteq \mathcal{N}_G$ , let  $p_*$  and  $\pi_*^{\mathcal{K}}$  be the optimal values for problems  $P^{DC}$  and  $\Pi^{\mathcal{K},DC}$ , respectively<sup>2</sup>. Now, we are ready to present the main result of this section.

<sup>2</sup>The notation  $p_*$  should not be confused with real power.

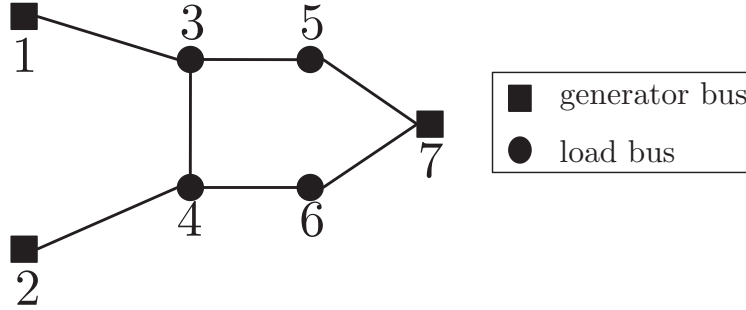


Figure 6.7: A sample network.

**Theorem 17.** *Suppose  $\mathcal{K} \subseteq \mathcal{N}_G$  and each node  $i \in \mathcal{K}$  has a single connection. If  $P^{DC}$  is feasible, then  $\Pi^{\mathcal{K}}$  is feasible and  $p_* = \pi_*^{\mathcal{K}}$ .*

Problem  $P^{DC}$ , in general, may have multiple optimal solutions, but Theorem 17 proves that there *always* exists an optimal allocation of storage capacities that places *no* storage at any subset of generation buses with single connections, regardless of the demand profiles, generation capacities, line-flow limits and characteristics of the storage technologies. We further discuss the applicability and uses of this result in Section 6.4.1.

Notice that we have restricted our attention to generator buses in  $\mathcal{K}$  that have single connections only. The result is not true, in general, if  $\mathcal{K}$  includes generator buses with multiple connections; see Section 6.4.1 for an example.

The storage capacity allocation at each bus has been assumed to be infinitely divisible, i.e., each  $b_k, k \in \mathcal{N}$  is feasible that satisfies the budget constraint  $\sum_{k \in \mathcal{N}} b_k \leq h$  in (6.7). But it might be impractical to implement an optimal allocation with arbitrarily small storage capacities. This, however, is not a limitation for the result in Theorem 17 as it only specifies zero storage capacities at some buses and does *not* characterize storage sizes at others.

## Proof of the main result

We only prove for the case where the round-trip efficiency is  $\alpha < 1$ , but the result holds for  $\alpha = 1$  as well. Assume  $P^{DC}$  is feasible throughout. Recall that for any variable  $z$ , let  $z^*$  be the value of the corresponding variable at the optimum. In our proof, we use the following technical result.

**Lemma 18.** *Suppose  $\phi : \mathbb{R} \rightarrow \mathbb{R}$  is convex. Then, for any  $x_1 < x_2$  and  $0 \leq \eta \leq (x_2 - x_1)$ :*

$$\phi(x_1 + \eta) + \phi(x_2 - \eta) \leq \phi(x_1) + \phi(x_2).$$

*Proof.* Applying Jensen's inequality to the convex function  $\phi(\cdot)$ , we have

$$\begin{aligned} \left(1 - \frac{\eta}{x_2 - x_1}\right) \phi(x_1) + \left(\frac{\eta}{x_2 - x_1}\right) \phi(x_2) &\geq \phi(x_1 + \eta), \\ \left(\frac{\eta}{x_2 - x_1}\right) \phi(x_1) + \left(1 - \frac{\eta}{x_2 - x_1}\right) \phi(x_2) &\geq \phi(x_2 - \eta). \end{aligned}$$

The result follows from adding the inequalities above. □

Consider node  $i \in \mathcal{K}$  and  $j \sim i$ . Node  $j$  is uniquely defined as  $i$  has a single connection. It can be shown that problem  $P^{DC}$ , in general, has multiple optima. In the following result, we characterize only a subset of these optima.

**Lemma 19.** *There exists an optimal solution of  $P^{DC}$  such that for all  $t \in [T]$  and all  $i \in \mathcal{K}, j \sim i$ ,*

(a)  $g_i^*(t)\gamma_i^*(t)\delta_i^*(t) = 0,$

(b)  $g_i^*(t) \leq f_{ij}.$

The first part of Lemma 19 essentially says that for some optimum solution of  $P^{DC}$ , the storage units should not charge and discharge at the same time step if there is positive generation at the same bus at that time step. This is expected since the round-trip efficiency of the storage devices  $\alpha = \alpha_\gamma \alpha_\delta$  is less than one and since the generation cost is a nondecreasing function. The second part can be interpreted as follows. Power that flows from bus  $i$  to bus  $j$  at each  $t \in [T]$  is  $p_{ij}(t) = g_i(t) - \gamma_i(t) + \delta_i(t)$  and we have  $p_{ij}(t) \leq f_{ij}$ . But Lemma 19(b) states that there exists an optimum for which,  $g_i^*(t), t \in [T]$  itself defines a feasible flow over this line.

*Proof.* The feasible set of problem  $P^{DC}$  is a bounded<sup>3</sup> polytope and the objective function is a continuous convex function. Hence the set of the optima of  $P^{DC}$  is a convex and compact set [55]. Now, with every point in the set of optimal solutions of  $P^{DC}$ , consider the function  $\sum_{i \in \mathcal{K}, t \in [T]} (\gamma_i(t) + \delta_i(t))$ . This is a linear and hence continuous function on the compact set of optima of  $P^{DC}$  and hence attains a minimum. Consider the optimum of  $P^{DC}$  where this minimum is attained. We show that for this optimum,  $g_i^*(t)\gamma_i^*(t)\delta_i^*(t) = 0$  and  $g_i^*(t) \leq f_{ij}$  for all  $t \in [T]$  and  $i \in \mathcal{K}, j \sim i$ .

(a) Suppose, on the contrary, we have  $g_i^*(t_0) > 0$ ,  $\gamma_i^*(t_0) > 0$  and  $\delta_i^*(t_0) > 0$  for some  $t_0 \in [T]$ .

Define

$$\Delta g' := \min \left\{ (1 - \alpha)\gamma_i^*(t_0), \frac{1 - \alpha}{\alpha}\delta_i^*(t_0), g_i^*(t_0) \right\}.$$

Note that  $\Delta g' > 0$ . Now, for bus  $i$ , construct modified generation, charging and discharging profiles  $\tilde{g}_i(t), \tilde{\delta}_i(t), \tilde{\gamma}_i(t), t \in [T]$  that differ from  $g_i^*(t), \delta_i^*(t), \gamma_i^*(t)$  only at  $t_0$  as follows:

$$\begin{aligned} \tilde{g}_i(t_0) &:= g_i^*(t_0) - \Delta g', \\ \tilde{\gamma}_i(t_0) &:= \gamma_i^*(t_0) - \frac{1}{1 - \alpha}\Delta g', \\ \tilde{\delta}_i(t_0) &:= \delta_i^*(t_0) - \frac{\alpha}{1 - \alpha}\Delta g'. \end{aligned}$$

Note that, for all  $t \in [T]$ , the storage level  $s_i(t)$  and the power  $p_{ij}(t)$  flowing from bus  $i$  to bus  $j$  remain unchanged throughout. It can be checked that the modified profiles define a feasible point of  $P^{DC}$ . Since  $c_i(\cdot)$  is non-decreasing, we have  $c_i(\tilde{g}_i(t_0)) \leq c_i(g_i^*(t_0))$  and hence the additivity of the objective in  $P^{DC}$  over  $i$  and  $t$  implies that this feasible point has an objective function value of at most  $p_*$ . It follows that this feasible point defines an optimal point of  $P^{DC}$ . However, we have  $\tilde{\gamma}_i(t_0) + \tilde{\delta}_i(t_0) < \gamma_i^*(t_0) + \delta_i^*(t_0)$  and

---

<sup>3</sup>Without loss of generality, let bus 1 be the slack bus and hence  $\theta_1(t) = 0$  for all  $t \in [T]$ . Boundedness of the set of feasible solutions of  $P^{DC}$  then follows from generation limits, power flow limits and storage operations in Section 6.2.

thus, this optimum of  $P^{DC}$  has a strictly lower  $\sum_{i \in \mathcal{K}, t \in [T]} (\gamma_i(t) + \delta_i(t))$ , contradicting our hypothesis. This completes the proof of  $g_i^*(t_0)\gamma_i^*(t_0)\delta_i^*(t_0) = 0$ .

(b) If  $g_i^*(t) = 0$  for all  $t \in [T]$ , then  $g_i^*(t) \leq f_{ij}$  clearly holds. Henceforth, assume  $\max_{t \in [T]} g_i^*(t) > 0$ , and consider any  $t_0 \in [T]$ , such that  $g_i^*(t_0) = \max_{t \in [T]} g_i^*(t)$ .

If  $\gamma_i^*(t_0) = 0$ , then,

$$\begin{aligned} \max_{t \in [T]} g_i^*(t) &= g_i^*(t_0) \\ &= \underbrace{p_{ij}^*(t_0)}_{\leq f_{ij}} + \underbrace{\gamma_i^*(t_0)}_{=0} - \underbrace{\delta_i^*(t_0)}_{\geq 0} \\ &\leq f_{ij}. \end{aligned} \tag{6.12}$$

and Lemma 19(b) holds.

Suppose now that  $\gamma_i^*(t_0) > 0$  and hence  $\delta_i^*(t_0) = 0$  from Lemma 19(a). First, we show that the storage device discharges at some point after  $t_0$ .

$$s_i^*(t_0) = \underbrace{s_i^*(t_0 - 1)}_{\geq 0} + \underbrace{\alpha_\gamma \gamma_i^*(t_0)}_{> 0} > 0.$$

We also have  $s_i^*(T) = s_i^0 = 0$  by hypothesis. Thus the storage device at node  $i$  needs to discharge in  $[t_0 + 1, T]$  and hence  $\alpha_\gamma \gamma_i^*(t) - \frac{1}{\alpha_\delta} \delta_i^*(t) < 0$  for some  $t \in [t_0 + 1, T]$ . Let  $t_1$  be the first time instant after  $t_0$  when the storage device at bus  $i$  is discharged, i.e.

$$t_1 := \min \left\{ t \in [t_0 + 1, T] \mid \alpha_\gamma \gamma_i^*(t) - \frac{1}{\alpha_\delta} \delta_i^*(t) < 0 \right\}. \tag{6.13}$$

Thus,  $\delta_i^*(t_1) > 0$ . Define

$$\Delta g := \min \left\{ \gamma_i^*(t_0), \frac{1}{\alpha} \delta_i^*(t_1), g_i^*(t_0) \right\}. \tag{6.14}$$

Then  $\Delta g > 0$ . Now, consider the case where:

$$g_i^*(t_1) > 0, \quad \text{and} \quad g_i^*(t_0) \leq g_i^*(t_1) + \alpha \Delta g. \quad (6.15)$$

Since  $g_i^*(t_1) > 0$  and  $\delta_i^*(t_1) > 0$ , then  $\gamma_i^*(t_1) = 0$ , by Lemma 19(a). In that case,  $g_i^*(t_1) + \delta_i^*(t_1) = p_{ij}^*(t_1)$  is the power that flows from bus  $i$  to bus  $j$  at time  $t_1$ . Combining (6.14) and (6.15), we have

$$\begin{aligned} \max_{t \in [T]} g_i^*(t) &= g_i^*(t_0) \\ &\leq g_i^*(t_1) + \alpha \Delta g \\ &\leq g_i^*(t_1) + \delta_i^*(t_1) \\ &= p_{ij}^*(t_1) \leq f_{ij}. \end{aligned}$$

Hence, Lemma 19(b) holds when (6.15) is satisfied. Next, we show that if (6.15) does not hold, then we can construct an optimum of  $P^{DC}$  with a lower  $\sum_{i \in \mathcal{K}, t \in [T]} (\gamma_i(t) + \delta_i(t))$  and this contradicts our hypothesis.

Suppose (6.15) does not hold. If  $g_i^*(t_1) = 0$ , then we have

$$g_i^*(t_0) \geq \Delta g > \alpha \Delta g = g_i^*(t_1) + \alpha \Delta g.$$

Thus, it suffices to only consider the following case:

$$g_i^*(t_0) > g_i^*(t_1) + \alpha \Delta g. \quad (6.16)$$

Construct the modified generation, charging and discharging profiles at node  $i$ ,  $\tilde{g}_i(t)$ ,  $\tilde{\delta}_i(t)$ ,  $\tilde{\gamma}_i(t)$

using (6.14), that differ from  $g_i^*(t), \delta_i^*(t), \gamma_i^*(t)$  only at  $t_0$  and  $t_1$  as follows:

$$\begin{aligned}\tilde{g}_i(t_0) &= g_i^*(t_0) - \Delta g, & \tilde{g}_i(t_1) &= g_i^*(t_1) + \alpha \Delta g, \\ \tilde{\gamma}_i(t_0) &= \gamma_i^*(t_0) - \Delta g, & \tilde{\gamma}_i(t_1) &= \gamma_i^*(t_1), \\ \tilde{\delta}_i(t_0) &= \delta_i^*(t_0) = 0, & \tilde{\delta}_i(t_1) &= \delta_i^*(t_1) - \alpha \Delta g.\end{aligned}$$

Also, define the modified storage level  $\tilde{s}_i(t)$  using  $\tilde{\gamma}_i(t)$  and  $\tilde{\delta}_i(t)$ . To provide intuition to the above modification, we essentially generate and store less at time  $t_0$  by an amount  $\Delta g$ . This means at a future time  $t_1$ , we can discharge  $\alpha \Delta g$  less from the storage device and hence have to generate  $\alpha \Delta g$  more to compensate. To check feasibility, it follows from (6.14), that for  $t = t_0, t_1$ , we have

$$\begin{aligned}0 &\leq \tilde{g}_i(t) \leq \bar{g}_i, \\ 0 &\leq \tilde{\gamma}_i(t) \leq \epsilon_\gamma b_i^*, \\ 0 &\leq \tilde{\delta}_i(t) \leq \epsilon_\delta b_i^*.\end{aligned}$$

Also, the line flows  $p_{ij}(t)$  remain unchanged. For the storage levels, it can be checked that the following holds:

$$\begin{aligned}0 \leq s_i^*(t_0 - 1) &\leq \tilde{s}_i(t) \leq s_i^*(t) \leq b_i^*, \text{ for } t \in [t_0, t_1 - 1], \\ \tilde{s}_i(t) &= s_i^*(t), \text{ otherwise.}\end{aligned}$$

This proves that the modified profiles define a feasible point for  $P^{DC}$ . The cost satisfies

$$\begin{aligned}c_i(\tilde{g}_i(t_0)) + c_i(\tilde{g}_i(t_1)) \\ \leq c_i(g_i^*(t_0) - \alpha \Delta g) + c_i(g_i^*(t_1) + \alpha \Delta g)\end{aligned}\tag{6.17a}$$

$$\leq c_i(g_i^*(t_0)) + c_i(g_i^*(t_1)).\tag{6.17b}$$

Equation (6.17a) follows from the non-decreasing nature of  $c_i(\cdot)$  and equation (6.17b)

follows from using (6.16) and Lemma 18. Thus the modified profiles  $\tilde{g}_i(t), \tilde{\delta}_i(t), \tilde{\gamma}_i(t)$  define a feasible point of  $P^{DC}$  with a cost at most  $p_*$  and, hence, are optimal for  $P^{DC}$ . However, we also have

$$\begin{aligned} & \tilde{\gamma}_i(t_0) + \tilde{\gamma}_i(t_1) + \tilde{\delta}_i(t_0) + \tilde{\delta}_i(t_1) \\ &= \gamma_i^*(t_0) + \gamma_i^*(t_1) + \delta_i^*(t_0) + \delta_i^*(t_1) - \underbrace{(1 + \alpha)\Delta g}_{>0}. \end{aligned}$$

Thus, the modified profiles define an optimum of  $P^{DC}$  with a lower  $\sum_{i \in \mathcal{K}, t \in [T]} (\gamma_i(t) + \delta_i(t))$ . This is a contradiction and completes the proof of the Lemma. □

To prove Theorem 17, consider the optimal solution of  $P^{DC}$  that satisfies Lemma 19(b). For all  $i \in \mathcal{K}$ ,  $g_i^*(t)$  itself defines a feasible flow over the line joining buses  $i$  and  $j$ , where  $j$  is the unique neighboring node of  $i$ . Now the proof idea is as follows. For  $i \in \mathcal{K}$ , transfer all storage capacities  $b_i^*$  and the associated charging/ discharging profiles  $(\gamma_i^*(t), \delta_i^*(t))$ , to the neighboring node  $j$ . In particular, consider the point  $(g_k^*(t), \hat{\gamma}_k(t), \hat{\delta}_k(t), \hat{\theta}_k(t), \hat{p}_{kl}(t), \hat{b}_k, k \in \mathcal{N}, k \sim l, t \in [T])$  defined as follows.

$$\begin{aligned} \hat{\gamma}_i(t) &= 0, & \hat{\gamma}_j(t) &= \gamma_i^*(t) + \gamma_j^*(t), & \hat{\gamma}_k(t) &= \gamma_k^*(t), & k \in \mathcal{N} \setminus \{i, j\}, \\ \hat{\delta}_i(t) &= 0, & \hat{\delta}_j(t) &= \delta_i^*(t) + \delta_j^*(t), & \hat{\delta}_k(t) &= \delta_k^*(t), & k \in \mathcal{N} \setminus \{i, j\}, \\ \hat{\theta}_i(t) &= \theta_i^*(t) + \frac{1}{y_{ij}}(\gamma_i^*(t) - \delta_i^*(t)), & \hat{\theta}_k(t) &= \theta_k^*(t), & k \in \mathcal{N} \setminus \{i\}, \\ \hat{b}_i &= 0, & \hat{b}_j &= b_i^* + b_j^*, & \hat{b}_k &= b_k^*, & k \in \mathcal{N} \setminus \{i, j\}, \\ \hat{p}_{ij}(t) &= p_{ij}^*(t) + \gamma_i^*(t) - \delta_i^*(t), & \hat{p}_{kl}(t) &= p_{kl}^*(t), & k \sim l, & (k, l) \neq (i, j). \end{aligned}$$

We do this successively for each  $i \in \mathcal{K}$  to obtain a feasible point of  $\Pi^{\mathcal{K}, DC}$ . Since the generation profiles remained invariant, the resulting point is optimal for  $\Pi^{\mathcal{K}, DC}$ . This completes the proof of Theorem 17.

## Discussion

Here, we explain our main result in more detail. First, we explore a few power networks, where Theorem 17 applies, i.e., network topologies with generator buses that have single connections. Consider the networks shown in Figure 6.8. The single generator single load case in Figure 6.8(a) models topologies where generators and loads are geographically separated and are connected by a transmission line, e.g., see [200]. This is common where the resources for the generation technology (like coal or natural gas) are available far away from where the loads are located in a network. Figure 6.8(b) is an example of a radial network, i.e., an acyclic graph. Most distribution networks conform to this topology<sup>4</sup> Also, isolated transmission networks, e.g., the power network in Catalina island [185] are radial in nature.

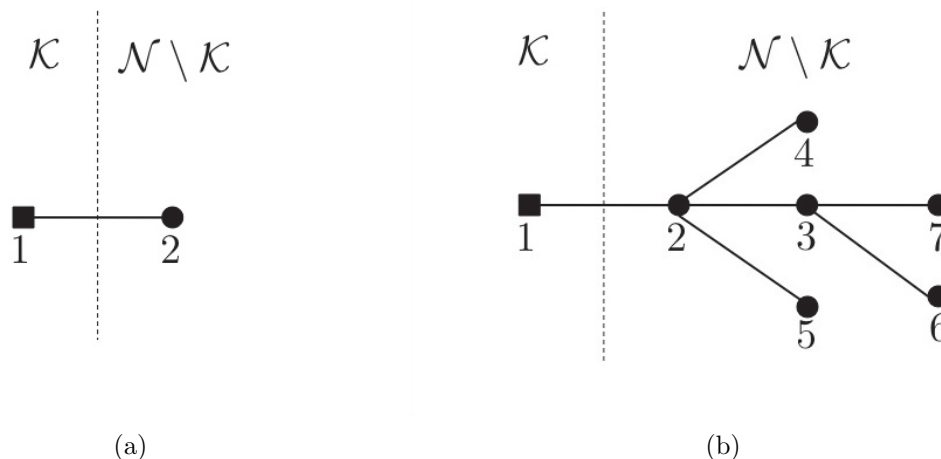


Figure 6.8: Examples of power networks (a) Single generator single load system (b) A radial network.

Next, we discuss how Theorem 17 is helpful for a network planner. Our result suggests that it remains optimal not to place any storage at buses in set  $\mathcal{K}$  even if the demand profiles, generation capacities, line flow capacities or admittances in the network change. We illustrate how this implies a robust investment strategy. Consider the example in Figure

---

<sup>4</sup>Two assumptions in our model hold for transmission networks but not strictly for distribution networks: (a) Resistances in distribution lines are not negligible and hence DC approximation does not generally apply [33], (b) Three different types of loads, namely, constant power, constant current and constant impedance loads show different behavior in distribution networks [8]; but in aggregate, demands can be modeled as constant power loads in transmission networks, as in IEEE benchmark systems, e.g., see [12, 63].

6.8(a). Suppose the line flow capacity is larger than the peak value of the demand profile, i.e.,  $f_{12} \geq \max_{t \in [T]} d_2(t)$ . It can be checked that placing all the available storage at the generator bus is an optimal solution. If at a later time during the operation of the network, the demand increases such that the peak demand surpasses the line capacity, this placement of storage no longer remains optimal and requires new infrastructure for storage to be built on the demand side to avoid load shedding. If, however, we use the optimum as suggested by the problem  $\Pi^{\mathcal{K}, DC}$  and place all storage on the demand side from the beginning, then this placement not only can accommodate the change in the demand, but, it also, remains optimal under the available storage budget. To explore another such direction, suppose another generator is built to supply the load in Figure 6.8(a). Our result suggests that we still do not need storage allocation at bus 1 even with the extended network. This illustrates how Theorem 17 implies an investment strategy that is robust to changes in many parameters in the network.

We end this section with remarks on the storage placement problem with concave cost functions and generator buses with multiple connections, respectively.

### On concave cost functions

We briefly discuss the role of convexity in the cost function. Suppose instead that  $c(\cdot)$  is concave then  $P^{DC}$  and  $\Pi^{\mathcal{K}, DC}$  are not convex programs and, hence, cannot be solved efficiently. Note that the results of Theorem 17 do *not* generally apply to such cases. For example, consider a two bus system, consisting of: (i) a generator bus (say, bus 1) with a concave cost function  $c(g) = 2g$ , if  $0 \leq g \leq 5$  and  $c(g) = 10 + (g - 5)$  otherwise, (ii) a load bus (say, bus 2) with  $T = 2$  and demand profile  $d_2 = (5, 5)$  and (iii) a single line with capacity  $f_{12} = 5$  connecting them. Further let  $h = 1$ ,  $\alpha = 1$ ,  $\epsilon_\gamma = \epsilon_\delta = 1$  and  $\bar{g}_1 = 8$ . All quantities are in per units. It can be checked that the optimal generation profile of  $\Pi^{\{1\}, DC}$  is  $(5, 5)$ , thus,  $\pi_*^{\{1\}} = 20$ . On the other hand, the generation profile  $(6, 4)$  is feasible for  $P^{DC}$ . Hence,  $p_* \leq 19 < \pi_*^{\{1\}}$ .

## On generators with multiple connections

Generator buses with multiple connections may not always have zero storage capacity in the optimal allocation. In this section, we illustrate this fact through a simple example. Consider a 3-node network as shown in Figure 6.9. All quantities are in per units. Let the cost of generation at node 1 be  $c_1(g) = g^2$ . Let  $T = 4$  and the demand profiles at nodes 2 and 3 be

$$d_2 = (9, 10, 0, 10) \quad \text{and} \quad d_3 = (0, 10, 9, 10).$$

Also, suppose that the line and generation capacities are  $f_{12} = f_{13} = 9.5$  and the available storage budget is  $h = 5$ . Finally, assume no losses and ignore the ramp constraints in the charging and discharging processes, i.e.  $\alpha = 1$  and  $\epsilon_\gamma = \epsilon_\delta = 1$ . The optimal storage allocation  $(b_1^*, b_2^*, b_3^*)$  for the two problems  $P^{DC}$  and  $\Pi^{\{1\}, DC}$  is  $(4, 0.5, 0.5)$  and  $(0, 2.5, 2.5)$ , respectively. Also, the optimal generation profile  $g_1^*(t), t = 1, 2, 3, 4$  for the two problems can be computed to be  $(14, 15, 14, 15)$  and  $(12, 17, 12, 17)$ , respectively. Thus,  $p_* = 842 < \pi_*^{\{1\}} = 866$ .

We provide some intuition behind the design of the counterexample above. First, notice that if demands at buses 2 and 3 are multiples of each other, i.e.,  $d_2(t) = \zeta d_3(t)$  for some constant  $\zeta \geq 0$ , the 3-node network can be roughly thought of as two single-generator-single-load systems with nodes  $(1, 2)$  and  $(1, 3)$ , respectively and Theorem 1 applies. Thus to expect  $b_1^* \neq 0$  in  $P^{DC}$ , we consider demand profiles that show opposite trends. Second, if  $h = \infty$ , we prove in Section A.2 that for such networks, there exists an optimal point with  $b_1^* = 0$ . Hence, we consider a small storage budget. Third, note that if line capacities are large, then an optimal allocation with  $b_1^* = 0$  trivially exists. Thus, we construct  $f_{12} = f_{13} = 9.5$  for which  $P^{DC}$  and  $\Pi^{\{1\}, DC}$  are feasible but the network is congested. This illustrates some key directions to look at for characterizing cases where  $b_1^* = 0$  for generator buses with multiple connections; this is a part of our ongoing research.

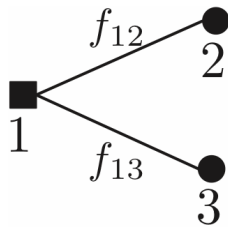


Figure 6.9: A network with a generator that has multiple connections.

## 6.5 Conclusions and future work

In this chapter, we formulated the optimal storage placement problem for load shifting at slow time scale for power network operations. Assuming a periodic demand profile, we study the infinite horizon problem over one cycle. First, we use a semidefinite conic relaxation of the power flow equations to observe salient features of the optimal placement. Then we use analytical tools to prove a property of the optimal solution of the same problem with a DC approximation.

There are quite a few natural directions to explore for this problem. We comment on a few here. (a) Our result in Theorem 17 only partially explains the observation made with SDP relaxations that optimal storage capacities seldom have large fractions on nodes with cheap generation resources. The counterexample in Section 6.4.1 suggests that such a general result does not hold beyond the settings in Theorem 17; however, it is unclear whether structural results can be identified when demand profiles and/ or network topologies are restricted to a certain class. (b) The analysis in Section 6.4 ignores losses in the network and only captures the interaction of load-shifting with line capacities. The SDP formulation, however, models the losses in the network and storage placements still show similar patterns. This hints on possible extensions of theoretical analysis to DC approximation with losses. (c) The current work only focusses on slow time scales of operation. Another important application of storage is to mitigate intermittency of renewables at faster time-scales. The interaction of the slower and faster time-scales would provide a unifying framework for studying investments in storage technologies.

# Appendix A

## Partial results on storage placement for specific network topologies

In this appendix, we present and prove some partial results on the DC version of the storage placement problem defined in Chapter 6. Please refer to Chapter 6 Section 6.2 for the notation. These results are intended to provide directions for future work. We hope that such results would spur further research into structural properties of optimal storage investment for the load-shifting problem.

Recall that  $\Pi^{\mathcal{K},DC}$  is the DC version of the restricted storage placement problem which places no storage capacity at the buses in set  $\mathcal{K}$ . Notice that in both problems  $P^{DC}$  and  $\Pi^{\mathcal{K},DC}$ , we solve for the optimal placement and control of storage in a power-network, given the demand profiles  $d_k(t), t \in [T]$ , the storage budget  $h$ , the capacities of the generators  $\bar{g}_k, k \in \mathcal{N}_G$  and other network parameters such as the line flow limits  $f_{kl}, k \sim l$ . Now we explore the behavior of the optimal cost of production as a function of these parameters. This provides valuable insights on various design issues, e.g., how much savings in terms of generation cost do we achieve by investing in an extra unit of storage. We explore such questions for specific network topologies.

We make a few simplifying assumptions in this section. Let  $c_k(\cdot), k \in \mathcal{N}_G$  be strictly convex and let  $\alpha = 1$  and  $\epsilon_\gamma = \epsilon_\delta = 1$ . The proofs are included in Section A.3.

## A.1 Single generator single load network

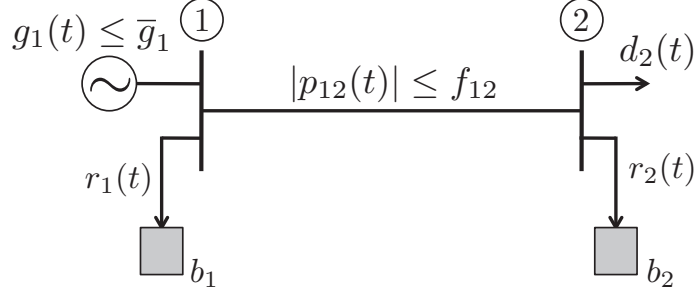


Figure A.1: Single generator single load network. Available storage budget is  $h \geq b_1 + b_2$ .

Consider the single generator single load network shown in Figure A.1. Generator at bus 1 is connected to a load (or demand) at bus 2 using a single line, i.e.,  $\mathcal{K} = \mathcal{N}_G = \{1\}$  and  $\mathcal{N}_D = \{2\}$ . For this network, placing all the available storage resources at the load bus is always optimal. This is an immediate consequence of Theorem 17. In this section, for any fixed demand profile  $d_2(t), t \in [T]$  of the load bus, we analyze the behavior of the optimal cost of production as a function of the generation capacity  $\bar{g}_1$ , the line flow capacity  $f_{12}$  and the available storage budget  $h$ ; in particular, let the parameterized storage placement problem be  $P^{DC}(\bar{g}_1, f_{12}, h)$  and its optimal cost be  $p_*(\bar{g}_1, f_{12}, h)$ . Similarly define,  $\Pi^{\{1\}, DC}(\bar{g}_1, f_{12}, h)$  and  $\pi_*^{\{1\}}(\bar{g}_1, f_{12}, h)$ .

At the optimum of  $P^{DC}(\bar{g}_1, f_{12}, h)$ , we have  $g_1^*(t) \leq f_{12}, t \in [T]$  from Lemma 19. Also, it satisfies  $g_1^*(t) \leq \bar{g}_1, t \in [T]$ . Thus, to characterize the optimal point of  $P^{DC}(\bar{g}_1, f_{12}, h)$ , it is equivalent to consider the constraint  $g_1(t) \leq \min\{\bar{g}_1, f_{12}\}, t \in [T]$ .

**Proposition 20.** *For any  $h \geq 0$ , problem  $P^{DC}(\bar{g}_1, f_{12}, h)$  is feasible iff  $\min\{\bar{g}_1, f_{12}\} \geq f_{\min}$ , where*

$$f_{\min} = \max \left\{ \max_{1 \leq t \leq T} \left( \frac{\sum_{\tau=1}^t d_2(\tau)}{t} \right), \max_{1 \leq t_1 < t_2 \leq T} \left( \frac{\sum_{\tau=t_1+1}^{t_2} d_2(\tau) - h}{t_2 - t_1} \right) \right\}. \quad (\text{A.1})$$

Moreover, if  $\min\{\bar{g}_1, f_{12}\} \geq f_{\min}$ , then  $p_*(\bar{g}_1, f_{12}, h) = p_*(f_{\min}, f_{\min}, h)$ .

We interpret this result as follows. If either the line flow limit  $f_{12} < f_{\min}$  or the generation capacity  $\bar{g}_1 < f_{\min}$ , the load cannot be satisfied. Notice that  $f_{\min}$  for  $h > 0$  is no more

than  $f_{min}$  for  $h = 0$ . Thus, storage can be used to reduce the cost of operation avoiding transmission upgrades and generation capacity expansion [194]. Interestingly, for  $f_{12} \geq f_{min}$  and  $\bar{g}_1 \geq f_{min}$ , the optimal cost of operation does not depend on the specific values of  $f_{12}$  and  $\bar{g}_1$ . From transmission or distribution planning perspective, investment in line and generation capacities over  $f_{min}$  do not reduce the cost of operation. We provide an illustrative example at the end of this section.

Next, we characterize the behavior of  $P^{DC}(\bar{g}_1, f_{12}, h)$  and its optimal cost  $p^*(\bar{g}_1, f_{12}, h)$  as a function of  $h$ . For a given  $f_{12}$  and  $\bar{g}_1$ , the minimum required storage budget to serve the load depends on the demand profile  $d_2(t), t \in [T]$ . This may or may not be zero, depending on  $d_2(t), t \in [T]$ ,  $f_{12}$  and  $\bar{g}_1$ . We calculate this minimum required storage budget, (say  $h_{min}$ ) in Proposition 21. Also, it is easy to observe that as we allow larger storage budget, the generation cost does not reduce beyond a point, i.e., there exists  $h_{sat}$  such that  $p_*(\bar{g}_1, f_{12}, h) = p_*(\bar{g}_1, f_{12}, h_{sat})$  for all  $h \geq h_{sat}$ . We also calculate  $h_{sat}$  in Proposition 21. First, we introduce some notation. Construct the sequence  $\{\tau_m\}_{m=0}^M$  as follows. Let  $\tau_0 = 0$ . Define  $\tau_m$  iteratively:

$$\tau_m = \arg \max_{\tau_{m-1}+1 \leq t \leq T} \left( \frac{\sum_{\tau=\tau_{m-1}+1}^t d_2(\tau)}{t - \tau_{m-1}} \right), \quad (\text{A.2})$$

for  $1 \leq m \leq M$ , where  $M$  is the smallest integer for which  $\tau_M = T$ . Note that the sequence depends only on the demand profile  $d_2(t), t \in [T]$ . For any  $x \in \mathbb{R}$ , let  $[x]^+ := \max(x, 0)$ .

**Proposition 21.** *Problem  $P^{DC}(\bar{g}_1, f_{12}, h)$  satisfies:*

- (a) *If  $\min \{\bar{g}_1, f_{12}\} < \max_{t \in [T]} \left( \frac{\sum_{\tau=1}^t d_2(\tau)}{t} \right)$ , then  $P^{DC}(\bar{g}_1, f_{12}, h)$  is infeasible for all  $h \geq 0$ .*
- (b) *Suppose,  $\min \{\bar{g}_1, f_{12}\} \geq \max_{t \in [T]} \left( \frac{\sum_{\tau=1}^t d_2(\tau)}{t} \right)$ . Then,  $P^{DC}(\bar{g}_1, f_{12}, h)$  is feasible iff  $h \geq h_{min}$  and  $p_*(\bar{g}_1, f_{12}, h)$  is convex and non-increasing in  $h$ , where*

$$h_{min} = \max_{0 \leq t_1 \leq t_2 \leq T} \left[ \sum_{\tau=t_1+1}^{t_2} (d_2(\tau) - \min \{\bar{g}_1, f_{12}\}) \right]^+. \quad (\text{A.3})$$

Furthermore,  $p_*(\bar{g}_1, f_{12}, h)$  is constant for all  $h \geq h_{sat}$ , where

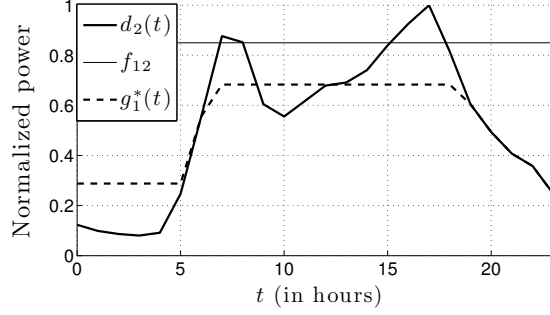
$$h_{sat} = \max_{1 \leq m \leq M} \left[ \max_{\tau_{m-1}+1 \leq t \leq \tau_m} \left\{ \left( \sum_{\tau=\tau_{m-1}+1}^{\tau_m} d_2(\tau) \right) \frac{t - \tau_{m-1}}{\tau_m - \tau_{m-1}} - \left( \sum_{\tau=\tau_{m-1}+1}^t d_2(\tau) \right) \right\} \right]. \quad (\text{A.4})$$

The condition  $\min \{\bar{g}_1, f_{12}\} \geq \max_{t \in [T]} \left( \frac{\sum_{\tau=1}^t d_2(\tau)}{t} \right)$  implies that there is some  $h > 0$  for which  $P^{DC}(\bar{g}_1, f_{12}, h)$  is feasible. If this condition is violated, the problem remains infeasible no matter how large the storage budget  $h$  is. More the storage budget, lesser is the generation cost and hence  $p^*(\bar{g}_1, f_{12}, h)$  is decreasing in  $h$ . The convexity, however, implies that there is diminishing marginal returns on the investment on storage, i.e., the benefit of the first unit installed is more than that from the second unit. As a final note, observe that  $h_{sat}$  is a function of only the demand profile and is independent of the generation and line flow capacities.

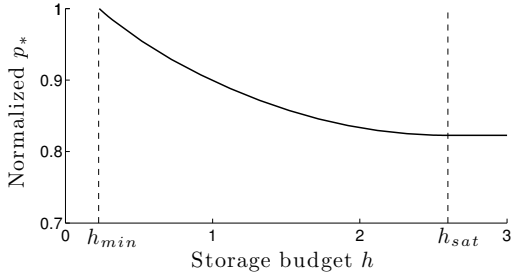
## Illustrative example

Now we explain Propositions 20 and 21 with an example. All quantities are in per units. Consider an hourly load profile  $d_2(t), t \in [T]$  as shown in Figure A.2(a). The optimal generation profile  $g_1^*(t), t \in [T]$  for  $P^{DC}(\bar{g}_1 = 1, f_{12} = 0.85, h = 1)$  has been plotted in the same Figure. Notice that  $\max_{t \in [T]} g_1^*(t) \leq f_{12}$  as stated in Lemma 19.

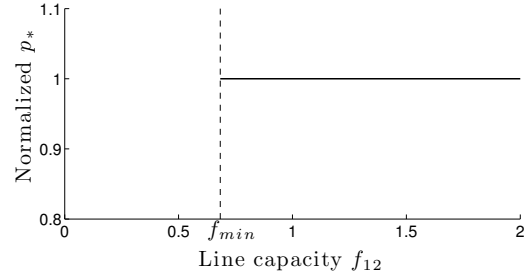
Consider the plots in Figures A.2(b) and A.2(c). We plot  $p^*(\bar{g}_1 = 1, f = 0.85, h)$  for  $h$  in  $[0, 3]$  in Figure A.2(b). Notice that  $f_{12} \leq \max_{t \in [T]} d_2(t)$ , i.e., the problem is infeasible in the absence of storage. We calculate  $h_{\min} = 0.226$  and  $h_{sat} = 2.598$  from Proposition 21. In Figure A.2(c), we plot  $p^*(\bar{g}_1 = 1, f_{12}, h = 1)$  for  $f_{12}$  in  $[0, 2]$ . As in Proposition 20, the problem is infeasible for  $f_{12} < f_{\min} = 0.683$  and the optimal cost remains constant for  $f_{12} \geq f_{\min}$ .



(a)



(b)



(c)

Figure A.2: Plots to illustrate Propositions 20 and 21. (a) Typical hourly load profile and optimal generation portfolio for line flow capacity  $f_{12} = 0.85$ , generation capacity  $\bar{g}_1 = 1$  and storage budget  $h = 1$  (b)  $p_*(\bar{g}_1 = 1, f_{12} = 0.85, h)$ . (c)  $p_*(\bar{g}_1 = 1, f_{12}, h = 1)$ .

## A.2 Star network

Consider a star network on  $n \geq 2$  nodes, where  $\mathcal{N}_G = \{1\}$  and  $\mathcal{N}_D = \{2, 3, \dots, n\}$  that are only linked with the generator node 1 through lines of capacities  $f_{1k}$ ,  $k \in \mathcal{N}_D$ . For fixed demand profiles  $d_k(t)$ ,  $t \in [T]$ ,  $k \in \mathcal{N}_D$ , line flow capacities  $f_{1k}$ ,  $k \in \mathcal{N}_D$  and capacity of the generator  $\bar{g}_1$ , let  $P^{DC}(h)$  and  $\Pi^{\{1\}, DC}(h)$  denote the DC versions of the storage placement problem and the restricted storage placement problem as functions of the available storage budget  $h$ . Also, let  $p_*(h)$  and  $\pi_*^{\{1\}}(h)$  be their optimal costs respectively.

In Section 6.4.1 we showed that placing zero storage at the generator bus of a star network with 3 nodes is not optimal, i.e., in general,  $p_*(h) \neq \pi_*(h)$ . In Figure A.3, we plot  $p_*(h)$  and  $\pi_*(h)$  for the 3-node star network shown in Figure 6.9 over a range of values of the total storage budget  $h$ . Observe that  $p_*(h) < \pi_*^{\{1\}}(h)$  for some values of  $h$  but they coincide at:

- Minimum value of  $h$  for which  $P^{DC}(h)$  and  $\Pi^{\{1\},DC}(h)$  are feasible.
- Large enough values of  $h$ .

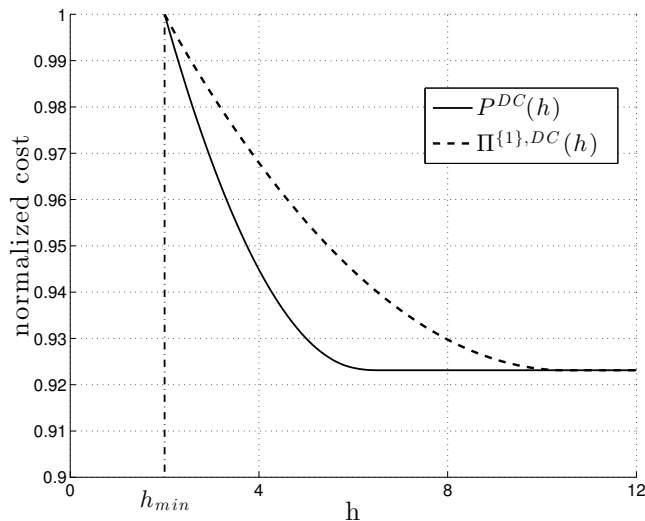


Figure A.3:  $P^{DC}(h)$  and  $\Pi^{\{1\}}(h)$  for the simple 3-node star network in Figure 6.9.

We formally state this for a general  $n$ -node star network in the following.

**Proposition 22.** Assume  $\bar{g} = \infty$ . Suppose  $f_{1k} \geq \max_{t \in [T]} \left( \frac{\sum_{\tau=1}^t d_k(\tau)}{t} \right)$  for all  $k \in \mathcal{N}_D$ . Then,  $P^{DC}(h)$  and  $\Pi^{\{1\},DC}(h)$  are feasible iff  $h \geq h_{min}$ , where

$$h_{min} = \sum_{k \in \mathcal{N}_D} \max_{0 \leq t_1 < t_2 \leq T} \left[ \sum_{\tau=t_1+1}^{t_2} (d_k(\tau) - f_{1k}) \right]^+. \quad (\text{A.5})$$

Moreover:

(a)  $p_*(h_{min}) = \pi_*^{\{1\}}(h_{min})$ ,

(b) There exists  $h_o \geq h_{min}$  such that  $p_*(h) = \pi_*^{\{1\}}(h)$  for all  $h \geq h_o$ .

## A.3 Proofs of results for specific network topologies

Here, we present the proofs of the results presented in Section A. For the single generator single node and the star network, we drop the voltage angles  $\theta_k(t), k \in \mathcal{N}, t \in [T]$ . For any value of the power flow  $p_{1k}(t)$  from bus 1 to bus  $k$ , voltage angles  $\theta_k(t)$  can always be chosen to satisfy the power flow constraints.

Furthermore, since  $\alpha = 1$ , define  $r_k(t) := \gamma_k(t) - \delta_k(t)$  as the power that flows into the storage device at node  $k \in \mathcal{N}$  at time  $t \in [T]$  as in Section 6.2. Notice that  $r_k(t)$  can be positive or negative depending on whether power flows in or out of the storage device. Also, the storage level of the storage device at node  $k \in \mathcal{N}$ , at time  $t$  can be written as  $s_k(t) = \sum_{\tau=1}^t r_k(\tau)$ .

### A.3.1 Proofs for single generator single load network

We drop subscripts from the variables  $d_2(t), g_1(t), t \in [T], f_{12}, \bar{g}_1, c_1(\cdot)$  and the superscripts from  $P^{DC}(\cdot), \Pi^{\{1\}, DC}(\cdot), \pi_*^{\{1\}}(\cdot)$  for ease of notation for the single generator single load networks.

**Proposition 20.** *For any  $h \geq 0$ , problem  $P^{DC}(\bar{g}, f, h)$  is feasible iff  $\min\{\bar{g}, f\} \geq f_{\min}$ , where*

$$f_{\min} = \max \left\{ \max_{t \in [T]} \left( \frac{\sum_{\tau=1}^t d(\tau)}{t} \right), \max_{1 \leq t_1 < t_2 \leq T} \left( \frac{\sum_{\tau=t_1+1}^{t_2} d(\tau) - h}{t_2 - t_1} \right) \right\}. \quad (\text{A.6})$$

Moreover, if  $\min\{\bar{g}, f\} \geq f_{\min}$ , then  $p_*(\bar{g}, f, h) = p_*(f_{\min}, f_{\min}, h)$ .

*Proof.* From Theorem 17, it suffices to show the claim for  $\Pi(\bar{g}, f, h)$  and  $\pi_*(\bar{g}, f, h)$ . First, we show that if  $\Pi(\bar{g}, f, h)$  is feasible, then  $\min\{\bar{g}, f\} \geq f_{\min}$ . Fix any  $h \geq 0$  and let  $g(t), t \in [T]$  be a feasible generation profile. Since  $\sum_{\tau=1}^t r_2(\tau) = s_2(t) \geq 0$ , we have for any  $t \in [T]$

$$\max_{t' \in [T]} g(t') \geq \frac{\sum_{\tau=1}^t g(\tau)}{t} = \frac{\sum_{\tau=1}^t d(\tau) + \sum_{\tau=1}^t r_2(\tau)}{t} \geq \frac{\sum_{\tau=1}^t d(\tau)}{t}. \quad (\text{A.7})$$

Furthermore, for any  $1 \leq t_1 < t_2 \leq T$ , the power extracted from the storage device

between time instants  $t_1$  and  $t_2$  cannot exceed the total storage budget  $h$  and hence we have

$$\max_{t' \in [T]} g(t') \geq \frac{\sum_{\tau=t_1+1}^{t_2} g(\tau)}{t_2 - t_1} = \frac{\sum_{\tau=t_1+1}^{t_2} d(\tau) + \sum_{\tau=t_1+1}^{t_2} r_2(\tau)}{t_2 - t_1} \geq \frac{\sum_{\tau=t_1+1}^{t_2} d(\tau) - h}{t_2 - t_1}. \quad (\text{A.8})$$

Since  $g(t), t \in [T]$  is feasible,  $g(t) \leq \min\{\bar{g}, f\}$  for all  $t \in [T]$ . Hence, combining (A.7) and (A.8), we get

$$\min\{\bar{g}, f\} \geq \max_{t' \in [T]} g(t') \geq f_{\min}.$$

Next, we show that  $\min\{\bar{g}, f\} \geq f_{\min}$  is sufficient for  $\Pi(\bar{g}, f, h)$  to be feasible. Consider the optimal generation profile  $g^*(t), t \in [T]$  for the relaxed problem  $\Pi(+\infty, +\infty, h)$ . Suppose it satisfies

$$\max_{t \in [T]} g^*(t) \leq f_{\min}. \quad (\text{A.9})$$

Then  $g^*(t), t \in [T]$  is also feasible and optimal for problem  $\Pi(\bar{g}, f, h)$  for  $\min\{\bar{g}, f\} \geq f_{\min}$ . Also,  $\pi_*(\bar{g}, f, h) = \pi_*(f_{\min}, f_{\min}, h)$  for  $\min\{\bar{g}, f\} \geq f_{\min}$ . It remains to show that (A.9) indeed holds. Consider the following notation.

$$t_{\max} := \max\{t \in [T] \mid g^*(t) = \max_{\tau \in [T]} g^*(\tau)\},$$

$$t_{\text{less}} := \max\{0 \leq t < t_{\max} \mid g^*(t) < g^*(t_{\max})\}.$$

In the above definition  $g^*(0) := 0$  for convenience. If  $g^*(t_{\max}) = 0$ , then (A.9) clearly holds. Henceforth, assume  $g^*(t_{\max}) > 0$ . Then,  $g^*(t), t \in [T]$  satisfies:

$$\begin{aligned} \max_{t \in [T]} g^*(t) &= \frac{\sum_{\tau=t_{\text{less}}+1}^{t_{\max}} g^*(\tau)}{t_{\max} - t_{\text{less}}} \\ &= \frac{\sum_{\tau=t_{\text{less}}+1}^{t_{\max}} [d(\tau) + r_2^*(\tau)]}{t_{\max} - t_{\text{less}}} \\ &= \frac{1}{t_{\max} - t_{\text{less}}} \left[ \left( \sum_{\tau=t_{\text{less}}+1}^{t_{\max}} d(\tau) \right) + s_2^*(t_{\max}) - s_2^*(t_{\text{less}}) \right] \end{aligned} \quad (\text{A.10})$$

Now, suppose the following holds:

$$s_2^*(t_{max}) = 0 \quad \text{and} \quad s_2^*(t_{less}) = \begin{cases} 0, & \text{if } t_{less} = 0, \\ h, & \text{otherwise.} \end{cases} \quad (\text{A.11})$$

If (A.11) holds, it follows from (A.10):

$$\begin{aligned} \max_{t \in [T]} g^*(t) &= \begin{cases} \frac{\sum_{\tau=1}^{t_{max}} d(\tau)}{t_{max}}, & \text{if } t_{less} = 0, \\ \frac{\sum_{\tau=t_{less}+1}^{t_{max}} d(\tau) - h}{t_{max} - t_{less}}, & \text{otherwise,} \end{cases} \\ &\leq f_{\min}. \end{aligned}$$

and hence (A.9) is satisfied. Next, we show that (A.11) indeed holds to complete the proof. First we prove that  $s_2^*(t_{max}) = 0$ , i.e., the storage device at node 2 fully discharges at time  $t_{max}$ . Suppose  $s_2^*(t_{max}) > 0$ . As in Lemma 19, we construct a modified generation profile and storage control policy that is feasible and has an objective function value no greater than  $\pi_*(+\infty, +\infty, h)$ . But, the optimal generation profile  $g^*(t), t \in [T]$  is unique since the cost function  $c(\cdot)$  is assumed to be strictly convex. Hence we derive a contradiction. By hypothesis,  $s_2^*(t_{max}) > 0$  and hence storage device at bus 2 discharges for some  $t > t_{max}$ . Let  $t_1$  be the first such time instant. Define

$$\Delta_1 := \min \{s_2^*(t_{max}), g^*(t_{max}), g^*(t_{max}) - g^*(t_1)\}.$$

Notice that  $\Delta_1 > 0$ . Consider the modified generation profile  $\tilde{g}(t)$  and control policy  $\tilde{r}_2(t)$ , that differ from  $g^*(t)$  and  $r_2^*(t)$  only at  $t_{max}$  and  $t_1$  as follows:

$$\begin{aligned} \tilde{g}(t_{max}) &= g^*(t_{max}) - \Delta_1, & \tilde{g}(t_1) &= g^*(t_1) + \Delta_1, \\ \tilde{r}_2(t_{max}) &= r_2^*(t_{max}) - \Delta_1, & \tilde{r}_2(t_1) &= r_2^*(t_1) + \Delta_1. \end{aligned}$$

Using Lemma 18, we have

$$c(\tilde{g}(t_{max})) + c(\tilde{g}(t_1)) \leq c(g^*(t_{max})) + c(g^*(t_1)).$$

It can be checked that the modified profiles are feasible for  $\Pi(+\infty, +\infty, h)$ . The details are omitted for brevity. This is a contradiction and hence  $s_2^*(t_{max}) = 0$ .

Next, we characterize  $s_2^*(t_{less})$ . If  $t_{less} = 0$ , then  $s_2^*(t_{less}) = s_2^0 = 0$ . If  $t_{less} > 0$ , we prove that  $s_2^*(t_{less}) = h$ , i.e., the storage device at node 2 is fully charged at time  $t_{less}$ . Suppose  $s_2^*(t_{less}) < h$ . As above, we construct a modified generation profile  $\tilde{g}(t)$  and storage control policy  $\tilde{r}_2(t)$  that achieves an objective value no greater than  $\pi_*(+\infty, +\infty, h)$  to derive a contradiction. In particular, define

$$\Delta_2 := \min \{h - s_2^*(t_{less}), g^*(t_{less} + 1), g^*(t_{less} + 1) - g^*(t_{less})\} > 0.$$

Consider  $\tilde{g}(t)$  and  $\tilde{r}_2(t)$ , that differ from  $g^*(t)$  and  $r_2^*(t)$  only at  $t_{less}$  and  $t_{less} + 1$  as follows:

$$\begin{aligned} \tilde{g}(t_{less}) &= g^*(t_{less}) + \Delta_2, & \tilde{g}(t_{less} + 1) &= g^*(t_{less} + 1) - \Delta_2, \\ \tilde{r}_2(t_{less}) &= r_2^*(t_{less}) + \Delta_2, & \tilde{r}_2(t_{less} + 1) &= r_2^*(t_{less} + 1) - \Delta_2. \end{aligned}$$

As above, this defines a feasible point for  $\Pi(+\infty, +\infty, h)$  and achieves an objective value strictly less than  $\pi_*(+\infty, +\infty, h)$ . This is a contradiction and hence  $s_2^*(t_{less}) = h$  for  $t_{less} > 0$ .  $\square$

**Proposition 21.** *Problem  $P(\bar{g}, f, h)$  satisfies:*

- (a) *If  $\min \{\bar{g}, f\} < \max_{t \in [T]} \left( \frac{\sum_{\tau=1}^t d(\tau)}{t} \right)$ , then  $P(\bar{g}, f, h)$  is infeasible for all  $h \geq 0$ .*
- (b) *Suppose,  $\min \{\bar{g}, f\} \geq \max_{t \in [T]} \left( \frac{\sum_{\tau=1}^t d(\tau)}{t} \right)$ . Then,  $P(\bar{g}, f, h)$  is feasible iff  $h \geq h_{min}$  and  $p_*(\bar{g}, f, h)$  is convex and non-increasing in  $h$ , where*

$$h_{min} = \max_{0 \leq t_1 \leq t_2 \leq T} \left[ \sum_{\tau=t_1+1}^{t_2} (d(\tau) - \min \{\bar{g}, f\}) \right]^+. \quad (\text{A.12})$$

Furthermore,  $p_*(\bar{g}, f, h)$  is constant for all  $h \geq h_{sat}$ , where

$$h_{sat} = \max_{1 \leq m \leq M} \left[ \max_{\tau_{m-1}+1 \leq t \leq \tau_m} \left\{ \left( \sum_{\tau=\tau_{m-1}+1}^{\tau_m} d(\tau) \right) \frac{t - \tau_{m-1}}{\tau_m - \tau_{m-1}} - \left( \sum_{\tau=\tau_{m-1}+1}^t d(\tau) \right) \right\} \right]. \quad (\text{A.13})$$

*Proof.* From Theorem 17, it suffices to prove the claim for  $\Pi(\bar{g}, f, h)$  and  $\pi_*(\bar{g}, f, h)$ .

- (a) To the contrary of the statement of the Proposition suppose that  $\min \{\bar{g}, f\} < \max_{t \in [T]} \left( \frac{\sum_{\tau=1}^t d(\tau)}{t} \right)$  and  $\Pi(\bar{g}, f, h)$  is feasible for some  $h \geq 0$ . Then, it follows directly from Proposition 20 that  $\min \{\bar{g}, f\} \geq f_{min} \geq \max_{t \in [T]} \left( \frac{\sum_{\tau=1}^t d(\tau)}{t} \right)$ , contradicting our hypothesis.
- (b) First we show that if  $\Pi(\bar{g}, f, h)$  is feasible then  $h \geq h_{min}$ . Suppose  $\Pi(\bar{g}, f, h)$  is feasible. Then, for all  $0 \leq t_1 < t_2 \leq T$  Proposition 20 implies that  $\min \{\bar{g}, f\} \geq f_{min} \geq \left( \sum_{\tau=t_1+1}^{t_2} d(\tau) - h \right) / (t_2 - t_1)$ . Rearranging this we get  $h \geq \sum_{\tau=t_1+1}^{t_2} (d(\tau) - \min \{\bar{g}, f\})$ . Also,  $h \geq 0$  and hence:

$$h \geq \max_{0 \leq t_1 < t_2 \leq T} \left[ \sum_{\tau=t_1+1}^{t_2} (d(\tau) - \min \{\bar{g}, f\}) \right]^+ = h_{min}.$$

Now we show that  $h \geq h_{min}$  is sufficient for  $\Pi(\bar{g}, f, h)$  to be feasible. The relation  $h \geq h_{min}$  can be equivalently written as follows:

$$\min \{\bar{g}, f\} \geq \frac{\sum_{\tau=t_1+1}^{t_2} d(\tau) - h}{t_2 - t_1}, \quad \text{for all } 0 \leq t_1 < t_2 \leq T. \quad (\text{A.14})$$

Also, by hypothesis, we have

$$\min \{\bar{g}, f\} \geq \max_{t \in [T]} \left( \frac{\sum_{\tau=1}^t d(\tau)}{t} \right). \quad (\text{A.15})$$

Combining (A.14) and (A.15), we get  $\min \{\bar{g}, f\} \geq f_{min}$ . Then, Proposition 20 implies that  $\Pi(\bar{g}, f, h)$  is feasible. Convexity and non-decreasing nature of  $p_*(\bar{g}, f, h)$  as a function of  $h$  follows from linear parametric optimization theory [55].

Finally, we prove that  $p_*(\bar{g}, f, h)$  is constant for all  $h \geq h_{sat}$ , where  $h_{sat}$  is as defined in (A.13). The proof idea here is as follows. We construct the optimal generation profile  $g^*(t), t \in [T]$  for the problem  $\Pi(+\infty, +\infty, +\infty)$  and show that it is feasible and hence optimal for the problem  $\Pi(\bar{g}, f, +\infty)$  provided  $\min\{\bar{g}, f\} \geq \max_{t \in [T]} \left( \frac{\sum_{\tau=1}^t d(\tau)}{t} \right)$  holds. Problem  $\Pi(+\infty, +\infty, +\infty)$  can be re-written as follows.

$$\begin{aligned} & \underset{g(t), t \in [T]}{\text{minimize}} && \sum_{t=1}^T c_1(g(t)) \\ & \text{subject to} && g(t) \geq 0, \quad \sum_{\tau=1}^t (g(\tau) - d(\tau)) \geq 0, \quad t \in [T], \end{aligned} \quad (\text{A.16a})$$

$$\sum_{\tau=1}^T g(\tau) = \sum_{\tau=1}^T d(\tau). \quad (\text{A.16b})$$

Let the Lagrange multipliers in equations (A.16a)–(A.16b) be  $\lambda(t)$ ,  $\ell(t)$ ,  $t \in [T]$  and  $\nu$ , respectively.

It can be checked that the following primal-dual pair satisfies the Karush-Kuhn-Tucker conditions and hence is optimal for the convex program  $\Pi(+\infty, +\infty, +\infty)$  and its Lagrangian dual [55]. We omit the details for brevity.

$$\begin{aligned} g^*(t) &= \frac{\sum_{\tau=\tau_{m-1}+1}^{\tau_m} d(\tau)}{\tau_m - \tau_{m-1}}, \quad t = \tau_{m-1} + 1, \dots, \tau_m \quad \text{and} \quad m = 1, 2, \dots, M, \\ \ell^*(t) &= \begin{cases} c'(g^*(\tau_m)) - c'(g^*(\tau_m + 1)), & \text{if } t = \tau_m, \quad m = 1, 2, \dots, M - 1 \\ 0, & \text{otherwise} \end{cases}, \quad t \in [T], \\ \lambda^*(t) &= 0, \quad t \in [T], \quad \text{and} \quad \nu^* = -c'(g^*(T)). \end{aligned}$$

The above profile  $g^*(t), t \in [T]$  of  $\Pi(+\infty, +\infty, +\infty)$  satisfies:

$$\max_{t \in [T]} g^*(t) = \max_{t \in [T]} \frac{\sum_{\tau=1}^t d(\tau)}{t} \leq \min\{\bar{g}, f\},$$

and hence is feasible and optimal for  $\Pi(\bar{g}, f, +\infty)$ . Note that  $\sum_{\tau=\tau_{m-1}+1}^{\tau_m} (g^*(\tau) - d(\tau)) =$

0 for all  $1 \leq m \leq M$ . Thus, for  $\tau_{m-1} < t \leq \tau_m$ , we have

$$\begin{aligned} s_2^*(t) &= \sum_{\tau=\tau_{m-1}}^t (g^*(\tau) - d(\tau)) \\ &= \frac{\sum_{\tau=\tau_{m-1}+1}^{\tau_m} d(\tau)}{\tau_m - \tau_{m-1}} (t - \tau_{m-1}) - \sum_{\tau=\tau_{m-1}+1}^t d(\tau). \end{aligned}$$

Maximizing the above relation over all  $t \in [T]$  we get  $\max_{t \in [T]} s_2^*(t) = h_{sat}$ . Therefore,  $g^*(t), t \in [T]$  is feasible and optimal for  $\Pi(\bar{g}, f, h)$  provided that  $h \geq h_{sat}$ .

□

### A.3.2 Proofs for star network

**Proposition 22.** *Suppose  $f_{1k} \geq \max_{t \in [T]} \left( \frac{\sum_{\tau=1}^t d_k(\tau)}{t} \right)$  for all  $k \in \mathcal{N}_D$ . Then,  $P(h)$  and  $\Pi^{\{1\}}(h)$  are feasible iff  $h \geq h_{min}$ , where*

$$h_{min} = \sum_{k \in \mathcal{N}_D} \max_{0 \leq t_1 < t_2 \leq T} \left[ \sum_{\tau=t_1+1}^{t_2} (d_k(\tau) - f_{1k}) \right]^+. \quad (\text{A.18})$$

Moreover:

(a)  $p_*(h_{min}) = \pi_*^{\{1\}}(h_{min})$ ,

(b) *There exists  $h_o \geq h_{min}$  such that  $p_*(h) = \pi_*^{\{1\}}(h)$  for all  $h \geq h_o$ .*

*Proof.* First we show that  $h \geq h_{min}$  is necessary for  $P(h)$  to be feasible. Consider any feasible solution of  $P(h)$ . For any  $k \in \mathcal{N}_D$  and  $0 \leq t_1 < t_2 \leq T$ , we have  $\sum_{\tau=t_1+1}^{t_2} r_k(\tau) \geq -b_k$ , since the power extracted from the storage device at node  $k$  cannot exceed the corresponding storage capacity  $b_k$ . Also, for any  $k \in \mathcal{N}_D$  the power flow on the line joining buses 1 and  $k$  satisfies  $p_{1k}(t) = d_k(t) + r_k(t) \leq f_{1k}$  for all  $t \in [T]$ . Combining the above relations and

rearranging, we get  $b_k \geq \sum_{\tau=t_1+1}^{t_2} (d_k(\tau) - f_{1k})$ . Also for  $k \in \mathcal{N}_D$ ,  $b_k \geq 0$  and hence

$$b_k \geq \max_{0 \leq t_1 < t_2 \leq T} \left[ \sum_{\tau=t_1+1}^{t_2} (d_k(\tau) - f_{1k}) \right]^+. \quad (\text{A.19})$$

Thus we get  $h \geq \sum_{k \in \mathcal{N}_D} b_k \geq h_{min}$ . If  $\Pi^{\{1\}}(h)$  is feasible, then  $P(h)$  is also feasible and hence  $h \geq h_{min}$  is necessary for both problems to be feasible. Now we prove that it is also sufficient. In particular, we show that for  $h = h_{min}$ ,  $\Pi^{\{1\}}(h)$  is feasible. For convenience, define

$$\tilde{h}_k := \max_{0 \leq t_1 < t_2 \leq T} \left[ \sum_{\tau=t_1+1}^{t_2} (d_k(\tau) - f_{1k}) \right]^+, \quad k \in \mathcal{N}_D. \quad (\text{A.20})$$

Then  $h_{min} = \sum_{k \in \mathcal{N}_D} \tilde{h}_k$ . Rearranging (A.20), we get

$$f_{1k} \geq \max_{0 \leq t_1 < t_2 \leq T} \left( \frac{\sum_{\tau=t_1+1}^{t_2} d_k(\tau) - \tilde{h}_k}{t_2 - t_1} \right). \quad (\text{A.21})$$

Also, by hypothesis, we have

$$f_{1k} \geq \max_{t \in [T]} \left( \frac{\sum_{\tau=1}^t d_k(\tau)}{t} \right). \quad (\text{A.22})$$

Combining equations (A.21) and (A.22), we have

$$f_{1k} \geq \max \left\{ \max_{0 \leq t_1 < t_2 \leq T} \left( \frac{\sum_{\tau=t_1+1}^{t_2} d_k(\tau) - \tilde{h}_k}{t_2 - t_1} \right), \max_{t \in [T]} \left( \frac{\sum_{\tau=1}^t d_k(\tau)}{t} \right) \right\}. \quad (\text{A.23})$$

For each  $k \in \mathcal{N}_D$ , consider a single generator single load system as follows. Let the demand profile be  $d_k(t)$ , the capacity of the transmission line be  $f_{1k}$  and the total available storage budget be  $\tilde{h}_k$ . For this system, the right hand side in (A.23) coincides with the definition of  $f_{min}$  in (A.1). From Proposition 20, it follows that there is a feasible generation profile (say  $g^{(k)}(t)$ ) and a storage control policy  $r_k(t)$  that define a feasible flow over this single generator single load system and meet the demand. Now, for the star network, construct

the generation profile  $g_1(t)$

$$g_1(t) = \sum_{k \in \mathcal{N}_D} g^{(k)}(t),$$

and operate the storage units at each node  $k \in \mathcal{N}_D$  with the control policy  $r_k(t)$  defined above. Also,  $r_1(t) = 0$  for all  $t \in [T]$ . It can be checked that this defines a feasible point for  $\Pi^{\{1\}}(h_{min})$ .

Next, we prove that  $p_*(h_{min}) = \pi_*^{\{1\}}(h_{min})$ . Let  $b_k^*, k \in \mathcal{N}$  be optimal storage capacities for problem  $P(h_{min})$ . Then the optimal storage capacities satisfy the following relations:

$$\sum_{k \in \mathcal{N}_D} b_k^* \geq h_{min}, \quad \text{and} \quad b_1^* + \sum_{k \in \mathcal{N}_D} b_k^* \leq h_{min}.$$

where the first one follows from (A.19) and the second one follows from the constraint on the total available storage capacities. Rearranging the above equations, we get  $b_1^* = 0$  and hence  $p_*(h_{min}) = \pi_*^{\{1\}}(h_{min})$ . This completes the proof of part (a).

To prove part (b) of Proposition 22, we start by showing that

$$p_*(\infty) = \pi_*^{\{1\}}(\infty). \tag{A.24}$$

Assume  $P(\infty)$  is feasible. For  $h = \infty$ , we drop the variables  $b_k, k \in \mathcal{N}$ , and consider the problems  $P(\infty)$  and  $\Pi^{\{1\}}(\infty)$  over the variables  $g_1(t), r_k(t), k \in \mathcal{N}$ . The variables  $p_{1k}(t)$  and  $s_k(t)$  are defined accordingly for all  $k \in \mathcal{N}$ . We argue that the optimal points of  $P(\infty)$  lie in a bounded set. Note that  $|p_{1k}(t)| = |d_k(t) + r_k(t)| \leq f_{1k}$  and thus the control policies  $r_k(t)$  are bounded for all  $k \in \mathcal{N}_D$ . Also, the cost function  $c_1(\cdot)$  is convex and hence its sub-level sets [55] are bounded. From the above arguments and the power-balance at bus 1, the optimal policy  $r_1(t)$  is also bounded. Thus, the set of optimal solutions of  $P(\infty)$  is a bounded set. Furthermore, this set is also closed since the objective function and the constraints are continuous functions. As in the proof of Lemma 19, associate the function  $\sum_{t \in [T]} |r_1(t)|$  with every point in the set of optimal solutions of  $P(\infty)$ . This is a continuous function on a compact set and hence attains a minimum. Consider the optimum of  $P(\infty)$

where this minimum is attained. We prove (A.24) by showing that  $r_1^*(t) = 0$  for all  $t \in [T]$  at this optimum.

Assume to the contrary, that  $r_1^*(t)$  is non-zero for some  $t \in [T]$ . Define

$$t_0 := \{t \in [T] \mid r_1(t_0) > 0\} \quad \text{and} \quad t_1 := \min \{t \in [t_0 + 1, T] \mid r_1^*(t) < 0\}.$$

Also, define  $\Delta := \min \{r_1^*(t_0), -r_1^*(t_1)\}$  and notice that  $\Delta > 0$ .

**Case 1:**  $g_1^*(t_0) > g_1^*(t_1) + \Delta$ : Construct the modified generation and charging/ discharging profiles  $\tilde{g}_1(t), \tilde{r}_1(t)$  that differ from  $g_1^*(t), r_1^*(t)$  only at  $t_0$  and  $t_1$  as follows:

$$\begin{aligned} \tilde{g}_1(t_0) &= g_1^*(t_0) - \Delta g, & \tilde{g}_1(t_1) &= g_1^*(t_1) + \Delta g, \\ \tilde{r}_1(t_0) &= r_1^*(t_0) - \Delta g, & \tilde{r}_1(t_1) &= r_1^*(t_1) + \Delta g, \end{aligned}$$

where  $\Delta g := \min \{\Delta, g_1^*(t_0)\} > 0$ . As in the proof of Lemma 19, this is feasible for  $P(\infty)$ .

Also, by Lemma 18:

$$c_1(\tilde{g}_1(t_0)) + c_1(\tilde{g}_1(t_1)) \leq c_1(g_1^*(t_0)) + c_1(g_1^*(t_1)).$$

The details are omitted for brevity. This feasible point satisfies

$$|\tilde{r}_1(t_0)| + |\tilde{r}_1(t_1)| = r_1^*(t_0) - \Delta - r_1^*(t_1) - \Delta < |r_1^*(t_0)| + |r_1^*(t_1)|, \quad (\text{A.25})$$

and hence defines an optimal point of  $P(\infty)$  with a strictly lower value of the function  $\sum_{t \in [T]} |r_1(t)|$ . This is a contradiction.

**Case 2:**  $g_1^*(t_0) \leq g_1^*(t_1) + \Delta$ : As above we construct modified storage control policies  $\tilde{r}_k(t)$  for all  $k \in \mathcal{N}$ , keeping the generation profile constant to define an optimal point of  $P(\infty)$  with a lower value of  $\sum_{t \in [T]} |r_1(t)|$  to derive a contradiction.

Let the modified control policy at bus 1 be as follows:

$$\tilde{r}_1(t_0) = r_1^*(t_0) - \Delta, \quad \tilde{r}_1(t_1) = r_1^*(t_1) + \Delta.$$

Instead, we distribute this to storage devices at  $k \in \mathcal{N}_D$ , as follows:

$$\tilde{r}_k(t_0) = r_k^*(t_0) + \psi_k, \quad \tilde{r}_k(t_1) = r_k^*(t_1) - \psi_k, \quad k \in \mathcal{N}_D,$$

for some  $\psi_k \geq 0, k \in \mathcal{N}_D$  and  $\sum_{k \in \mathcal{N}_D} \psi_k = \Delta$ . To ensure feasibility of the modified profiles it suffices to check that the line flow constraints are satisfied at  $t_0$  and  $t_1$ . In other words, we show that there exists  $\psi_k, k \in \mathcal{N}_D$  such that for all  $k \in \mathcal{N}_D$ ,

$$\psi_k \geq 0, \quad p_{1k}^*(t_0) + \psi_k \leq f_{1k}, \quad p_{1k}^*(t_1) - \psi_k \geq -f_{1k}, \quad \sum_{k \in \mathcal{N}_D} \psi_k = \Delta.$$

Equivalently, we prove that

$$\sum_{k \in \mathcal{N}_D} \min \{f_{1k} - p_{1k}^*(t_0), f_{1k} + p_{1k}^*(t_1)\} \geq \Delta.$$

Recall that  $p_{1k}^*(t_0)$  and  $p_{1k}^*(t_1)$  are feasible for  $P(\infty)$ . Thus  $p_{1k}^*(t_0) \leq f_{1k}$  and  $p_{1k}^*(t_1) \geq -f_{1k}$ . Also,  $g_1^*(t) - r_1^*(t) = \sum_{k \in \mathcal{N}_D} p_{1k}^*(t)$  at  $t = t_0$  and  $t = t_1$ . Thus, we have

$$\begin{aligned} \sum_{k \in \mathcal{N}_D} \min \{f_{1k} - p_{1k}^*(t_0), f_{1k} + p_{1k}^*(t_1)\} &\geq \sum_{k \in \mathcal{N}_D} (p_{1k}^*(t_1) - p_{1k}^*(t_0)) \\ &= \underbrace{g_1^*(t_1) - g_1^*(t_0)}_{\geq -\Delta} - \underbrace{r_1^*(t_1)}_{\leq -\Delta} + \underbrace{r_1^*(t_0)}_{\geq \Delta} \\ &\geq \Delta, \end{aligned}$$

where the last inequality follows from the hypothesis  $g_1^*(t_0) \leq g_1^*(t_1) + \Delta$ . The modified profiles satisfy  $|\tilde{r}_1(t_0)| + |\tilde{r}_1(t_1)| < |r_1^*(t_0)| + |r_1^*(t_1)|$  as in (A.25). As argued above this is a contradiction and hence (A.24) holds.

For  $P(\infty)$ ,  $s_k^*(t), k \in \mathcal{N}, t \in [T]$  is finite. Define  $h_o := \sum_{k \in \mathcal{N}_D} \max_{t \in [T]} s_k^*(t)$ . Then, note that  $(g_1^*(t), r_k^*(t), t \in [T], k \in \mathcal{N})$  are also feasible for  $\Pi^{\{1\}}(h)$  and  $P(h)$  for all  $h \geq h_o$ . This completes the proof of Proposition 22.  $\square$

# Bibliography

- [1] B. Lesieutre, D. Molzahn, A. Borden, and C. L. DeMarco, “Examining the limits of the application of semidefinite programming to power flow problems,” in *Proc. Allerton Conference*, 2011.
- [2] C. Weare, *The California Electricity Crisis: Causes and Policy Options*, 2003, published: Public Policy Institute of San Francisco, [http://www.ppic.org/content/pubs/report/R\\_103CWR.pdf](http://www.ppic.org/content/pubs/report/R_103CWR.pdf).
- [3] J. Carpentier, “Contribution to the economic dispatch problem,” *Bulletin de la Societe Francoise des Electriciens*, vol. 3, no. 8, p. 431447, 1962.
- [4] J. L. Sweeney, *The California electricity crisis*. Hoover Press, 2008.
- [5] Wikipedia, “Deregulation wikipedia, the free encyclopedia,” 2014, [Online; accessed 8-May-2014]. [Online]. Available: <http://en.wikipedia.org/w/index.php?title=Deregulation&oldid=605503841>
- [6] T. Karl, R. Knight, and K. Trenberth, *JM Melillo, and TC Peterson, Eds., 2009: Global Climate Change Impacts in the United States*. Cambridge University Press, 2009.
- [7] “Energy, climate change and our environment,” 2009. [Online]. Available: <http://www.whitehouse.gov/energy>
- [8] A. R. Bergen and V. Vittal, *Power Systems Analysis*, 2nd ed. Prentice Hall, 2000.
- [9] D. Kirschen and G. Strbac, *Fundamentals of power system economics*. Wiley, 2004.

- [10] F. C. Schweppe, R. D. Tabors, M. Caraminis, and R. E. Bohn, "Spot pricing of electricity," 1988.
- [11] S. Bose, S. H. Low, T. Teeraratkul, and B. Hassibi, "Equivalent relaxations of optimal power flow," *Accepted at IEEE Trans. on Automatic Control*, 2014. [Online]. Available: <http://smart.caltech.edu/papers/equivalence.pdf>
- [12] S. Bose, D. F. Gayme, S. H. Low, and K. M. Chandy, "Quadratically constrained quadratic programs on acyclic graphs with application to power flow," *arXiv preprint arXiv:1203.5599*, 2012, submitted to IEEE Transactions on Control of Networked Systems, 2014.
- [13] S. Bose, C. Wu, Y. Xu, A. Wierman, and H. Mohsenian-Rad, "Unifying measure for market power in deregulated electricity markets," *Under review in IEEE Transactions in Power Systems*, 2014.
- [14] S. Bose, D. Cai, S. Low, and A. Wierman, "The role of a market maker in networked cournot competition," *arXiv preprint arXiv:1403.7286*, 2014, submitted to Annual Conference on Decision and Control, 2014.
- [15] S. Bose, D. Gayme, S. H. Low, and K. M. Chandy, "Optimal power flow over tree networks," in *Proc. Allerton Conf. on Comm., Ctrl. and Computing*, Oct. 2011.
- [16] C. Thrampoulidis, S. Bose, and B. Hassibi, "Optimal placement of distributed energy storage in power networks," *arXiv preprint arXiv:1303.5805*, 2013.
- [17] H. Dommel and W. Tinney, "Optimal power flow solutions," *Power Apparatus and Systems, IEEE Transactions on*, vol. PAS-87, no. 10, pp. 1866–1876, Oct. 1968.
- [18] J. A. Momoh, *Electric Power System Applications of Optimization*, ser. Power Engineering, H. L. Willis, Ed. Markel Dekker Inc.: New York, USA, 2001.
- [19] M. Huneault and F. D. Galiana, "A survey of the optimal power flow literature," *IEEE Trans. on Power Systems*, vol. 6, no. 2, pp. 762–770, 1991.

- [20] J. A. Momoh, M. E. El-Hawary, and R. Adapa, “A review of selected optimal power flow literature to 1993. part II: newton, linear programming and interior point methods,” *IEEE Trans. on Power Systems*, vol. 14, no. 1, pp. 105 – 111, 1999.
- [21] —, “A review of selected optimal power flow literature to 1993. part i: Nonlinear and quadratic programming approaches,” *IEEE Trans. on Power Systems*, vol. 14, no. 1, p. 96104, 1999.
- [22] K. S. Pandya and S. K. Joshi, “A survey of optimal power flow methods,” *J. of Theoretical and Applied Information Technology*, vol. 4, no. 5, p. 450458, 2008.
- [23] S. Frank, I. Steponavice, and S. Rebennack, “Optimal power flow: a bibliographic survey i, II,” *Energy Systems*, vol. 3, no. 3, p. 221289, 2012.
- [24] M. B. Cain, R. P. O’Neill, and A. Castillo, “History of optimal power flow and formulations (OPF paper 1),” US FERC, Tech. Rep., Dec. 2012.
- [25] R. P. O’Neill, A. Castillo, and M. B. Cain, “The IV formulation and linear approximations of the AC optimal power flow problem (OPF paper 2),” US FERC, Tech. Rep., Dec. 2012.
- [26] —, “The computational testing of AC optimal power flow using the current voltage formulations (OPF paper 3),” US FERC, Tech. Rep., Dec. 2012.
- [27] A. Castillo and R. P. O’Neill, “Survey of approaches to solving the ACOPF (OPF paper 4),” US FERC, Tech. Rep., Mar. 2013.
- [28] —, “Computational performance of solution techniques applied to the ACOPF (OPF paper 5),” US FERC, Tech. Rep., Mar. 2013.
- [29] S. H. Low, “Convex relaxation of optimal power flow: a tutorial,” in *IREP Symposium Bulk Power System Dynamics and Control (IREP)*, Rethymnon, Greece, Aug. 2013.
- [30] B. Stott and O. Als, “Fast decoupled load flow,” *IEEE Trans. on Power Apparatus and Systems*, vol. PAS-93, no. 3, p. 859869, 1974.

- [31] O. Alsa, J. Bright, M. Prais, and B. Stott, "Further developments in LP-based optimal power flow," *IEEE Trans. on Power Systems*, vol. 5, no. 3, p. 697711, 1990.
- [32] K. Purchala, L. Meeus, D. Van Dommelen, and R. Belmans, "Usefulness of DC power flow for active power flow analysis," in *Proc. of IEEE PES General Meeting*. IEEE, 2005, p. 24572462.
- [33] B. Stott, J. Jardim, and O. Alsa, "DC power flow revisited," *IEEE Trans. on Power Systems*, vol. 24, no. 3, p. 13011309, Aug. 2009.
- [34] C. Coffrin and P. V. Hentenryck, "A linear-programming approximation of AC power flows," 2012, CoRR, abs/1206.3614.
- [35] X. Bai, H. Wei, K. Fujisawa, and Y. Wang, "Semidefinite programming for optimal power flow problems," *Int'l J. of Electrical Power & Energy Systems*, vol. 30, no. 6-7, p. 383392, 2008.
- [36] J. Lavaei and S. H. Low, "Zero duality gap in optimal power flow problem," *IEEE Trans. on Power Systems*, vol. 27, no. 1, p. 92107, Feb. 2012.
- [37] B. Zhang and D. Tse, "Geometry of the injection region of power networks," *IEEE Trans. Power Systems*, vol. 28, no. 2, p. 788797, 2013.
- [38] S. Sojoudi and J. Lavaei, "Physics of power networks makes hard optimization problems easy to solve," in *IEEE Power & Energy Society General Meeting*, 2012.
- [39] J. Lavaei, A. Rantzer, and S. H. Low, "Power flow optimization using positive quadratic programming," in *Proceedings of IFAC World Congress*, 2011.
- [40] L. Gan and S. H. Low, "Optimal power flow in DC networks," in *52nd IEEE Conference on Decision and Control*, Dec. 2013.
- [41] M. E. Baran and F. F. Wu, "Optimal capacitor placement on radial distribution systems," *IEEE Trans. Power Delivery*, vol. 4, no. 1, p. 725734, 1989.

- [42] —, “Optimal sizing of capacitors placed on a radial distribution system,” *IEEE Trans. Power Delivery*, vol. 4, no. 1, p. 735743, 1989.
- [43] R. Cespedes, “New method for the analysis of distribution networks,” *IEEE Trans. Power Del.*, vol. 5, no. 1, p. 391396, Jan. 1990.
- [44] A. G. Expsito and E. R. Ramos, “Reliable load flow technique for radial distribution networks,” *IEEE Trans. Power Syst.*, vol. 14, no. 13, p. 10631069, Aug. 1999.
- [45] R. Jabr, “Radial distribution load flow using conic programming,” *IEEE Trans. on Power Systems*, vol. 21, no. 3, p. 14581459, Aug. 2006.
- [46] M. Farivar, C. R. Clarke, S. H. Low, and K. M. Chandy, “Inverter VAR control for distribution systems with renewables,” in *Proceedings of IEEE SmartGridComm Conference*, Oct. 2011.
- [47] J. A. Taylor and F. S. Hover, “Convex models of distribution system reconfiguration,” *IEEE Trans. Power Systems*, 2012.
- [48] R. A. Jabr, “Exploiting sparsity in SDP relaxations of the OPF problem,” *Power Systems, IEEE Transactions on*, vol. 27, no. 2, p. 11381139, 2012.
- [49] M. Farivar and S. H. Low, “Branch flow model: relaxations and convexification (parts i and II),” *IEEE Trans. on Power Systems*, vol. 28, no. 3, p. 25542572, Aug. 2013.
- [50] L. Gan, N. Li, U. Topcu, and S. H. Low, “On the exactness of convex relaxation for optimal power flow in tree networks,” in *Prof. 51st IEEE Conference on Decision and Control*, Dec. 2012.
- [51] N. Li, L. Chen, and S. Low, “Exact convex relaxation of OPF for radial networks using branch flow model,” in *IEEE International Conference on Smart Grid Communications*, Nov. 2012.

- [52] M. Fukuda, M. Kojima, K. Murota, and K. Nakata, “Exploiting sparsity in semidefinite programming via matrix completion i: General framework,” *SIAM Journal on Optimization*, vol. 11, p. 647674, 2001.
- [53] E. d. Klerk, “Exploiting special structure in semidefinite programming: A survey of theory and applications,” *European Journal of Operational Research*, vol. 201, no. 1, p. 110, 2010.
- [54] M. S. Lobo, L. Vandenberghe, S. Boyd, and H. Lebret, “Applications of second-order cone programming,” *Linear Algebra and its Applications*, vol. 284, p. 193228, 1998.
- [55] S. P. Boyd and L. Vandenberghe, *Convex optimization*. Cambridge University Press, 2004.
- [56] X. Bai and H. Wei, “A semidefinite programming method with graph partitioning technique for optimal power flow problems,” *Int’l J. of Electrical Power & Energy Systems*, vol. 33, no. 7, p. 13091314, 2011.
- [57] S. Bose, S. H. Low, and M. Chandy, “Equivalence of branch flow and bus injection models,” in *50th Annual Allerton Conference on Communication, Control, and Computing*, Oct. 2012.
- [58] W. H. Kersting, *Distribution systems modeling and analysis*. CRC, 2002.
- [59] D. Shirmohammadi, H. W. Hong, A. Semlyen, and G. X. Luo, “A compensation-based power flow method for weakly meshed distribution and transmission networks,” *IEEE Transactions on Power Systems*, vol. 3, no. 2, p. 753762, May 1988.
- [60] H.-D. Chiang and M. E. Baran, “On the existence and uniqueness of load flow solution for radial distribution power networks,” *IEEE Trans. Circuits and Systems*, vol. 37, no. 3, p. 410416, Mar. 1990.
- [61] L. Gan, N. Li, U. Topcu, and S. H. Low, “Optimal power flow in distribution networks,” in *Proc. 52nd IEEE Conference on Decision and Control*, Dec. 2013.

- [62] —, “Exact convex relaxation of optimal power flow in radial networks,” *IEEE Trans. Automatic Control*, 2014.
- [63] R. D. Zimmerman, C. E. Murillo-Snchez, and R. J. Thomas, “MATPOWER: steady-state operations, planning, and analysis tools for power systems research and education,” *IEEE Trans. on Power Systems*, vol. 26, no. 1, p. 1219, 2011.
- [64] R. Horn and C. Johnson, *Matrix analysis*. Cambridge university press, 2005.
- [65] H. Wolkowicz, R. Saigal, and L. Vandenberghe, *Handbook of semidefinite programming: theory, algorithms, and applications*. Springer Netherlands, 2000, vol. 27.
- [66] Y. Nesterov and A. Nemirovskii, *Interior-point polynomial algorithms in convex programming*. Society for Industrial Mathematics, 1987, vol. 13.
- [67] F. Alizadeh, “Interior point methods in semidefinite programming with applications to combinatorial optimization,” *SIAM Journal on Optimization*, vol. 5, no. 1, p. 1351, 1995.
- [68] J. Lavaei, D. Tse, and B. Zhang, “Geometry of power flows and optimization in distribution networks,” *Power Systems, IEEE Transactions on*, vol. PP, no. 99, pp. 1–12, 2013.
- [69] A. Y. S. Lam, B. Zhang, A. Domnguez-Garca, and D. Tse, “Optimal distributed voltage regulation in power distribution networks,” *arXiv*, Apr. 2012.
- [70] S. Sojoudi and J. Lavaei, “Semidefinite relaxation for nonlinear optimization over graphs with application to power systems,” *Preprint*, 2013.
- [71] D. R. Fulkerson and O. A. Gross, “Incidence matrices and interval graphs,” *Pacific Journal of Mathematics*, vol. 15, no. 3, p. 835855, 1965.
- [72] D. J. Rose, R. E. Tarjan, and G. S. Lueker, “Algorithmic aspects of vertex elimination on graphs,” *SIAM Journal on Computing*, vol. 5, no. 2, p. 266283, 1976.

- [73] N. Biggs, *Algebraic graph theory*. Cambridge University Press, 1993, Cambridge Mathematical Library.
- [74] R. Grone, C. R. Johnson, E. M. S, and H. Wolkowicz, “Positive definite completions of partial hermitian matrices,” *Linear Algebra and its Applications*, vol. 58, p. 109124, 1984.
- [75] T. Tsuchiya, “A polynomial primal-dual path-following algorithm for second-order cone programming,” *Research Memorandum*, vol. 649, 1997.
- [76] M. Grant and S. Boyd, “CVX: matlab software for disciplined convex programming, version 2.0 beta,” Sep. 2012. [Online]. Available: <http://cvxr.com/cvx>
- [77] J. F. Sturm, “Using SeDuMi 1.02, a MATLAB toolbox for optimization over symmetric cones,” *Optimization Methods and Software*, vol. 11, no. 1-4, pp. 625–653, 1999.
- [78] A. Gershman, N. Sidiropoulos, S. Shahbazpanahi, M. Bengtsson, and B. Ottersten, “Convex optimization-based beamforming,” *IEEE Signal Processing Magazine*, vol. 27, no. 3, p. 6275, 2010.
- [79] N. Sidiropoulos, T. Davidson, and Z. Luo, “Transmit beamforming for physical-layer multicasting,” *IEEE Trans. on Signal Processing*, vol. 54, no. 6, p. 22392251, 2006.
- [80] A. So, Y. Ye, and J. Zhang, “A unified theorem on SDP rank reduction,” *Mathematics of Operations Research*, vol. 33, no. 4, p. 910920, 2008.
- [81] Y. Huang and D. Palomar, “Rank-constrained separable semidefinite programming with applications to optimal beamforming,” *IEEE Trans. on Signal Processing*, vol. 58, no. 2, p. 664678, 2010.
- [82] P. Biswas, T. Lian, T. Wang, and Y. Ye, “Semidefinite programming based algorithms for sensor network localization,” *ACM Trans. on Sensor Networks (TOSN)*, vol. 2, no. 2, p. 188220, 2006.

- [83] M. McCoy and J. Tropp, “Two proposals for robust PCA using semidefinite programming,” *Arxiv preprint arXiv:1012.1086*, 2010.
- [84] M. Goemans and D. Williamson, “Improved approximation algorithms for maximum cut and satisfiability problems using semidefinite programming,” *Journal of the ACM (JACM)*, vol. 42, no. 6, p. 11151145, 1995.
- [85] A. Frieze and M. Jerrum, “Improved approximation algorithms for max-cut and max bisection,” *Algorithmica*, vol. 18, no. 1, p. 6781, 1997.
- [86] T. S. Motzkin and E. G. Straus, “Maxima for graphs and a new proof of a theorem of turn,” *Canadian J. of Mathematics*, vol. 17, no. 4, p. 533540, 1965.
- [87] M. Giandomenico, A. N. Letchford, F. Rossi, and S. Smriglio, “A new approach to the stable set problem based on ellipsoids,” in *Integer Programming and Combinatorial Optimization*. Springer, 2011, p. 223234.
- [88] Y. Nesterov and A. Nemirovskii, “Polynomial barrier methods in convex programming,” *Ekonom. i Mat. Metody*, vol. 24, no. 6, p. 10841091, 1988.
- [89] Z. Luo, W. Ma, A. So, Y. Ye, and S. Zhang, “Semidefinite relaxation of quadratic optimization problems,” *Signal Processing Magazine, IEEE*, vol. 27, no. 3, pp. 20–34, May 2010.
- [90] Y. Nesterov, “Quality of semidefinite relaxation for nonconvex quadratic optimization,” Universite catholique de Louvain, Center for Operations Research and Econometrics (CORE), CORE Discussion Papers 1997019, 1997. [Online]. Available: <http://EconPapers.repec.org/RePEc:cor:louvco:1997019>
- [91] —, “Semidefinite relaxation and nonconvex quadratic optimization,” *Optimization methods and software*, vol. 9, no. 1-3, p. 141160, 1998.
- [92] D. Bertsimas and Y. Ye, “Semidefinite relaxations, multivariate normal distributions, and order statistics,” *Handbook of Combinatorial Optimization*, vol. 3, p. 119, 1998.

- [93] Y. Ye, “Approximating quadratic programming with bound and quadratic constraints,” *Mathematical Programming*, vol. 84, no. 2, p. 219226, 1999.
- [94] S. Kim and M. Kojima, “Exact solutions of some nonconvex quadratic optimization problems via SDP and SOCP relaxations,” *Computational Optimization and Applications*, vol. 26, no. 2, p. 143154, 2003.
- [95] S. Zhang, “Quadratic maximization and semidefinite relaxation,” *Mathematical Programming*, vol. 87, no. 3, p. 453465, 2000.
- [96] A. Ben-Tal and A. Nemirovski, “Lectures on modern convex optimization,” *Technion-Israel Institute of Technology*, 2000.
- [97] Y. C. d. Verdiere, “Multiplicities of eigenvalues and tree-width graphs,” *Journal of Combinatorial Theory*, vol. 74, p. 121146, 1998, series B.
- [98] H. v. d. Holst, “Graphs whose positive semidefinite matrices have nullity at most two,” *Linear Algebra and its Applications*, vol. 375, p. 111, 2003.
- [99] C. Johnson, A. Leal Duarte, C. Saiago, B. Sutton, and A. Witt, “On the relative position of multiple eigenvalues in the spectrum of an hermitian matrix with a given graph,” *Linear Algebra and its Applications*, vol. 363, p. 147159, 2003.
- [100] J. Bonnans and A. Shapiro, “Optimization problems with perturbations: A guided tour,” *SIAM review*, vol. 40, no. 2, p. 228264, 1998.
- [101] E. Yldrm and M. Todd, “Sensitivity analysis in linear programming and semidefinite programming using interior-point methods,” *Mathematical Programming*, vol. 90, no. 2, p. 229261, 2001.
- [102] X. Bai and H. Wei, “Semi-definite programming-based method for security-constrained unit commitment with operational and optimal power flow constraints,” *IET Generation, Transmission & Distribution*, vol. 3, no. 2, p. 182197, 2009.

- [103] I. A. Hiskens and R. Davy, “Exploring the power flow solution space boundary,” *IEEE Trans. Power Systems*, vol. 16, no. 3, p. 389395, 2001.
- [104] B. C. Lesieutre and I. A. Hiskens, “Convexity of the set of feasible injections and revenue adequacy in FTR markets,” *IEEE Trans. Power Systems*, vol. 20, no. 4, p. 17901798, 2005.
- [105] Y. V. Makarov, Z. Y. Dong, and D. J. Hill, “On convexity of power flow feasibility boundary,” *IEEE Trans. Power Systems*, vol. 23, no. 2, p. 811813, May 2008.
- [106] S. Borenstein, J. Bushnell, and F. Wolak, “Measuring market inefficiencies in california’s restructured wholesale electricity market,” *The American Economic Review*, vol. 92, no. 5, p. 13761405, 2002.
- [107] “FERC, JP morgan unit agree to \$410 million in penalties, disgorgement to ratepayers,” 2009. [Online]. Available: <http://www.ferc.gov/media/news-releases/2013/2013-3/07-30-13.asp#.UymzZPldUtN>
- [108] S. Stoft, *Power System Economics: Designing Market for Power*. Piscataway, NJ: IEEE Press, 2002.
- [109] P. Twomey, R. Green, K. Neuhoff, and D. Newbery, “A review of the monitoring of market power the possible roles of TSOs in monitoring for market power issues in congested transmission systems,” Tech. Rep., Jan. 2005. [Online]. Available: <http://ideas.repec.org/p/cam/camdae/0504.html>
- [110] P. Samuelson and W. Nordhaus, *Microeconomics*. Mcgraw-Hill Irwin, New York, 2001.
- [111] A. K. David and F. Wen, “Market power in electricity supply,” *IEEE Trans. on Energy Conversion*, vol. 16, no. 4, pp. 352–360, Dec. 2001.
- [112] S. Borenstein, J. Bushnell, E. Kahn, and S. Stoft, “Market power in california electricity markets,” *Utilities Policy*, vol. 5, no. 3, p. 219236, 1995.

- [113] S. Berenstein, J. Bushnell, and S. Stoft, *The Competitive Effects of Transmission Capacity in a Deregulated Electricity Industry*. Iowa State University, Department of Economics, Jun. 2000.
- [114] S. S. Oren, "Economic inefficiency of passive transmission rights in congested electricity systems with competitive generation," *ENERGY JOURNAL-CAMBRIDGE MA THEN CLEVELAND OH-*, vol. 18, p. 6384, 1997.
- [115] J. B. Cardell, C. C. Hitt, and W. Hogan, "Market power and strategic interaction in electricity networks," *Resource and Energy Economics*, vol. 19, no. 1, pp. 109–137, Mar. 1997.
- [116] F. A. Wolak and R. H. Patrick, "The impact of market rules and market structure on the price determination process in the england and wales electricity market," National Bureau of Economic Research, Tech. Rep., 2001.
- [117] A. Sheffrin, *Critical Actions Necessary for Effective Market Monitoring, Draft comments Dept. of Market Analysis, California ISO, FERC RTO Workshop*. October, 2001.
- [118] P. Joskow and E. Kahn, "A quantitative analysis of pricing behavior in california's wholesale electricity market during summer 2000," National Bureau of Economic Research, Tech. Rep., 2001.
- [119] S. Harvey, W. Hogan, and T. Schatzki, "A hazard rate analysis of mirant's generating plant outages in california," in *Toulouse Conference*, 2004.
- [120] R. Schmalensee and B. W. Golub, "Estimating effective concentration in deregulated wholesale electricity markets," *RAND Journal of Economics*, vol. 15, no. 1, pp. 12–26, Mar. 1984.
- [121] J. Bushnell and C. Day, *An international comparison of models for measuring market power in electricity*, 1999, published: Energy Modeling Forum Stanford University.

- [122] A. Y. Sheffrin and J. Chen, “Predicting market power in wholesale electricity markets,” in *Proc. of the Western Conference of the Advances in Regulation and Competition*, South Lake Tahoe, 2002.
- [123] “Market power and competitiveness,” Market Surveillance Unit California ISO, Tech. Rep., Jun. 1999. [Online]. Available: [http://www.caiso.com/Documents/Chapter7\\_1998AnnualReport\\_MarketIssuesandPerformance.pdf](http://www.caiso.com/Documents/Chapter7_1998AnnualReport_MarketIssuesandPerformance.pdf)
- [124] “Electric reliability council of texas market protocols,” 2001. [Online]. Available: <http://www.ercot.com/mktrules>
- [125] D. T. Scheffman and P. T. Spiller, “Geographic market definition under the US department of justice merger guidelines,” *JL & Econ.*, vol. 30, p. 123, 1987.
- [126] L. Xu and R. Baldick, “Transmission-constrained residual demand derivative in electricity markets,” *IEEE Trans. on Power Systems*, vol. 22, no. 4, pp. 1563–1573, Nov. 2007.
- [127] L. Xu and Y. Yu, “Transmission constrained linear supply function equilibrium in power markets: method and example,” in *Proc. of International Conference on Power System Technology (Powercon 2002)*, vol. 3. IEEE, 2002, p. 13491354.
- [128] C. Wu, S. Bose, A. Wierman, and H. Mohsenian-Rad, “A unifying approach to assessing market power in deregulated electricity markets,” in *Proc. of the IEEE PES General Meeting*, Vancouver, BC, Jul. 2013.
- [129] J. Chen, M. Macauley, and A. Marathe, “Network topology and locational market power,” *Computational Econ.*, vol. 34, pp. 21–35, 2009.
- [130] K. Atkins, J. Chen, V. S. A. Kumar, M. Macauley, and A. Marathe, “Locational market power in network constrained markets,” *J. of Economic Behavior & Organization*, vol. 70, no. 1, pp. 416–430, May 2009.

- [131] Y. Y. Lee, R. Baldick, and J. Hur, “Firm-based measurements of market power in transmission-constrained electricity markets,” *IEEE Trans. on Power Systems*, vol. 26, no. 4, pp. 1962–1970, Nov. 2011.
- [132] D. Gan and D. Bourcier, “Locational market power screening and congestion management: experience and suggestions,” *IEEE Trans. on Power Systems*, vol. 17, no. 1, p. 180185, 2002.
- [133] P. Wang, Y. Xiao, and Y. Ding, “Nodal market power assessment in electricity markets,” *IEEE Trans. on Pow. Sys.*, vol. 19, no. 3, p. 13731379, 2004.
- [134] N. S. Rau, “Issues in the path toward an RTO and standard markets,” *IEEE Trans. on Power Systems*, vol. 18, no. 2, p. 435443, 2003.
- [135] ———, *Optimization principles: practical applications to the operation and markets of the electric power industry*. John Wiley & Sons, Inc., 2003.
- [136] J. Lavaei and S. Sojoudi, “Competitive equilibria in electricity markets with nonlinearities,” in *Proceedings of American Control Conference*. IEEE, 2012, p. 30813088.
- [137] S. Bose, D. Gayme, U. Topcu, and K. Chandy, “Optimal placement of energy storage in the grid,” *Proceedings of IEEE Conference on Decision and Control*, 2012.
- [138] K.-C. Toh, M. J. Todd, and R. H. Ttnc, “SDPT3 a MATLAB software package for semidefinite programming, version 1.3,” *Optimization methods and software*, vol. 11, no. 1-4, p. 545581, 1999.
- [139] N. Karmarkar, “A new polynomial-time algorithm for linear programming,” in *Proceedings of the 16th annual ACM symposium on Theory of computing*, 1984, p. 302311.
- [140] Y. Nesterov and A. Nemirovskii, *Interior-point polynomial algorithms in convex programming*, ser. Studies in Applied and Numerical Mathematics. SIAM, 1994, vol. 13.
- [141] P. Klemperer and M. A. Meyer, “Supply function equilibria in oligopoly under uncertainty,” *Econometrica*, vol. 57, no. 6, pp. 1243–1277, 1989.

- [142] R. Green and D. Newbery, “Competition in the british electricity spot market,” *Journal of Political Economy*, vol. 100, no. 5, pp. 929–953, Oct. 1992.
- [143] R. J. Green, “Increasing competition in the british electricity spot market,” *The journal of Industrial economics*, p. 205216, 1996.
- [144] D. W. Bunn and F. S. Oliveira, “Agent-based simulation-an application to the new electricity trading arrangements of england and wales,” *Evolutionary Computation, IEEE Transactions on*, vol. 5, no. 5, p. 493503, 2001.
- [145] ———, “Evaluating individual market power in electricity markets via agent-based simulation,” *Annals of Operations Research*, vol. 121, no. 1-4, p. 5777, 2003.
- [146] R. Baldick and W. Hogan, *Capacity constrained supply function equilibrium models of electricity markets: stability, non-decreasing constraints, and function space iterations*. University of California Energy Institute, 2001.
- [147] A. Rudkevich, “On the supply function equilibrium and its applications in electricity markets,” *Decision Support Systems*, vol. 40, no. 3, p. 409425, 2005.
- [148] R. Baldick, R. Grant, and E. Kahn, “Theory and application of linear supply function equilibrium in electricity markets,” *Journal of Regulatory Economics*, vol. 25, no. 2, p. 143167, 2004.
- [149] R. Johari and J. N. Tsitsiklis, “Parameterized supply function bidding: Equilibrium and efficiency,” *Operations research*, vol. 59, no. 5, p. 10791089, 2011.
- [150] R. Wilson, “Supply function equilibrium in a constrained transmission system,” *Operations research*, vol. 56, no. 2, p. 369382, 2008.
- [151] A. Mas-Colell, M. Whinston, J. Green *et al.*, *Microeconomic theory*. New York: Oxford university press, 1995, vol. 1.
- [152] M. Ventosa, A. Ballo, A. Ramos, and M. Rivier, “Electricity market modeling trends,” *Energy policy*, vol. 33, no. 7, p. 897913, 2005.

- [153] B. Willems, I. Rumiantseva, and H. Weigt, “Cournot versus supply functions: What does the data tell us?” *Energy Economics*, vol. 31, no. 1, p. 3847, 2009.
- [154] R. Johari and J. N. Tsitsiklis, “Efficiency loss in cournot games,” in *Harvard University*, 2005.
- [155] J. N. Tsitsiklis and Y. Xu, “Efficiency loss in a cournot oligopoly with convex market demand,” in *Game Theory for Networks*. Springer, 2012, p. 6376.
- [156] —, “Profit loss in cournot oligopolies,” *Operations Research Letters*, vol. 41, no. 4, p. 415420, 2013.
- [157] K. Neuhoff, J. Barquin, M. G. Boots, A. Ehrenmann, B. F. Hobbs, F. A. Rijkers, and M. Vazquez, “Network-constrained cournot models of liberalized electricity markets: the devil is in the details,” *Energy Economics*, vol. 27, no. 3, p. 495525, 2005.
- [158] J. Barquin and M. Vazquez, “Cournot equilibrium calculation in power networks: An optimization approach with price response computation,” *Power Systems, IEEE Transactions on*, vol. 23, no. 2, pp. 317–326, May 2008.
- [159] J. Barquin and M. Vazquez, “Cournot equilibrium in power networks,” *Instituto de Investigacin Tecnolgica, Universidad Pontificia Comillas, Madrid*, 2005.
- [160] J. Yao, S. Oren, and I. Adler, “Computing cournot equilibria in two settlement electricity markets with transmission constraint,” in *System Sciences, 2004. Proceedings of the 37th Annual Hawaii International Conference on*. IEEE, 2004, p. 9pp.
- [161] —, “Two-settlement electricity markets with price caps and cournot generation firms,” *European journal of operational research*, vol. 181, no. 3, p. 12791296, 2007.
- [162] J. Yao, I. Adler, and S. Oren, “Modeling and computing two-settlement oligopolistic equilibrium in a congested electricity network,” *Operations Research*, vol. 56, no. 1, p. 3447, 2008.

- [163] J. Y. Wei and Y. Smeers, “Spatial oligopolistic electricity models with cournot generators and regulated transmission prices,” *Operations Research*, vol. 47, no. 1, pp. 102–112, 1999.
- [164] R. Ilklic, “Cournot competition on a network of markets and firms,” 2009.
- [165] F. Li and R. Bo, “DCOPF-Based LMP simulation: Algorithm, comparison with ACOPF, and sensitivity,” *Power Systems, IEEE Transactions on*, vol. 22, no. 4, pp. 1475–1485, Nov. 2007.
- [166] CAISO, *Technical Bulletin*, 2009. [Online]. Available: <http://caiso.com/Documents/TechnicalBulletin-MarketOptimizationDetails.pdf>
- [167] NYISO, *Transmission and Dispatching Operations Manual*, 2012. [Online]. Available: [http://www.nyiso.com/public/webdocs/markets\\_operations/documents/Manuals\\_and\\_Guides/Manuals/Operations/trans\\_disp.pdf](http://www.nyiso.com/public/webdocs/markets_operations/documents/Manuals_and_Guides/Manuals/Operations/trans_disp.pdf)
- [168] F. Wu, P. Varaiya, P. Spiller, and S. Oren, “Folk theorems on transmission access: Proofs and counterexamples,” *Journal of Regulatory Economics*, vol. 10, no. 1, p. 523, 1996.
- [169] G. Debreu, “A social equilibrium existence theorem,” *Proceedings of the National Academy of Sciences of the United States of America*, vol. 38, no. 10, p. 886, 1952.
- [170] F. Facchinei and C. Kanzow, “Generalized nash equilibrium problems,” *Annals of Operations Research*, vol. 175, no. 1, p. 177211, 2010.
- [171] T. Ichiishi, *Game theory for economic analysis*. Academic press New York, 1983.
- [172] S. Chu and A. Majumdar, “Opportunities and challenges for a sustainable energy future,” *Nature*, vol. 488, no. 7411, p. 294303, 2012.
- [173] “Electrical energy storage,” *IEC White paper*, 2011.

- [174] D. Rastler, *Electricity Energy Storage Technology Options: A White Paper Primer on Applications, Costs and Benefits*. Electric Power Research Institute, 2010.
- [175] “2020 strategic analysis of energy storage in california,” *California Energy Commission*, Nov. 2011.
- [176] R. Schainker, “Executive overview: Energy storage options for a sustainable energy future,” in *Proc. of IEEE PES General Meeting*, 2004, p. 23092314.
- [177] A. Nourai, “Installation of the first distributed energy storage system at american electric power,” *Sandia Nat. Labs*, 2007.
- [178] P. Denholm, E. Ela, B. Kirby, and M. Milligan, “The role of energy storage with renewable electricity generation,” *Nat. Renewable Ener. Lab.*, 2010.
- [179] P. P. Varaiya, F. F. Wu, and J. W. Bialek, “Smart operation of smart grid: Risk-limiting dispatch,” *Proceedings of the IEEE*, vol. 99, no. 1, p. 4057, Jan. 2011.
- [180] J. Eyer and G. Corey, “Energy storage for the electric grid: Benefits and market potential assessment guide,” *Sandia Nat. Lab.*, 2010.
- [181] J. Greenberger, “The smart grid’s problem may be storage’s opportunity,” 2011. [Online]. Available: <http://theenergycollective.com/jim-greenberger/70813/smart-grids-problem-may-be-storages-opportunity>
- [182] D. Lindley, “Smart grids: The energy storage problem.” *Nature*, vol. 463, no. 7277, p. 18, 2010.
- [183] “Distributed energy storage serving national interests: Advancing wide-scale DES in the united states,” *KEMA Inc*, 2012.
- [184] Y. M. Atwa and E. F. El-Saadany, “Optimal allocation of ESS in distribution systems with a high penetration of wind energy,” *IEEE Trans. on Power Systems*, 2010.

- [185] H. Xu, U. Topcu, S. Low, C. Clarke, and K. Chandy, "Load-shedding probabilities with hybrid renewable power generation and energy storage," in *48th Annual Allerton Conf. on Comm., Control, and Comp.* IEEE, 2010, p. 233239.
- [186] C. Budischak, D. Sewell, H. Thomson, L. Mach, D. Veron, and W. Kempton, "Cost-minimized combination of wind power, solar power and electrochemical storage, powering the grid up to 99.9% of the time," *Jour. of Pow. Sources*, 2012.
- [187] D. Biello, "Storing the breeze: New battery might make wind power more reliable," 2008. [Online]. Available: <http://www.scientificamerican.com/article.cfm?id=storing-the-breeze-new-battery-might-make-wind-power-reliable>
- [188] I. Koutsopoulos, V. Hatzi, and L. Tassiulas, "Optimal energy storage control policies for the smart power grid," in *IEEE Int. Conf. on Smart Grid Comm.* IEEE, 2011, p. 475480.
- [189] H. Su and A. Gamal, "Modeling and analysis of the role of fast-response energy storage in the smart grid," *arXiv preprint arXiv:1109.3841*, 2011.
- [190] M. Chandy, S. Low, U. Topcu, and H. Xu, "A simple optimal power flow model with energy storage," in *Proc. of Conf. on Decision and Control*, 2010.
- [191] Y. Kanoria, A. Montanari, D. Tse, and B. Zhang, "Distributed storage for intermittent energy sources: Control design and performance limits," in *Proc. of 49th Annual Allerton Conf. on Comm., Control, and Comp.* IEEE, 2011, p. 13101317.
- [192] D. Gayme and U. Topcu, "Optimal power flow with large-scale storage integration," *Power Systems, IEEE Transactions on*, vol. 28, no. 2, p. 709717, 2013.
- [193] M. Kraning, Y. Wang, E. Akuiyibo, and S. Boyd, "Operation and configuration of a storage portfolio via convex optimization," in *Proc. of the IFAC World Congress*, 2010, p. 1048710492.

- [194] P. Denholm and R. Sioshansi, "The value of compressed air energy storage with wind in transmission-constrained electric power systems," *Energy Policy*, vol. 37, p. 31493158, 2009.
- [195] P. Harsha and M. Dahleh, "Optimal management and sizing of energy storage under dynamic pricing for the efficient integration of renewable energy," 2012, in preparation.
- [196] "CAISO realtime demand data: Today's outlook," 2013. [Online]. Available: <http://www.caiso.com/outlook/SystemStatus.html>
- [197] M. Korpaas, A. T. Holen, and R. Hildrum, "Operation and sizing of energy storage for wind power plants in a market system," *Int. Jour. of Elec. Pow. & Energy Sys.*, vol. 25, no. 8, p. 599606, 2003.
- [198] J. Lofberg, "YALMIP: a toolbox for modeling and optimization in MATLAB," in *IEEE Int'l Symposium on Computer Aided Control Systems Design*, 2004, p. 284289.
- [199] "Western wind and solar integration study," G. E. Energy, Tech. Rep., 2010, subcontract report NREL/SR-550-47434. [Online]. Available: <http://www.osti.gov/bridge/>
- [200] L. Gaillac, J. Castaneda, A. Edris, D. Elizondo, C. Wilkins, C. Vartanian, and D. Mendelsohn, "Tehachapi wind energy storage project: Description of operational uses, system components, and testing plans," in *IEEE PES Transmission and Distribution Conf. and Expo.*, 2012, pp. 1–6.